JOINT TRANSPORTATION
RESEARCH PROGRAM
INDIANA DEPARTMENT OF TRANSPORTATION
AND PURDUE UNIVERSITY

Moisture-Strength-Constructability Guidelines for Subgrade Foundation Soils Found in Indiana

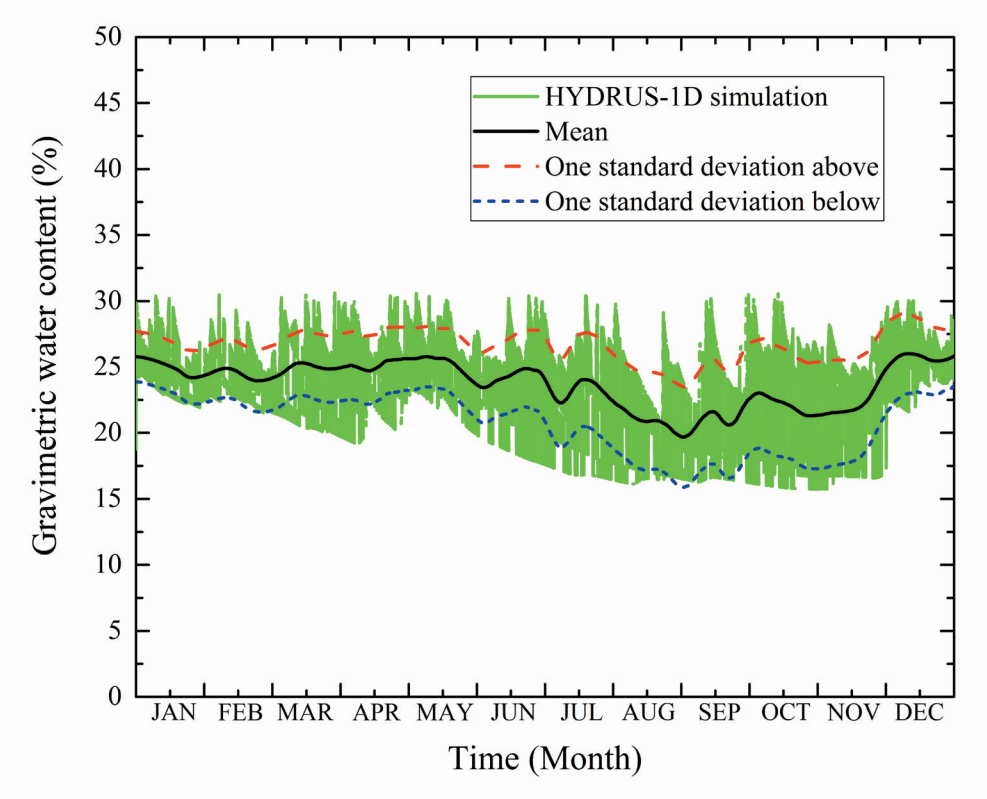

Eshan Ganju, Shahedur Rahman, Monica Prezzi,
Rodrigo Salgado, Nayyarzia Siddiki

SPR-3811 • Report Number: FHWA/IN/JTRP-2016/27 • DOI: 10.5703/1288284316354

RECOMMENDED CITATION

Ganju, E., Rahman, S., Prezzi, M., Salgado, R., & Siddiki, N. (2016). *Moisture-strength-constructability guidelines for subgrade foundation soils found in Indiana* (Joint Transportation Research Program Publication No. FHWA/IN/JTRP-2016/27). West Lafayette, IN: Purdue University. http://dx.doi.org/10.5703/1288284316354

AUTHORS

Eshan Ganju
Shahedur Rahman
Graduate Research Assistants
Lyles School of Civil Engineering
Purdue University

Monica Prezzi, PhD
Professor of Civil Engineering
Lyles School of Civil Engineering
Purdue University
(765) 494-5034
mprezzi@purdue.edu
Corresponding Author

Rodrigo Salgado, PhD
Charles Pankow Professor in Civil Engineering
Lyles School of Civil Engineering
Purdue University
(765) 494-5030
salgado@purdue.edu
Corresponding Author

Nayyarzia Siddiki, PhD, PE
Geotechnical Operations Manager
Indiana Department of Transportation

JOINT TRANSPORTATION RESEARCH PROGRAM

The Joint Transportation Research Program serves as a vehicle for INDOT collaboration with higher education institutions and industry in Indiana to facilitate innovation that results in continuous improvement in the planning, design, construction, operation, management and economic efficiency of the Indiana transportation infrastructure. https://engineering.purdue.edu/JTRP/index_html

Published reports of the Joint Transportation Research Program are available at http://docs.lib.purdue.edu/jtrp/.

NOTICE

COPYRIGHT

Print ISBN: 978-1-62260-441-8
ePUB ISBN: 978-1-62260-442-5

TECHNICAL REPORT STANDARD TITLE PAGE

1. Report No.	2. Government Accession No.	3. Recipient's Catalog No.
FHWA/IN/JTRP-2016/27		

4. Title and Subtitle	5. Report Date
Moisture-Strength-Constructability Guidelines for Subgrade Foundation Soils Found in Indiana	September 2016
	6. Performing Organization Code

7. Author(s)	8. Performing Organization Report No.
Eshan Ganju, Shahedur Rahman, Monica Prezzi, Rodrigo Salgado, Nayyarzia Siddiki	FHWA/IN/JTRP-2016/27

9. Performing Organization Name and Address	10. Work Unit No.
Joint Transportation Research Program Purdue University 550 Stadium Mall Drive West Lafayette, IN 47907-2051	11. Contract or Grant No. SPR-3811

12. Sponsoring Agency Name and Address	13. Type of Report and Period Covered
Indiana Department of Transportation State Office Building 100 North Senate Avenue Indianapolis, IN 46204	Final Report
	14. Sponsoring Agency Code

15. Supplementary Notes
Prepared in cooperation with the Indiana Department of Transportation and Federal Highway Administration.

16. Abstract

Soil moisture is an important indicator of constructability in the field. Construction activities become difficult when the soil moisture content is excessive, especially in fine-grained soils. Change orders caused by excessive soil moisture during construction projects drive up construction costs for INDOT and cause unexpected delays. To alleviate these problems and minimize change order costs associated with having unexpectedly high soil moisture conditions at the time of construction, a methodology was developed to allow INDOT engineers to estimate in situ soil moisture conditions early in the design phases of projects. The soil moisture prediction methodology is based on results from soil moisture flow simulations carried out using the HYDRUS-1D software. The soil moisture flow simulations in HYDRUS-1D required i) weather data, ii) groundwater table data and iii) in situ soil hydraulic (saturated and unsaturated) and index property data. These data were collected for all the counties in Indiana from five different sources: i) Indiana Department of Transportation (INDOT), ii) Indiana Geological Survey (IGS), iii) United States Department of Agriculture's (USDA's) Soil Survey Geographic (SSURGO), iv) the Department of Natural Resources (DNR) and v) Indiana State Climate Office (Iclimate). The results obtained from initial soil moisture flow simulations were first validated using field measurements from six IGS test sites located in Indiana where soil property data and continuous in situ soil moisture measurements at multiple depths were available for up to 3 years (2011-2014). Good agreement was observed between moisture content measurements and predictions. After validation of the developed moisture prediction methodology, ten-year moisture content simulations using HYDRUS 1D were performed for typical profiles in each county in Indiana using as input weather data from the iclimate database, groundwater data from DNR database and soil properties from IGS, INDOT and the SSURGO databases. Yearly results from these ten-year soil moisture flow simulations were then overlapped to ascertain how the profiles of the in situ soil moisture content within the depth of interest varied monthly within this period of time in each county. Using the results of these simulations for typical soil profile(s) for each county, a constructability criteria was developed that is based on determining how the in situ soil moisture content deviates from the optimum soil moisture content obtained from standard Proctor compaction tests (these are often performed by INDOT in routine projects). Recommendations are made for in situ soil moisture constructability assessment that can be implemented by INDOT in pilot projects and further refined as needed.

17. Key Words	18. Distribution Statement
soil moisture, seasonal soil moisture variation, constructability, in situ soils in Indiana	No restrictions. This document is available to the public through the National Technical Information Service, Springfield, VA 22161.

19. Security Classif. (of this report)	20. Security Classif. (of this page)	21. No. of Pages	22. Price
Unclassified	Unclassified	135	

Form DOT F 1700.7 (8-69)

EXECUTIVE SUMMARY

MOISTURE-STRENGTH-CONSTRUCTABILITY GUIDELINES FOR SUBGRADE FOUNDATION SOILS FOUND IN INDIANA

Introduction

One of the most important factors in earthwork-related design is the correct estimation of the water content of *in situ* soil because its mechanical response to loading and construction activities depends strongly on its water content at the time of construction. However, because the time between site investigation, design and construction phases varies substantially for any given project, initial estimates of soil water content may no longer apply. Occurrence of excessive soil moisture in the *in situ* soil at the time of construction leads to low strength, which inevitably results in constructability problems, particularly for fine-grained soils. If the strength of the foundation soil is too low, it is not capable of sustaining the loads due to construction activities. Changes in soil moisture over time have led to a larger number of change orders for INDOT. Once a change order is seen as necessary, INDOT engineers and contractors working at a jobsite have to then agree on how to proceed and spend extra time and effort to bring the water content of the *in situ* soil to the desired level or redo the design for current conditions before the construction process can actually begin.

This report presents a methodology that can be used to estimate the water content of fine-grained soils (A-4, A-6 and A-7-6 according to the AASHTO classification system) found in Indiana near the ground surface (within the top 5 ft. (150 cm)) and to assess the impact of changes in water content of fine-grained soils on their constructability.

Findings

HYDRUS-1D, a free soil moisture flow software, was used to simulate unsaturated soil moisture flow for typical soil profiles of the 92 counties in the state of Indiana. Input data for the simulations were obtained from various government agencies, such as the United States Department of Agriculture (USDA), the Department of Natural Resources (DNR), the Indiana Geological Survey (IGS) and Purdue State Climate (Iclimate). In order to validate the methodology used in this research, results from the soil moisture simulations were compared to measured soil moisture data collected for a period of 3 years from six IGS test sites (in four counties) located across Indiana. Since good agreement was obtained between predicted and measured water content values at these sites, the methodology was used to generate *in situ* soil water content profiles for all 92 counties using as input 10 years of weather and groundwater table data. The 10-year soil moisture simulations were superimposed to get daily ranges for the *in situ* soil water content of representative soil profiles for each county. Constructability of soils can be assessed by comparing the estimated *in situ* soil water content with the optimum value required for compaction. Based on INDOT specifications, it is suggested that if the *in situ* soil moisture is above 2% of the optimum water content, then a poor constructability rating be given to coarse-grained soil. On the other hand, for fine-grained soils, it is suggested that a poor constructability rating be given when the *in situ* soil moisture is 3% above of the optimum water content.

Implementation

In this report, yearly water content plots obtained from the overlapping of HYDRUS-1D soil moisture simulations for a period of 10 years are provided. From these plots, INDOT engineers can obtain the expected daily range for the soil water content of representative soil profiles in each Indiana county. These plots can also be used to obtain the daily range for the *in situ* soil moisture at project locations at any time of the year; the estimated soil water contents can be considered by INDOT engineers when making construction and design decisions at different phases of a project.

The constructability rating given to soils, which is based on the difference between the *in situ* soil moisture at any time of the year and the optimum water content obtained from standard Proctor compaction tests, can be considered when INDOT is preparing construction contracts. The methodology proposed in this report can be further improved by (i) taking into consideration the topography and vegetation at the project locations, (ii) performing additional HYDRUS-1D simulations for all the counties in Indiana for *in situ* soil profiles with specific laboratory characterization of soil properties, and (iii) implementing the developed methodology in pilot projects to fine-tune and refine the water content prediction methodology.

CONTENTS

LIST OF TABLES

LIST OF FIGURES

1. INTRODUCTION AND PROBLEM STATEMENT

1.1 Introduction

One of the most important factors in earthwork-related design is the estimation of the *in situ* soil water content because the mechanical response of a soil to loading and construction activities depends strongly on its water content at the time of construction (Holtz, Kovacs, & Sheahan, 2010; Rodriguez, del Castillo, & Stowers, 1988). For this reason, surveys carried out by INDOT before the beginning of construction activities include the soil water content measured during the soil investigation phase of projects. However, because the time between site investigation, design and construction phases varies substantially for any given project, the initial estimates of soil water content may no longer apply. Occurrence of excessive *in situ* soil moisture at the time of construction leads to low strength, which inevitably results in constructability problems, particularly for fine-grained soils. If the strength of the foundation soil is too low, it is not capable of sustaining the loads due to construction activities.

Changes in soil moisture over time have led to a larger number of change orders for INDOT over the years. Once a change order is seen as necessary, INDOT engineers and contractors working at a jobsite have to then agree on how to proceed and spend extra time and effort to bring the water content of the *in situ* soil to the desired level or redo the design for current conditions before the construction process can actually begin. Depending on the site conditions and ground water level, other solutions, such as providing under drainage for the excess water, excavating and replacing the problematic soils with a compacted layer of aggregate and doing chemical stabilization, may be adopted.

Deviations from the planned sequence of project activities or change orders (caused by but not just limited to changes in soil moisture conditions) are a major source of unforeseen project overruns and amount to substantial excess costs each fiscal year. A JTRP study (Mohan, Prezzi, & McCullouch, 2011) showed that the majority of the contracts that experienced geotechnical change orders are road and bridge contracts (the average geotechnical change order amount per year per district was 1.34% of the total construction cost per district per year). One-third of these geotechnical change orders were caused by "Changes in Field Conditions: Soils Related" or what is known as "Reason Code 405" in the INDOT jargon. The main reason for these change orders is the change in water content of the soil between the site investigation, design and the construction phases of the project.

During the year starting on July 1, 2012 and ending on June 30, 2013, change orders that had reason codes of either "Errors & Omissions, Soils Related" or "Changed Conditions, Soils Related" amounted to $14,722,963. Out of this total of $14,722,963, $877,725 was due to change orders caused by excessive soil moisture at the time of construction (cost overruns ranging from $15,000–300,000 were approved in 15–30 days). Even a small reduction in the occurrence of these change orders can lead to accumulated savings and reductions in time delays for INDOT in the long term. In addition, armed with the knowledge of temporal variation in soil moisture, INDOT engineers can schedule construction activities to avoid or to effectively deal with high moisture conditions *in situ*.

This problem of change orders due to change in soil moisture conditions is most critical when the geotechnical work is planned based on reconnaissance and *in situ* tests performed under unsaturated conditions, while construction takes place under saturated or nearly saturated conditions. Geotechnical engineers at INDOT would like to be proactive to minimize the occurrence of these soil moisture-related change orders. In order to achieve this goal, a methodology was developed in this research that makes it possible for INDOT engineers to estimate approximately the water content of foundation soils (located near the ground surface) at any phase of a project and to consider its impact on construction activities. INDOT engineers when planning the geotechnical work and designing the subgrade soil that supports geotechnical structures (such as embankments and foundations) will then be able to use the moisture prediction methodology to consider, during the design phase of projects, the impact of expected soil moisture changes on soil strength and constructability and to consider best options to improve the foundation soils during the construction phase of projects, in case such remediation measures are needed. This all-inclusive approach to geotechnical projects that accounts for changes in soil properties with time will allow INDOT to address potential problems that may arise in projects and propose upfront mitigating solutions that are cost-effective, allowing for the required work to be competitively bid.

1.2 Problem Statement

The water content of *in situ* soils oscillates throughout the year. Its value at any given time and depth depends on the nature of the soil strata, the topography, the prevalent weather conditions and the location of the groundwater table. Water content of natural soils is of particular interest to INDOT engineers because often naturally occurring *in situ* soils are compacted to construct a pavement subgrade layer. Whenever *in situ* soils are not used for construction of the compacted subgrade layer, they are the foundation soils for the subgrade layer itself.

The strength of a soil and its ability to carry loads is dependent on its intrinsic parameters (critical-state friction angle) and its state parameters (density, water content, over consolidation ratio). Under the most general conditions, a soil is weakest when fully saturated and when completely dry. When a soil is partially saturated, tightly held pore water provides additional confinement to the soil due to the formation of air-water interfaces, shown schematically in a two-particle system in Figure 1.1.

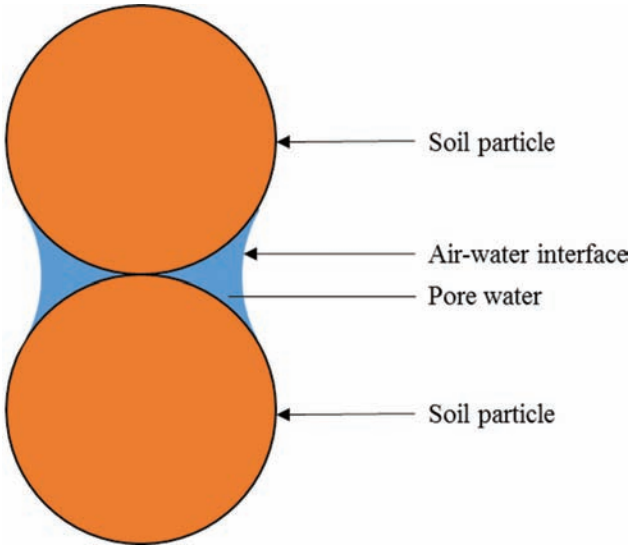

Figure 1.1 Air-water interface in unsaturated soil.

The curvature of the air-water interface is due to the difference in the pore-air and pore-water pressure in the soil (the pore-water pressure being smaller than the pore-air pressure). As the soil dries out from an initially saturated state, the difference between the pore-water and pore-air pressure (defined as the matric suction) pulls the particles together, thereby increasing the strength of the soil mass (Fredlund, Rahardjo, & Fredlund, 2012d). When a soil completely dries out, it no longer has any suction to contribute to an increase to its strength.

These facts present some important issues to the geotechnical engineer since the state of the *in situ* soil will be different depending on the timing of the site investigation for each project. Changes in soil water content between the site investigation, design and construction phases of a project cause geotechnical change orders every year. In order to reduce the number of those soil moisture-related change orders, this report includes:

i. A methodology that can be used to estimate the water content of fine-grained soils (A-4, A-6 and A-7-6 according to the AASHTO classification system) found in Indiana near the ground surface (within the top 3 ft. (90 cm)).
ii. A methodology to assess the impact of changes in water content of fine-grained soils found in Indiana on soil strength and constructability.

1.3 Sections of the Report

This report has been divided into six chapters. A literature review on the topics of soil moisture prediction and unsaturated flow in soils is presented in chapter 2. Chapter 3 describes the research methodology. Chapter 4 presents the experimental results obtained from laboratory and field tests. The developed soil moisture prediction methodology, which is based on the laboratory and field data and the results of the simulations carried out in HYDRUS-1D, is presented in chapter 5. Chapter 6 presents the conclusions and recommendations for implementation reached from the findings of this study and discusses topics for further research.

2. LITERATURE REVIEW

Soil moisture prediction, especially near the ground surface (within a depth of 5 ft.), is of significant importance for agricultural scientists and hydrologists. It allows for an assessment of the water available for root uptake and agricultural planning. For the purpose of assessing constructability of a soil at a site, the zone of interest is also within this shallow depth range of approximately 3–5 feet. This is because the loads due to construction activities are carried mostly by the soil mass within this depth (Holtz et al., 2010; Rodriguez et al., 1988). Therefore, the focus of this research is on the estimation of the soil water content of this top layer and its change throughout the seasons.

2.1 Soil Moisture Prediction

Water enters the soil mass due to precipitation and leaves the zone of interest due to surface run off, evapotranspiration and deep drainage, as shown in Figure 2.1. Our goals are to predict how much water remains inside the zone of interest (at different depths) as a function of time and how the water is distributed in the zone of interest. This allows us to assess changes in the strength and stiffness characteristics of the soil (due to changes in water content) and to make recommendations regarding the constructability of soils in different seasons.

Historically, soil water content has been obtained from direct methods (by making gravimetric and volumetric moisture measurements) or indirect methods (by using soil moisture probes, remote sensing and

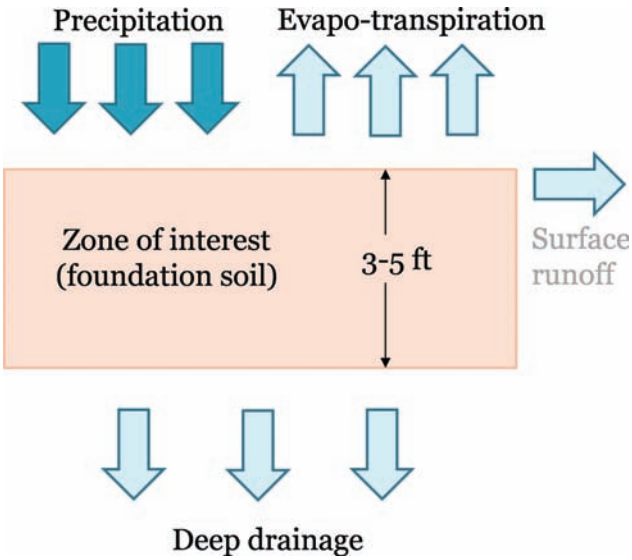

Figure 2.1 Water balance and zone of interest in a soil profile.

water-balance models) (Gorthi, 2011). In one of the most common forms of the indirect approach, soil moisture probes are inserted into the soil mass at the desired depths to measure soil water content over time (Naylor, Letsinger, Ficklin, Ellet, & Olyphant, 2014). Another form of indirect approach that has gained considerable support in industrial and academic research is the use of remote sensing equipment for the estimation of soil moisture (Hu, Islam, & Cheng, 1997; Njoku & Entekhabi, 1996). This method relies on the concept that the magnitude of reflected or emitted electromagnetic (most commonly optical, infrared and microwave) radiation is affected by the near-surface *in-situ* soil moisture. The electromagnetic waves, recorded as signals via satellites and sensors mounted on aircrafts, can subsequently be converted to soil moisture values using empirical models. One of the major shortcoming of this approach from the perspective of the current research project is that commercial remote sensing equipment has only been successful in obtaining the *in-situ* soil moisture accurately up to a depth of 5–10 cm from the ground surface (Nichols, Zhang, & Ahmad, 2011). In addition to the shallow depth of penetration, these methods tend to be cost prohibitive and time consuming. Due to the cost associated with the indirect and direct approaches of soil moisture measurement, researchers have often resorted to the use of soil-moisture-flow simulations to estimate and effectively obtain *in situ* soil moisture profiles instead of relying on the above methods to obtain site-specific maps (Gorthi, 2011).

Soil moisture flow simulations can be carried out using commercially available software or in-house developed software to estimate the water content of soil with depth over time (Chen, Willgoose, & Saco, 2014). Water-balance models that rely on the measurement of precipitation run off and other hydrological parameters to estimate the amount of water that the soil retains can be utilized. While the water-balance model approach is useful for agricultural purposes, there is no straightforward way of estimating the distribution of water in the soil mass for construction purposes.

Water content estimation using the indirect approach, while more accurate, is not always cost effective. It requires the calibration and installation of soil moisture probes at several locations in a site, data acquisition and transfer, maintenance and protection of the probes against vandalism and upkeep of expensive equipment. This method may be suitable for long-term water content monitoring (i.e., in farmlands and forest conservation areas), but for the purpose of monitoring the water content of soils in transient earthwork and assessing soil constructability, the soil-moisture-flow simulation method may be more preferable since it is less expensive. Less expensive also implies some loss of accuracy, hence a probabilistic approach should be considered when using the simulation path.

The approach of soil moisture flow simulation using HYDRUS-1D seems to be more suited for the purpose of soil moisture prediction with respect to transient earthwork activities (with the simulations, it is possible to obtain soil moisture profiles at any time). Soils are often unsaturated and the rate of flow of moisture through them is affected by the degree of saturation. To simulate the flow of soil moisture through an unsaturated soil mass, the equation proposed by Richards (1931) is widely used. Soil moisture flow simulations are commonly done using software such as HYDRUS-1D, which relies on solving Richard's 1D unsaturated soil moisture flow equation to simulate water flow:

$$\frac{\partial \theta}{\partial t} = \frac{\partial}{\partial z}\left[K\frac{\partial}{\partial z}(h+z)\right] - S \tag{2.1}$$

where θ is the volumetric water content of the soil (volume of water per unit volume of soil mass), h is the soil matric head (matric potential per unit weight of water), K is the hydraulic conductivity (which is a function of the degree of saturation), t is the time, S is the sink term used to account for root water uptake, and z is the elevation above an assumed datum. The underlying concepts behind Equation 2.1 will be discussed in the following section.

2.2 Unsaturated Flow in Soils

Equation 2.1 is based on the concept of the soil matric potential h. To describe the workings of this equation, let's consider the mechanism of flow of pore fluid through a soil mass. The energy of an element of the pore fluid per unit weight of fluid is defined as the total hydraulic head at the location of the element. Water tends to flow from a location of higher total head to a location of lower total head. The total hydraulic head h_{total} in the case of pore water (pore fluid) in the soil mass consists of three main components:

$$h_{total} = h_{elevation} + h_{pressure} + h_{velocity} \tag{2.2}$$

where $h_{elevation}$ is the elevation head, $h_{pressure}$ is the pressure head and $h_{velocity}$ is the velocity head of the pore water. Equation 2.2 can be rewritten as:

$$h_{total} = z + \frac{u_w}{\rho \times g} + \frac{v^2}{2 \times g} \tag{2.3}$$

where z is the elevation of water above an assumed datum, u_w is the pore water pressure, ρ is the mass density of water, g is the acceleration of gravity (9.81 m/s^2) and v is the average flow rate of water (m^3/s/m^2). For saturated soils, with relatively slow rate of flow, the magnitude of the total head is dominated by the elevation head (height of water above a datum) and the pressure head (pressure of pore fluid per unit weight of pore fluid). The velocity head is small enough and can be neglected for all practical purposes.

In the context of unsaturated soils, Equation 2.2 is found to be adequate in describing the flow of pore water, the only change from the saturated case is that the pressure head becomes negative (Fredlund, Rahardjo, & Fredlund, 2012c). The reason behind a negative pressure head is that the pore water pressure in an unsaturated soil

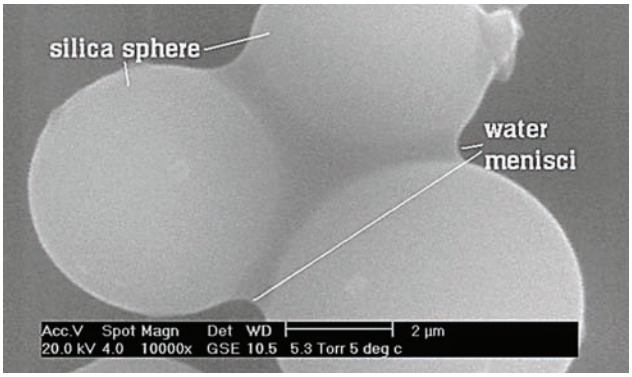

Figure 2.2 ESEM micrographs of silica spheres showing water-air-water interfaces and menisci (after Lourenço et al., 2008).

mass is always below the atmospheric pressure due to development of air-water interfaces and water menisci (Blight, 2013; Fredlund, Rahardjo, & Fredlund, 2012b; Lourenço et al., 2008), as shown schematically in Figure 1.1 and via Environmental Scanning Electron Microscope (ESEM) micrographs in Figure 2.2. The concave curvature of the pore water in Figure 1.1 and Figure 2.2 indicates that the pore-water pressure is lower than the pore-air pressure. In engineering practice, the negative of the pore-water pressure (u_w) in unsaturated soils is called matric suction (s) and is defined as:

$$s = -u_w \tag{2.4}$$

Therefore, Equation 2.3 can be re-written for unsaturated soils as:

$$h_{total} = z + \frac{u_w}{\rho \times g} = z + \frac{-s}{\rho \times g} \tag{2.5}$$

where the second term $\left(\frac{-s}{\rho \times g}\right)$ is the matric head term h in Equation 2.1.

An important relationship that describes the hydraulic behavior of unsaturated soils is that between the degree of saturation (or volumetric water content) of the soil and the matric suction retained in it. A Soil-Water Characteristic Curve (SWCC) or Soil-Water Retention Curve (SWRC) is a relationship between the degree of saturation (or volumetric water content) vs. suction. Figure 2.3 shows typical SWCCs for pure sand, silt and clay soils. As can be observed from Figure 2.3, the degree of saturation (volumetric water content) of sand drops fairly quickly as the suction retained in the soil mass increases, i.e., as the soil dries out, the pore-water pressure becomes more negative and the value of matric suction increases. For silts and clays, significantly higher suction needs to develop in the soil before the degree of saturation changes significantly. Figure 2.3 shows that the SWCCs for all three soil types can be divided into three distinct regions: (i) the initial flat region where the degree of saturation does not change considerably as suction increases (called the air-entry region), (ii) the middle region where a significant drop

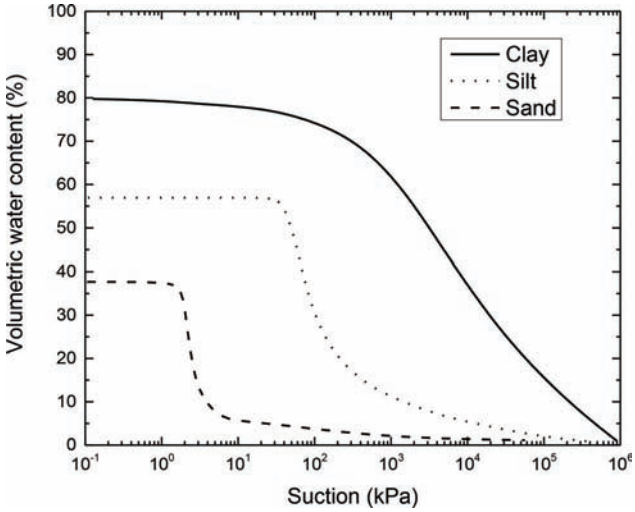

Figure 2.3 Soil Water Characteristic Curve (SWCC) for typical sand, silt and clay soils (after Fredlund et al., 2012c).

in saturation is observed as suction increases (called the capillary-water region), and (iii) the tail end of the SWCC where the saturation does not decrease significantly even as the suction reaches very high values (called the residual-water region). When the soil is in the air-entry region, pore water fills all pores of the soil mass, even though it may have pressure below the atmospheric pressure. In the capillary-water region, the water forms thin films around the soil particles, and the particle and pore water arrangement is similar to that seen in Figure 1.1 and Figure 2.2. In the residual-water region, the water in the soil is mostly in the form of adsorbed water on the surface of the soil particles.

The hydraulic conductivity of a soil depends on the properties of the fluid in the pores, the index properties and the void ratio e (or density) of the soil. Clayey soils have low saturated hydraulic conductivity K_s, while sandy soils have comparatively high K_s. Densely packed soils have lower K_s than loosely packed soils. In the case of unsaturated soils, the hydraulic conductivity is also affected by the amount of water that is present in the soil mass for flow to occur, i.e., the degree of saturation of the soil (Fredlund et al., 2012c).

Experiments conducted by Childs and Collis-George (1950) have shown that the hydraulic conductivity of a porous medium depends significantly on its degree of saturation. Following the initial work by Childs and Collis-George (1950), research done on the relative influence of void ratio and saturation on the hydraulic conductivity of soils indicates that the influence of void ratio on the hydraulic conductivity of a soil is less in comparison to that of the degree of saturation (Blight, 2013; Fredlund et al., 2012d).

As an illustration, Figure 2.4 (a) shows how the hydraulic conductivity of two soils changes with suction. Suction is related to the degree of saturation via the SWCC (with the degree of saturation known, the matric suction can be obtained from the SWCC, which, in turn, can then be used to estimate the unsaturated hydraulic

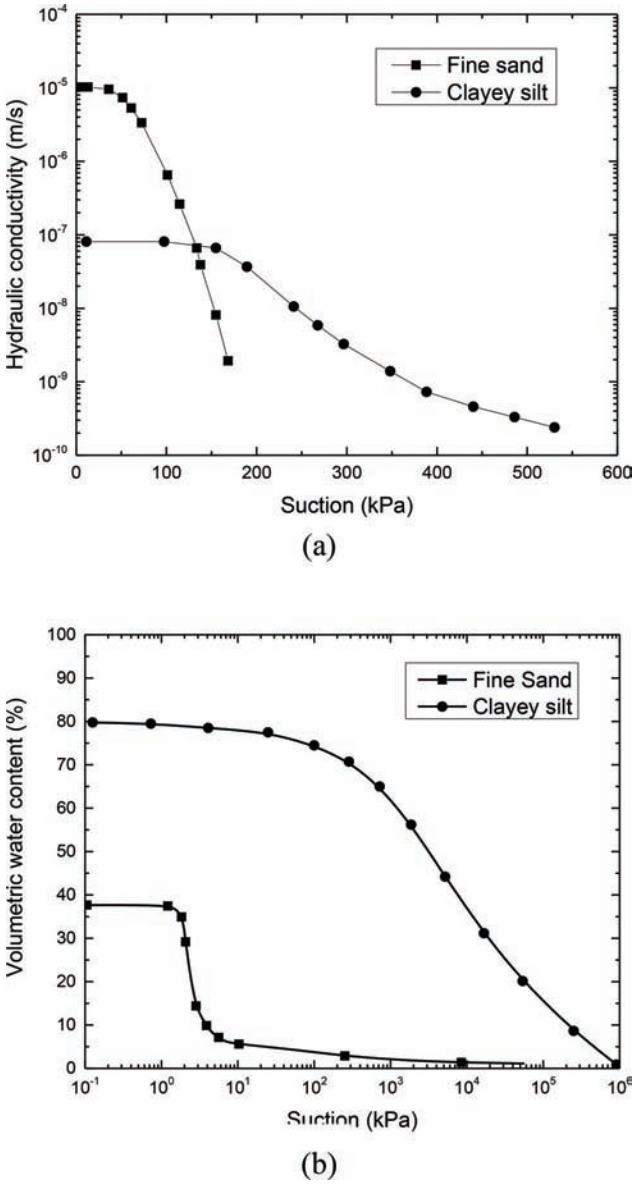

Figure 2.4 Change in (a) hydraulic conductivity and (b) volumetric water content with the suction retained in fine sand and clayey silt soils (after Fredlund et al., 2012a).

conductivity of the soil). Comparing Figure 2.4 (a) with the SWCC in Figure 2.4 (b), we can observe that as suction increases beyond a certain value, the degree of saturation of the soil starts to drop significantly (this is observed right at the end of the air-entry region, as described in Figure 2.3). It is after the air-entry value of suction that we observe a corresponding steep change in the hydraulic conductivity of the soil. This is attributed to the change in degree of saturation, and the resulting lack of availability of water and connected pore water in the soil structure. This trend of change in hydraulic conductivity with suction, similar to that observed for the SWCC, can be observed in both sands and clays and is closely related to the air-entry value of suction.

The most commonly used way of estimating the hydraulic conductivity of an unsaturated soil, also used in HYDRUS-1D, is based on the method proposed by van Genuchten (1980). This method relies on the estimation of fitting parameters for the SWCC along with the measured saturated hydraulic conductivity to obtain the unsaturated hydraulic conductivity of the soil. The equation used to fit the SWCC data by van Genuchten (1980) is:

$$\theta = \theta(s) = \theta_r + \frac{\theta_s - \theta_r}{[1 + (\alpha s)^n]^m} \tag{2.6}$$

where $\theta(s)$ is the volumetric water content of the soil mass at a given suction s, θ_r is the residual volumetric water content of the soil mass (i.e., the volumetric water content at the start of the residual water region in the SWCC), θ_s is the saturated volumetric water content of the soil mass, and α, n and m are fitting parameters.

Using the fitting parameters from the SWCC curve, the unsaturated hydraulic conductivity of the soil is computed using the equation proposed by van Genuchten (1980):

$$K(\theta_e) = K_s \theta_e^{0.5} \left[1 - \left(1 - \theta_e^{1/m}\right)^m\right]^2 \tag{2.7}$$

where K_s is the saturated hydraulic conductivity of the soil and θ_e is the non-dimensional effective volumetric water content given by:

$$\theta_e = \frac{\theta - \theta_r}{\theta_s - \theta_r} \tag{2.8}$$

where θ is the volumetric water content at which the hydraulic conductivity is to be estimated.

2.3 Estimation of Unsaturated Soil Hydraulic Conductivity from SWCC

The unsaturated hydraulic conductivity of a soil is required as input in unsaturated flow simulations. Therefore, it is important to fully understand the process through which the unsaturated hydraulic conductivity can be estimated from the SWCC of a soil. Consider as an example the SWCC presented in Figure 2.5. The SWCC was obtained from an undisturbed soil sample collected from a depth of 3 feet at a test site located in Muncie, Indiana (google maps location). The index and hydraulic properties of the soil are presented in Table 2.1. As described in Table 2.1, the soil is a low plasticity clay, classified as A-7-6 soil according to the AASHTO soil classification system. The SWCC of this soil was obtained using the Decagon-HYPROP device, which is a tensiometer-based device commonly used in geotechnical engineering laboratories to obtain the SWCCs of soils.

The van Genuchten (1980) equation (Equation 2.6) was used to fit the SWCC data of Figure 2.5. From the regression analysis of the SWCC data collected from the HYPROP, the van Genuchten (1980) SWCC fitting parameters (θ_s, θ_r, α, n and m) were obtained.

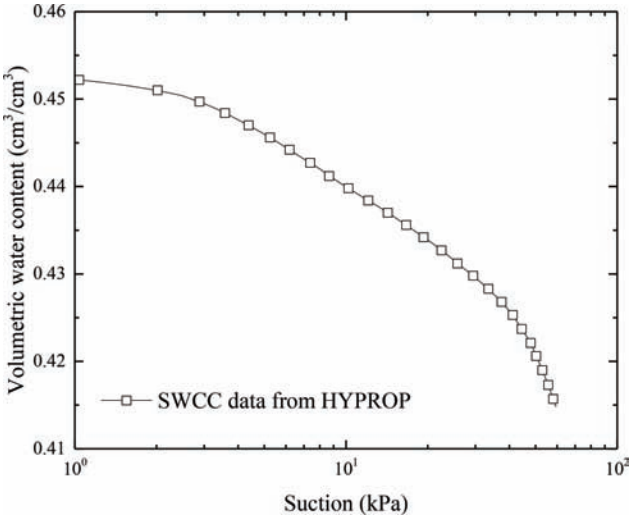

Figure 2.5 Soil-water characteristic curve for the test site located in Muncie, Indiana obtained from Decagon HYPROP.

The values of these parameters are given in Table 2.1 under the heading of hydraulic parameters. The SWCC data fitting parameters were used in Equation 2.7 to obtain the hydraulic conductivity vs. matric suction curve shown in Figure 2.6. In addition to the estimated hydraulic conductivity vs. matric suction curve, also plotted in Figure 2.6 is the hydraulic conductivity measured by the Decagon HYPROP using the evaporation method (Schindler, Durner, von Unold, & Müller, 2010) for suction values of up to 100 kPa. As you can see, good agreement is observed between the predicted and measured data.

2.4 Methods of Generating an SWCC

The SWCC of a soil can be obtained in the laboratory by measuring suction and the corresponding measure of soil water content (degree of saturation, gravimetric water content and volumetric water content) simultaneously for the entire range of saturation (from saturated to very dry conditions). SWCCs can either be wetting-SWCCs (suction is measured as a soil sample is wetted from a completely dry state to a completely saturated state) or drying-SWCCs (suction is measured as a soil sample is dried out from a slurry to a completely dry state). During either of these wetting or drying processes, the suction and degree of saturation are measured to generate the SWCCs. The drying and wetting SWCCs are different from each other due to the phenomenon of hydraulic hysteresis exhibited by soils (Fredlund, Rahardjo, & Fredlund, 2012a). For most applications, including the simulations in this report, the drying-SWCCs are used to obtain estimates of the van Genuchten (1980) unsaturated hydraulic parameters. However, hydraulic hysteresis should be considered to get more accurate predictions.

There are four different types of devices that can be used to obtain drying-SWCCs in the laboratory.

TABLE 2.1
Index and hydraulic properties of soil samples collected from Muncie (depth of 3 feet from surface).

Location	Classification		Sand (%)	Silt (%)	Clay (%)	Liquid Limit (%)	Plastic Limit (%)	Plasticity Index (%)	Hydraulic Fitting Parameters*					
	USCS	AASHTO							α (1/cm)	n	m	θr (cm^3/cm^3)	θs (cm^3/cm^3)	Ks (cm/day)
Muncie, Indiana	CL	A-7-6	50	27.5	22.5	47	15	32	$9.7 \times 10\text{-}4$	1.226	0.227	0.000	0.442	0.0214

*Obtained from curve fitting results from Decagon HYPROP.

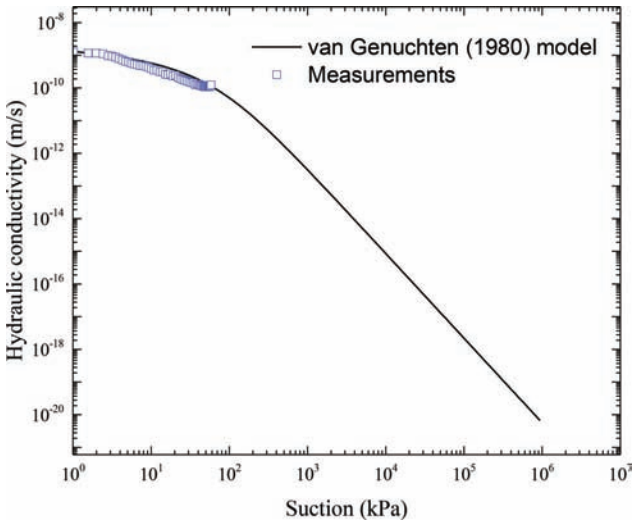

Figure 2.6 Unsaturated hydraulic conductivity versus suction curves obtained from measurements using the Decagon HYPROP and the van Genuchten (1980) model.

These are: (i) hanging column-based devices (optimal matric suction range of 0–80 kPa), (ii) pressure plate devices (with volumetric or gravimetric measurements) (optimal matric suction range of 0–1500 kPa), (iii) chilled-mirror hygrometer-based devices (optimal matric suction range of 0.5–00 MPa) and (iv) tensiometer-based devices (optimal matric suction range of 0–100 kPa).

2.4.1 Hanging Column-Based Devices

A hanging column-based device consists of a water-saturated, highly permeable porous ceramic plate connected to a water column and a reservoir open to the atmosphere. A hanging column-based apparatus is shown in Figure 2.7. A saturated sample of soil is placed in a metallic ring, which is placed on top of the flat ceramic plate when the height of water in the reservoir is the same as the top surface of the ceramic plate. The reservoir is subsequently lowered to a new height, a certain distance below the top of the ceramic plate. Due to a difference in elevation head, the water flows from the soil sample through the ceramic plate to the reservoir until the matric suction generated in the soil offsets the elevation head generated due to the difference in soil and reservoir water height. When equilibrium is restored, and no more water flow is occurring from the soil sample to the reservoir, the soil sample is removed and gravimetric or volumetric water content is measured. It is possible to perform the hanging column test in a wetting mode or a drying mode and thus obtain the wetting and drying SWCCs, respectively.

2.4.2 Pressure Plate Devices

A pressure plate type of device uses the axis-translation technique (Fredlund et al., 2012a) to obtain the SWCC. It consists of an airtight chamber enclosing a porous

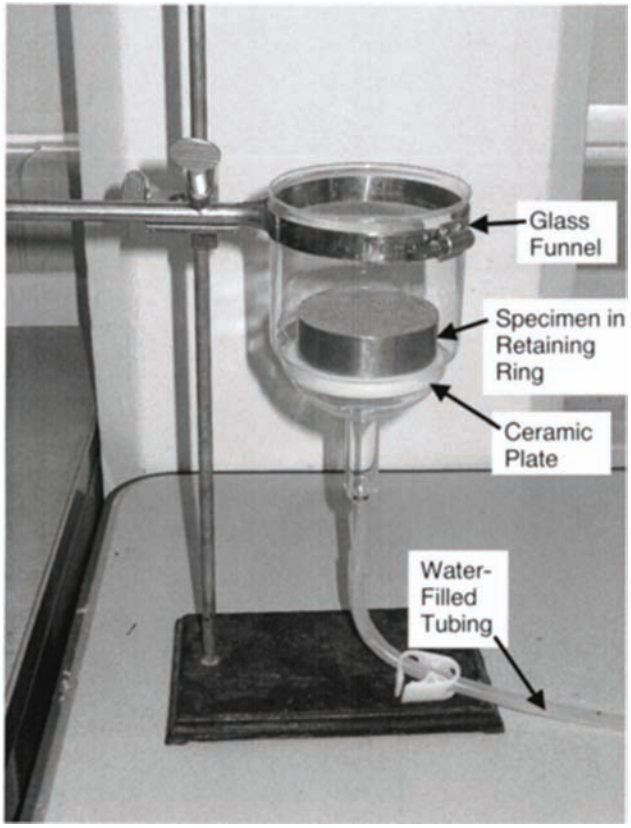

Figure 2.7 Hanging-column apparatus (ASTM D6836, 2008).

ceramic plate, the underside of which is connected to two volume change tubes that are open to the atmosphere, as shown in Figure 2.8. Saturated soil samples are packed into rings, which are then placed on top of the ceramic stone in the airtight chamber. The chamber is pressurized to produce an increase in the pore-air pressure, resulting in water flowing out from the soil pores through the ceramic stone and into the volume change tubes (which have water at atmospheric pressure). The increase in air pressure, while keeping the water pressure constant, results in an increase in the matric suction of the soil. At equilibrium conditions, flow through the tube ceases. Water content measurements are obtained by measuring the amount of water drained from the soil sample. The process is repeated with different increments in air pressure to obtain the SWCC for the entire suction range.

2.4.3 Chilled-Mirror Hygrometer Based Devices

In this type of instrument, a soil sample is placed in a sealed chamber. At equilibrium, the water potential of the air in the sealed chamber is the same as the water potential of the soil sample. The water potential of the sample is obtained from the relative humidity of the air inside the chamber by using Kelvin's equation.

WP4 is a commercially available instrument, which uses the chilled-mirror dew point technique to measure the water potential of a soil sample. The device consists of a sealed chamber with a photoelectric cell and an

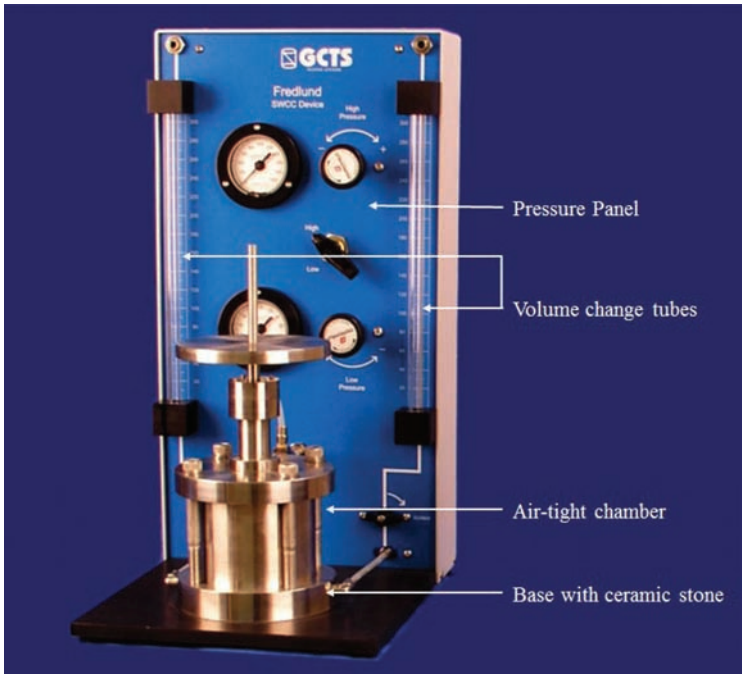

Figure 2.8 GCTS pressure plate device (courtesy GCTS).

infrared thermometer. A soil sample is placed in a stainless steel or plastic container, which is inserted into a temperature-controlled chamber. The chamber is closed, and the soil sample is thermodynamically equilibrated with the chamber environment. A cooling system is used to reduce the temperature on the surface of a mirror to the dew point temperature. A photoelectric cell detects the first sign of condensation on the mirror. The temperature at which moisture appears on the mirror corresponds to the dew point. The dew point temperature is measured using a thermocouple, and an infrared thermometer is used to measure the temperature of the chamber (it is assumed to be the same as the temperature of the soil sample at equilibrium conditions). The relative humidity is calculated from dew point temperature and actual temperature of the soil sample. Kelvin's equation is then used to calculate the total suction of the soil sample from the relative humidity. The process is repeated for soil samples at different degrees of saturation to obtain the entire SWCC. A commercially available chilled mirror potentiometer is shown in Figure 2.9.

Figure 2.9 WP4 chilled-mirror water potentiometer (courtesy of Decagon Devices http://www.decagon.com/en/).

2.4.4 Tensiometer-Based Devices

Tensiometers are often used to measure the negative pore-water pressure (soil suction) retained in soil. Tensiometer-based devices rely on continuous measurement of soil suction and soil sample weight as the soil dries out to generate the SWCCs. Soil suction is obtained from a direct measurement of negative pore water pressure using tensiometers, while the degree of saturation is obtained from loss of weight recorded as the soil dries out.

In the present research, a commercially available tensiometer-based device (Decagon-HYPROP), as shown in Figure 2.10, was used to obtain the SWCCs of the soils tested. The HYPROP device consists of a sensor base where two tensiometers are installed at two different depths. An undisturbed soil sample is placed inside a sampling ring and saturated by keeping it partially submerged in a trough of water for 24 hours. Two small holes are bored in the soil sample to fit the tensiometers at two different depths. The upper side of the soil sample is kept open to the atmosphere so that soil moisture can evaporate. The entire test setup (sensor base, tensiometer and soil sample in the sampling ring) is placed on a high precision weighing scale, which measures the change of the soil sample's mass due to evaporation.

The tensiometers measure the suction in the soil at two different depths as the soil dries out. The suction measurements from the two tensiometers are used to calculate the average suction in the soil sample. The corresponding degree of saturation is obtained from the

Figure 2.10 Decagon HYPROP device for tensiometer measurements.

initial sample water content and the loss of sample mass (due to water evaporation) recorded by the weighing scale. The average suction and the degree of saturation in the soil sample are measured at different times as the soil sample dries out; these measurements are then used to obtain the complete SWCC. In addition to the SWCC, the suction measured at the two different depths is used to calculate the hydraulic gradient in the soil. The hydraulic gradient and change in degree of saturation with time are used to get an estimate of the unsaturated hydraulic conductivity of the soil at different degrees of saturation (or volumetric water content). The details of these calculation process are described next.

At different points of time t^i the following are measured: (1) suction in the soil sample at the depths h_1^i and h_2^i of the two tensiometers and (2) the weight of the soil sample. The initial water content of the soil sample is estimated by adding up the total loss of water due to evaporation and the loss of water by oven drying of the soil sample after conclusion of the test. The volumetric water content $\overline{\theta}$, derived from the initial water content and loss of sample mass, and the average suction $\overline{s}$ give a discrete value of $\overline{\theta}(\overline{s})$ for the SWCC function at any time t^i.

For the calculation of the hydraulic conductivity function, it is assumed that, between two time steps t^{i-1} and t^i, the rate q^i of flow of water through a horizontal cross section at a point situated exactly between the two tensiometers in the soil sample is given by:

$$q^i = \frac{1}{2}\frac{\Delta V^i}{\Delta t^i A} \tag{2.9}$$

where ΔV^i is the water loss in cm^3 determined from weight changes, $\Delta t^i = t^i - t^{i-1}$ is the time interval considered and A is the area of the horizontal cross section of the soil sample in cm^2. The unsaturated hydraulic conductivity K^i is estimated using Darcy's equation:

$$K^i\left(\overline{\overline{h^i}}\right) = -\frac{q^i}{\Delta h^i/\Delta z + 1} \tag{2.10}$$

$$\overline{\overline{h^i}} = \frac{h_1^{i-1} + h_2^{i-1} + h_1^i + h_2^i}{4} \tag{2.11}$$

$$\Delta h^i = \frac{\left(h_2^{i-1} - h_1^{i-1}\right) + \left(h_2^i - h_1^i\right)}{2} \tag{2.12}$$

where $\overline{\overline{h^i}}$ is the medial suction head between two measurement points at the time step i, h_1 and h_2 are the suction heads at the two tensiometers measured at the i and i-1 time steps, Δh^i is the medial difference of the suction head of the two tensiometers and Δz is the distance between them.

The range of measurement of soil suction depends on the capacity of the tensiometers. The SWCC obtained using the HYPROP device is fitted by a nonlinear optimization function using a program called HYPROP-FIT. HYPROP-FIT provides SWCC functions that fit five basic types of water retention models. The five basic types of water retention models are: (1) Brooks and Corey, (2) Fredlund-Xing, (3) Kosugi, (4) van Genuchten with a constraint on the parameter m appearing in Equation 2.6, van Genuchten without a constraint on the parameter m. The curve fitting process allows for extrapolation of the SWCC based on the measured suction values to higher values of suction than measured.

3. RESEARCH METHODOLOGY

HYDRUS-1D, a free soil moisture flow software, was used to simulate unsaturated soil moisture flow for typical soil profiles of 92 counties in the state of Indiana. Input data for the simulations were obtained from various government agencies, such as the United States Department of Agriculture (USDA), the Department of Natural Resources (DNR), the Indiana Geological Survey (IGS) and Purdue State Climate (Iclimate). In order to validate the methodology used in this research, results from the soil moisture simulations were compared to measured soil moisture data collected for a period of 3 years from six IGS test sites (in four counties) located across Indiana.

Since good agreement was obtained between predicted and measured water content at these sites, the methodology was used to determine the *in situ* soil water content profiles for all the counties in Indiana using 10 years of weather and groundwater table data as input. The ten-year soil moisture simulations were superimposed to get a range for the *in situ* soil water content for each county. Figure 3.1 shows an overview of the methodology.

3.1 Soil Moisture Prediction

Estimates of soil water content from water flow simulations require validation with field data. However, once a methodology is carefully validated, it can be used to predict soil water content with minimal effort and recurring costs. HYDRUS-1D is one of the most commonly used free software for simulation of soil moisture flow (Chen et al., 2014; https://www.pc-progress.com/en/Default.aspx?hydrus-1d). HYDRUS-1D simulates water flow through the soil mass by solving Richard's (1931) 1D equation. Figure 3.2 shows the interface of the software.

The input data necessary to perform water flow simulations using HYDRUS-1D include:

1. Soil profile and layer properties:
   i. Index properties
   ii. Hydraulic properties
   iii. Unsaturated soil properties
2. Initial water content of the soil at a given time
3. Precipitation and weather records
4. Ground water table depth

Out of the input requirements, not all could be obtained directly, as the associated time requirement and fiscal cost of carrying out such an endeavor would be huge. For unsaturated hydraulic properties, a hierarchical approach was adopted, as outlined by Fredlund and Houston (2009), i.e., to obtain each input data, a combination of sources was used.

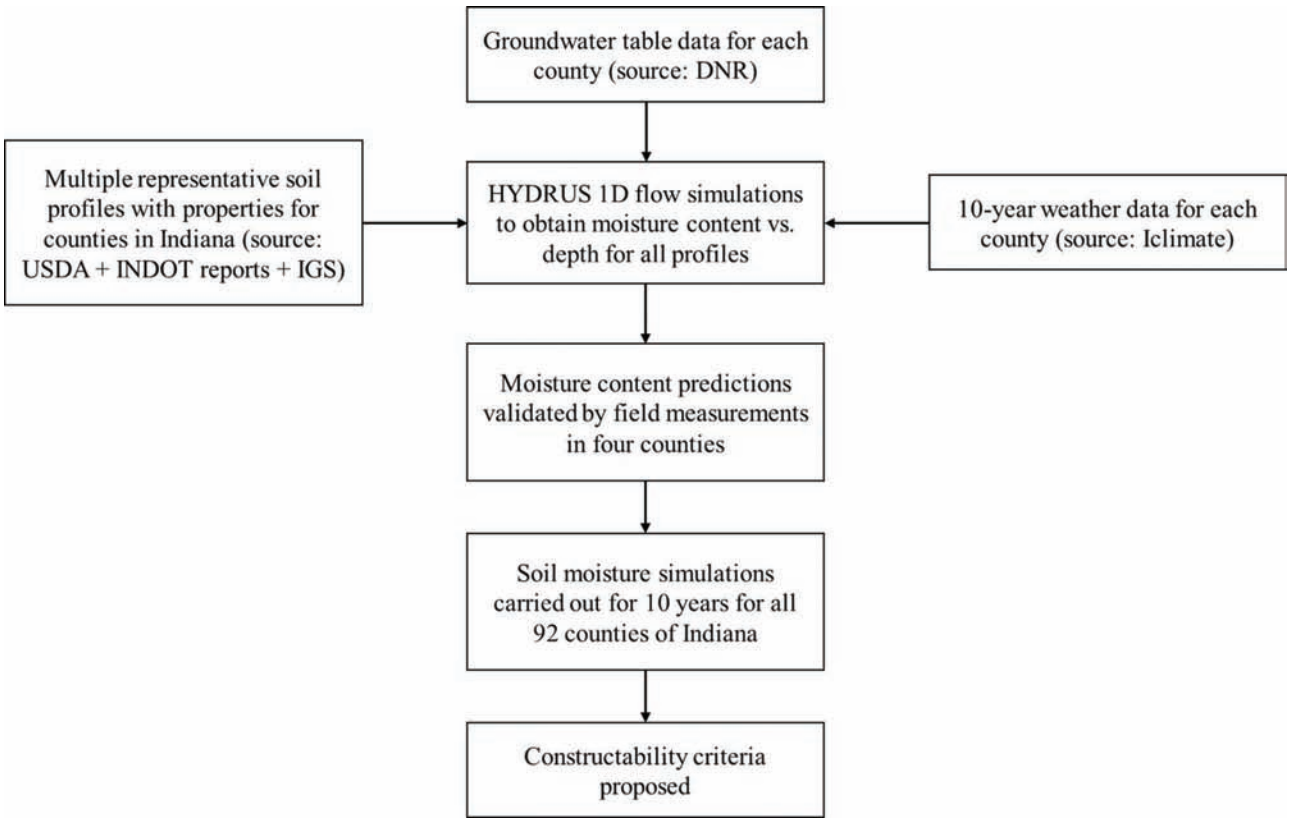

Figure 3.1 Research methodology outline.

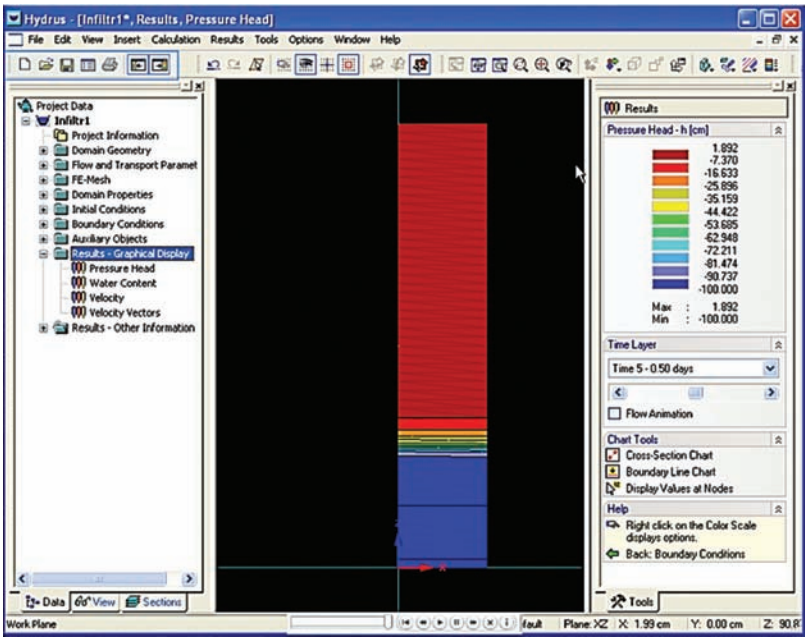

Figure 3.2 HYDRUS-1D interface.

3.1.1 Soil Properties and In Situ *Conditions*

Soil properties and *in situ* conditions were obtained from the following sources:

1. USDA's SSURGO database: The SSURGO (Soil Survey Geographic) database contains information about soil collected by the National Cooperative Soil Survey over the course of a century. The information was gathered by surveyors by reconnaissance and visual observation of soil layering. Soil samples were collected and tested to obtain basic soil classification indices (grain size distribution and plasticity limits) and *in situ* hydraulic properties (saturated hydraulic conductivity). SSURGO datasets consist of map and tabular data containing the different soil profiles and associated soil layer properties.
2. INDOT soil reports: Soil reports obtained from geotechnical site investigations from INDOT were also used as a source of soil properties and *in situ* conditions. These reports, while less broad in area covered than the SSURGO database, were more detailed and contained more soil index properties than the general SSURGO database.
3. IGS data: The data from the six IGS sites in Indiana also contained soil properties from laboratory tests (the IGS data were used to validate the soil moisture flow methodology proposed in this research). These IGS reports had more details on the soil hydraulic properties and unsaturated soil properties than either the SSURGO database or INDOT reports.

3.1.2 Initial Water Content

To carry out the soil moisture flow simulations, it is necessary to have an initial soil moisture condition. In the validation studies, initial soil moisture values were obtained from field measurements carried out by Naylor et al. (2014) for the 6 IGS test sites. However, for the 10-year flow simulations, the soil profile was assumed to be initially at field capacity (i.e., at the maximum water content that a soil layer can hold under free draining conditions when flow is occurring only due to gravity). HYDRUS-1D (https://www.pc-progress.com/en/Default.aspx?hydrus-1d) has a built-in algorithm that estimates field capacity of soil layers based on the USDA textural classification of soil.

3.1.3 Weather Data

To carry out soil moisture flow simulations in HYDRUS-1D, the following weather data parameters were needed:

1. Precipitation
2. Solar radiation
3. Wind speed
4. Temperature
5. Relative humidity

Obtaining all the above data accurately for each location in Indiana was not possible. Therefore, for the purpose of this research, the state of Indiana was divided into 6 weather regions, as shown in Figure 3.3. The division was based on the proximity of the counties from one of the six weather stations marked in Figure 3.3 that had reliable weather data with all of the five parameters listed above for an extended period of at least 10 years. The six weather stations chosen are monitored by the Indiana State Climate Office and can be reliably assumed to be representative of the region assigned to them.

3.1.4 Groundwater Table Data

Ground water table data were obtained from the Department of Natural Resources (DNR) for the state

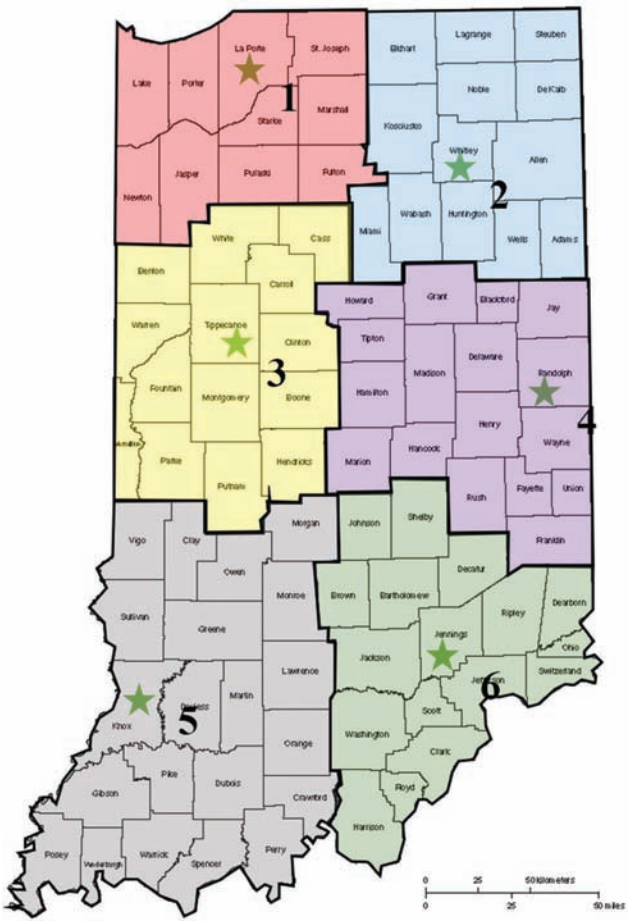

Figure 3.3 Six weather regions for the state of Indiana.

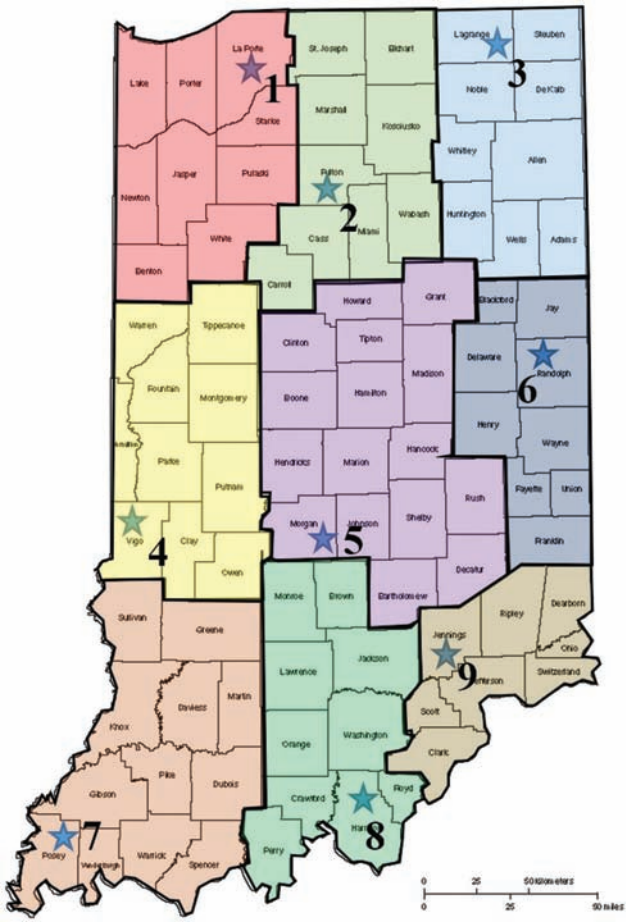

Figure 3.4 Climatic regions for state of Indiana (DNR).

of Indiana. DNR divides the state of Indiana into nine climatic regions based on the similarity of the ground water conditions in these regions, as shown in Figure 3.4. Each of these 9 regions is represented by a single constantly monitored well within each region which is marked by a star on the state map in Figure 3.4.

Ground water table in these regions are in the form of confined aquifers or unconfined aquifers. The ground water level in unconfined aquifers is very close to the soil surface (as opposed to the ground water level in confined aquifers). For soil moisture simulations at shallow depths, the water level from unconfined aquifers was considered as the bottom boundary condition. For locations where the ground water level was far below the ground surface in confined aquifers, free drainage was considered as the bottom boundary condition.

3.1.5 HYDRUS-1D Simulations

Using the data from the sources cited previously, soil moisture flow simulations were carried out using HYDRUS-1D. The steps that needed to be followed to carry out soil water flow simulations in HYDRUS-1D are shown in Figure 3.5. The corresponding screenshots from the software are shown in Figure 3.6 through Figure 3.17. Simulations can be carried out in HYDRUS-1D for any extended period of time.

Figure 3.6 shows the new project screen of HYDRUS-1D where the project is named and saved. Once a project is started, the first information that needs to be provided to the software is the type of simulation that needs to be carried out, as shown in Figure 3.7. HYDRUS-1D can carry out simulations for vapor flow, heat transport, solute transport, root water uptake and CO_2 transport. For our application, we select water flow and root water uptake by pastures. After specifying the type of simulation to be run, the next information is the geometry of the soil profile. Figure 3.8 shows the input box for the soil profile geometry. After defining the soil profile geometry, the time increments and the start and end times of the simulation need to be specified, as shown in Figure 3.9. Figure 3.10 shows the input box for defining the print information and how to output the results. Figure 3.11 shows the input box for the iteration criteria for the simulations. In the input box shown in Figure 3.12, the user can choose the soil hydraulic model (the function used to fit the SWCC) and the method used to calculate the unsaturated hydraulic conductivity of the soil with change in degree of saturation. As described earlier, the van Genuchten (1980) model was selected for all the

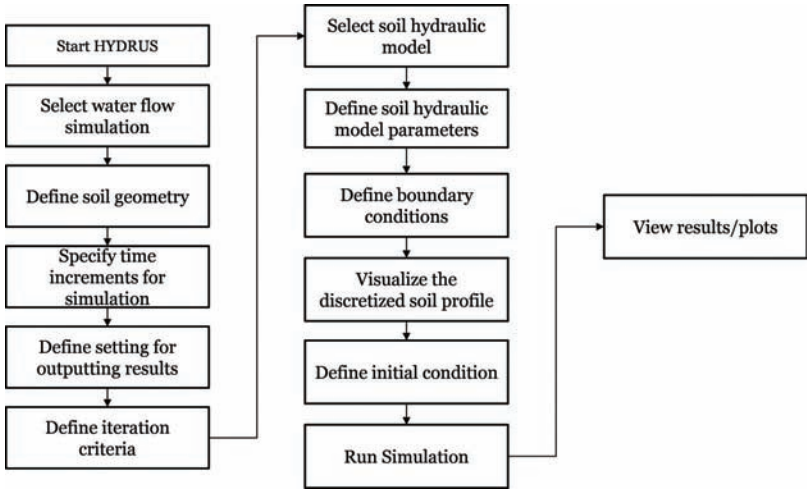

Figure 3.5 Procedure for soil moisture flow simulations using HYDRUS-1D.

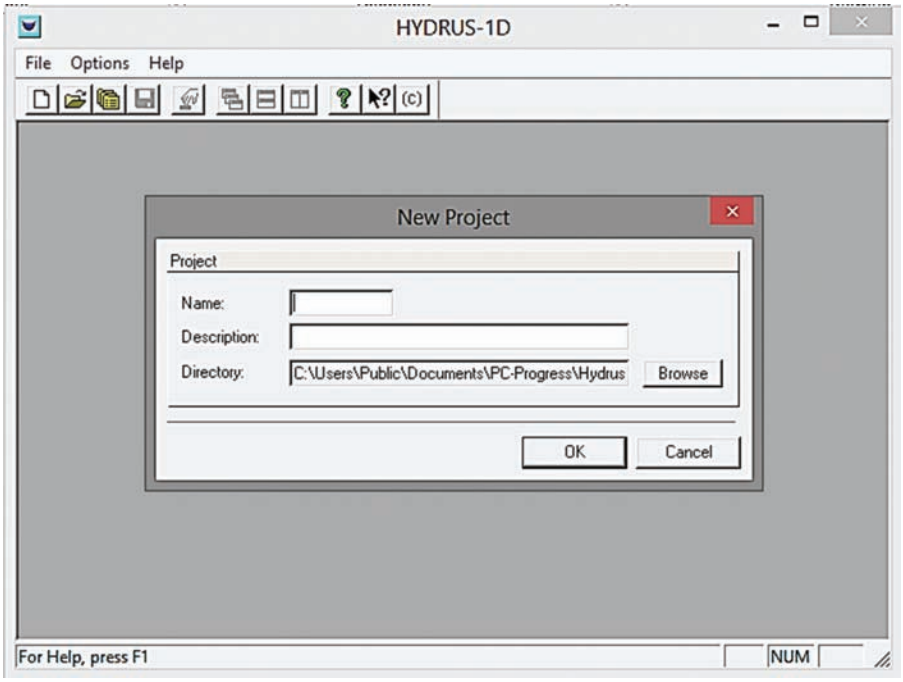

Figure 3.6 Start project screen HYDRUS.

simulations carried out in this study. The parameters for the van Genuchten (1980) model are inputted in the data box shown in Figure 3.13. The boundary conditions (rainfall events) are then inputted in the input box shown in Figure 3.14, and the initial condition values (initial water contents) are inputted in the data box shown in Figure 3.16. Finally, after all input data are provided to the software, simulations are run from the main interface, as shown in Figure 3.17.

3.2 Constructability Criteria of Natural Soils

In situ soil moisture profiles were obtained for typical soil profiles in each county in Indiana from the results of the HYDRUS-1D soil moisture simulations carried out following the procedure previously described. During construction activities, it is beneficial that the field soil moisture conditions be optimal. Since change orders have in the past been associated with high water content at the time of construction, in this research, constructability has been defined as the ease with which construction can be carried out in the field with reference to the *in situ* soil moisture conditions. With occurrence of high *in situ* soil moisture, it becomes difficult to bring construction equipment to the job site. In addition, wet subgrade soil needs to be dried out to reach appropriate *in situ* moisture specifications before compaction can get underway.

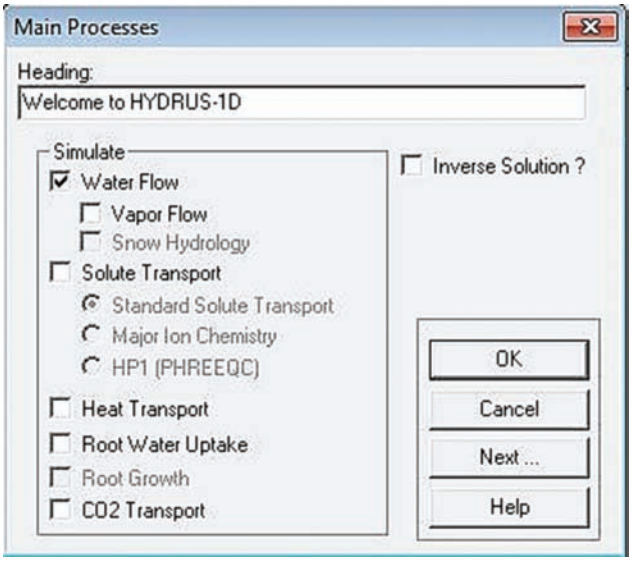

Figure 3.7 Select soil water flow simulation.

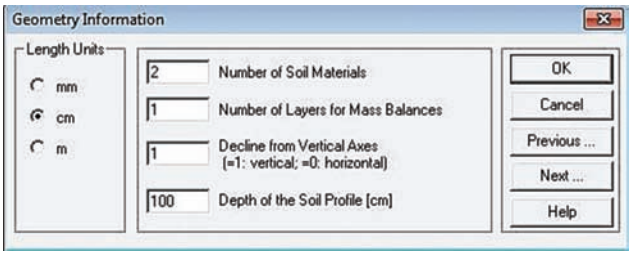

Figure 3.8 Define geometry of the soil profile.

To establish constructability criteria, the Optimum Water content (OMC) of a soil can be used as a reference. If the *in situ* soil water content is found to be higher than a predefined limit above the OMC of the soil, it can be tagged to have bad or poor constructability. Consider the example shown in Figure 3.18 where the predicted soil moisture from HYDRUS-1D is plotted alongside the measured soil moisture at a

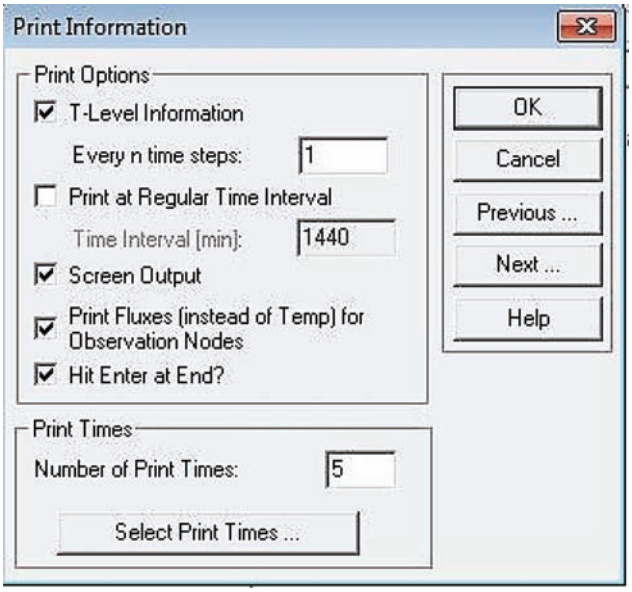

Figure 3.10 Define setting for outputting results.

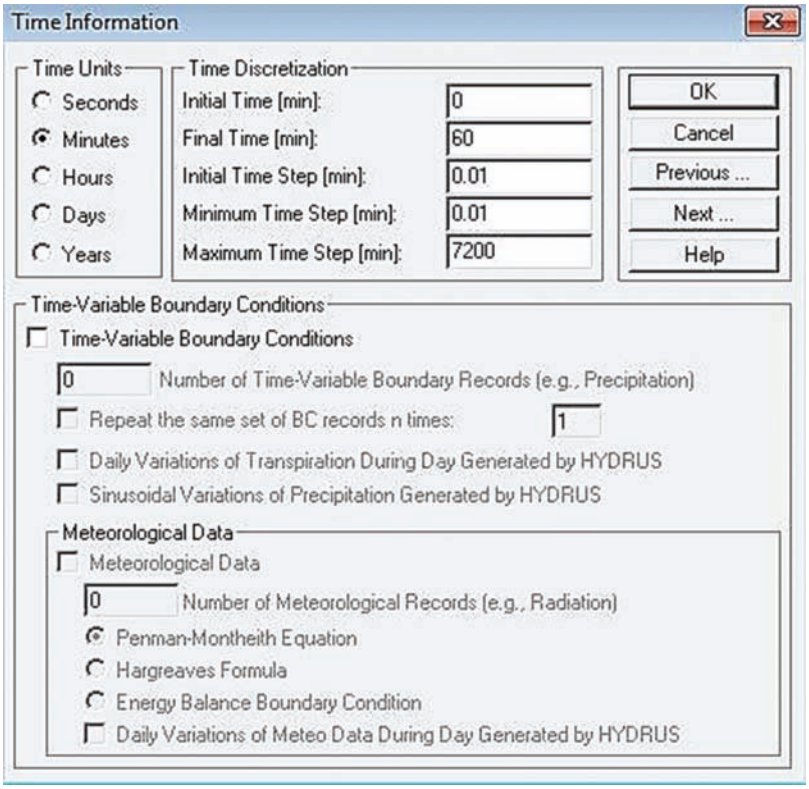

Figure 3.9 Specify time increments of simulation.

depth of 30 cm from the surface for a time period from January 2012 to October 2014 for a test site located in Shelbyville, Indiana (IGS test site). Also marked on the plot are the 80%, 90% and 100% saturation lines along with the OMC of the soil. The OMC and maximum dry density obtained from the standard Proctor test is shown in Figure 3.19, together with the INDOT family of curves. It can be observed that from January to May, the *in situ* soil water content at this location is consistently higher than the OMC by 4% (considering gravimetric water content). Under these conditions, the site would be considered to have poor constructability during this period and, accordingly, INDOT engineers would then have to make plans for remediation activities if construction were to take place during these months. INDOT specifications state that for proper soil compaction, the water content of a soil should not be greater than 2% above optimum for coarse-grained soils and 3% above optimum for fine-grained soils. Therefore, for fine-grained soils, a poor constructability rating could be assigned whenever the soil water content exceeds the OMC by 3% or more, but for coarse-grained soils, this limit is set lower at about 2% above the OMC.

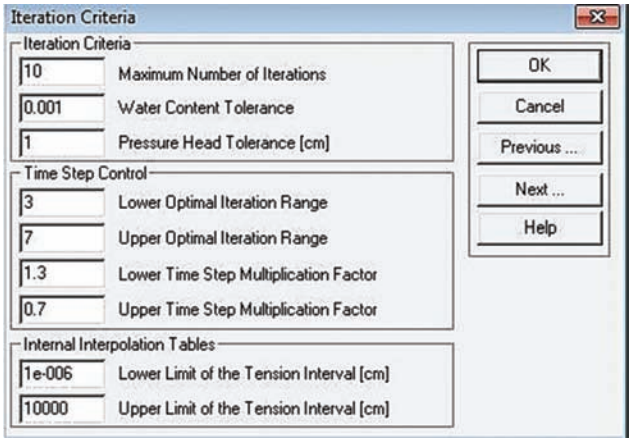

Figure 3.11 Define iteration criteria.

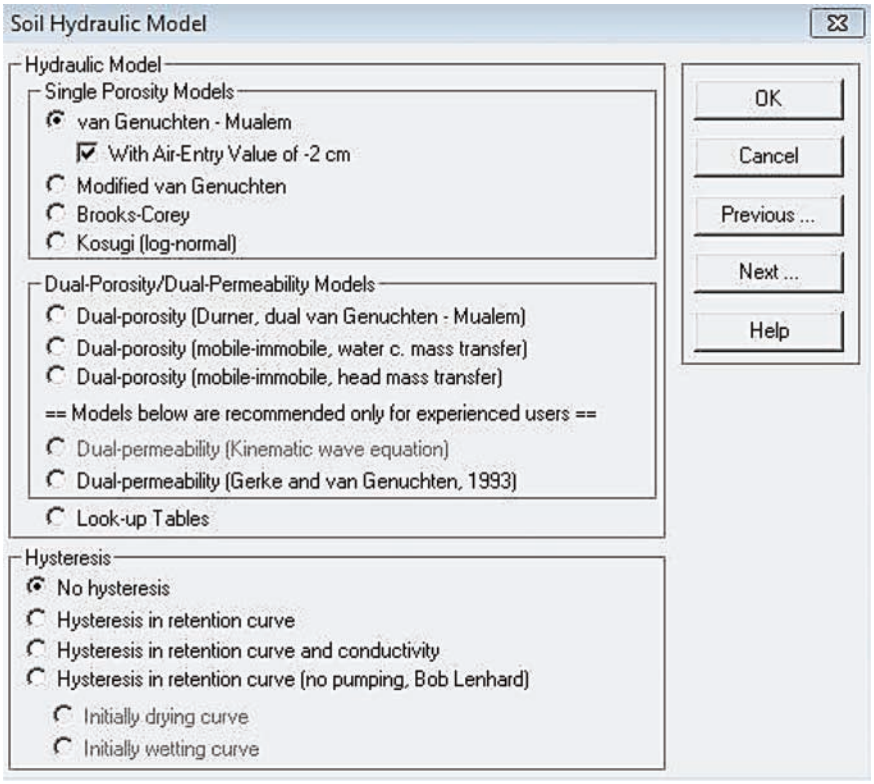

Figure 3.12 Choose soil hydraulic model.

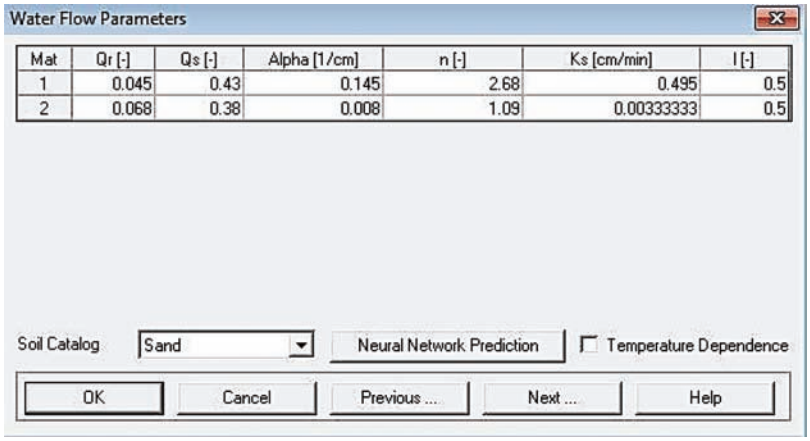

Figure 3.13 Define soil hydraulic model parameters.

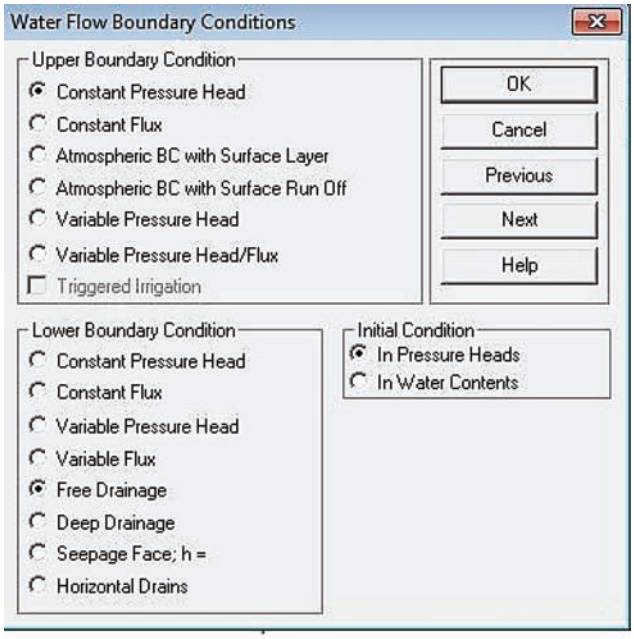

(a)

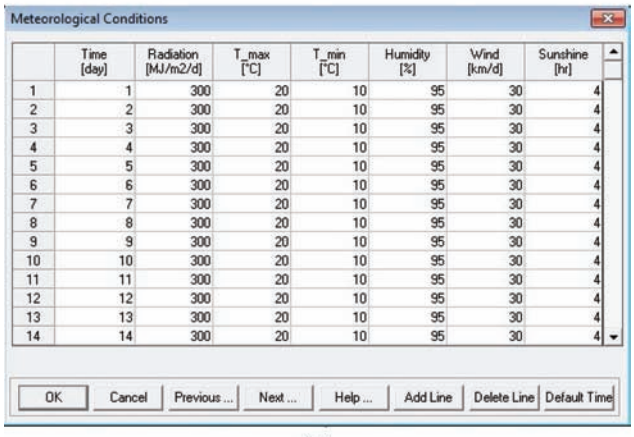

(b)

Figure 3.14 Define boundary conditions: (a) water flow boundary condition and (b) meteorological boundary condition.

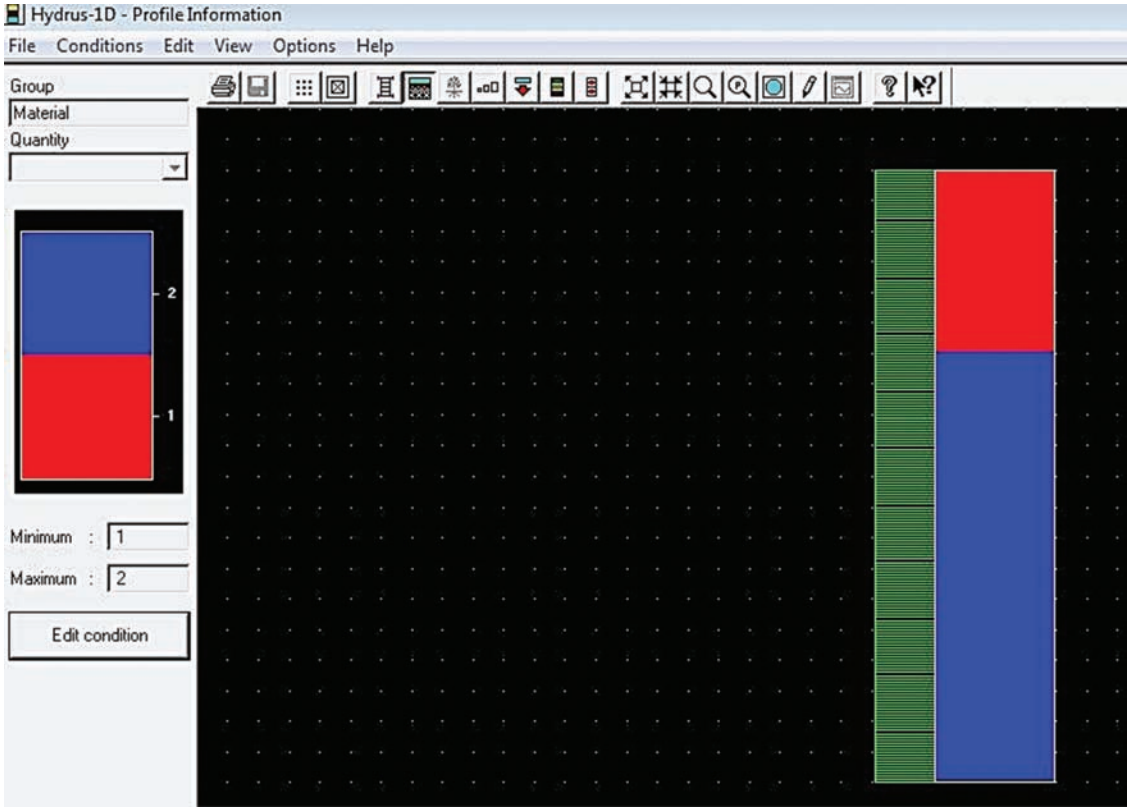

Figure 3.15 Visualize discretized profile.

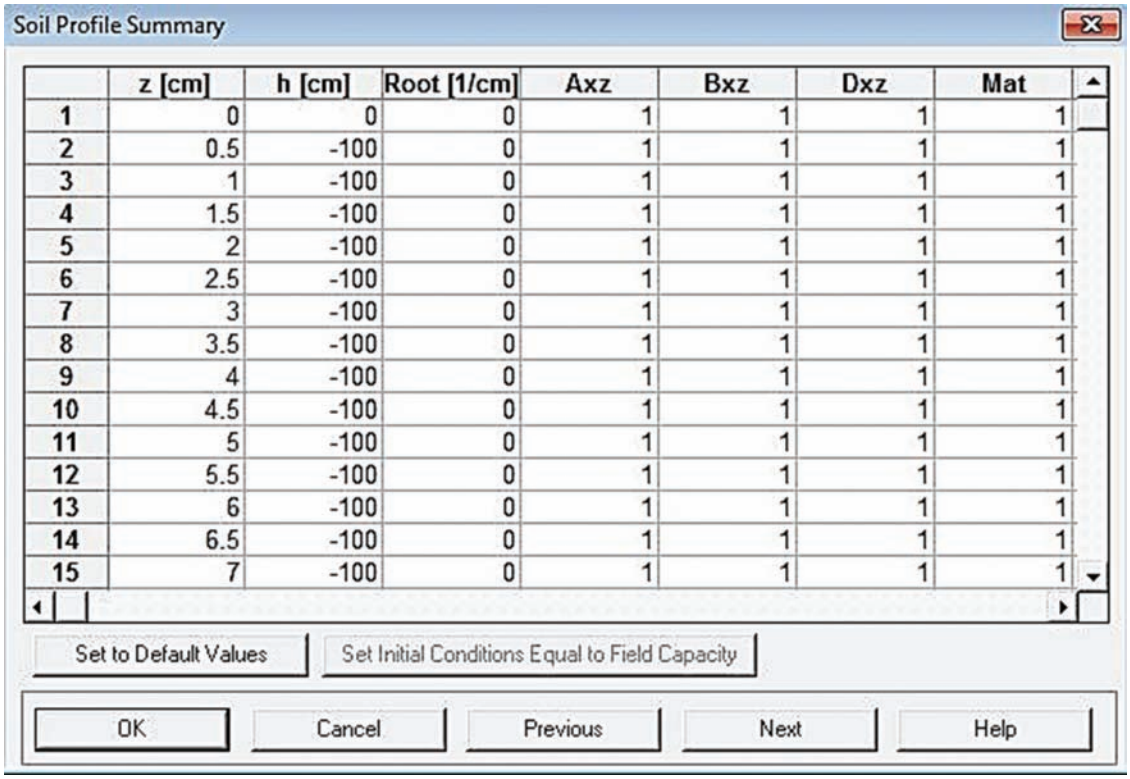

Figure 3.16 Define initial condition.

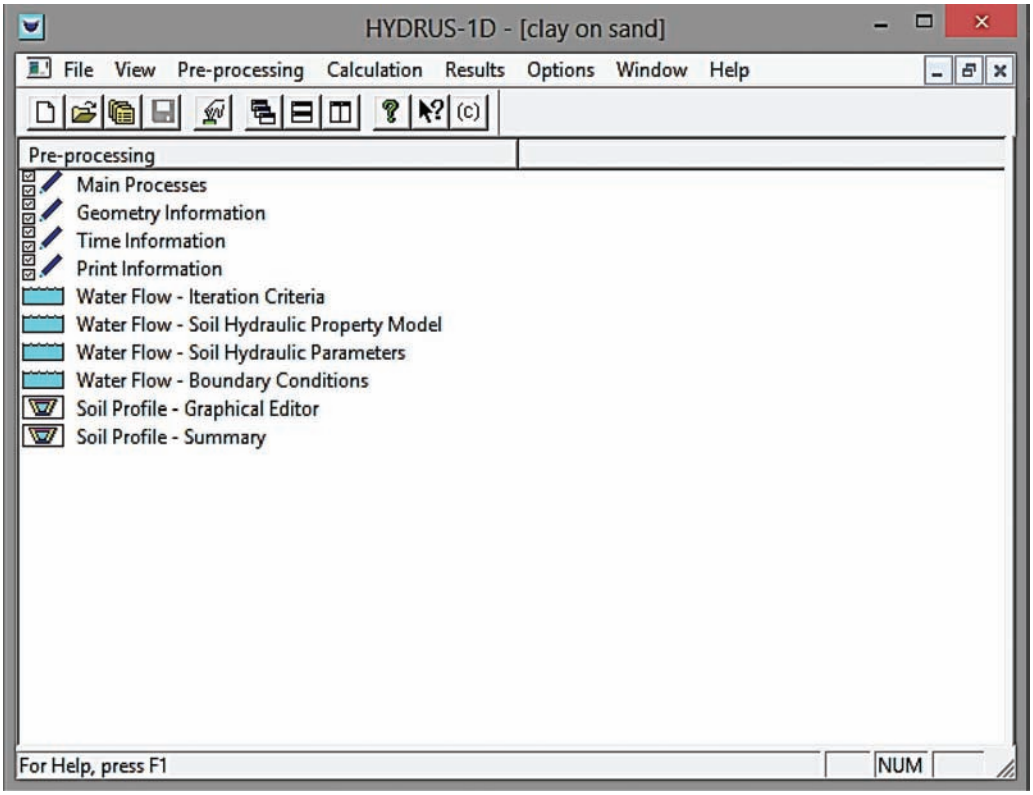

Figure 3.17 Run simulation.

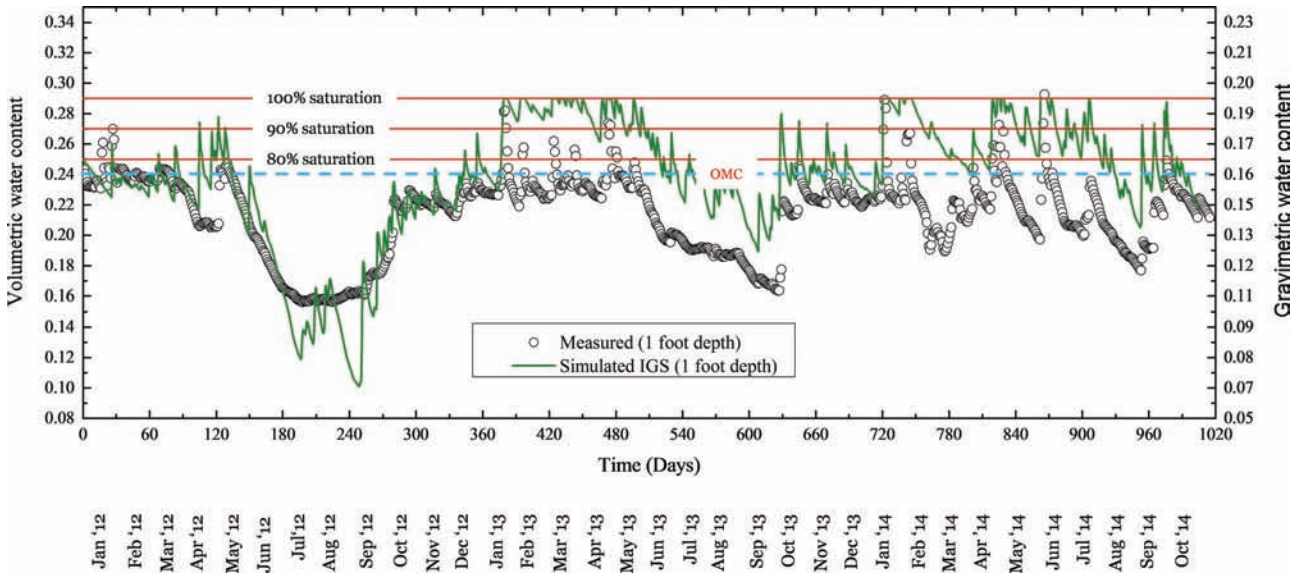

Figure 3.18 Measured and predicted volumetric and gravimetric soil water contents at a depth of 30 cm below the ground surface at Shelbyville (IGS site), Indiana.

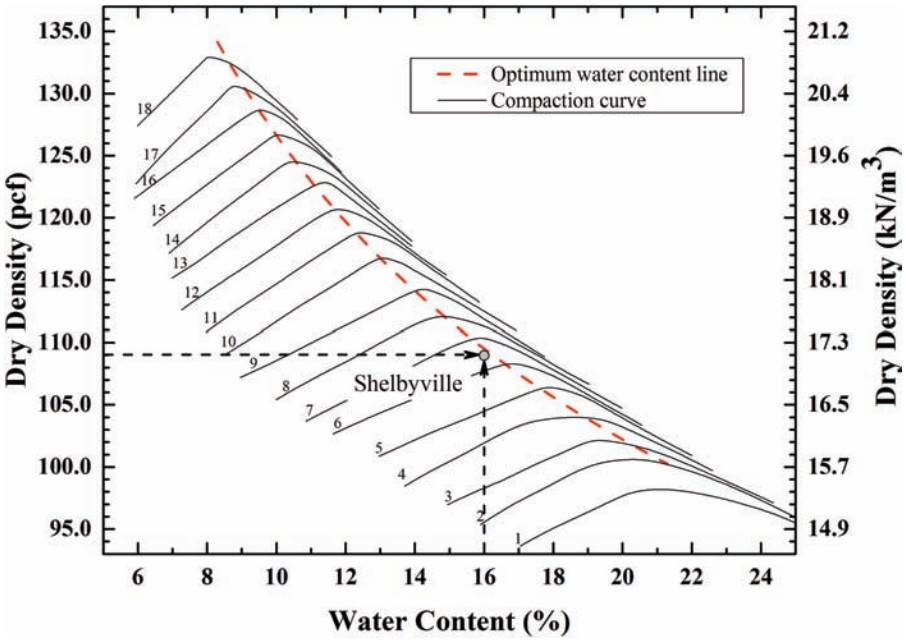

Figure 3.19 Shelbyville test site one-point Proctor test results along with INDOT family of curves.

4. EXPERIMENTAL RESULTS

4.1 *In Situ* Soil Data from INDOT

INDOT provided geotechnical reports for different ongoing projects. Field visits were also made by the research team to collect soil samples for laboratory experiments. The researchers met with the site engineers to learn of the problems that were faced because of excessive soil moisture during construction at those sites. Geotechnical reports were collected from projects in Fort Wayne on I-469 in Gibson County, SR-44 in Franklin County, SR-32 in Winchester County and Greenwood on I-65 in Johnson County. Figure 4.1 shows the location of the four INDOT field test sites.

4.2 Soil Data from IGS

The Indiana Geological Survey (IGS) has six locations in Indiana where they have continuous soil moisture measurements at different depths since 2012. IGS also has determined soil texture data from laboratory experiments for those sites. There are weather stations next to soil moisture measurement locations to collect daily solar radiation, temperature, wind speed, humidity and precipitation data. Figure 4.2 shows the locations of the six IGS field sites. The properties of the soils, available through the IGS database, at those locations are shown in Table 4.1.

4.3 Laboratory Test Results

Soil samples were collected from various locations in Indiana for laboratory experiments. A total of six sites were selected for this purpose. Three of the selected sites were INDOT construction sites and the other three of the selected sites were IGS field sites with continuous soil moisture measurements. The INDOT sites were chosen on the basis of the type of soil present *in situ*. Priority was given to sites with fine-grained soils, mostly clays and silts with low or high plasticity. The locations of field test sites from where soil samples were collected are shown in Figure 4.3. Disturbed and undisturbed soil samples were collected from these sites. A drilling rig and a hand-held split-spoon sampler were used to collect deep and shallow soil samples, respectively. Pictures of undisturbed soil sample collection by a drilling rig are shown in Figure 4.4. In addition to the undisturbed soil samples, disturbed bag samples of *in situ* soil were collected from these locations and used for soil texture classification.

ASTM-D422 and ASTM-D4318 were followed to obtain the grain size distribution curves and the Atterberg limits of the soil samples collected, respectively. The grain size distribution curves and the plasticity chart (plasticity index vs. liquid limit) with the results for the test soils are shown in Figure 4.5 and Figure 4.6, respectively. In addition to the grain size distribution curves and Atterberg limits, unconsolidated-undrained triaxial compression tests were also performed with a total confining stress of 250 kPa in accordance with AASHTO-T297. A summary of the laboratory test results is given in Table 4.2.

The undisturbed core samples collected in Shelby tubes were used for determination of the soil-water characteristic curve and the unsaturated hydraulic properties of the test soils using the HYPROP device. The Shelby tube samples were cut into the standard size (diameter = 7.5 cm; height = 5 cm) required for running the tests with the Decagon HYPROP, as shown in Figure 4.7.

After complete sample saturation, as described in section 2.4.4, two tensiometers were installed at 1.25 cm and 3.75 cm from the base of soil sample. Then, the sample was placed on a scale. The upper side of the sample was open to the atmosphere so that the moisture in the soil

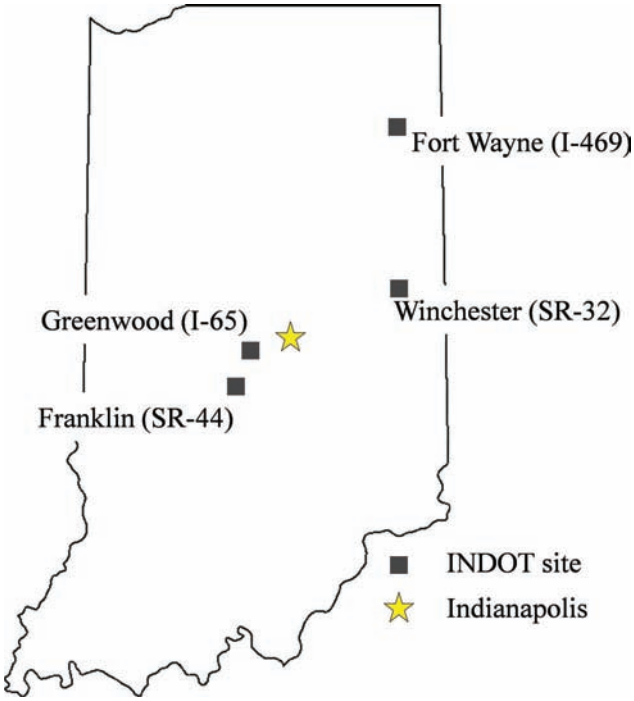

Figure 4.1 Field test sites of INDOT.

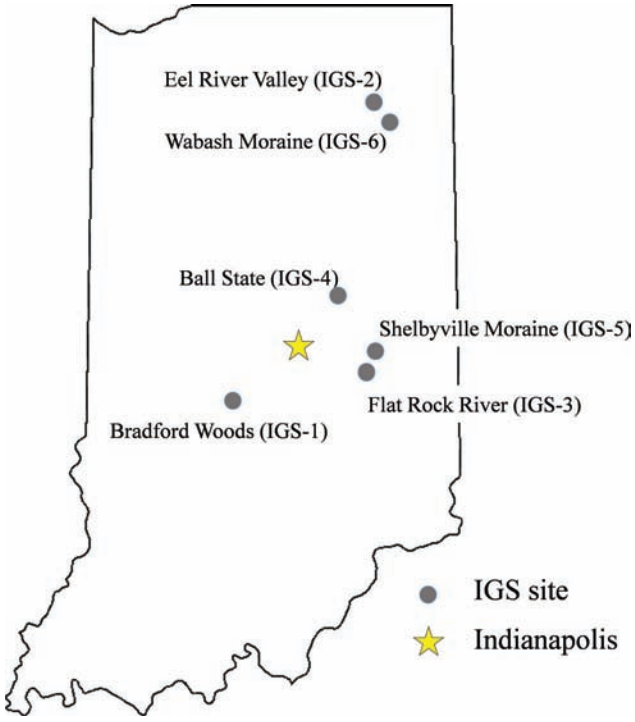

Figure 4.2 Data collection sites of IGS.

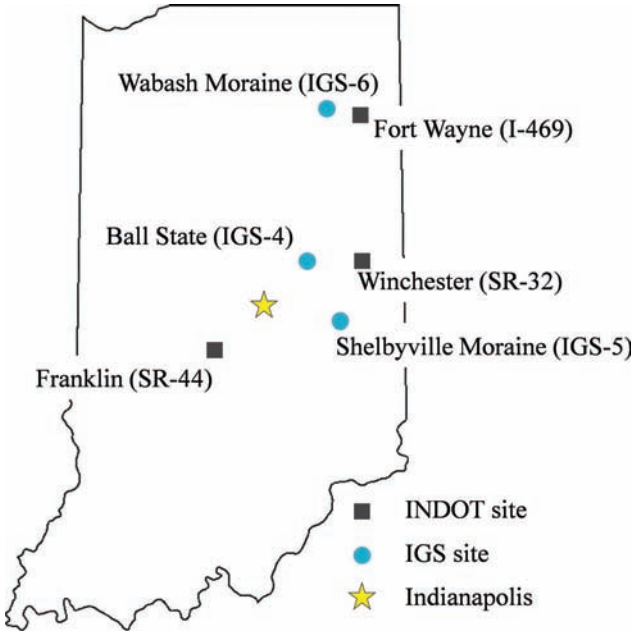

Figure 4.3 Soil sample collection sites in Indiana.

could evaporate. From the readings of the tensiometers, the mean matric potential and the hydraulic gradient were calculated. The loss of mass measured by the scale was used to calculate the volumetric water content and the flow rate.

The soil-water characteristic curves developed using the HYPROP for the undisturbed soil samples collected from three different locations (IGS-4, IGS-5 and IGS-6) are shown in Figure 4.8 (measurements were made for suction values of up to 100kPa; based on these initial measurements, the SWCCs were extrapolated to higher suction values using the van Genuchten model). These three results are for samples collected from 0 to 2 feet from the ground surface. At these depths, low plasticity clays with PI in the range of 20–30% are encountered. Table 4.3 shows the van Genuchten unsaturated hydraulic parameters of the test soils obtained using the HYPROP device.

TABLE 4.1
Soil profile and laboratory test data collected from IGS test sites (Naylor et al., 2015).

Site ID	Site Name	Depth cm	Density g/cc	Porosity	Sand %	Silt %	Clay %	Guelph Ks cm/day
IGS-1	Bradford Woods	0-40	1.67	0.37	69	24	7	27.7
		40-208	1.43	0.46	10	75	15	1.11
IGS-2	Eel River Valley	0-46	1.64	0.38	62	33	5	0.43
		46-108	1.74	0.35	50	32	18	0.18
		108-200	1.57	0.41	62	27	11	0.92
IGS-3	Flat Rock River	0-40	1.61	0.39	57	27	15	4.31
		40-105	1.57	0.41	52	19	29	10.9
		105-180	1.42	0.47	56	21	23	
		180-260			63	23	14	
IGS-4	Ball State	0-32.5	1.66	0.39	11	60	29	0.58
		32.5-60	1.65	0.39	16	44	40	
		60-230	1.77	0.35	18	50	32	
IGS-5	Shelbyville Moraine	0-32	1.48	0.44	6	71	23	237
		32-130	1.52	0.44	3	68	29	11.8
		130-215	1.88	0.31	34	44	22	
IGS-6	Wabash Moraine	0-35	1.58	0.4	31	50	19	0.32
		35-86	1.64	0.39	18	42	40	4.19
		86-250	1.82	0.33	22	49	29	

Figure 4.4 Collection of undisturbed soils by drilling rig.

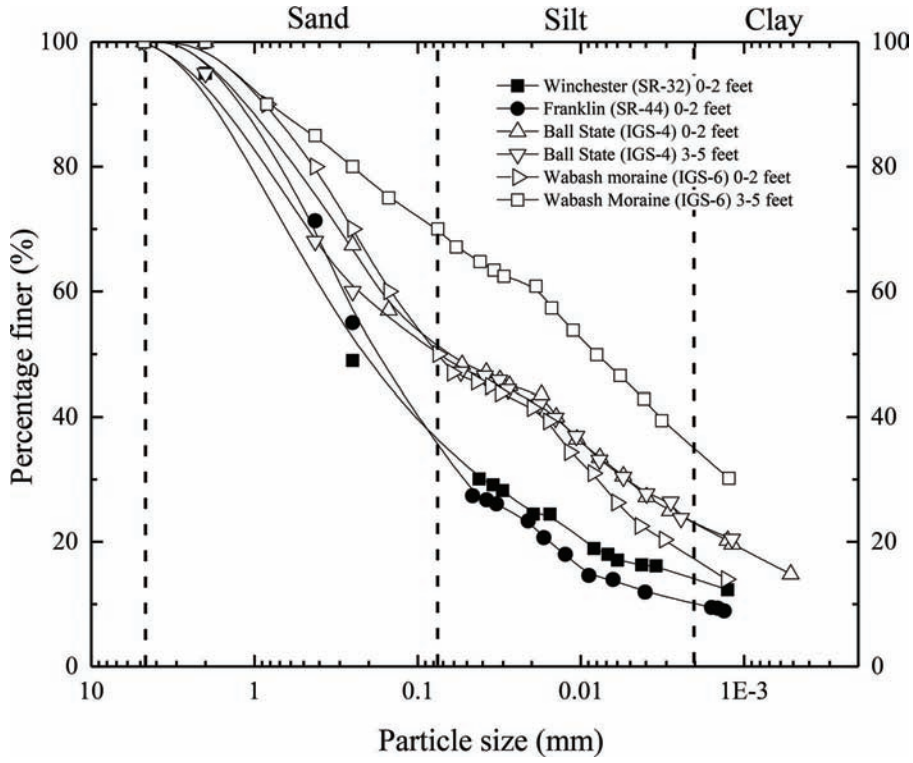

Figure 4.5 Grain size distribution curves for the test soils.

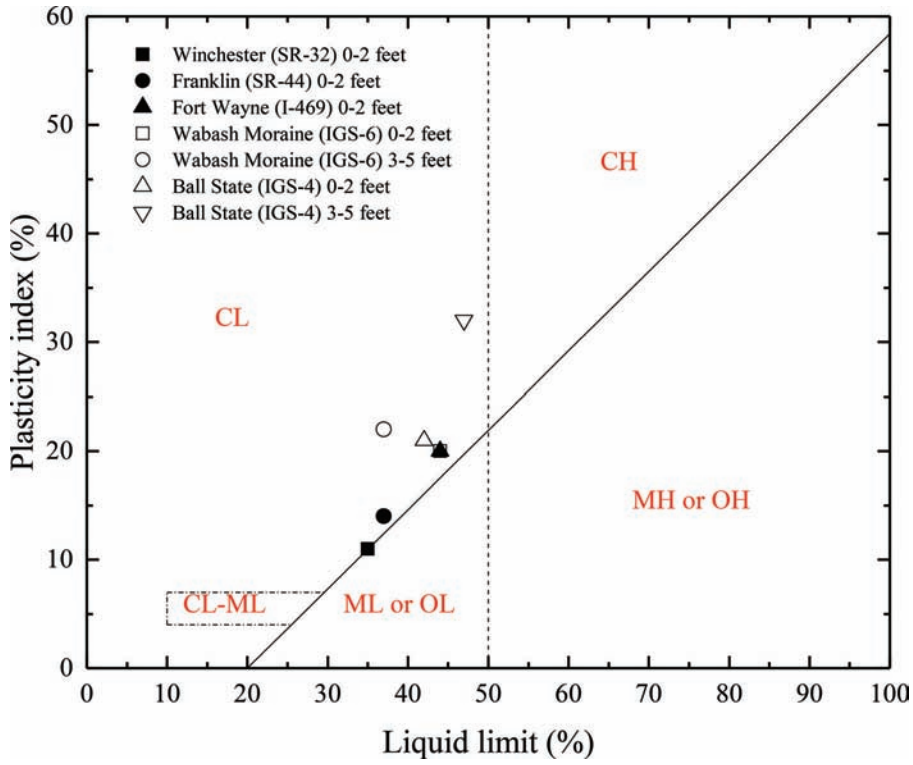

Figure 4.6 Plasticity index vs. liquid limit of the collected soils.

TABLE 4.2
Summary of laboratory test results for the soils tested.

Site	Depth (feet)	LL	PL	PI	Specific Gravity	Su (kPa)	USCS Classification
Winchester (SR 32)	0.0-2.0	35	24	11	2.71	Undisturbed sample not available	CL
Franklin (SR 44)	0.0-2.0	37	23	14	2.74		CL
Fort Wayne (I-469)	0.0-2.0	44	24	20	2.71		CL
Ball state (IGS-4)	0.0-2.0	42	21	21	2.74	100	CL
Ball state (IGS-4)	3.5-5.0	47	15	32	2.77	150	CL
Shelbyville (IGS-5)	0.0-2.0	Sampler damaged, sample could not be recovered				100	NA
Shelbyville (IGS-5)	3.0-5.0					130	
Wabash Moraine (IGS-6)	0.0-2.0	44	24	20	2.77	37	CL
Wabash Moraine (IGS-6)	3.0-5.0	37	15	22	2.77	68	CL

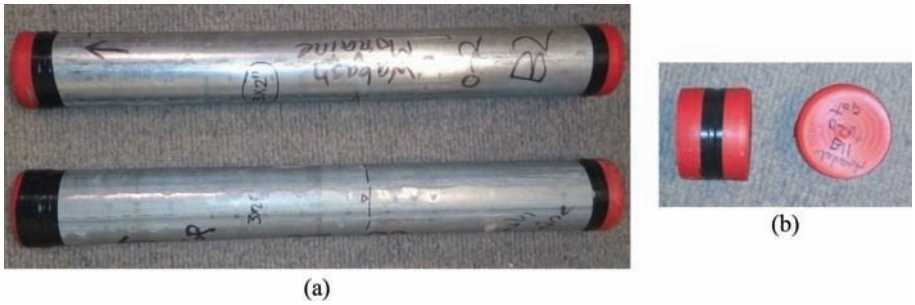

Figure 4.7 Undisturbed samples collected in Shelby tubes: (a) entire sample and (b) soil sample cut into small sizes required for testing with the HYPROP.

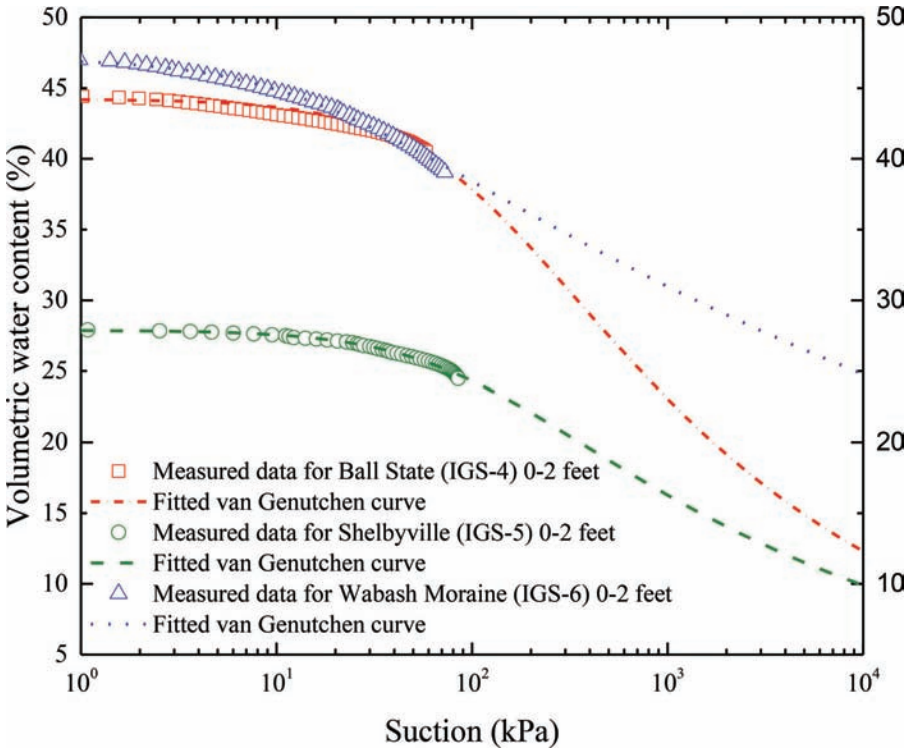

Figure 4.8 Soil-water characteristic curves for three undisturbed samples developed using the HYPROP device.

TABLE 4.3
Van Genuchten unsaturated hydraulic parameters determined from HYPROP tests.

Sample	van Genuchten Parameters				
	α (1/cm)	n*	θr (cm^3/cm^3)	θs (cm^3/cm^3)	Ks (cm/day)
Ball State (IGS-4)	0.00097	1.226	0.000	0.442	0.0214
Shelbyville (IGS-5)	0.00109	1.220	0.000	0.279	1.93
Wabash Moraine (IGS-6)	0.00730	1.097	0.000	0.471	85.0

*m = 1 - 1/n according to van Genuchten (1980).

5. SIMULATION RESULTS, VALIDATION AND IMPLEMENTATION

5.1 Seasonal *In Situ* Moisture Predictions Using HYDRUS-1D

Modeling unsaturated water flow and obtaining estimates of the soil water content at different depths require determination of the soil hydraulic properties of each layer of a soil profile. Although measurements are the most obvious and precise way to obtain soil hydraulic properties, financial and time constraints place limits on how much can be determined in the field or in the laboratory. Spatial variability of soil hydraulic characteristics further makes it doubtful whether limited soil hydraulic measurements are representative of the area considered (Šimůnek et al., 2013). Another alternative method is the use of pedotransfer functions (PTFs) for determining soil hydraulic properties from soil index properties. PTFs are empirical relations between soil hydraulic properties and index properties developed from data collected from 2,134 different soil samples (Schaap et al., 1998). A neural network-based prediction program called Rosetta implements PTFs to predict the van Genuchten (1980) water-retention parameters and saturated hydraulic conductivity by using as input textural class, textural distribution, bulk density and one or two points of a soil-water characteristic curve.

Appropriate estimation of soil hydraulic properties is a key step in the modeling of water flow through unsaturated soil. Therefore, to validate the method of determining soil hydraulic properties based on PTFs, HYDRUS-1D simulations were performed with hydraulic properties determined from PTFs. The results of the simulations were compared with measured data. Six IGS sites were selected for this purpose.

IGS has continuous soil moisture measurements for six locations in Indiana since 2012. Moisture measurement sensors were installed at 30 cm intervals from the ground surface up to a depth of 180 cm. Laboratory tests were carried out on soil samples to obtain the index properties of the soils at the IGS test sites. Each IGS site has a weather station to collect the weather-related parameters required for the HYDRUS-1D simulations. Hydraulic properties based on texture data for each soil layer were used as input for the HYDRUS-1D simulations performed in this research. A time-variable atmospheric boundary was considered at the top surface. The inputs for the top boundary were precipitation and evaporation. Evaporation from the top soil was calculated based on the Penman-Montheith equation:

$$ET_o = ET_{rad} + ET_{aero} = \frac{1}{\lambda}\left[\frac{\Delta(R_n - G)}{\Delta + \gamma(1 + r_c/r_a)} + \frac{\rho c_p (e_a - e_d)/r_a}{\Delta + \gamma(1 + r_c/r_a)}\right] \quad (5.1)$$

where ET_o is the evapotranspiration rate (mm/day), ET_{rad} is the radiation term (mm/day), ET_{aero} is the aerodynamic term (mm/day), λ is the latent heat of vaporization (MJ/kg), R_n is the net radiation at the surface (MJ/m^2/day), G is the soil heat flux (MJ/m^2/day), ρ is the atmospheric density (kg/m^3), c_p is the specific heat of moist air (i.e., 1.013 KJ/kg/°C), $(e_a\text{-}e_d)$ is the vapor pressure deficit (kPa), e_a is the saturation vapor pressure at a temperature T (kPa), e_d is the actual vapor pressure (kPa), r_c is the crop canopy resistance (s/m), and r_a is the aerodynamic resistance (s/m). The slope of the vapor pressure curve, Δ (KPa/°C), and the psychrometric constant, λ (KPa/°C) are defined as follows:

$$\Delta = \frac{4098 e_a}{(T + 237.3)^2} \quad (5.2)$$

$$\gamma = \frac{c_p P}{\varepsilon \lambda} \times 10^{-3} = 0.00163 \frac{P}{\lambda} \quad (5.3)$$

where T is the average air temperature (°C), P is the atmospheric pressure (kPa), ε is the ratio of the molecular weights of water vapor and dry air (i.e., 0.622), and λ is the latent heat (MJ/kg).

The depth of the groundwater table from the surface was provided as the bottom boundary condition for the soil profiles. Root water uptake by vegetation was considered in the simulations to represent the actual conditions at these sites (vegetation cover by pasture was selected). Feddes's parameter for root water uptake and root distribution model were selected from the HYDRUS-1D database (Feddes & Zaradny, 1977). Field capacity of soil moisture was selected as the initial condition for these simulations.

A comparison between the measured soil moisture for a period of three years and the predicted soil moisture from the simulations are shown in Figure 5.1 for the Bradford Woods site.

5.2 Soil Moisture Predictions for the State of Indiana

Soil moisture simulations were performed for a period of 10 years, from 2006 to 2015, using available climate data, groundwater level data and soil hydraulic properties data. Soil texture classification for each county of Indiana was obtained from the SSURGO database. Rosetta implemented PTFs were used to determine the soil hydraulic properties of representative soil profiles for each county. Weather and groundwater table data were obtained for different zones of Indiana for a period of 10 years, from 2006 to 2015. HYDRUS-1D simulations were carried out using these data for each county of Indiana. Soil moisture estimates at the depths of 60 cm and 90 cm were obtained from the HYDRUS-1D simulations. Depths of 60 and 90 cm from the ground surface were chosen because greater scatter was observed in the measured near-surface *in situ* soil moisture data.

Figure 5.2(a) and Figure 5.2(b) show the soil gravimetric water content vs. time for the Bradford Woods test site at a depth of 60 and 90 cm. The predicted soil water content is also presented in terms of one standard deviation above and below the estimated average water content values based on weather input data for a period of 10 years, from 2006 to 2015 (note that the 10-year simulation results are plotted together for a period of 12 months). The measured and simulated water content values in Figure 5.1 show good agreement with the 10 year overlapped simulation results shown in Figure 5.2. The simulation results for all Indiana counties are provided in Appendix A.

5.3 Example of Soil Moisture Prediction by HYDRUS-1D

HYDRUS-1D simulations were performed for the LaGrange County as an example. (See Table 5.1 for soil index properties of the profile used.) From the SSURGO database, the prominent type of soil in this county, based on the percentage of maximum area coverage, was a loamy sand (names Boyer loamy sand, according to the SSURGO database). 15,706 acres of land in LaGrange County is covered by this type of soil, which is approximately 6.3% of the entire land area of the county. LaGrange County is located in zone 2 of the Indiana weather map that considers proximity of weather stations, as previously shown in Figure 3.3. Based on the groundwater table map prepared by the Department of Natural Resources, it can be observed from Figure 3.4 that LaGrange County is located in zone 3. Numerical simulations of soil moisture flow by HYDRUS-1D provides soil moisture values at the desired depths at different times of the year. Soil moisture simulations were carried out for weather and groundwater table data input from 2006 to 2015. The steps followed to simulate soil moisture flow for the chosen soil profile in LaGrange County are described next.

The first step of a HYDRUS-1D simulation is to select the type of simulation. Here, water flow simulation with root water uptake was selected, as shown in Figure 5.3.

The second step of the simulation is to define the soil geometry. A vertical soil profile of 152 cm depth with 3 types of soil was selected for LaGrange County, as shown in Figure 5.4.

In the next step of the simulation, the time increments and the number of time variable data input were selected, as shown in Figure 5.5. The simulation was carried out for 3,652 days, which is equivalent to 10 years. A time-variable boundary condition was also selected to account for precipitation during that period of time. The Penman-Montheith model was used to calculate water loss due to evapo-transpiration, as previously described.

In the next step of the simulation, the convergence criteria for iterations is selected. The following needs to be specified: (i) maximum number of iterations, (ii) water content tolerance limits, and (iii) pressure head tolerance limits. The limits for the iteration criteria selected for the simulations are shown in Figure 5.6.

In the next step, the soil hydraulic model is chosen, based on which of the soil moisture flow simulation are carried out by HYDRUS. The van Genuchten (1980) single porosity hydraulic model with no hysteresis was selected for the simulations, as shown in Figure 5.7.

In the next step, input parameters for the chosen soil hydraulic model were given appropriate values depending on the engineering properties of the layers in the chosen soil profile, as shown in Figure 5.8. The parameters for the van Genuchten (1980) model were selected from an in-built soil catalog in HYDRUS-1D which uses a Rosetta pedotransfer function (Schaap, Leij, & van Genuchten, 2001) to get the soil hydraulic parameters from the soil's texture.

The top and bottom boundary conditions of the soil profile were selected in the next step of the simulations, as shown in Figure 5.9. An atmospheric boundary condition was selected as the top boundary condition, which implies that the loss/gain of water from the top surface of the soil mass was controlled by the atmospheric demand/supply. Depending on the depth of the ground water table, the bottom boundary condition can either be: (i) free drainage boundary condition (in case the water table is significantly far from the region of interest) or (ii) variable pressure head boundary condition (in case the ground water table lies within the region of interest). For the case of LaGrange County, the ground water table was found to be at a depth of 3.5 m or more from the ground surface for the time period of 2006 – 2015. Therefore, a free drainage bottom boundary condition was chosen for this case. In addition to the boundary conditions, the type of initial condition was also selected in this step. Depending on the nature of data available, the initial condition can be either in terms of pressure head (if tensiometer readings are available) or

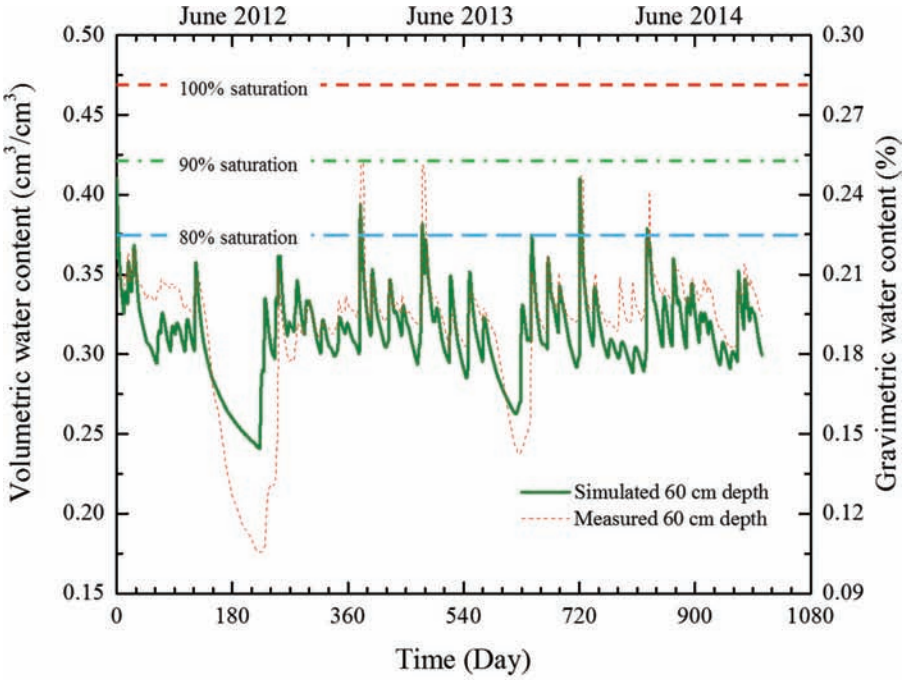

(a)

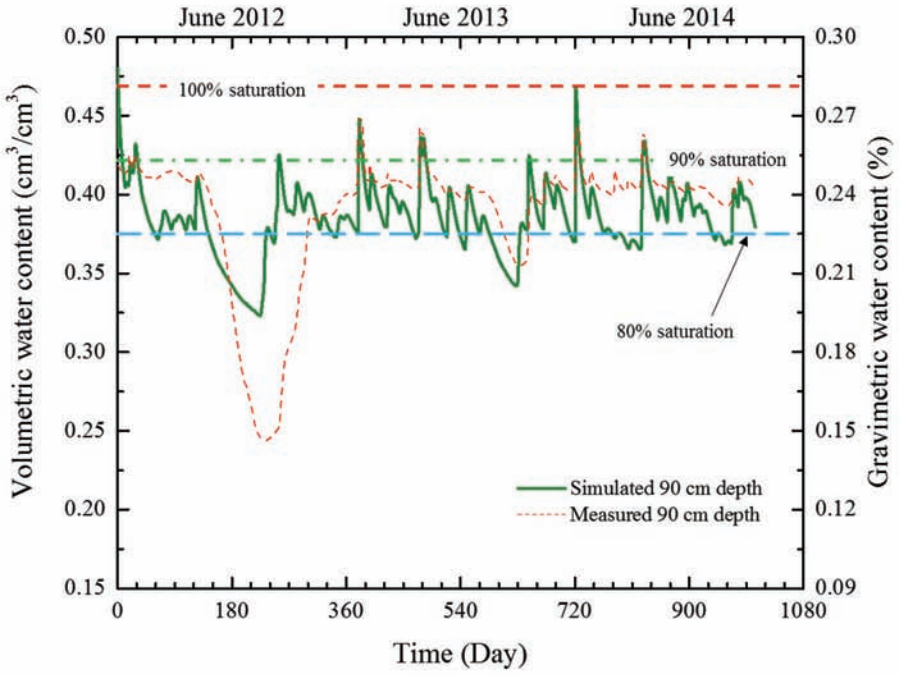

(b)

Figure 5.1 Simulated vs. measured soil moisture at a depth of (a) 60 cm and (b) 90 cm for Bradford Woods site (IGS-1) from January 2012 to September 2014.

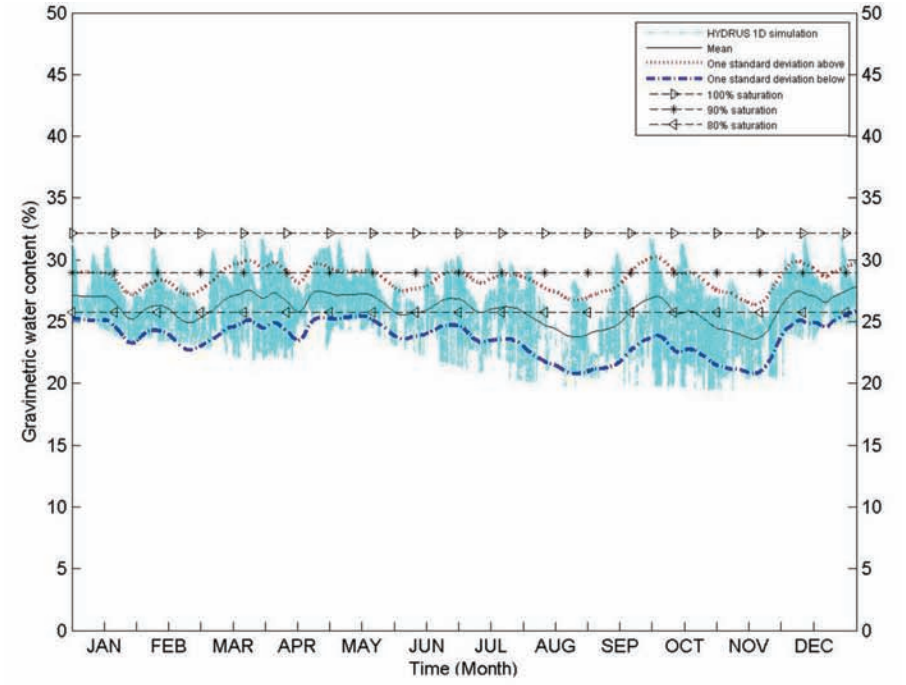

(a)

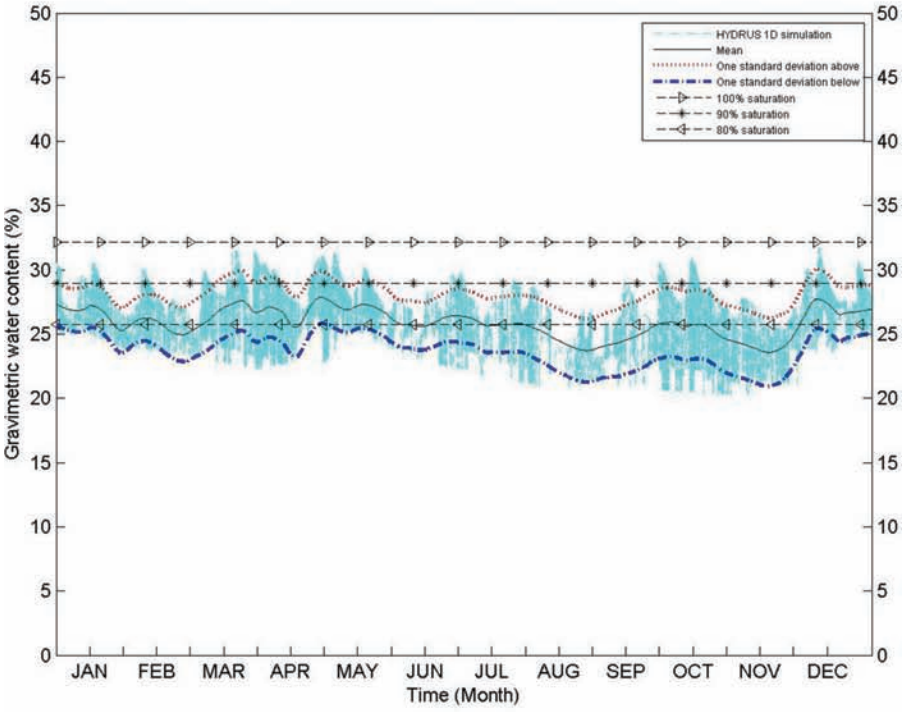

(b)

Figure 5.2 10-year overlapped soil moisture predictions with ± 1 standard deviation lines for the Bradford Woods site (IGS -1) at depths of (a) 60 cm and (b) 90 cm.

TABLE 5.1
Soil index properties for chosen soil profile in LaGrange County (from SSURGO database).

Layer Depth (cm)	USDA	USCS	AASHTO	In Situ Bulk Density (g/cm^3)*	Sand (%)*	Silt + Clay (%)*
0-46	loamy sand	SM	A-2-4	1.55	60	30
46-91	sandy clay loam	SC-SM	A-2	1.7	60	20
91-152	sand	SW	A-1	1.7	60	10

*Average for the layer taken.

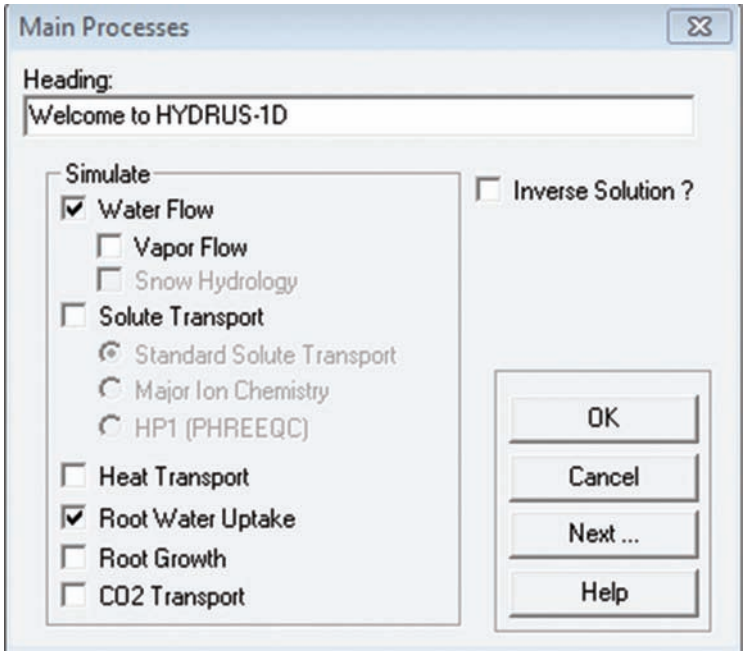

Figure 5.3 Selection of simulation type.

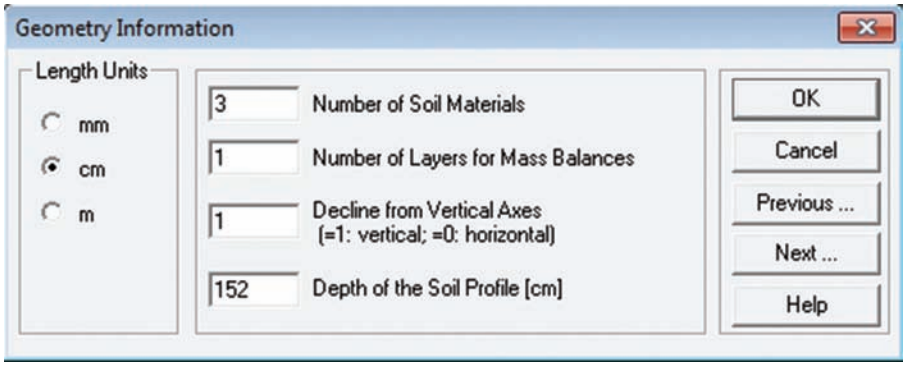

Figure 5.4 Selection of soil geometry.

in terms of volumetric water content of the soil. As the initial condition was not available at the time of the simulation, a pressure head based initial condition was chosen. It was assumed that the soil profile was at field capacity, *i.e.,* the condition under which there is no flow of water due to gravity within the soil mass.

The next step in the simulations was to select the root water uptake model based on the type of vegetation prevalent at the site of interest. As a majority of the county area of LaGrange is under grass or farmland cover, the Feddes and Zaradny (1977) root water uptake model was used assuming pasture type vegetative cover

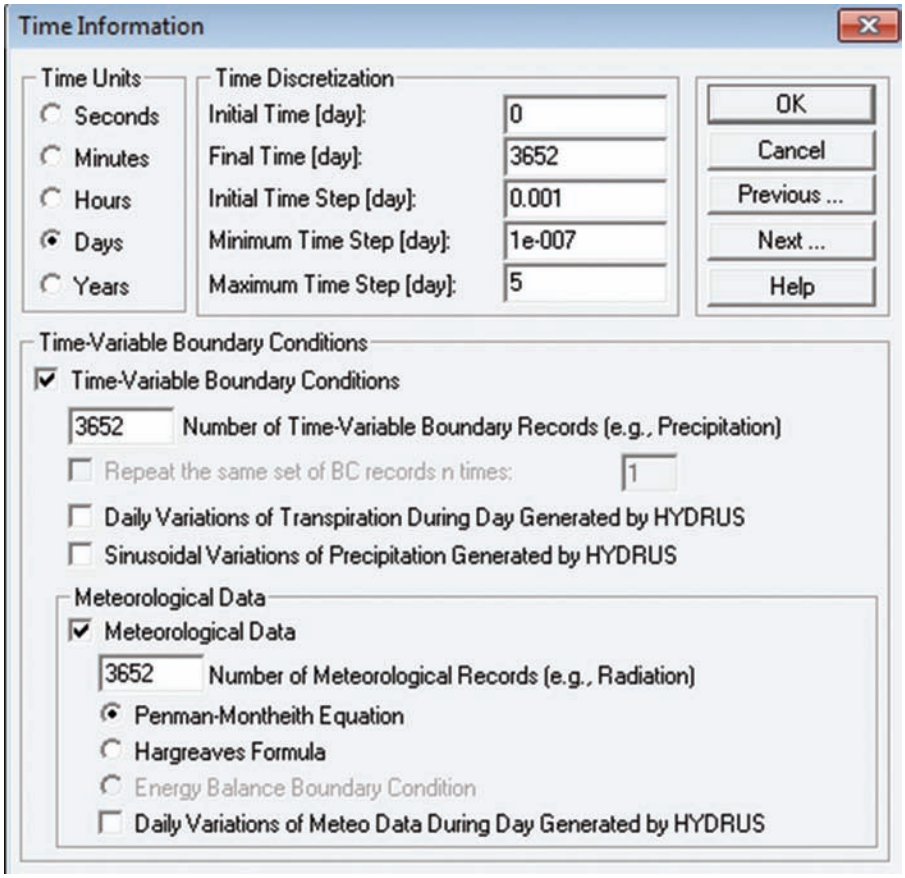

Figure 5.5 Selection of time increments and time variable data input.

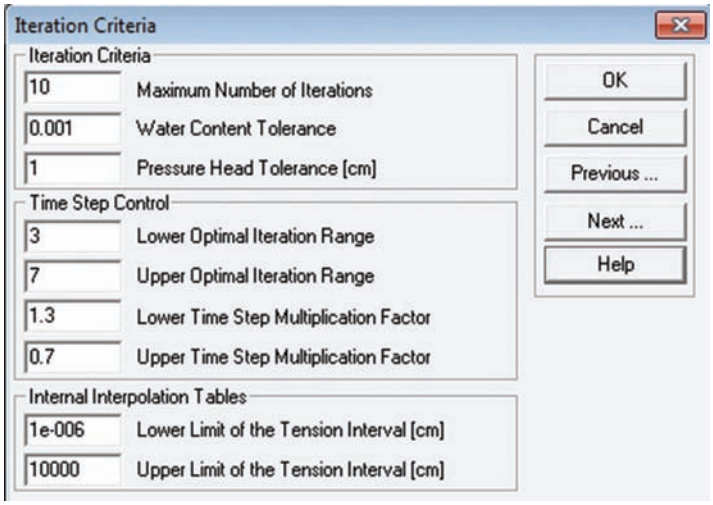

Figure 5.6 Defining iteration criteria.

for which the parameters were obtained from Wesseling (1991). (See Figure 5.10.)

Time variable boundary data was given as input in the next step of the simulations. Precipitation data was given as input for each day of the simulation time period (January 2006 to December 2015). For LaGrange County, the precipitation data was collected from a weather station located in zone 2 of the weather map shown in Figure 3.3. As the ground water table was far below the zone of interest, free drainage was assumed and no input of ground water table was necessary. In a general case, if the groundwater table is within the zone of interest, it should be obtained from the ground water table database maintained by the Department of

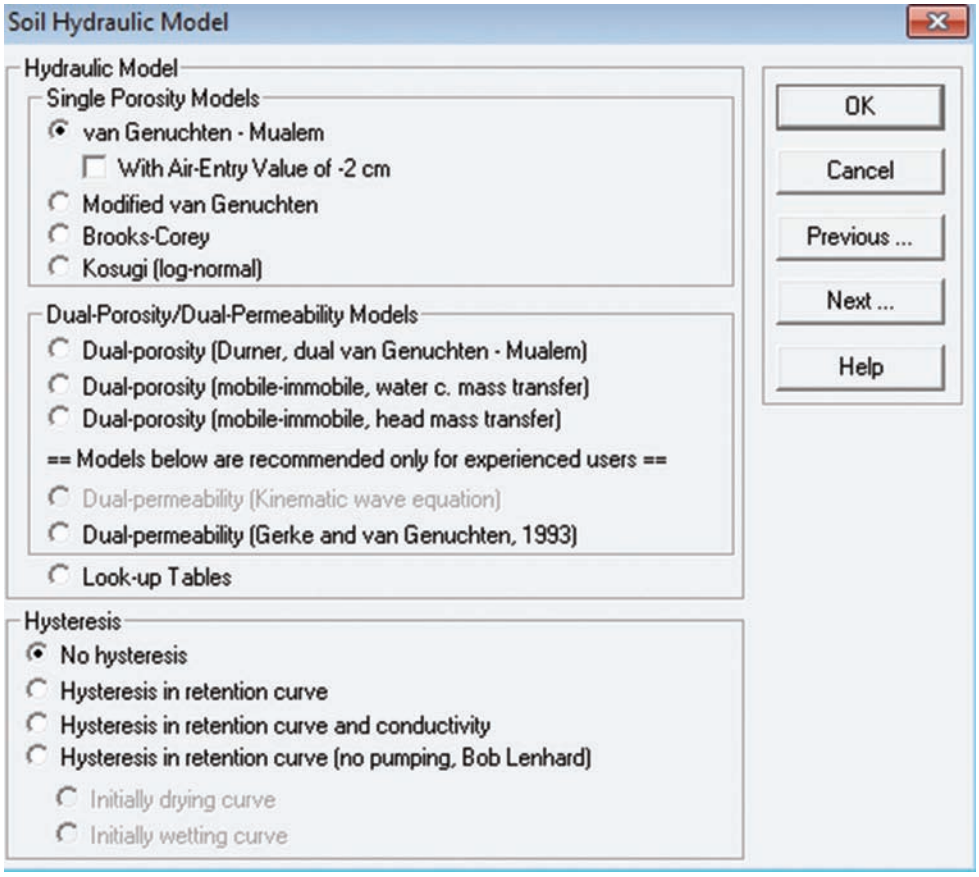

Figure 5.7 Selection of soil hydraulic model.

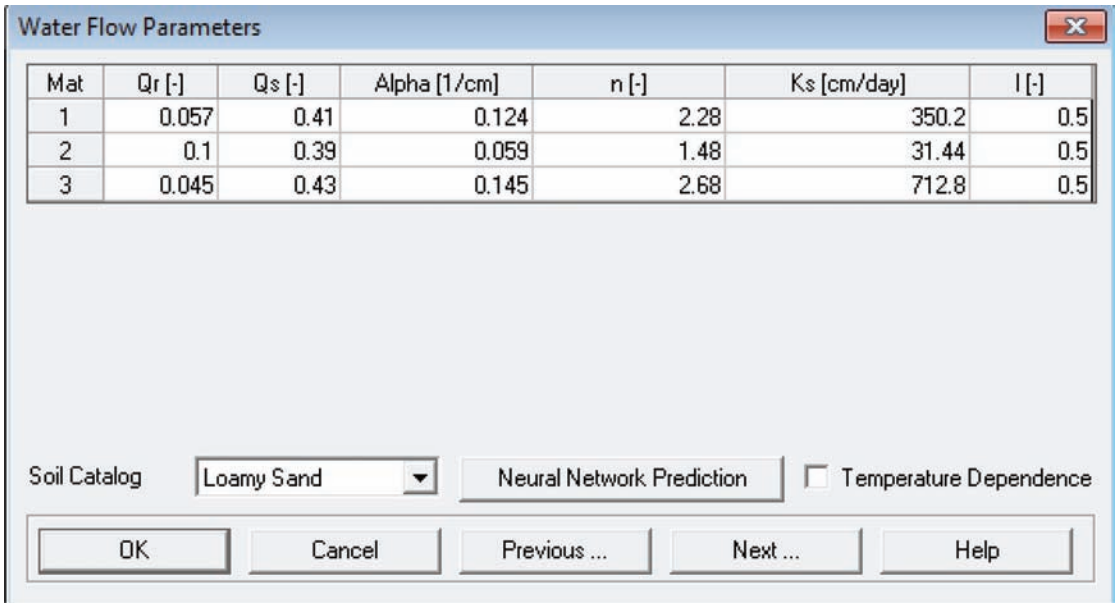

Figure 5.8 Selection of water flow parameters.

Natural Resources (DNR; as previously described). The precipitation data is shown in Figure 5.11.

In the next step of the simulations, the meteorological data was provided as input to HYDRUS-1D for calculation of the potential evaporation using the Penman-Montheith equation (Monteith, 1965). For LaGrange County, the meteorological data were collected from a weather station located in zone 2 from

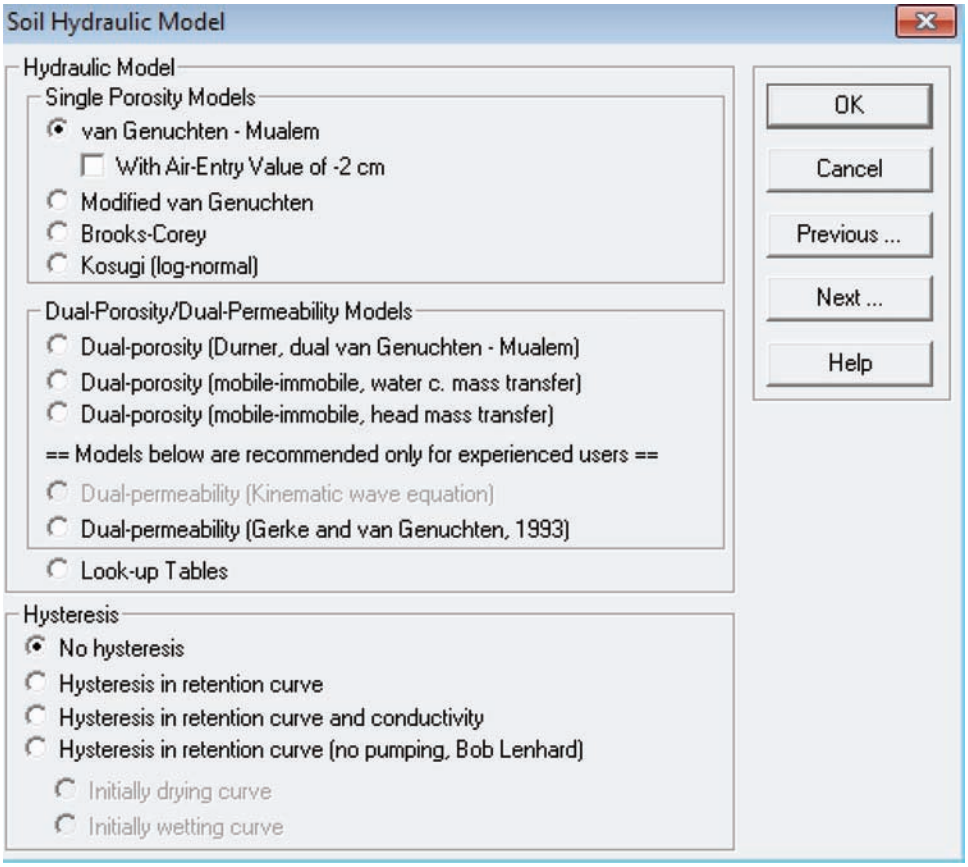

Figure 5.9 Selection of water flow boundary conditions.

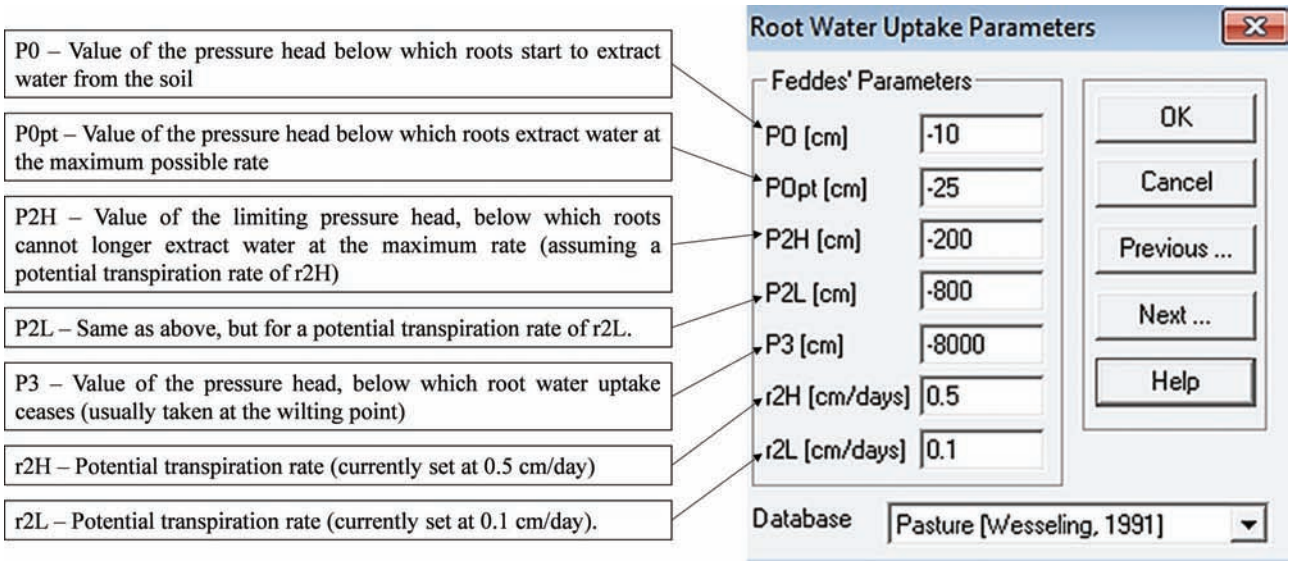

Figure 5.10 Root water uptake parameter for pasture.

1994 to 2004. Here solar radiation, wind speed, relative humidity, maximum and minimum daily temperature were provided as meteorological input parameters to HYDRUS-1D. The meteorological data are shown in Figure 5.12 to Figure 5.15.

Finally, from the graphical editor, the depth of the soil layer for each type of soil was defined. The initial water content, assuming the soil was at field capacity, was selected throughout the soil profile. Observation nodes were also placed in the graphical editor at the

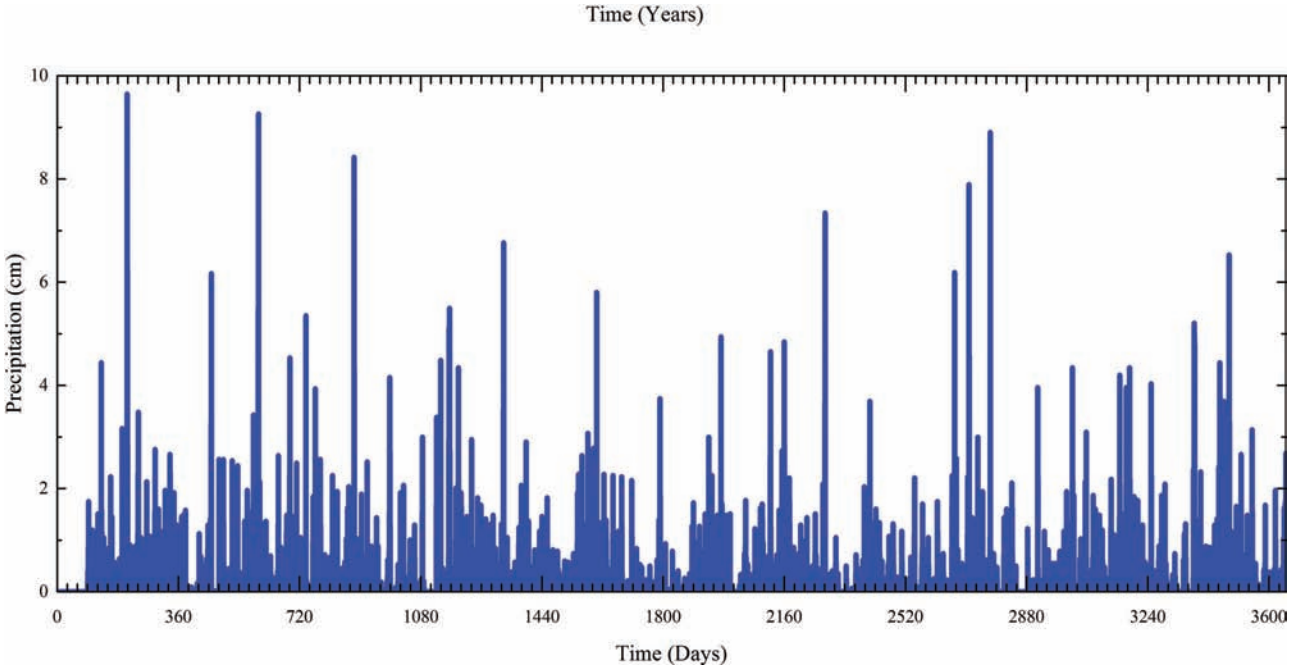

Figure 5.11 Precipitation data for LaGrange -County from year 2006 to 2015 (Iclimate-Purdue).

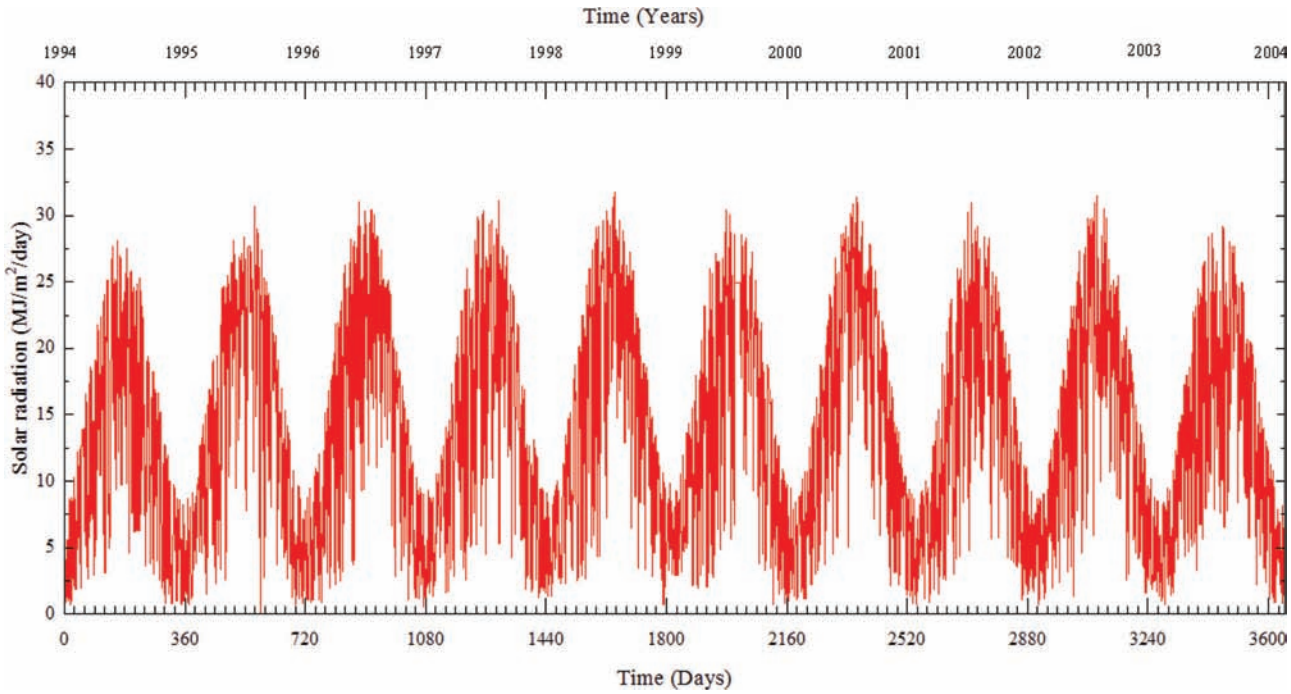

Figure 5.12 Solar radiation data for LaGrange County.

desired depths to get the soil moisture results from the simulations. The distribution of plant root within the soil profile was defined for root water uptake calculations. The distribution of roots of pasture from a depth of 0 cm to 90 cm was selected from the HYDRUS-1D database.

The simulations were carried out for the input weather data from 2006 to 2015 for LaGrange County for the chosen soil profiles. The soil moisture profiles at a depth of 60 cm from the surface were obtained from these simulations. The results of the simulations for a period of 10 years were overlapped to obtain the average daily soil

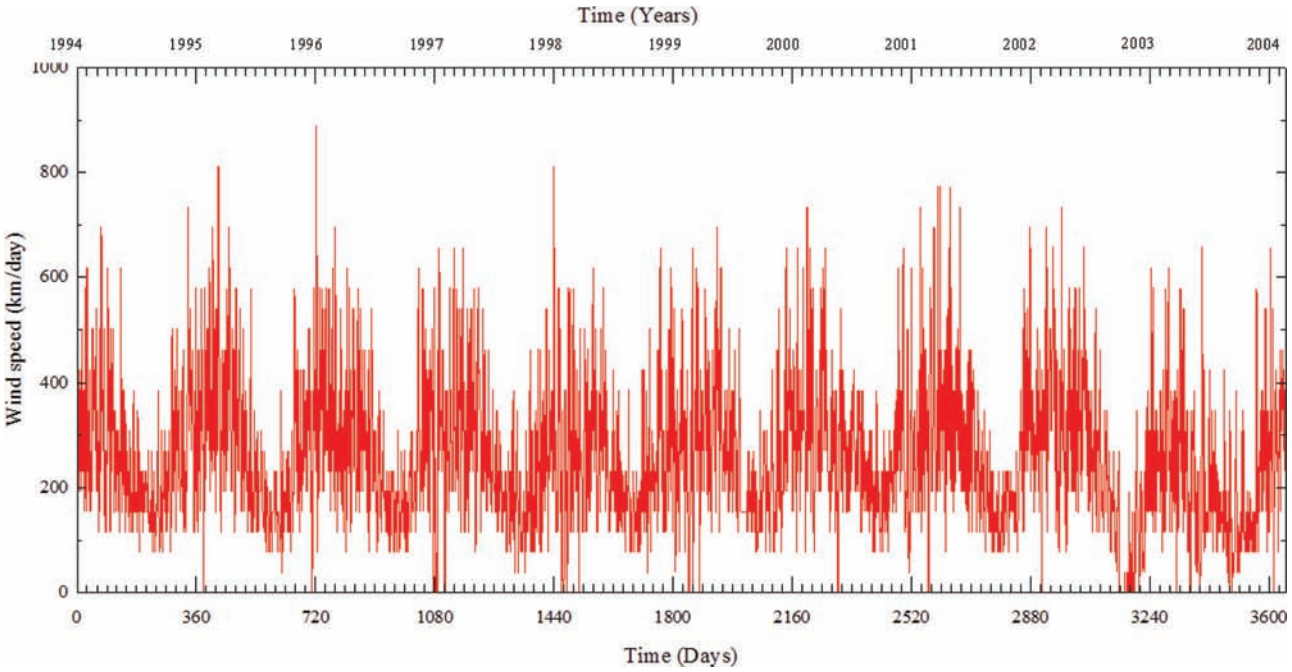

Figure 5.13 Wind speed data for LaGrange County.

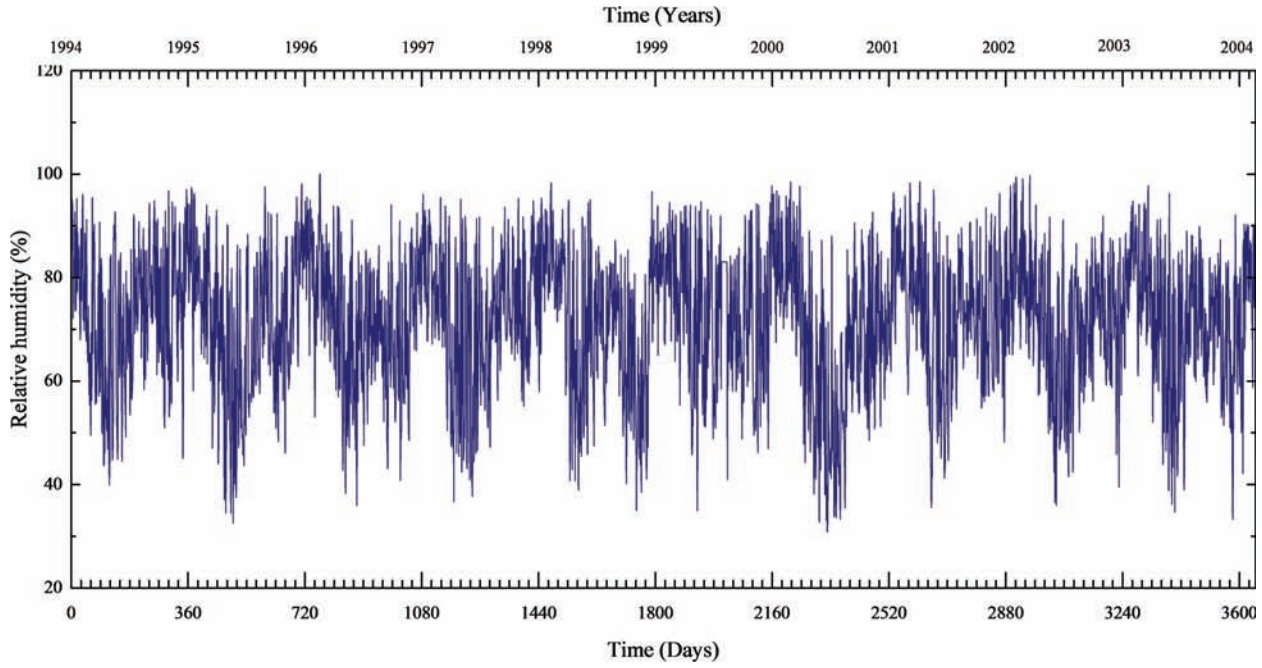

Figure 5.14 Relative humidity data for LaGrange County.

moisture in a calendar year. Statistical analyses were carried out to estimate the average daily soil moisture at a specific depth within a calendar year. Water content values corresponding to one standard deviation above and below the average daily soil moisture were also calculated in order to have a daily range for the expected water content. The results of the LaGrange County soil moisture predictions for a depth of 60 cm are shown in Figure 5.16.

Similar simulations were carried out for all the other counties in the state of Indiana. Multiple soil profiles were chosen for each county, based on the area covered, to get a representative set of soil profiles for the entire state of Indiana. The estimated yearly *in situ* soil moisture vs. time plots corresponding to depths of 60 cm and 90 cm for all the selected soil profiles for all the counties of the state of Indiana are presented in Appendix A.

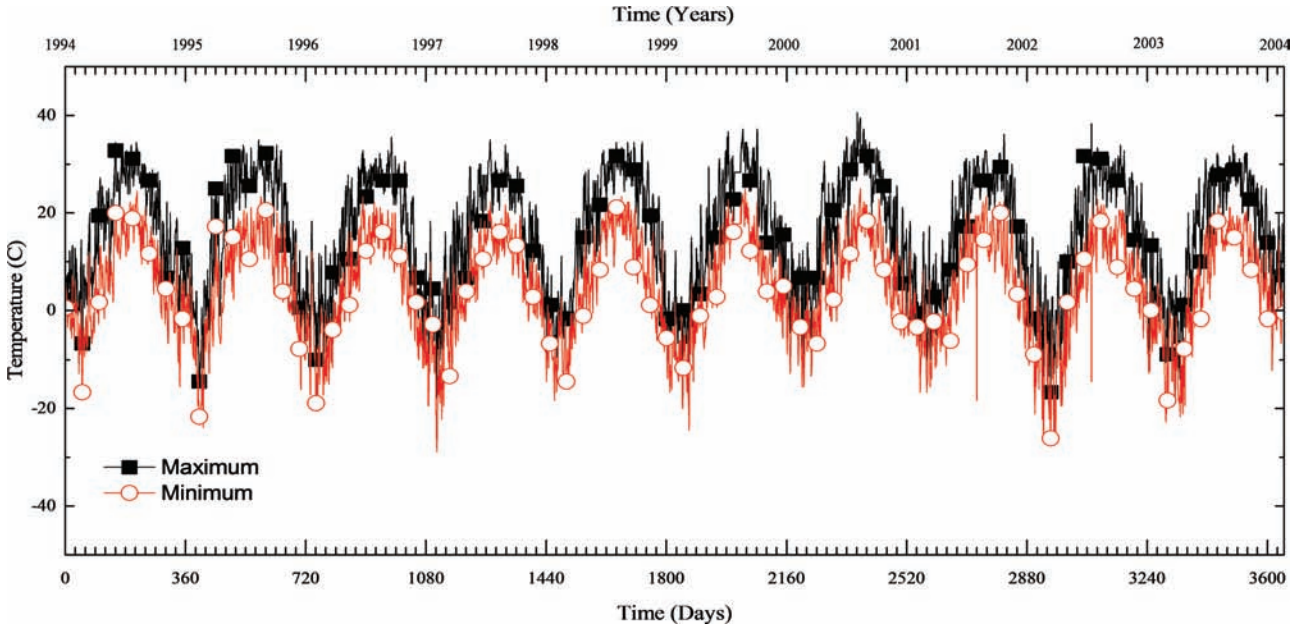

Figure 5.15 Maximum and minimum temperature data for LaGrange County.

5.4 Validation of Soil Moisture

To validate the process of determining the soil moisture at any depth from the numerical simulations with soil hydraulic properties estimated from soil texture data, the simulation results were compared with measured water content data for Wabash moraine site (IGS-6) in Allen County and Ball state site (IGS-4) in Delaware County. The two locations were chosen because continuous soil moisture measurement data was available at these two sites for more than one year and the soil type were of great interest to the project. The soil properties for the profiles chosen from the two sites are presented in Table 5.2. The comparison of measured and simulated soil moisture for IGS-6 and IGS-4 is presented in Figure 5.17 and Figure 5.18 respectively. As can be observed, the simulated results show good agreement with the measured values in the field, therefore the methodology can be used for other simulations. Similar results were obtained from other IGS test sites.

5.5 Preliminary Implementation Procedure for the Soil Moisture Prediction Methodology

The preliminary methodology proposed can provide guidance to INDOT engineers when making decisions regarding the need to improve or replace *in situ* soils at the time of construction. Further refinements to the methodology proposed in this report can be made during the implementation phase of this research project by performing additional laboratory tests to better characterize the soil properties of each layer of representative soil profiles at pilot project locations and by performing additional HYDRUS-1D simulations using as input weather and groundwater data specifically obtained at the desired locations.

The implementation of the methodology can be done in routine geotechnical engineering projects. The process of implementation is as follows:

1. Choose from this project report Appendix, the county in Indiana where the construction project of interest is located. As an illustration, three counties are chosen:
   i. Gibson County (Fine-grained soil profile)
   ii. LaPorte County (Coarse-grained soil profile)
   iii. Fayette County (Fine-grained soil profile)
2. For each county, a number of representative soil profiles are available in the appendices of this report. From the available options, choose the soil profile that is most similar to the soil profile at the construction project of interest. Three example profiles are provided in Figure 5.19, Figure 5.20 and Figure 5.21 for Gibson, LaPorte and Fayette counties, respectively. For each selected soil profile, a yearly plot of *in situ* soil moisture vs. time can be obtained from this report.
3. Figure 5.22, Figure 5.23 and Figure 5.24 show the yearly *in situ* soil moisture vs. time plots at 60 and 90 cm depths (these plots show the overlapped results of HYDRUS-1D simulations carried out for a period of 10 years of weather and groundwater table data for the Gibson, LaPorte and Fayette counties). Obtain from these plots the water content ranges for the expected months for the investigation and construction phases of a project of interest (note that the range of soil moisture values obtained from these plots at the time of the site investigation of a project can be compared with those obtained from the geotechnical report).

From Figure 5.22, Figure 5.23 and Figure 5.24, it can be observed that the *in situ* soil moisture for the fine-grained soils (Figure 5.22 and Figure 5.24) varies much less annually than the *in situ* soil moisture for

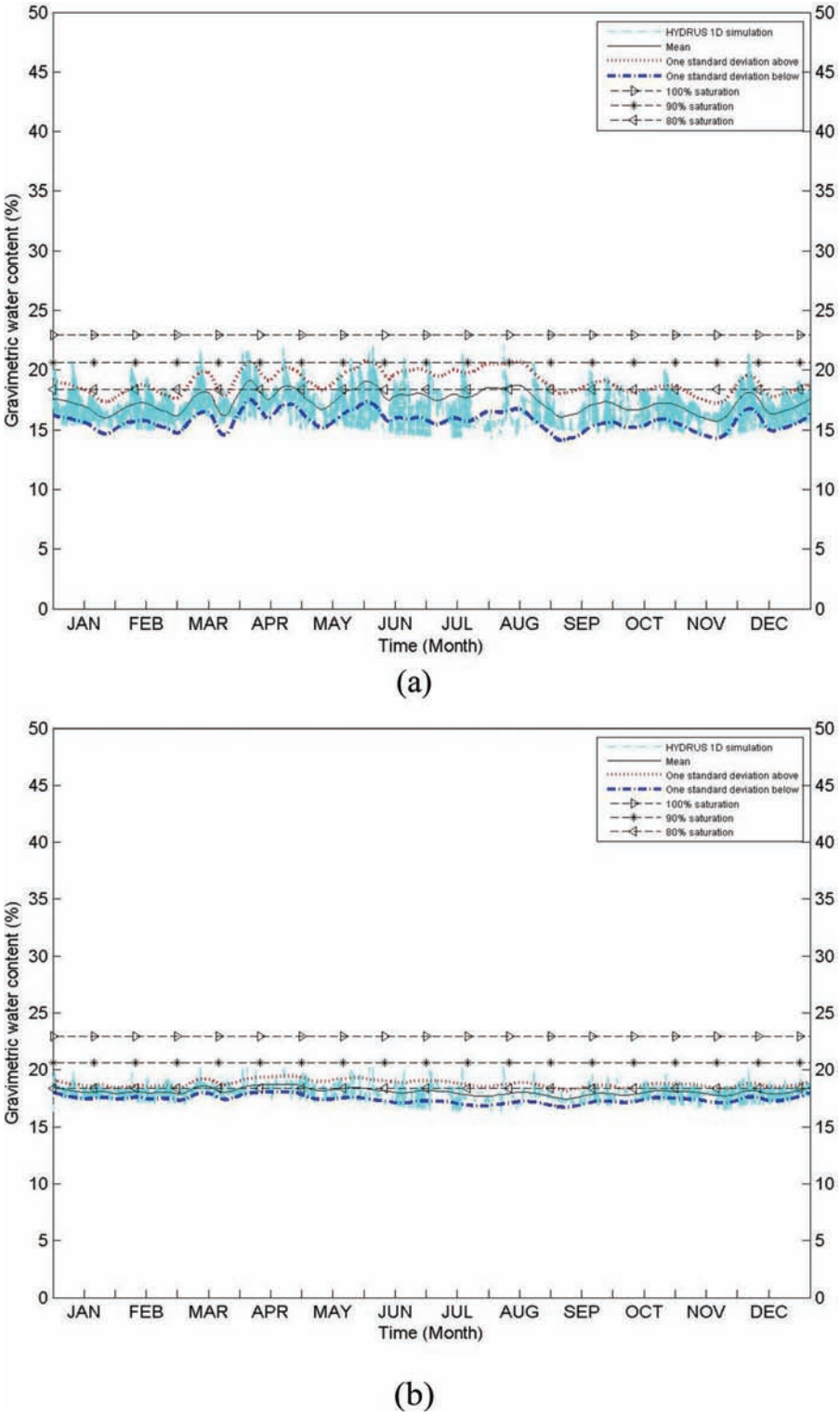

Figure 5.16 Soil moisture prediction range for LaGrange County.

coarse-grained soils (Figure 5.23). This can be attributed to the fact that the hydraulic conductivity of the fine-grained soil is much smaller than that of coarse-grained soils and, therefore, fine-grained soils have a tendency to hold on to moisture. Furthermore, for the soil moisture plots for coarse-grained soil presented in Figure 5.23, it can be seen that the moisture increases significantly and oscillates in the first half of the year (January to June), while in the second half of the year, soil moisture values are smaller. This can be attributed to the fact that: (i) for LaPorte County, the ground water table rises close to the ground surface in the first half of the year (January to

TABLE 5.2
Soil index and hydraulic properties for IGS-4 and IGS-6.

Location	Layer Depth (cm)	In Situ Density (g/cc)	Sand (%)	Silt (%)	Clay (%)	θr	θs	α	n	Saturated Hydraulic Conductivity (cm/day)	USDA Classification
Ball State (IGS-4)	0-32.5	1.66	11	60	29	0.0734	0.3799	0.0081	1.4676	2.83	silty clay loam
	32.5-60	1.65	16	44	40	0.0816	0.3905	0.0122	1.3369	2.31	silty clay
	60-230	1.77	18	50	32	0.068	0.3472	0.0116	1.3344	1.47	silty clay loam
Wabash Moraine (IGS-6)	0-35	1.58	31	50	19	0.0564	0.3589	0.0085	1.5132	6.88	silt loam
	35-85	1.64	18	42	40	0.0815	0.3916	0.0125	1.33	2.49	silty clay
	86-250	1.82	22	49	29	0.0606	0.3269	0.013	1.3048	1.3048	clay loam

June) and lowers down in the second half of the year (July to August), resulting in the higher soil moisture observed in the first half of the year, and (ii) the soil, being coarse grained, allows water to move easily through it, resulting in quick oscillations of the soil moisture.

4. From the *in situ* soil moisture vs. time plots, assess the constructability of the soil at different times of the year by comparing the OMC of the soil with the range of soil moisture values obtained from the moisture simulation plots. If the water content of the *in situ* soil is higher than the OMC, it may indicate potential constructability issues such as: (i) difficulty in achieving the desired density during compaction and (ii) difficulty in performing construction activities and maneuvering construction equipment at the construction site.
    a. For fine-grained soils, if the estimated *in situ* soil moisture is above 3% of the OMC, then potential constructability issues may be faced during construction
    b. For coarse-grained soils, if the estimated *in situ* soil moisture is above 2% of the OMC, then potential constructability issues may be faced during construction

To obtain the OMC, the one-point Proctor test (in tandem with the Purdue One-Point Proctor Program) and the INDOT family of curves (shown in Figure 5.25 or ITM 152-15T) can be used as a resource.

Consider as an example, the soil profile presented in Figure 5.20. If we assume that the soil layer at a depth of 60 cm has an OMC of 14% and a maximum dry density of 115 pcf (18 kN/m^3), then we can see from Figure 5.26 that the expected *in situ* soil moisture is higher than the (OMC +2%) from January until the month of July. Therefore, soil improvement or other remediation measures may be required in this soil profile whenever construction is scheduled to take place before the month of July.

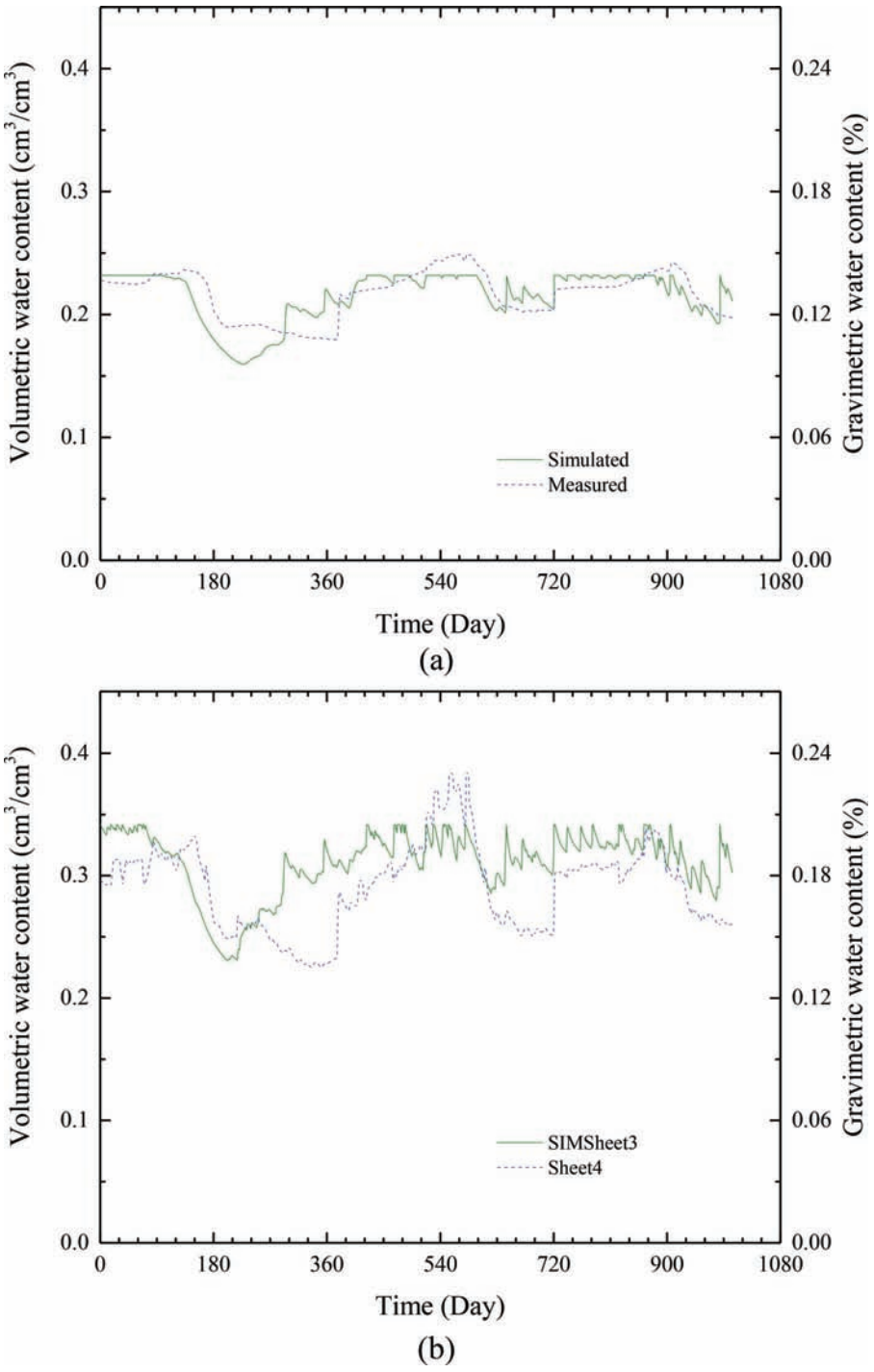

Figure 5.17 Simulated vs. measured in situ water content for wabash moraine (IGS-6) for depth of (a) 60 cm and (b) 90 cm.

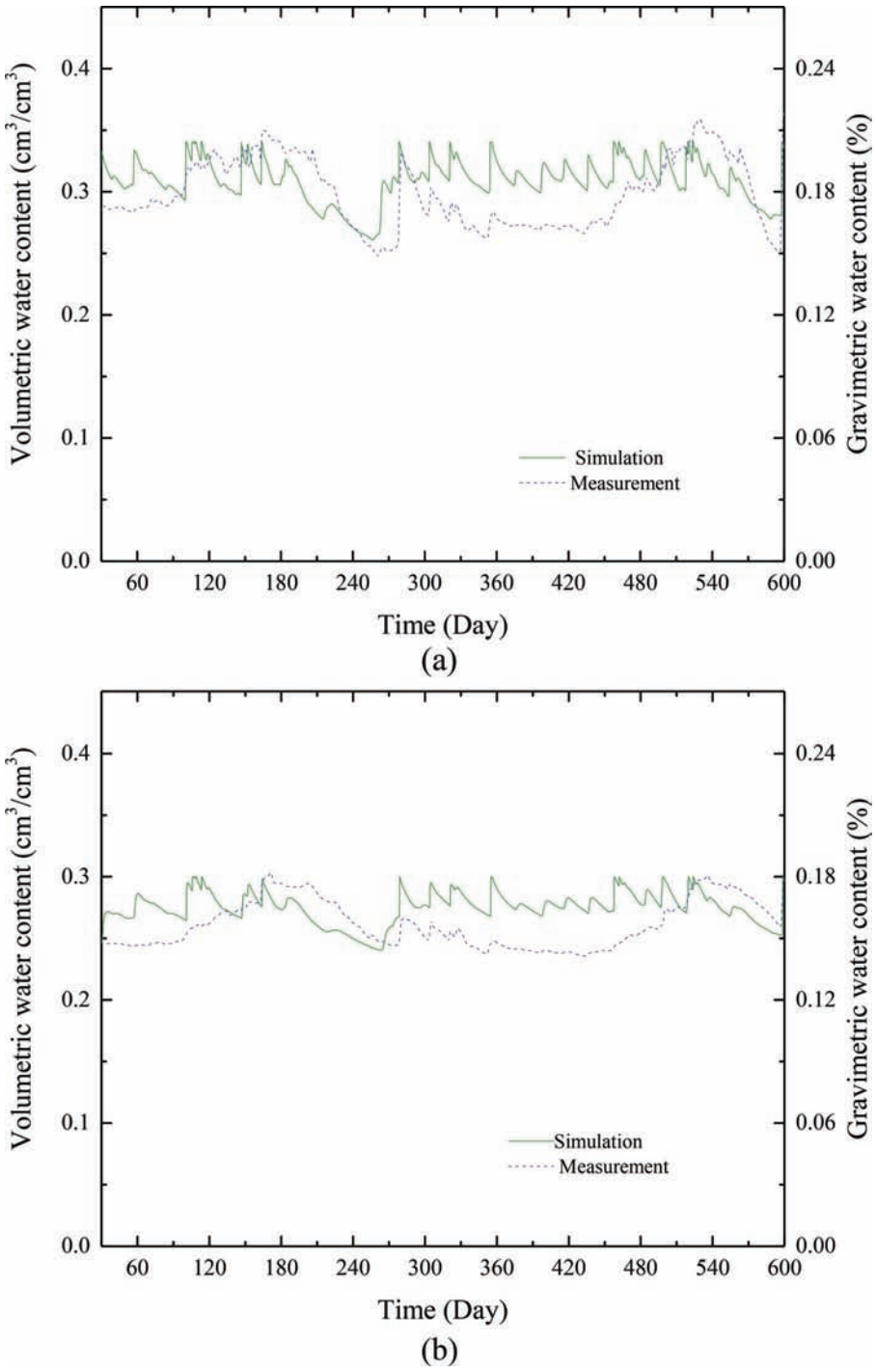

Figure 5.18 Simulated vs. measured in situ water content for Ball State (IGS-4) for depth of (a) 60 cm and (b) 90 cm.

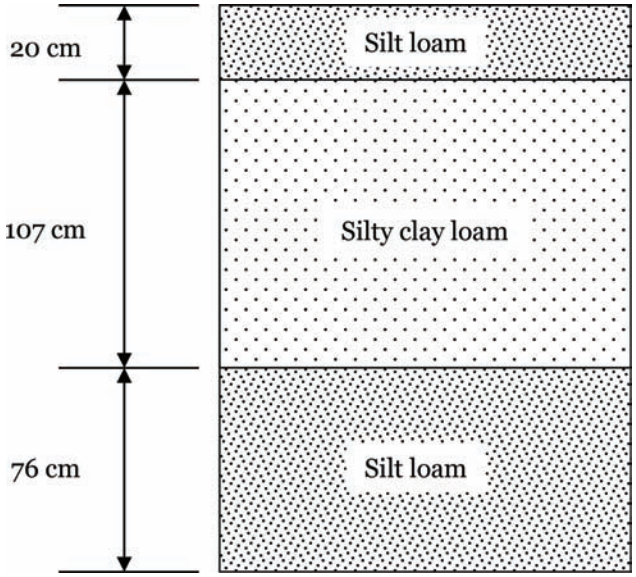

Figure 5.19 Selected soil profile for Gibson County.

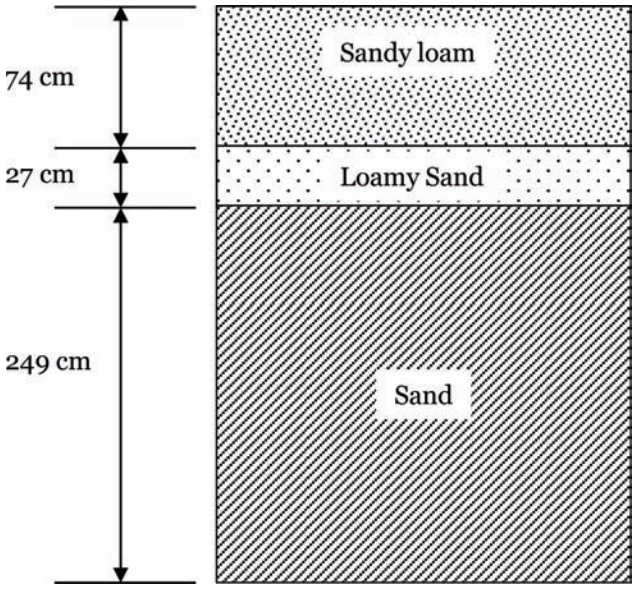

Figure 5.20 Selected soil profile for LaPorte County.

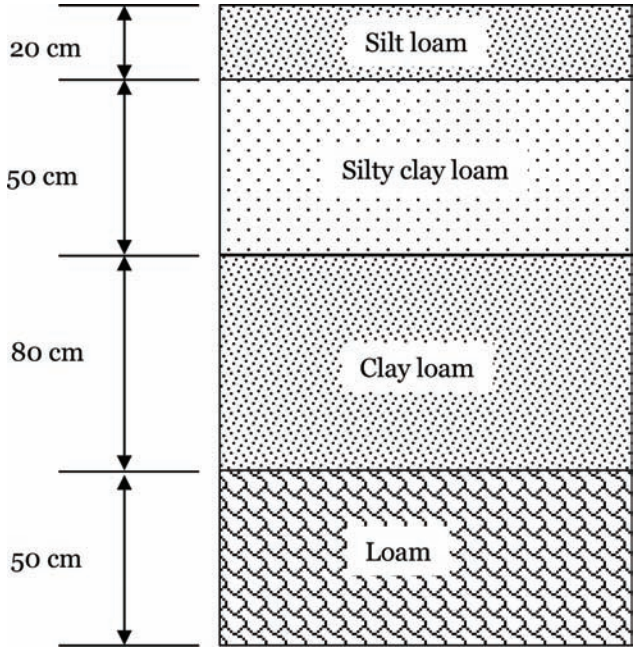

Figure 5.21 Selected soil profile for Fayette County.

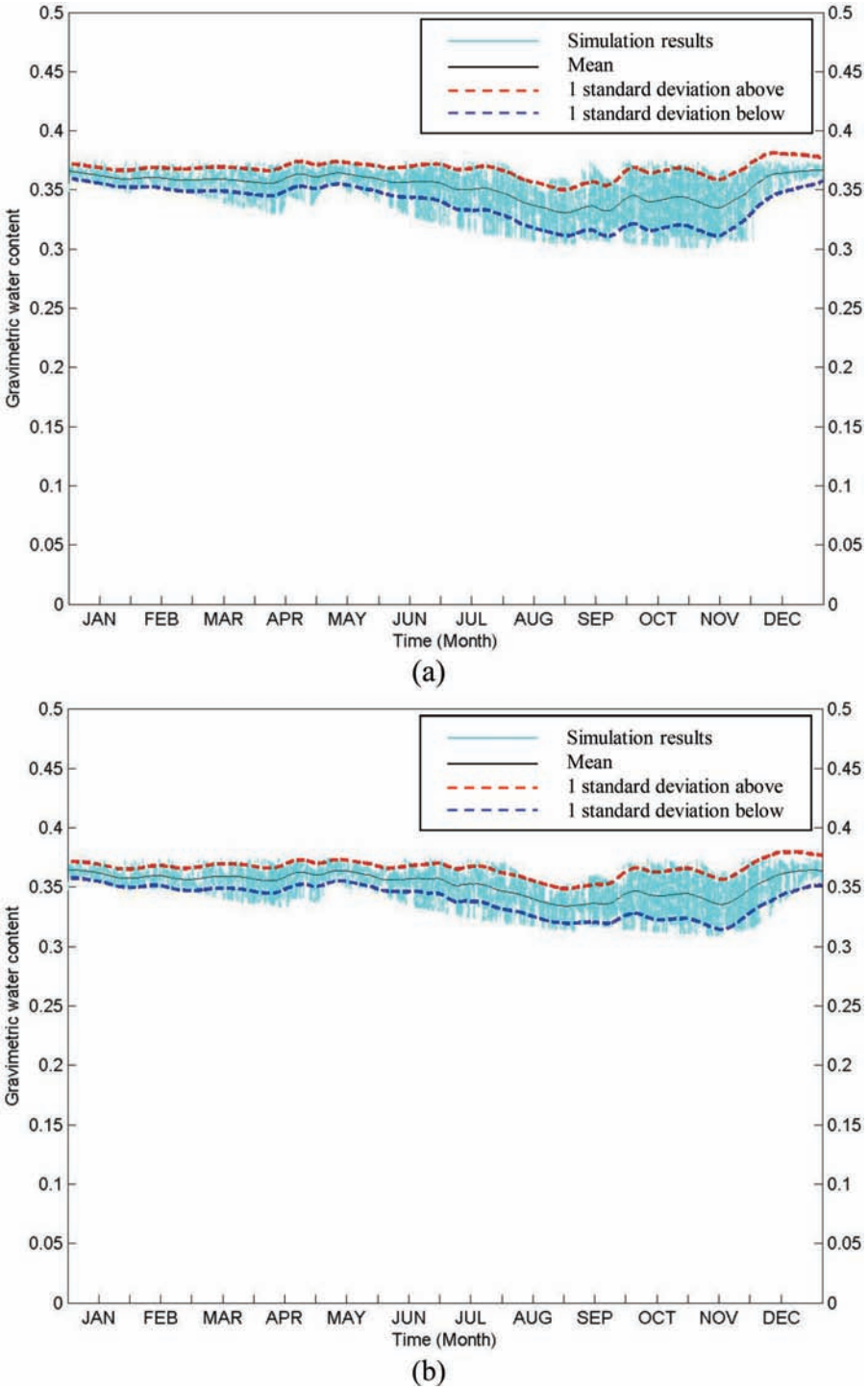

Figure 5.22 Soil moisture variation based on 10 years of weather and ground water table data for soil profile selected for Gibson County at depth of: (a) 60 cm and (b) 90 cm from the ground surface.

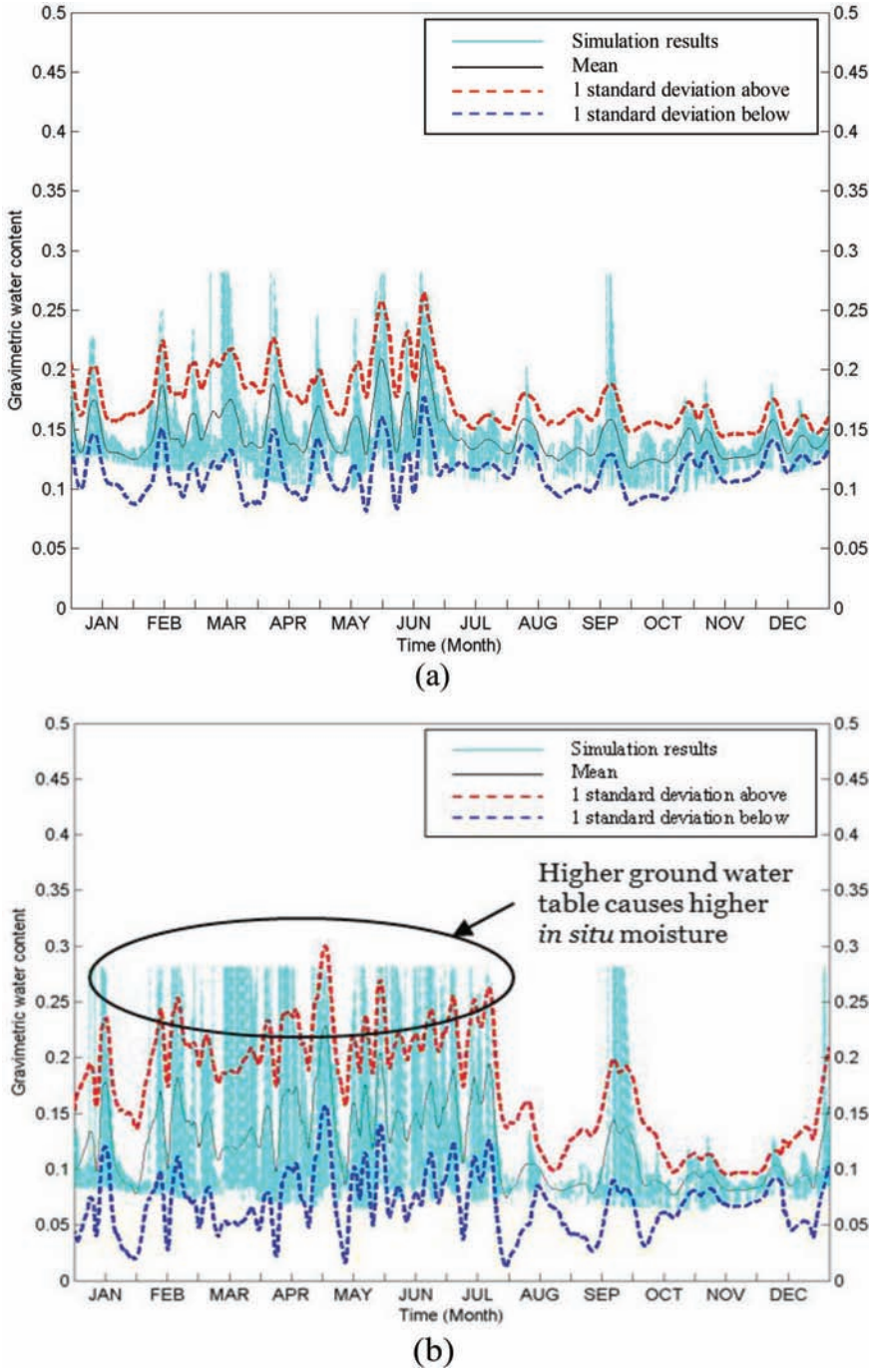

Figure 5.23 Soil moisture variation based on 10 years of weather and ground water table data for soil profile selected for LaPorte County at depth of: (a) 60 cm and (b) 90 cm from the ground surface.

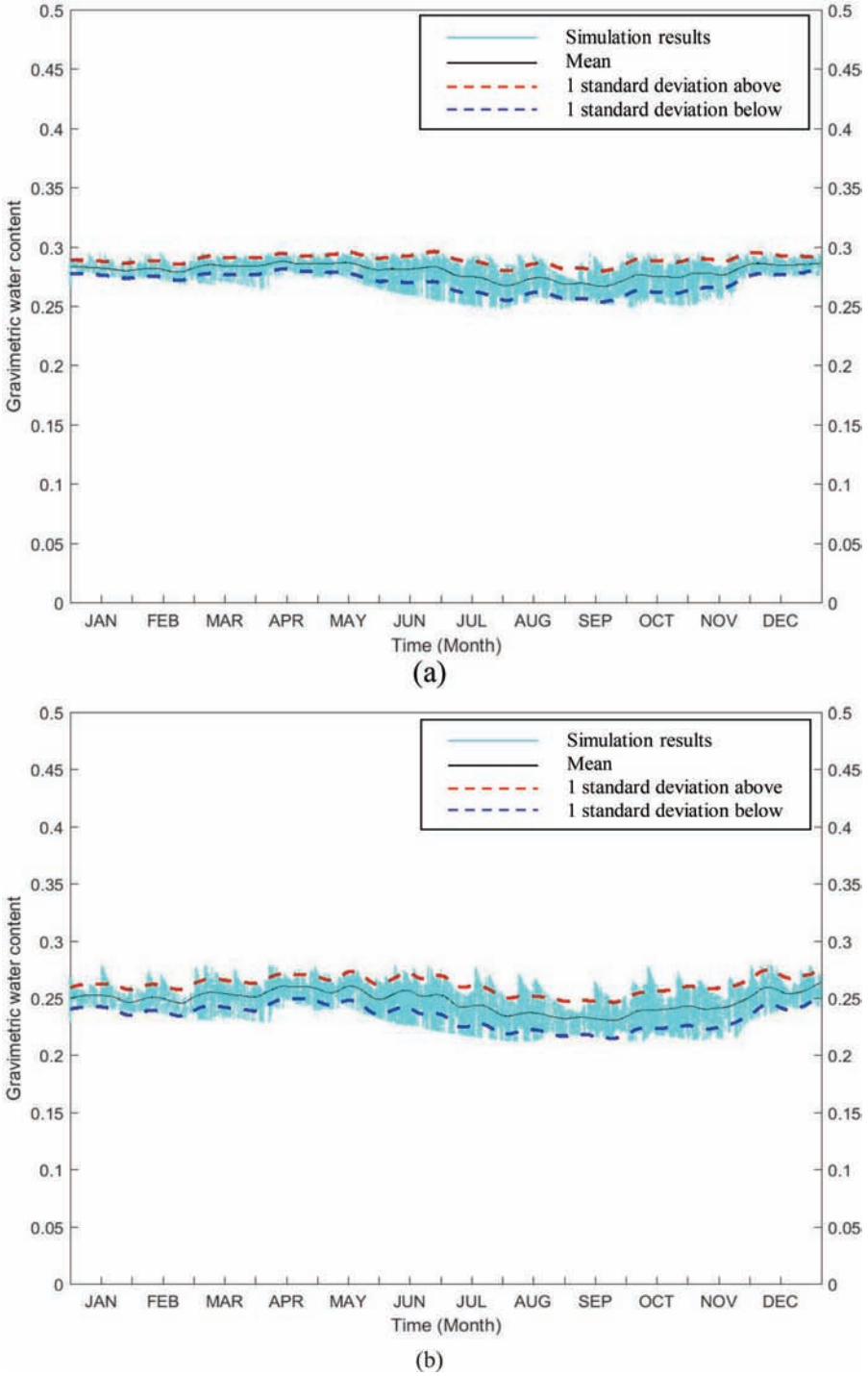

Figure 5.24 Soil moisture variation based on 10 years of weather and ground water table data for soil profile selected for Fayette County at depth of: (a) 60 cm and (b) 90 cm from the ground surface.

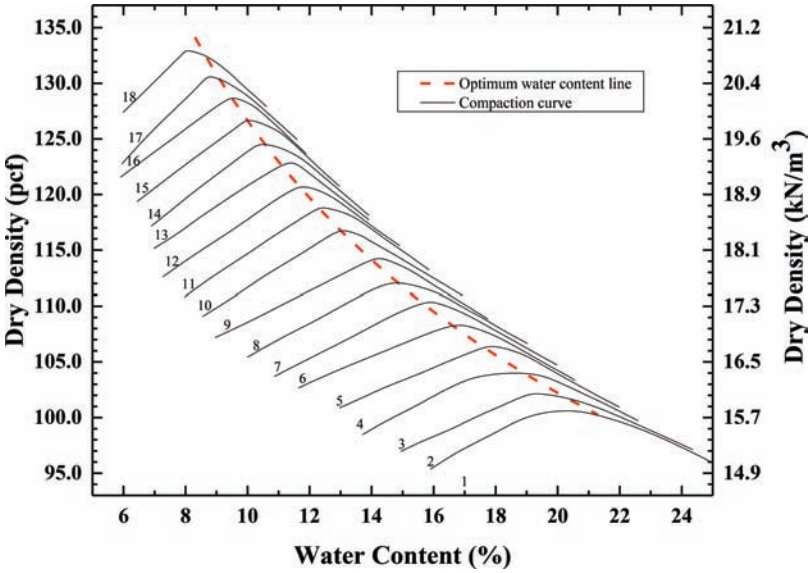

Figure 5.25 INDOT family of curves for standard proctor compaction.

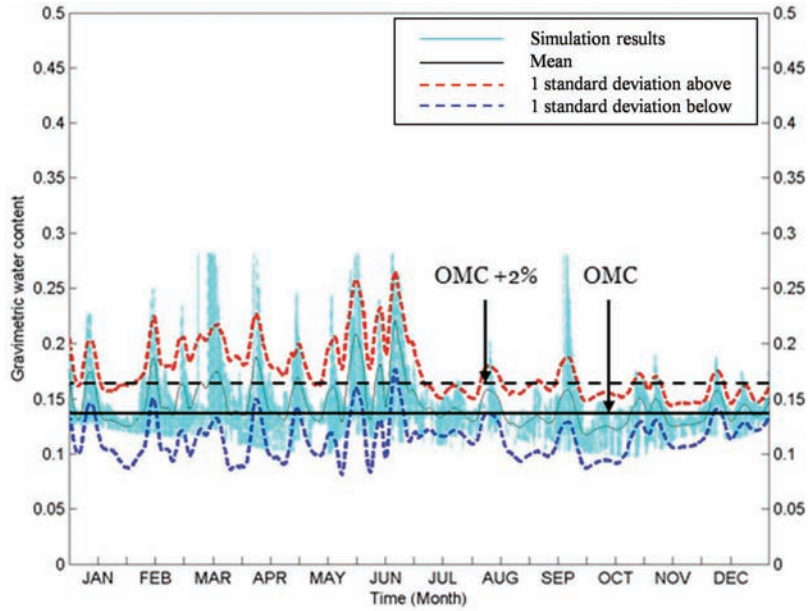

Figure 5.26 Yearly soil moisture vs. time plot and OMC for comparison at a depth of 60 cm for a soil profile located in LaPorte County.

6. CONCLUSIONS AND RECOMMENDATIONS

The presence of excessive soil moisture hinders earthwork construction activities. Inability to predict the soil moisture before the start of construction activities causes increase in cost of construction and sometimes project completion delays. It is important to assess constructability at a site based on the expected *in situ* soil moisture conditions at the construction phase of a project. This requires a prediction methodology to estimate the soil water content at depths of interest at any time of the year.

Simulations were performed using HYDRUS-1D to estimate the soil moisture near the ground surface at specific times of the year. Determination of the hydraulic properties for all the soil layers within the depth of interest is necessary to obtain reliable soil moisture predictions. The hydraulic properties of the soil profiles considered in this report were estimated based on their textural classification and index properties. To validate the process of determining the soil moisture at any depth from the numerical simulations with soil hydraulic properties estimated from soil texture data, the simulation results were compared with measured water content data for Wabash moraine site (IGS-5) in Allen County and Ball state site (IGS-6) in Delaware County. The comparison between the measured data and the simulated results showed good agreement. This methodology was followed by simulations of water flow through unsaturated soil for soil profiles representative of every county in Indiana. These simulations were performed using 10 years of weather and ground water table data. The SSURGO database created by USDA was used to obtain multiple representative soil profiles for each county in Indiana based on the area covered. Weather and water table data for the past 10 years were collected from the Indiana Climate Office and DNR, respectively. A statistical deviation of one standard deviation was applied above and below the predicted average soil moisture for a period of 10 years. Constructability of soil was determined by comparing the estimated *in situ* soil water content with the optimum value required for compaction. Based on INDOT specifications, if the *in situ* soil moisture is above 2% of optimum, then a poor constructability rating is given to coarse-grained soil. In case of fine-grained soils, a poor constructability rating is given when the *in situ* soil moisture is 3% above of optimum.

The methodology can be implemented in the field by use of the soil moisture prediction plots provided in the appendices of this report for each county in the state of Indiana. The geotechnical engineers at INDOT at the time of design can use these plots to obtain the expected *in situ* soil moisture at the construction phase of a project and account for the expected soil water content in their design considerations. This methodology of rating the constructability of *in situ* soils based on the estimated water content at any depth and time of the year is useful when INDOT is preparing construction contracts. The proposed methodology can be further improved by (i) consideration of the topography and vegetation of each county in Indiana, (ii) inclusion of additional soil profiles with better soil property characterization throughout the state, and (iii) implementation of the developed methodology for soil moisture estimation in pilot projects to fine-tune and refine the methodology proposed herein.

7. ACKNOWLEDGMENTS

This research was funded with the support provided by the Indiana Department of Transportation through the Joint Transportation Research Program at Purdue University. The authors would like to thank the agency for the support.

The authors would like to thank Mr. Athar Khan, Mr. Nayyar Zia, Dr. Tommy Nantung, Mr. Kumar Dave, Mr. Tom Duncan for their useful inputs and their support during the project. We are also very grateful for the assistance we received from Mr. Iqbal Khan, and Mr. Brian Dunbar for laboratory testing carried out during the project duration. Last but not the least, the authors would like to thank Mr. Kevin Ellett (Indiana Geological Survey) and Mr. Shawn Naylor Ellett (Indiana Geological Survey) for the help received during field testing and sampling at the test sites maintained by IGS.

REFERENCES

ASTM D6836. (2008). *Standard test methods for determination of the soil water characteristic curve for desorption using a hanging column, pressure extractor, chilled mirror hygrometer, and/or centrifuge*. West Conshohocken, PA: ASTM International.

Blight, G. E. (2013). Interactions between the atmosphere and the Earth's surface: Destructive interactions—Water and wind erosion, piping erosion. In *Unsaturated soil mechanics in geotechnical practice* (pp. 263–310). London, UK: Taylor & Francis. http://dx.doi.org/10.1201/b15239-6

Chen, M., Willgoose, G. R., & Saco, P. M. (2014). Spatial prediction of temporal soil moisture dynamics using HYDRUS-1D. *Hydrological Processes*, *28*(2), 171–185. http://dx.doi.org/10.1002/hyp.9518

Childs, E. C., & Collis-George, N. (1950). The permeability of porous materials. In *Proceedings of the Royal Society A: Mathematical, Physical and Engineering Sciences*, *201*(1066), 392–405. http://dx.doi.org/10.1098/rspa.1950.0068

Feddes, R., & Zaradny, H. (1977). *Numerical model for transient water flow in non-homogeneous soil-root systems with groundwater influence*. Wageningen, The Netherlands: ICW Publications.

Fredlund, D. G., Rahardjo, H., & Fredlund, M. D. (2012a). Soil-water characteristic curves for unsaturated soils. *Unsaturated soils in engineering practice* (pp. 184–272). Hoboken, NJ: John Wiley & Sons. http://dx.doi.org/10.1002/9781118280492.ch5

Fredlund, D. G., Rahardjo, H., & Fredlund, M. D. (2012b). Theory of water flow through unsaturated soils. In *Unsaturated soils in engineering practice* (pp. 327–374). Hoboken, NJ: John Wiley & Sons. http://dx.doi.org/10.1002/9781118280492.ch7

Fredlund, D. G., Rahardjo, H., & Fredlund, M. D. (2012c). Theory to practice of unsaturated soil mechanics. In *Unsaturated soils in engineering practice* (pp. 1–28). Hoboken, NJ: John Wiley & Sons. http://dx.doi.org/10.1002/9781118280492.ch1

Fredlund, D. G., Rahardjo, H., & Fredlund, M. D. (2012d). *Unsaturated soil mechanics in engineering practice*. Hoboken, NJ: John Wiley & Sons. http://dx.doi.org/10.1002/9781118280492

Gorthi, S. (2011). *Prediction models for estimation of moisture content* (Master's thesis). Logan, UT: Utah State Univerity.

Holtz, R. D., Kovacs, W. D., & Sheahan, T. C. (2010). *An introduction to geotechnical engineering*. Englewood Cliffs, NJ: Prentice Hall.

Hu, Z., Islam, S., & Cheng, Y. (1997). Statistical characterization of remotely sensed soil moisture images. *Remote Sensing of Environment*, *61*(2), 310–318.

Lourenço, S. D. N., Toll, D. G., Augarde, C. E., Gallipoli, D., Congreve, A., Smart, T., & Evans, F. D. (2008). Observations of unsaturated soils by Environmental Scanning Electron Microscopy in dynamic mode. In *Unsaturated soils: Advances in geo-engineering—Proceedings of the 1st European conference*. London, UK: Taylor & Francis. http://dx.doi.org/10.1201/9780203884430.ch15

Mohan, V. K. D., Prezzi, M., & McCullouch, B. (2011). *Analysis of change orders in geotechnical engineering work at INDOT* (Joint Transportation Research Program Publication No. FHWA/IN/JTRP-2011/10). West Lafayette, IN: Purdue University. http://dx.doi.org/10.5703/1288284314623

Monteith, J. L. (1965). Evaporation and environment. *Symposia of the Society for Experimental Biology*, *19*(4), 205–224.

Naylor, S., Letsinger, S., Ficklin, D., Ellet, K., & Olyphant, G. (2014). A hydropedological approach to quantifying groundwater recharge in various glacial setting of the mid-continental USA. *Hydrological Processes*, *30*(10), 1594–1608. http://dx.doi.org/10.1002/hyp.10718

Nichols, S., Zhang, Y., & Ahmad, A. (2011). Review and evaluation of remote sensing methods for soil-moisture estimation. *Journal of Photonics for Energy, Spie Reviews*, *2*, 28001. http://dx.doi.org/10.1117/1.3534910

Njoku, E. G., & Entekhabi, D. (1996). Passive microwave remote sensing of soil moisture. *Journal of Hydrology*, *184*(1–2), 101–129. http://dx.doi.org/10.1016/0022-1694(95)02970-2

Richards, L. A. (1931). Capillary conduction of liquids through porous mediums. *Journal of Applied Physics*, *1*(5), 318–333. http://dx.doi.org/10.1063/1.1745010

Rodriguez, A. R., del Castillo, H., & Sowers, G. F. (1988). *Soil mechanics in highway engineering*. Clausthal-Zellerfeld, Federal Republic of Germany: Trans Tech Publications.

Schaap, M. G., Leij, F. J., & van Genuchten, M. T. (2001). Rosetta: A computer program for estimating soil hydraulic parameters with hierarchical pedotransfer functions. *Journal of Hydrology*, *251*(3–4), 163–176. http://dx.doi.org/10.1016/S0022-1694(01)00466-8

Schaap, M. G., Leij, F. J., & van Genuchten, M. Th. (1998). Neural network analysis for hierarchical prediction of soil hydraulic properties. *Soil Science Society of America Journal*, *62*, 847–855.

Schindler, U., Durner, W., von Unold, G., & Müller, L. (2010). Evaporation method for measuring unsaturated hydraulic properties of soils: Extending the measurement range. *Soil Science Society of America Journal*, *74*(4), 1071. http://dx.doi.org/10.2136/sssaj2008.0358

Šimůnek, J., Šejna, M., Saito, H., Sakai, M., & van Genuchten, M. Th. (2013). *The Hydrus-1D software package for simulating the movement of water, heat, and multiple solutes in variably saturated media* (Version 4.16, HYDRUS Software Series 3). Riverside, CA: Department of Environmental Sciences, University of California Riverside.

Van Genuchten, M. T. (1980). A closed-form equation for predicting the hydraulic conductivity of unsaturated soils. *Soil Science Society of America Journal*, *44*(5), 892–898. http://dx.doi.org/10.2136/sssaj1980.03615995004400050002x

Wesseling, J. (1991). *CAPSEV: Steady state moisture flow theory: Program description: User manual*. Wageningen, The Netherlands: The Winand Staring Centre.

APPENDIX A: SOIL MOISTURE SIMULATIONS

In this appendix the simulations are represented for soil moisture at depths of 60 and 90 cm from ground surface. Counties have been arranged alphabetically. Soil profiles used for simulation are presented in Appendix B.

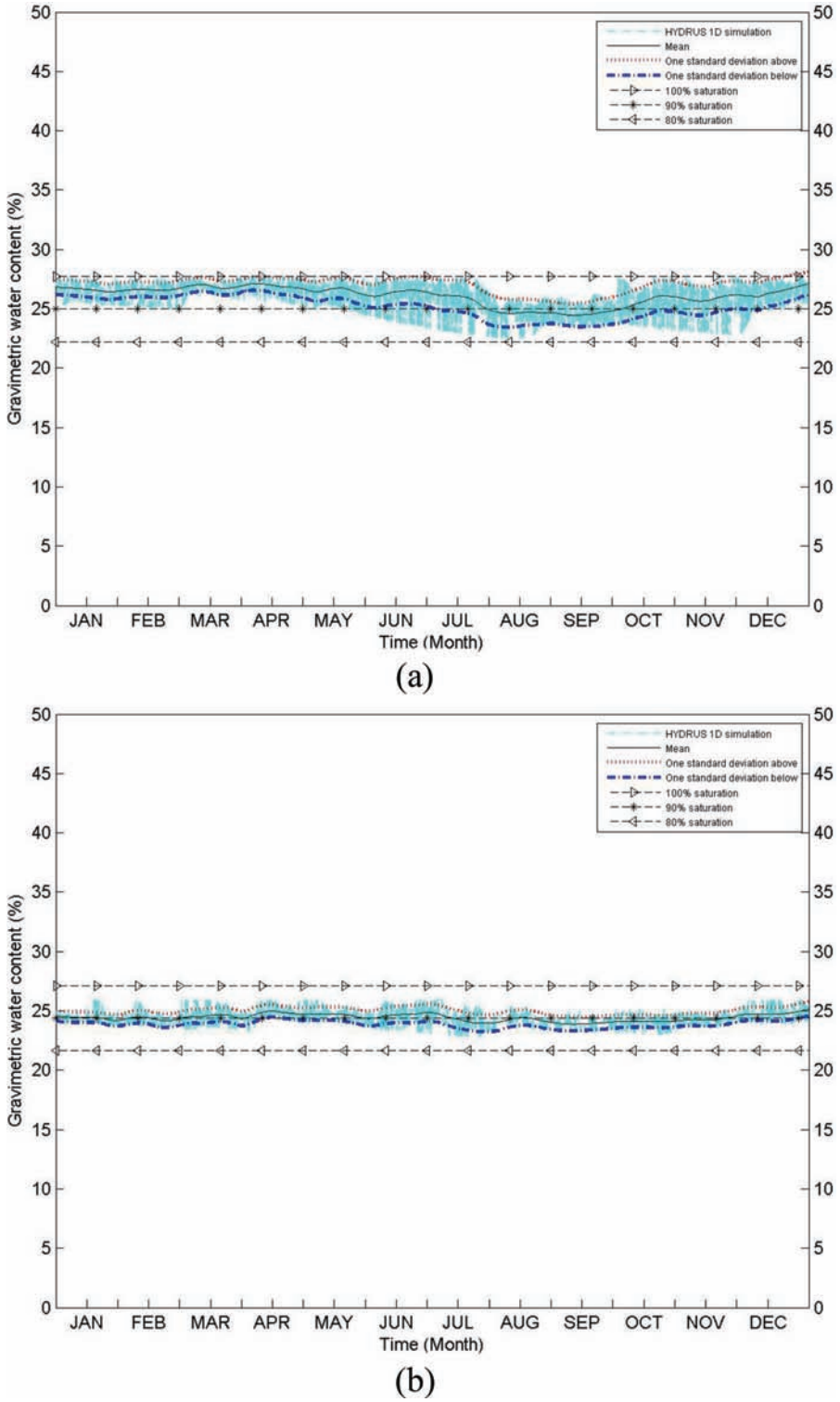

Figure A.1 Annual soil moisture variation for (a) 60 cm depth and (b) 90 cm depth for Adams County for profile (ADA-1).

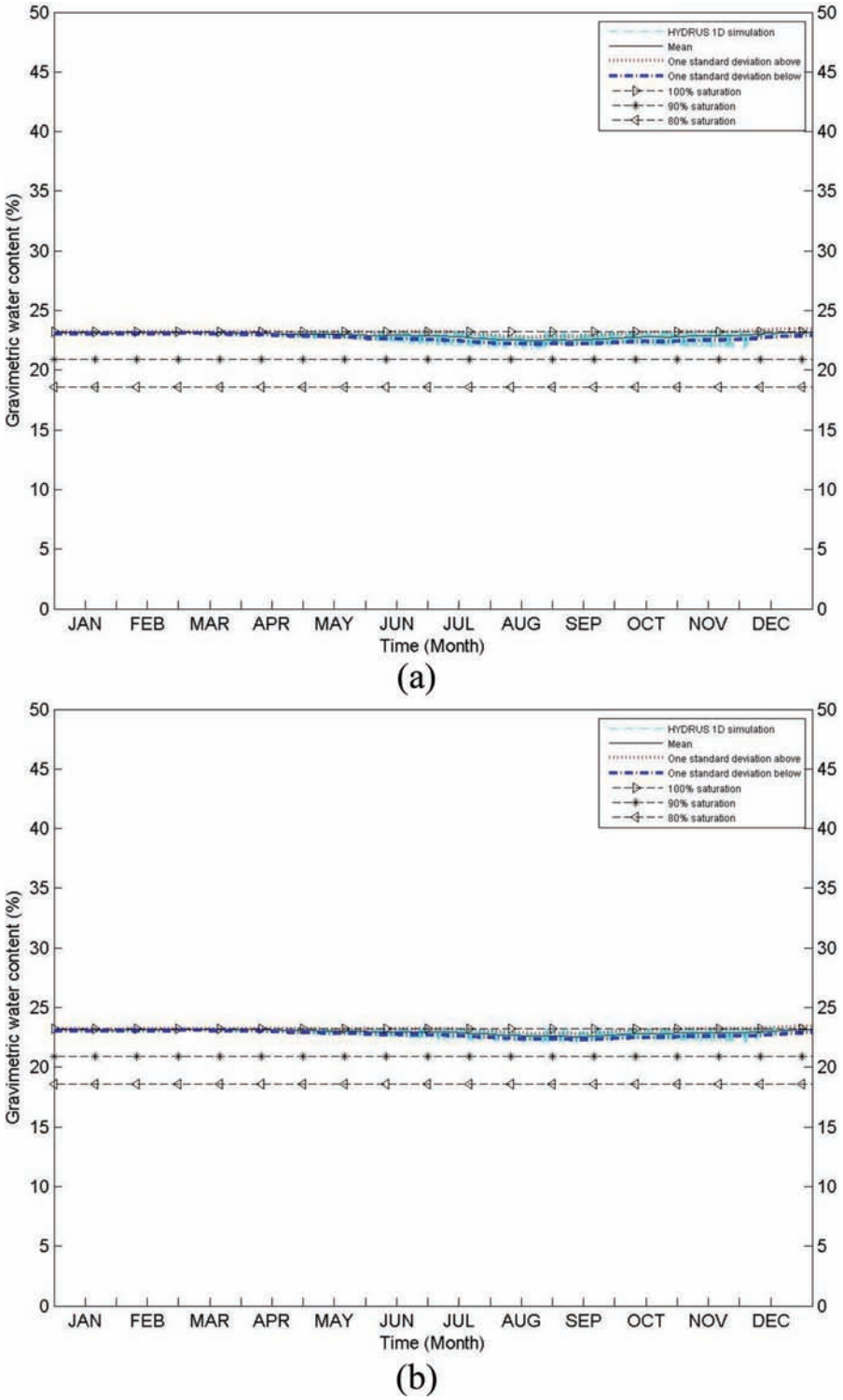

Figure A.2 Annual soil moisture variation for (a) 60 cm depth and (b) 90 cm depth for Allen County for profile (ALL-1).

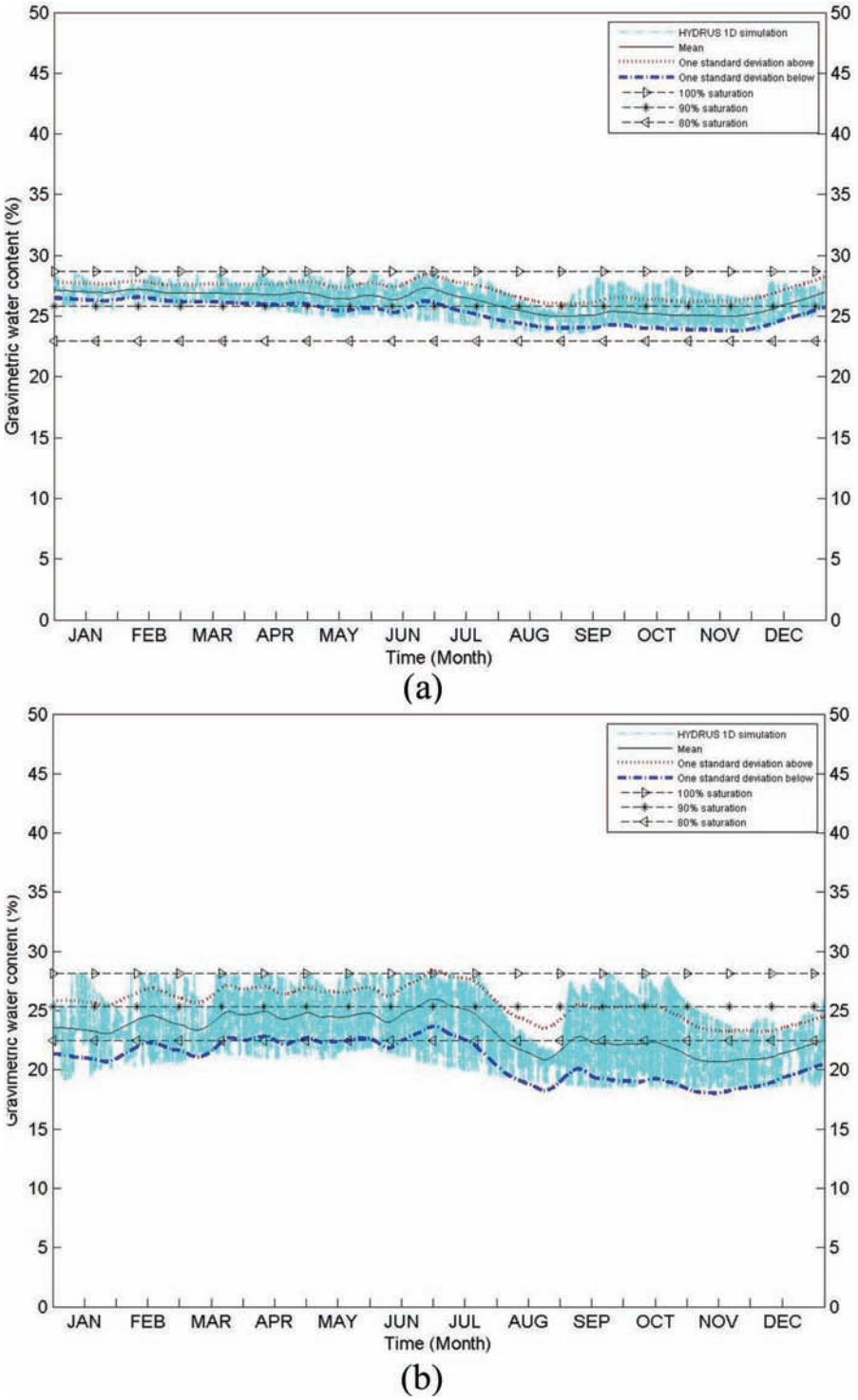

Figure A.3 Annual soil moisture variation for (a) 60 cm depth and (b) 90 cm depth for Benton County for profile (BEN-1).

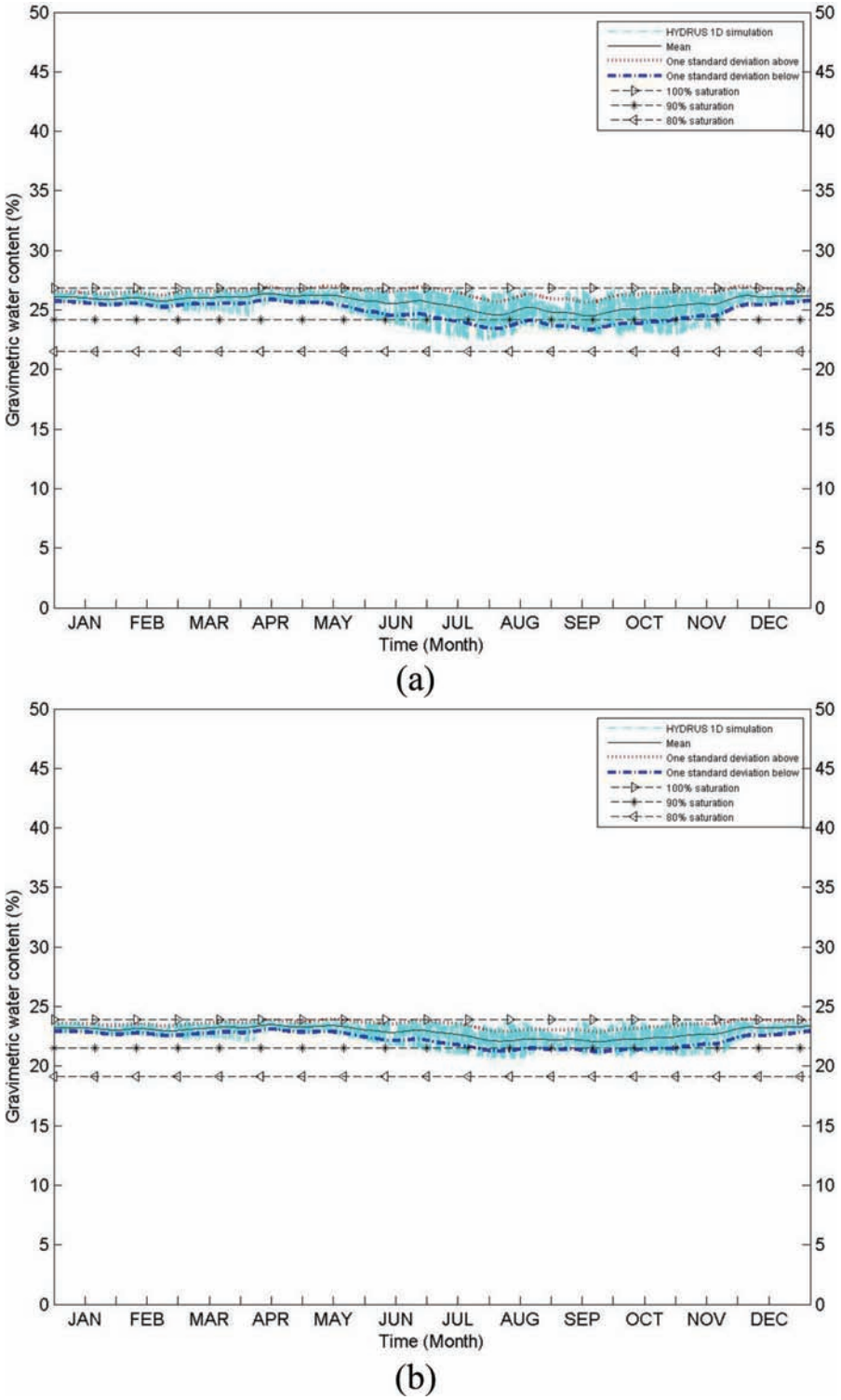

Figure A.4 Annual soil moisture variation for (a) 60 cm depth and (b) 90 cm depth for Blackford County for profile (BLA-1).

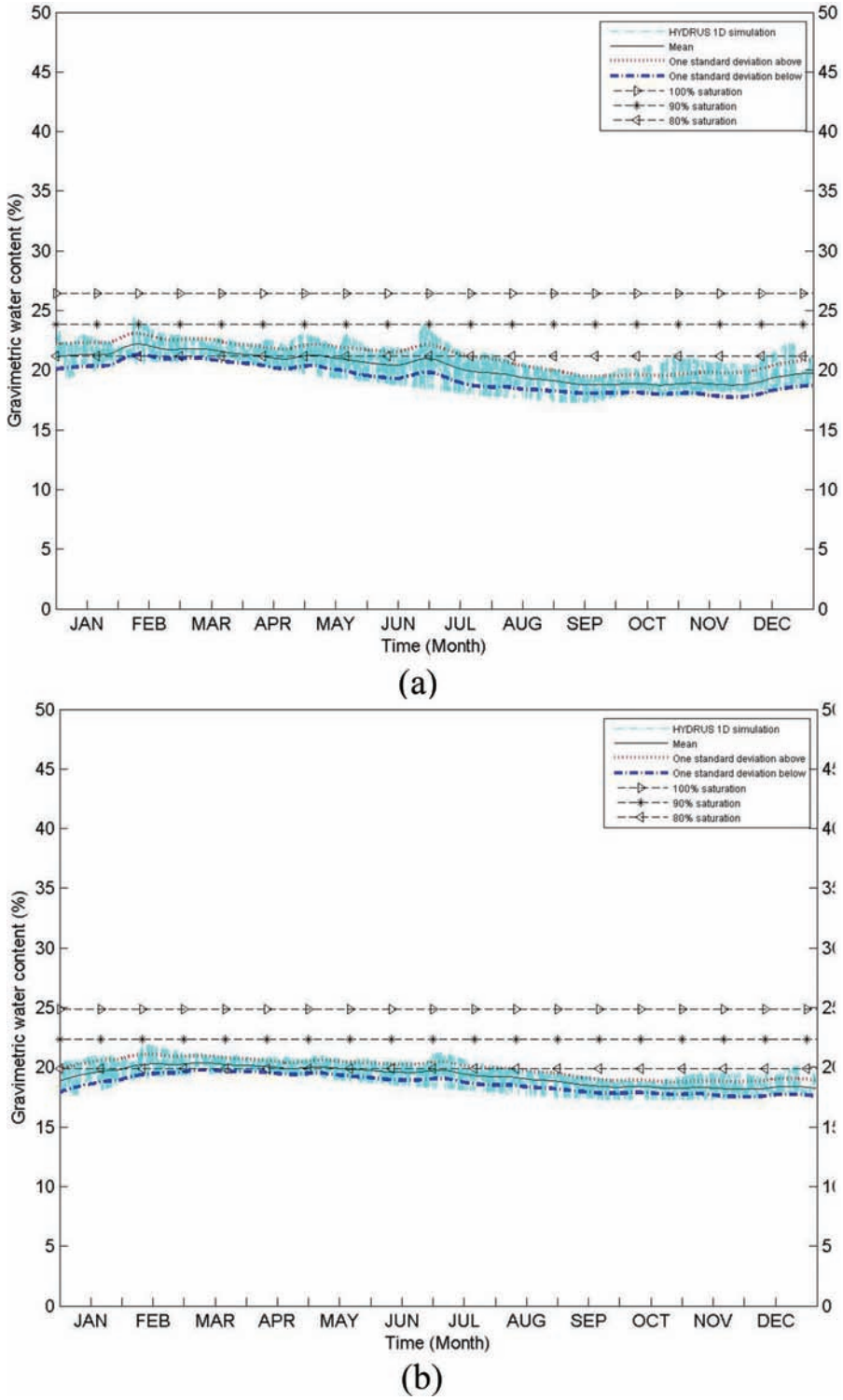

Figure A.5 Annual soil moisture variation for (a) 60 cm depth and (b) 90 cm depth for Boone County for profile (BOO-1).

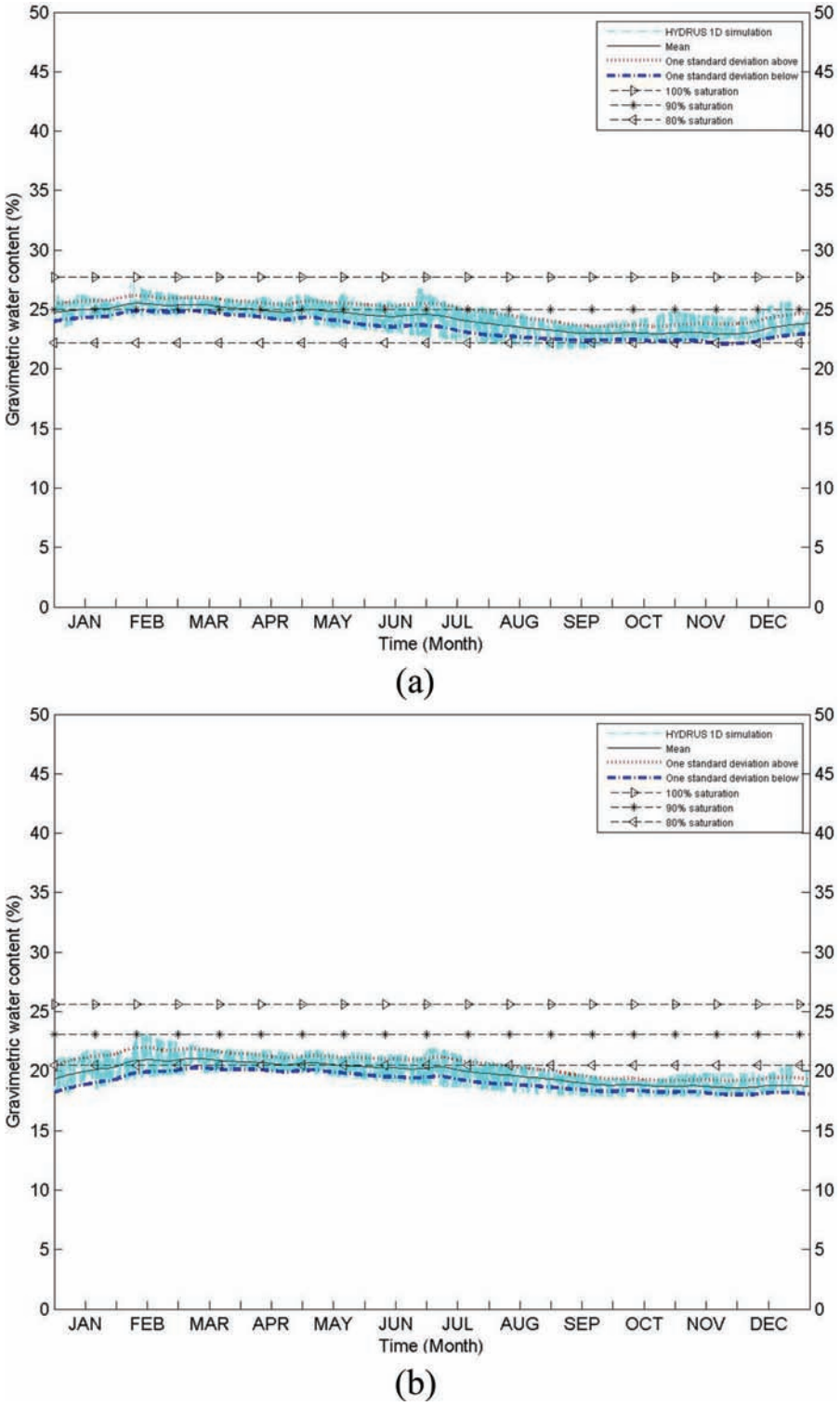

Figure A.6 Annual soil moisture variation for (a) 60 cm depth and (b) 90 cm depth for Carrol County for profile (CAR-1).

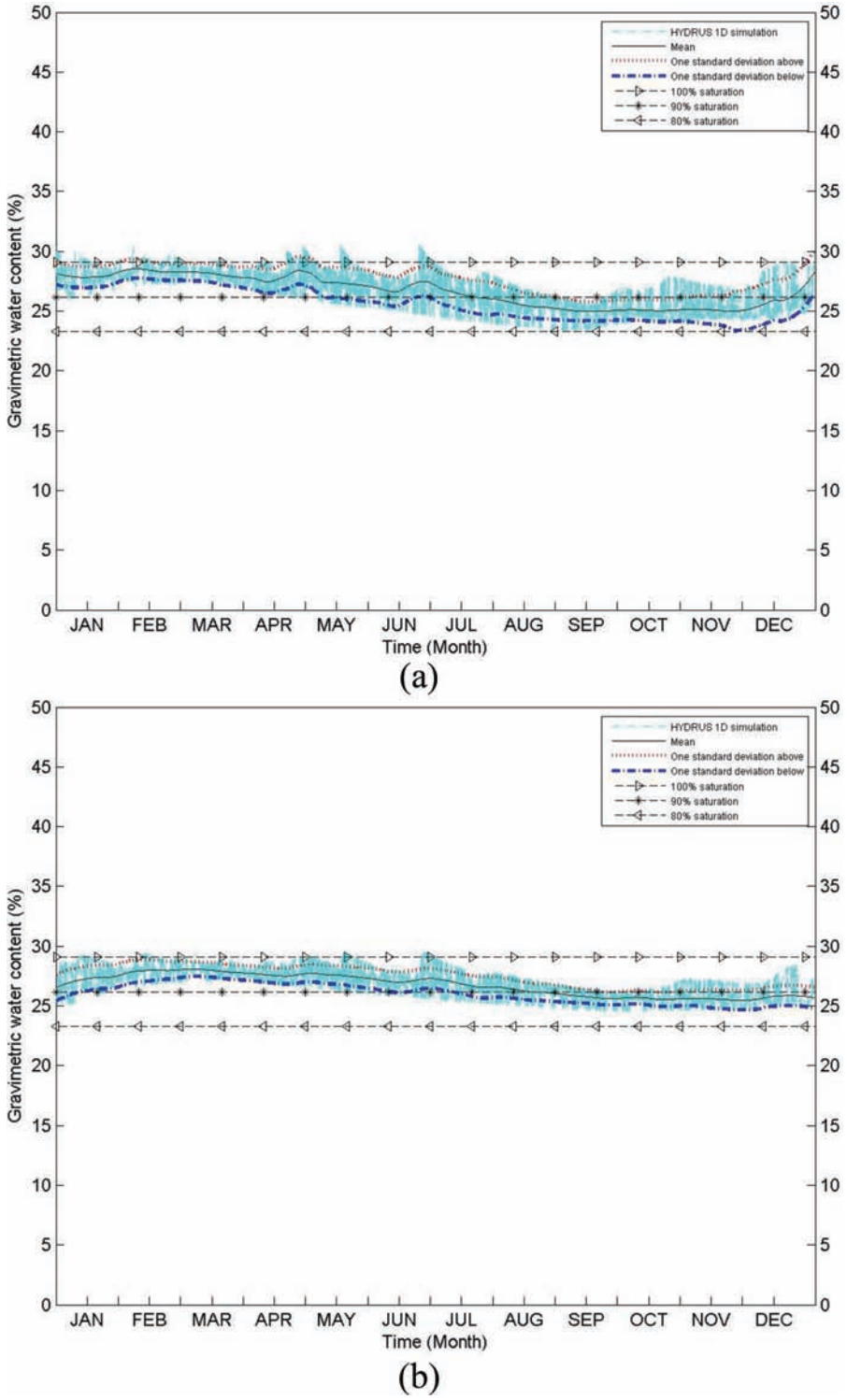

Figure A.7 Annual soil moisture variation for (a) 60 cm depth and (b) 90 cm depth for Cass County for profile (CAS-1).

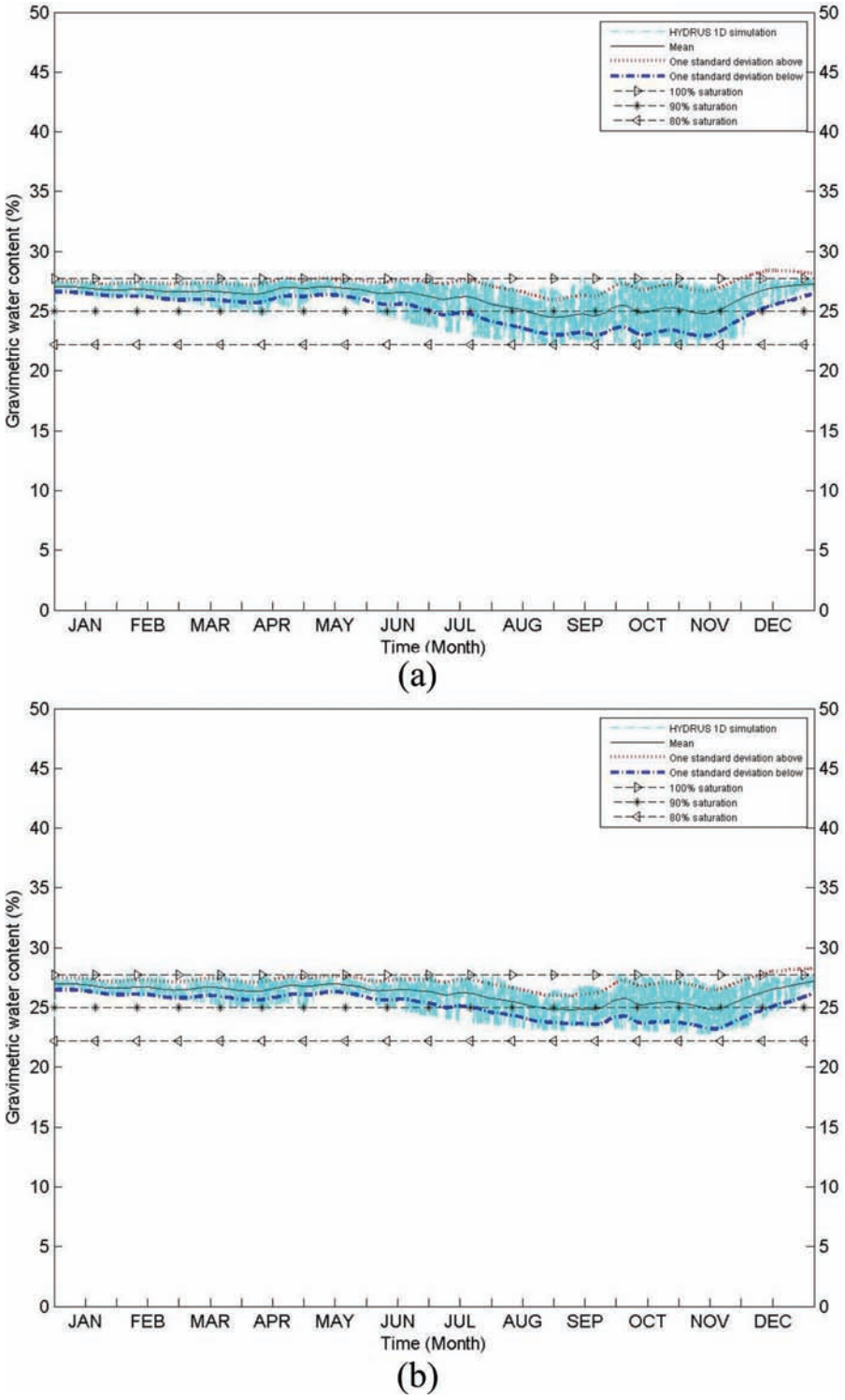

Figure A.8 Annual soil moisture variation for (a) 60 cm depth and (b) 90 cm depth for Clay County for profile (CLA-1).

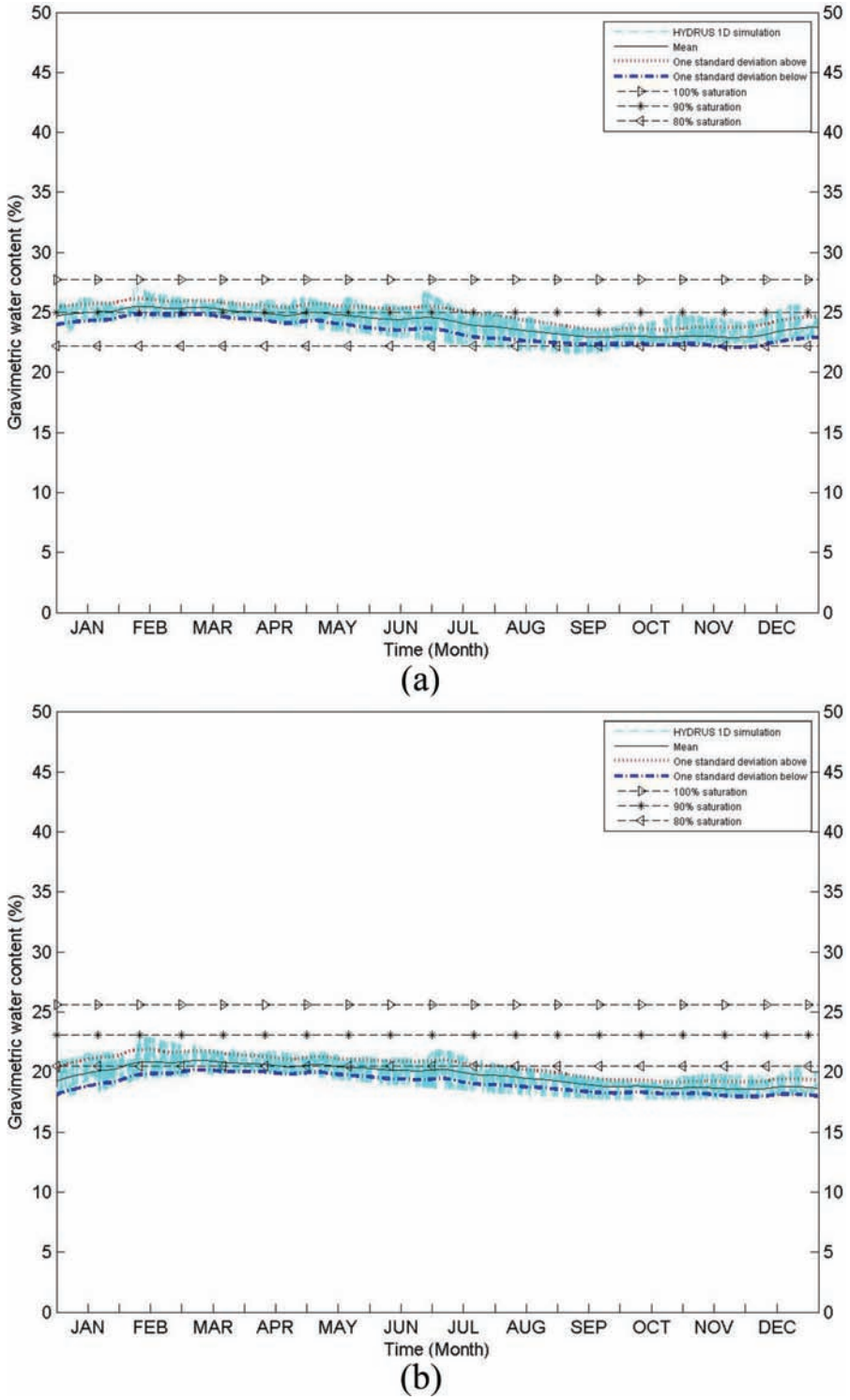

Figure A.9 Annual soil moisture variation for (a) 60 cm depth and (b) 90 cm depth for Clinton County for profile (CLI-1).

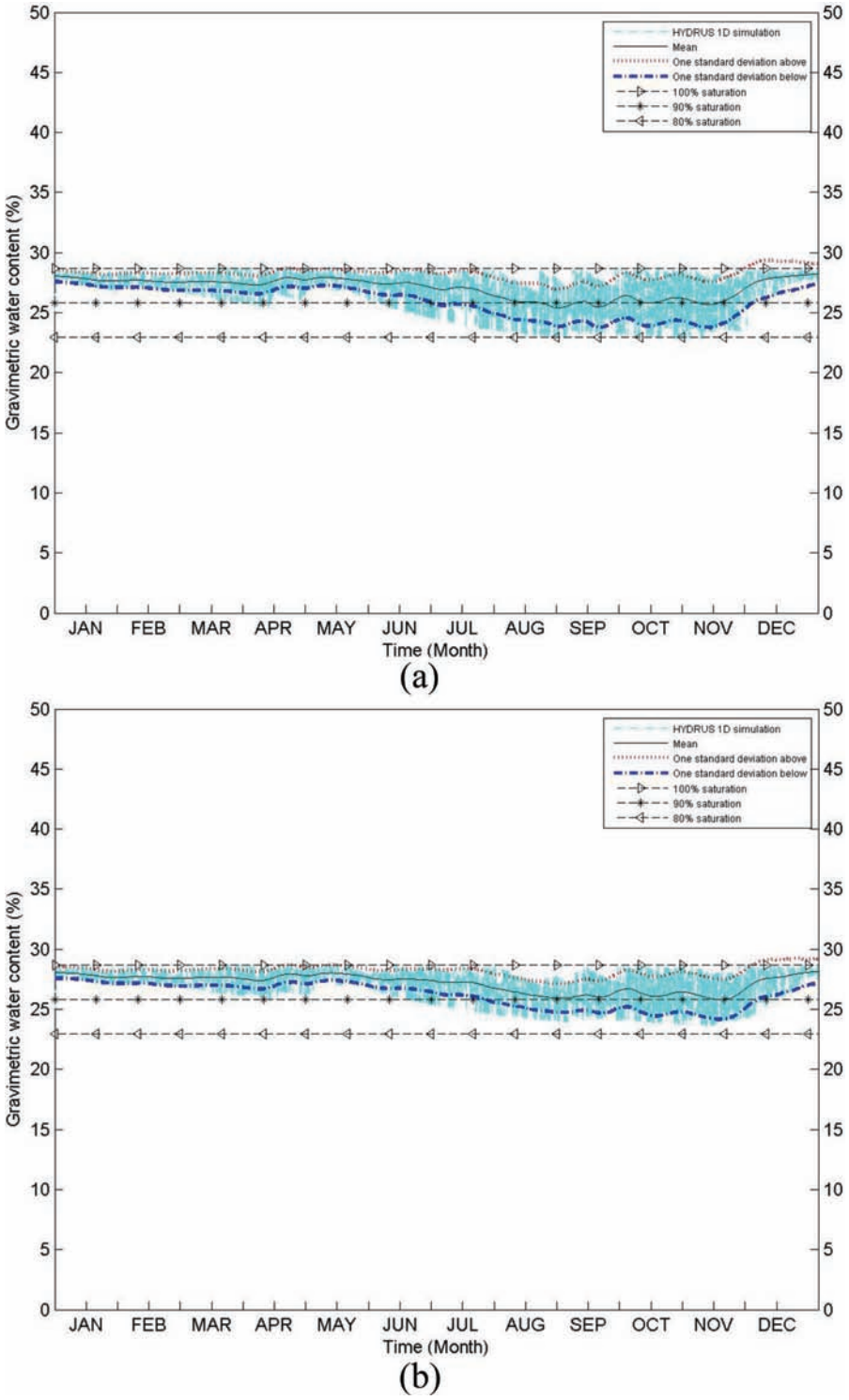

Figure A.10 Annual soil moisture variation for (a) 60 cm depth and (b) 90 cm depth for Crawford County for profile (CRA-1).

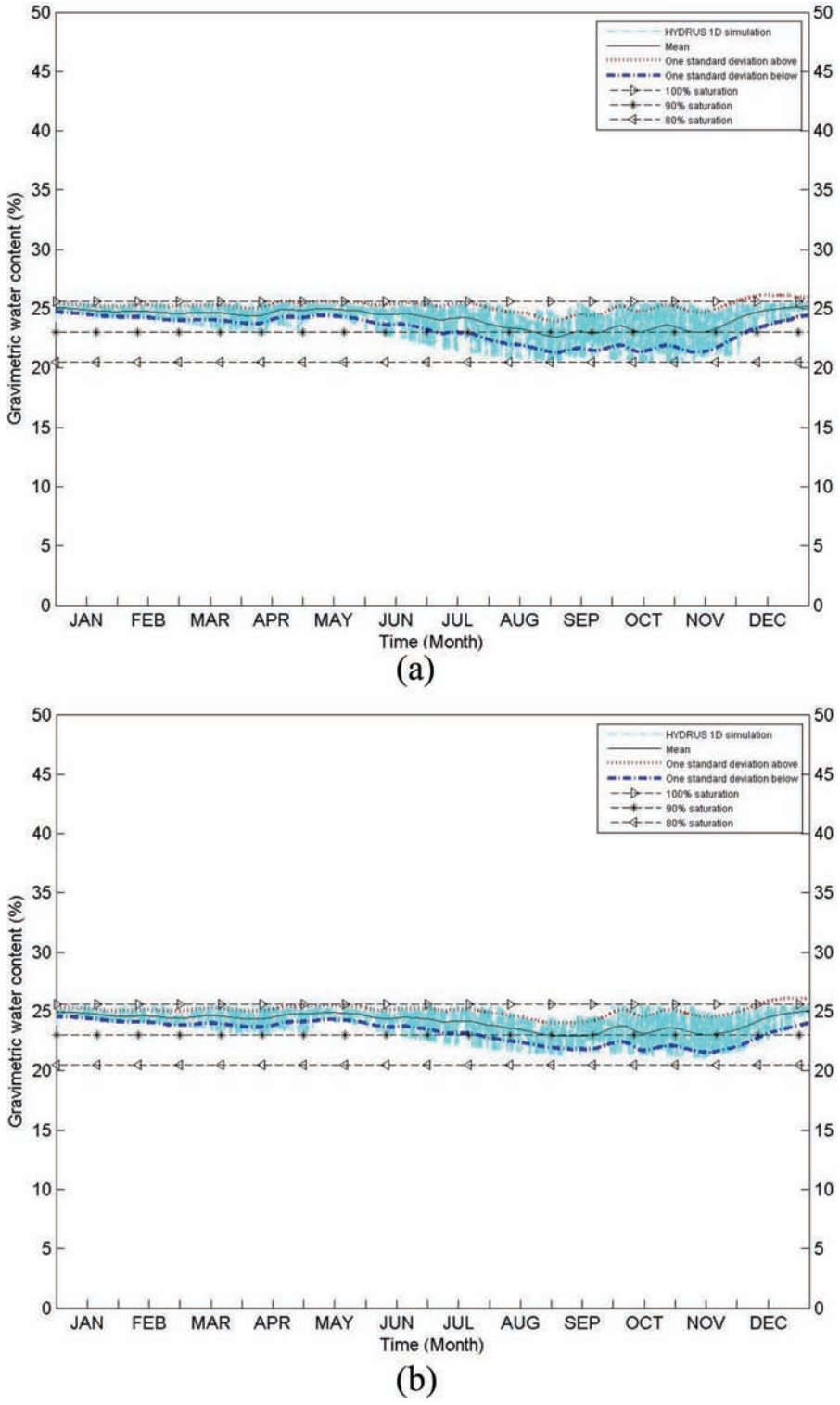

Figure A.11 Annual soil moisture variation for (a) 60 cm depth and (b) 90 cm depth for Daviess County for profile (DAV-1).

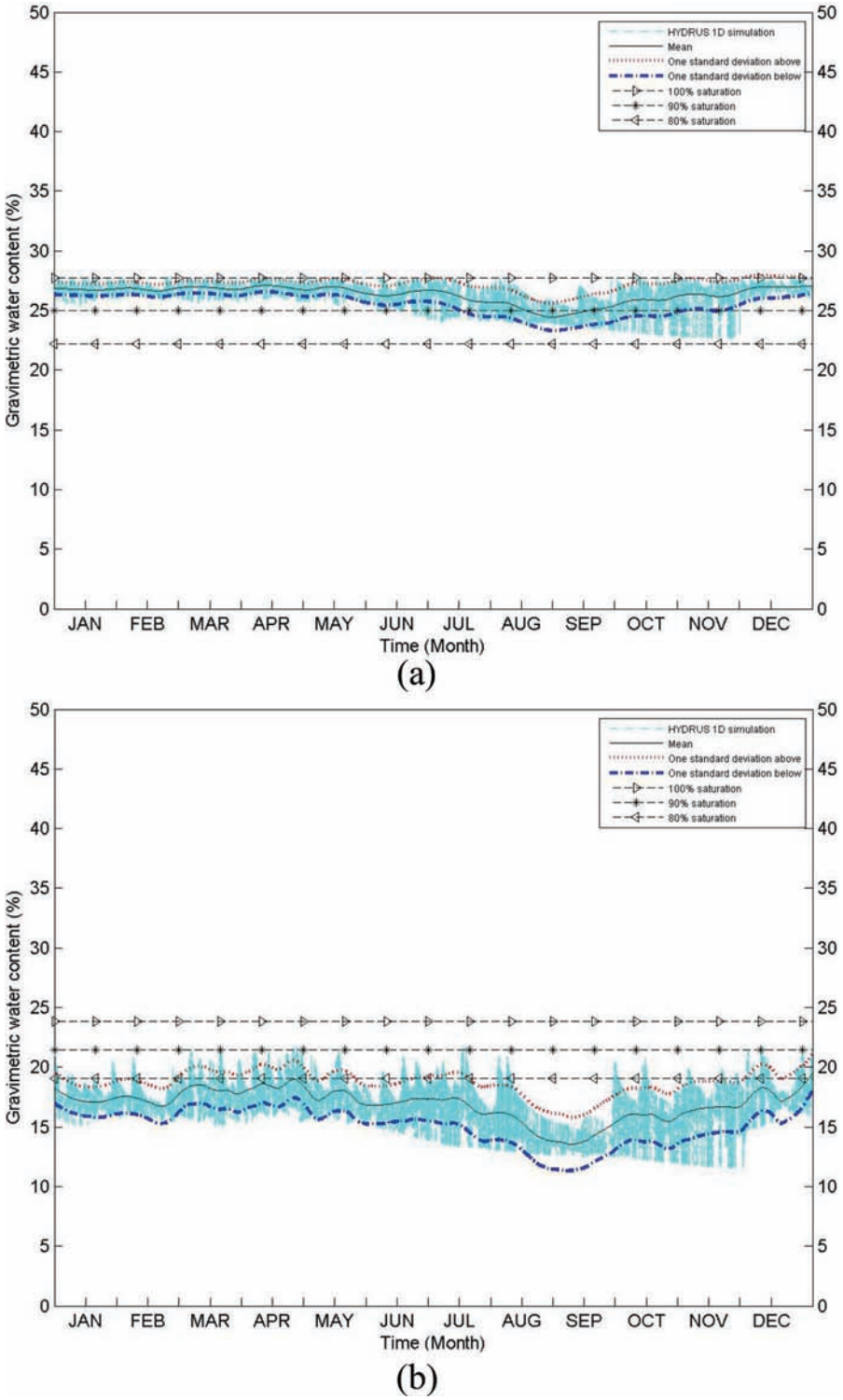

Figure A.12 Annual soil moisture variation for (a) 60 cm depth and (b) 90 cm depth for Dearborn County for profile (DEA-1).

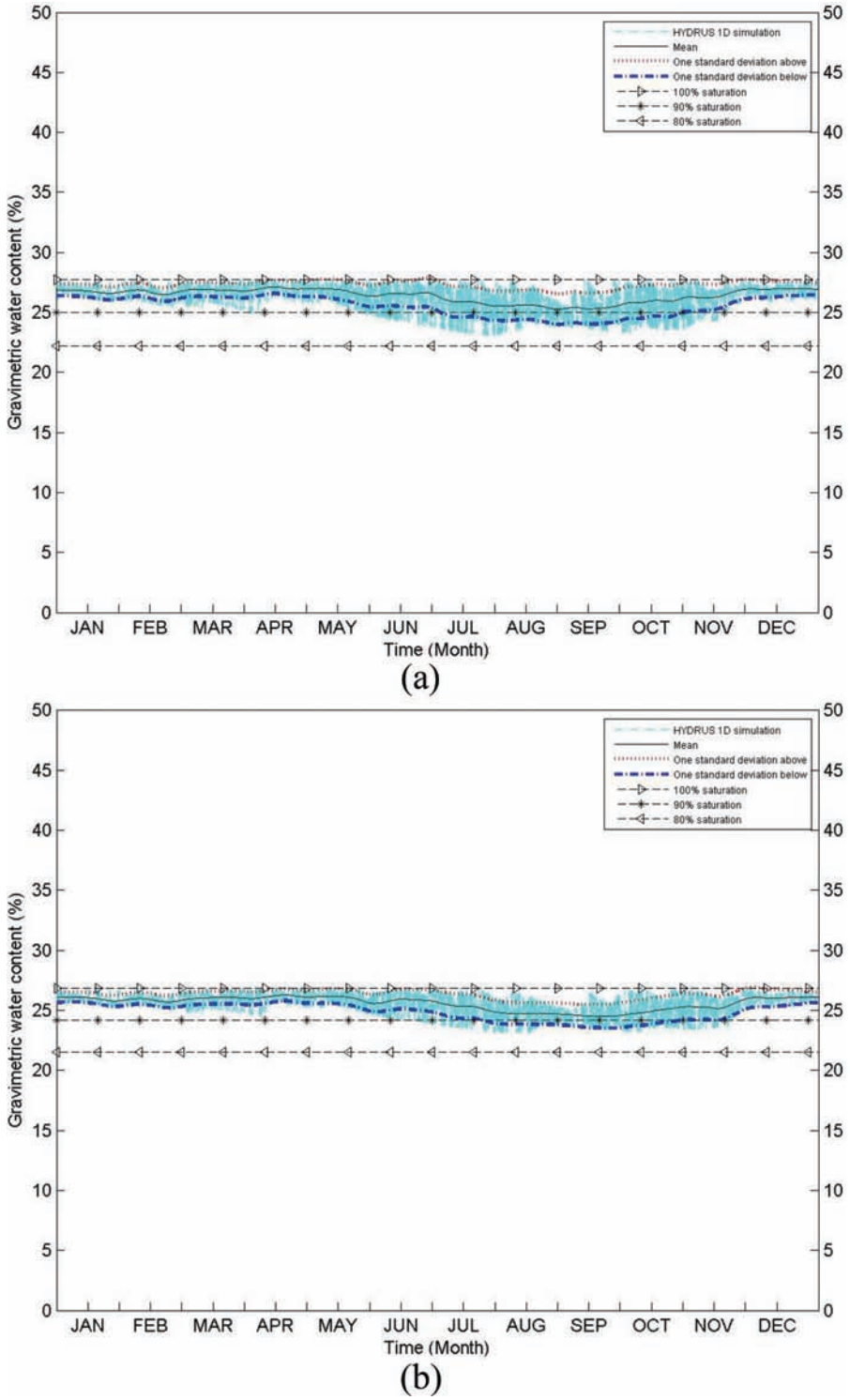

Figure A.13 Annual soil moisture variation for (a) 60 cm depth and (b) 90 cm depth for Delaware County for profile (DEL-1).

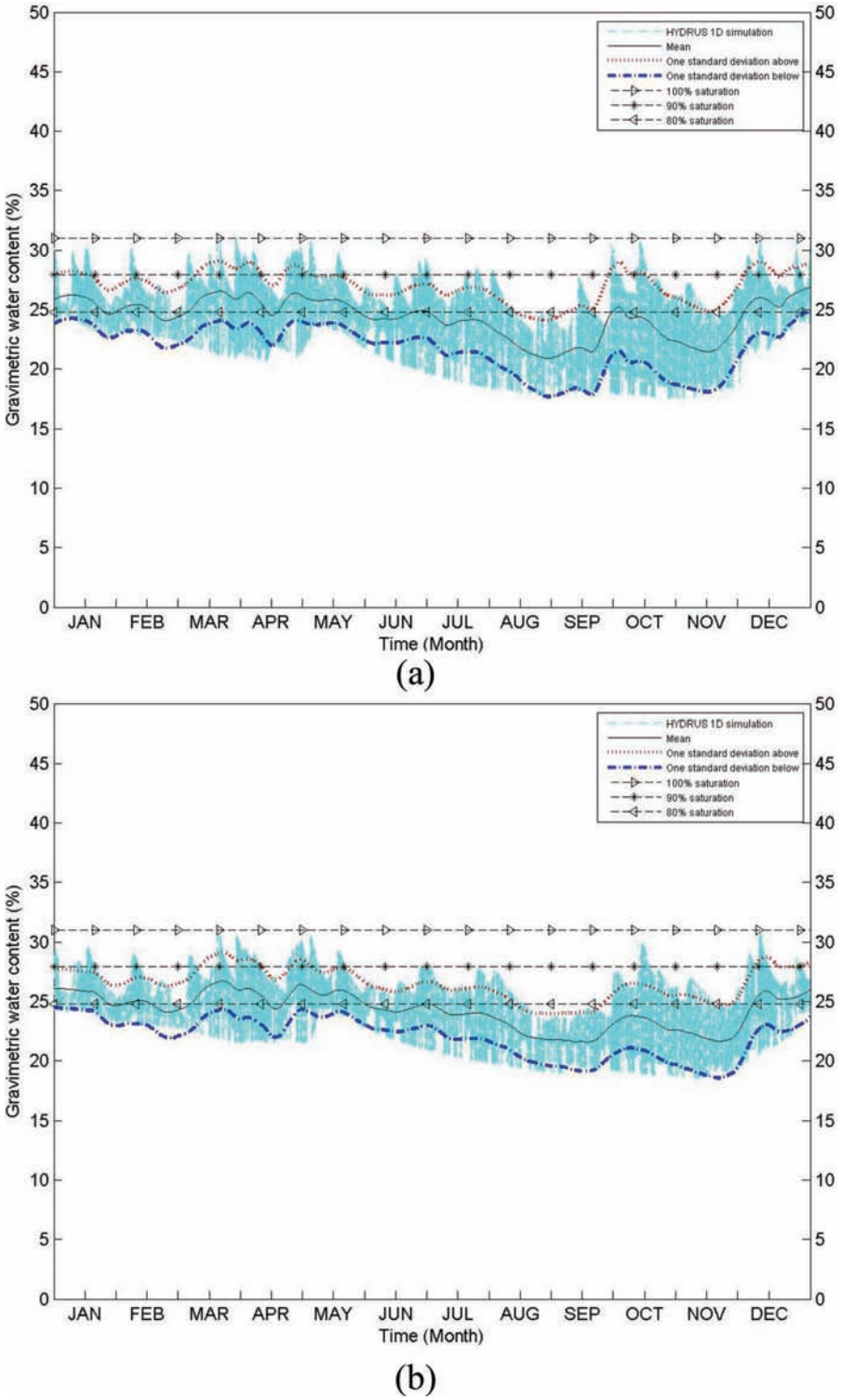

Figure A.14 Annual soil moisture variation for (a) 60 cm depth and (b) 90 cm depth for Dubois County for profile (DUB-1).

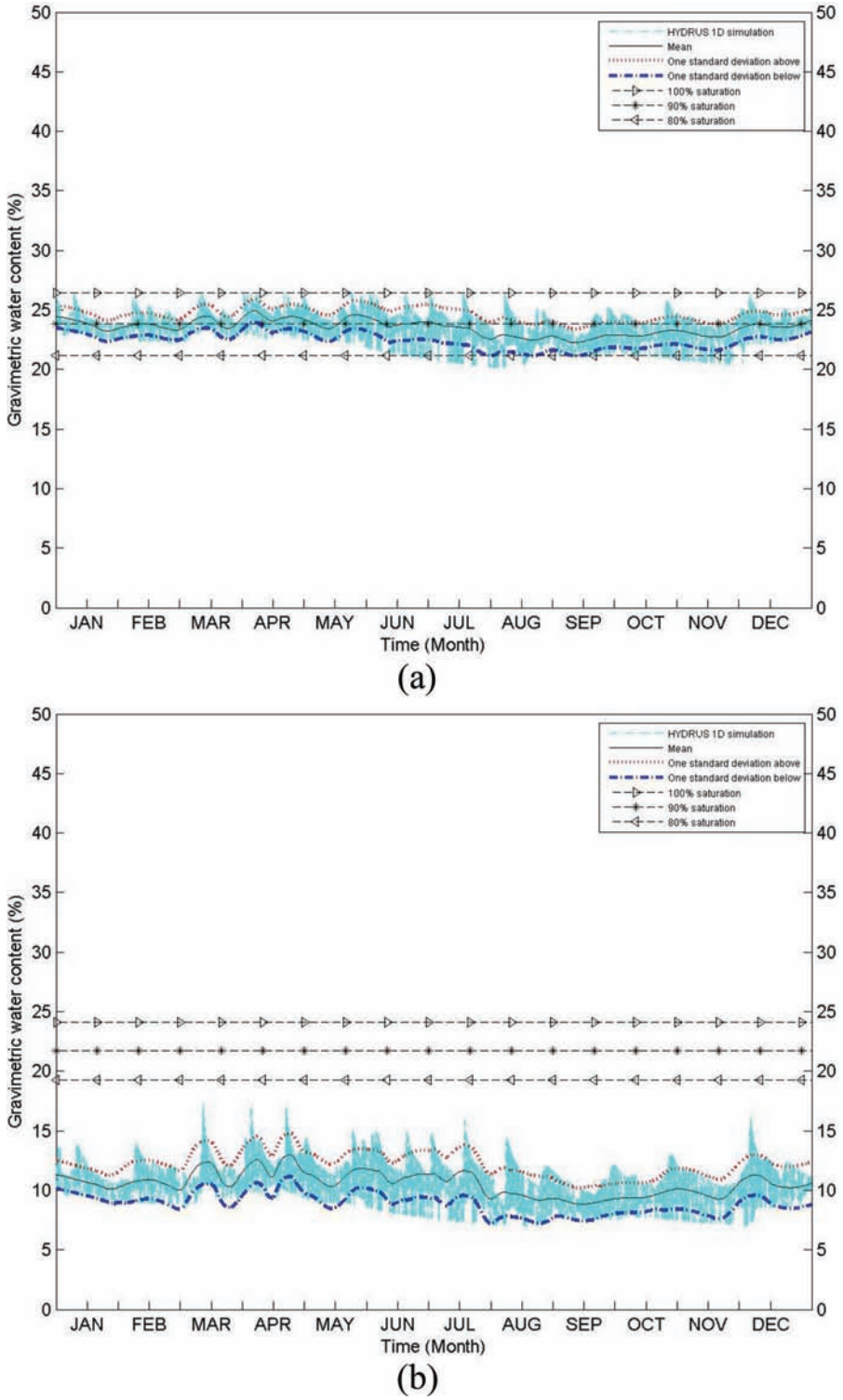

Figure A.15 Annual soil moisture variation for (a) 60 cm depth and (b) 90 cm depth for Elkhart County for profile (ELK-1).

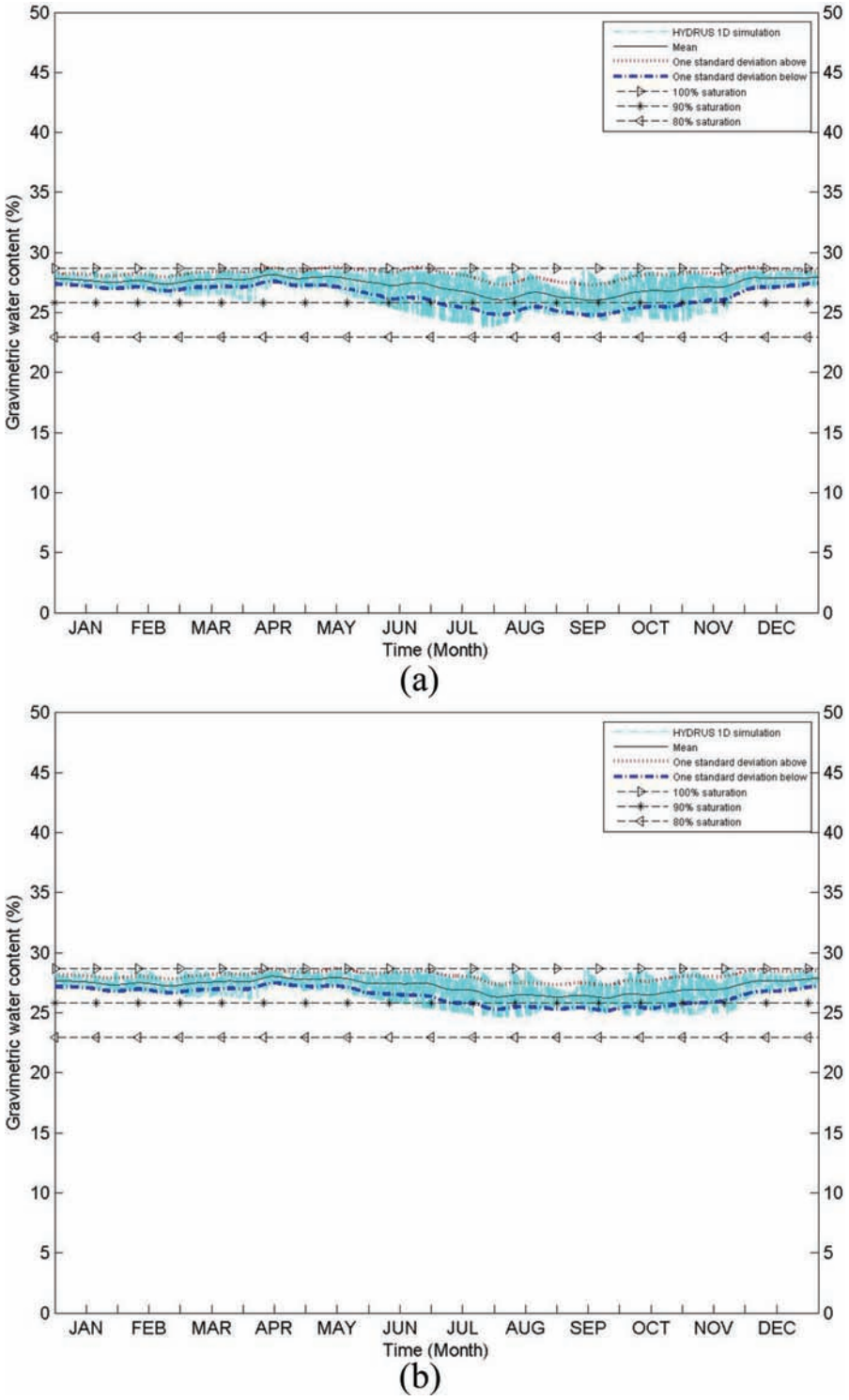

Figure A.16 Annual soil moisture variation for (a) 60 cm depth and (b) 90 cm depth for Fayette County for profile (FAY-1).

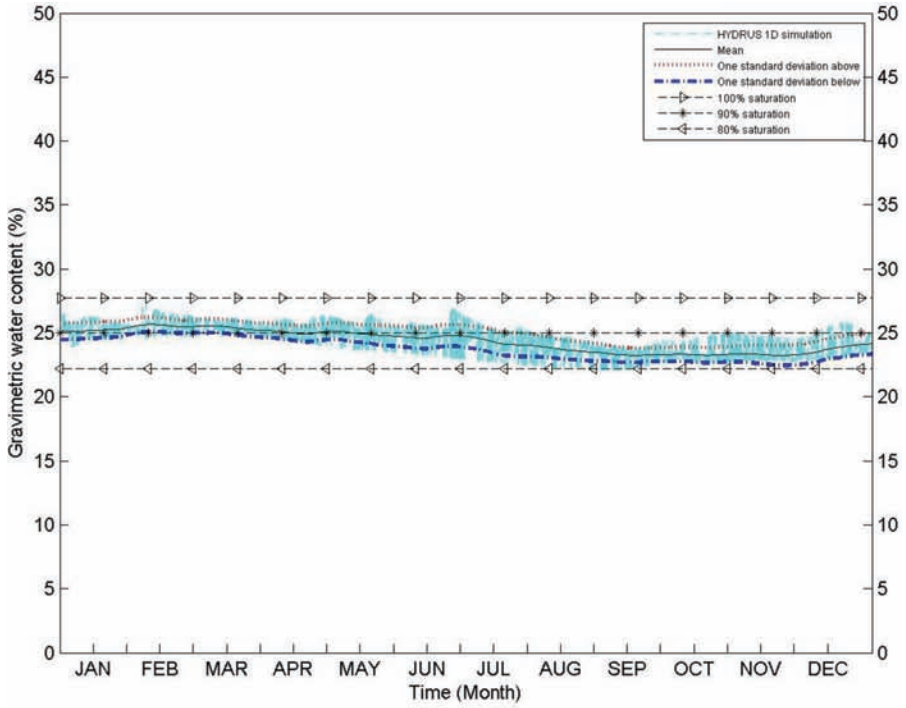

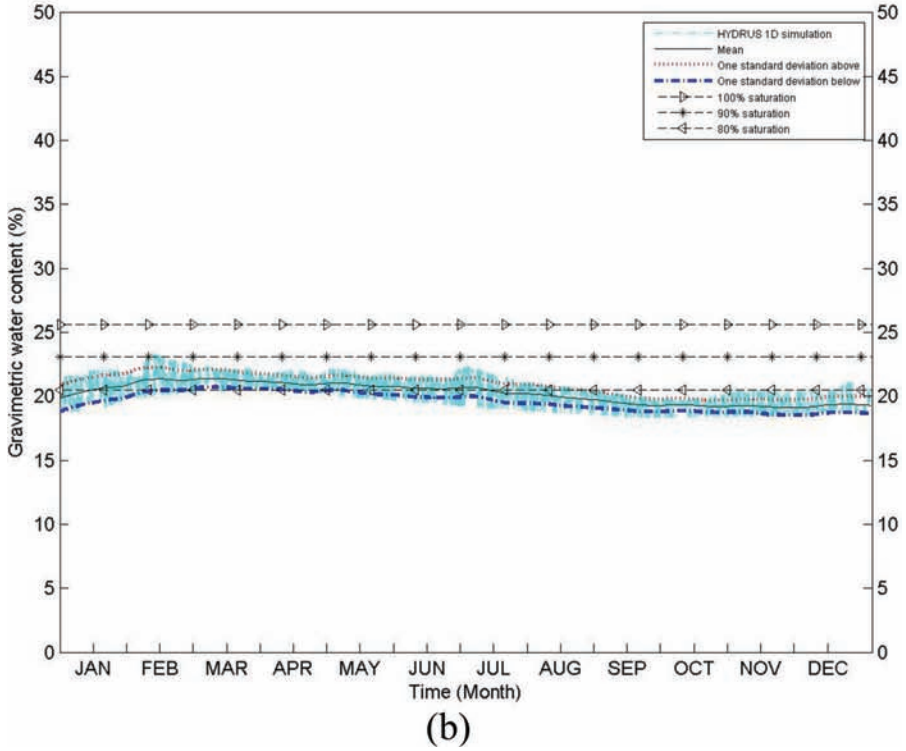

Figure A.17 Annual soil moisture variation for (a) 60 cm depth and (b) 90 cm depth for Fountain County for profile (FOU-1).

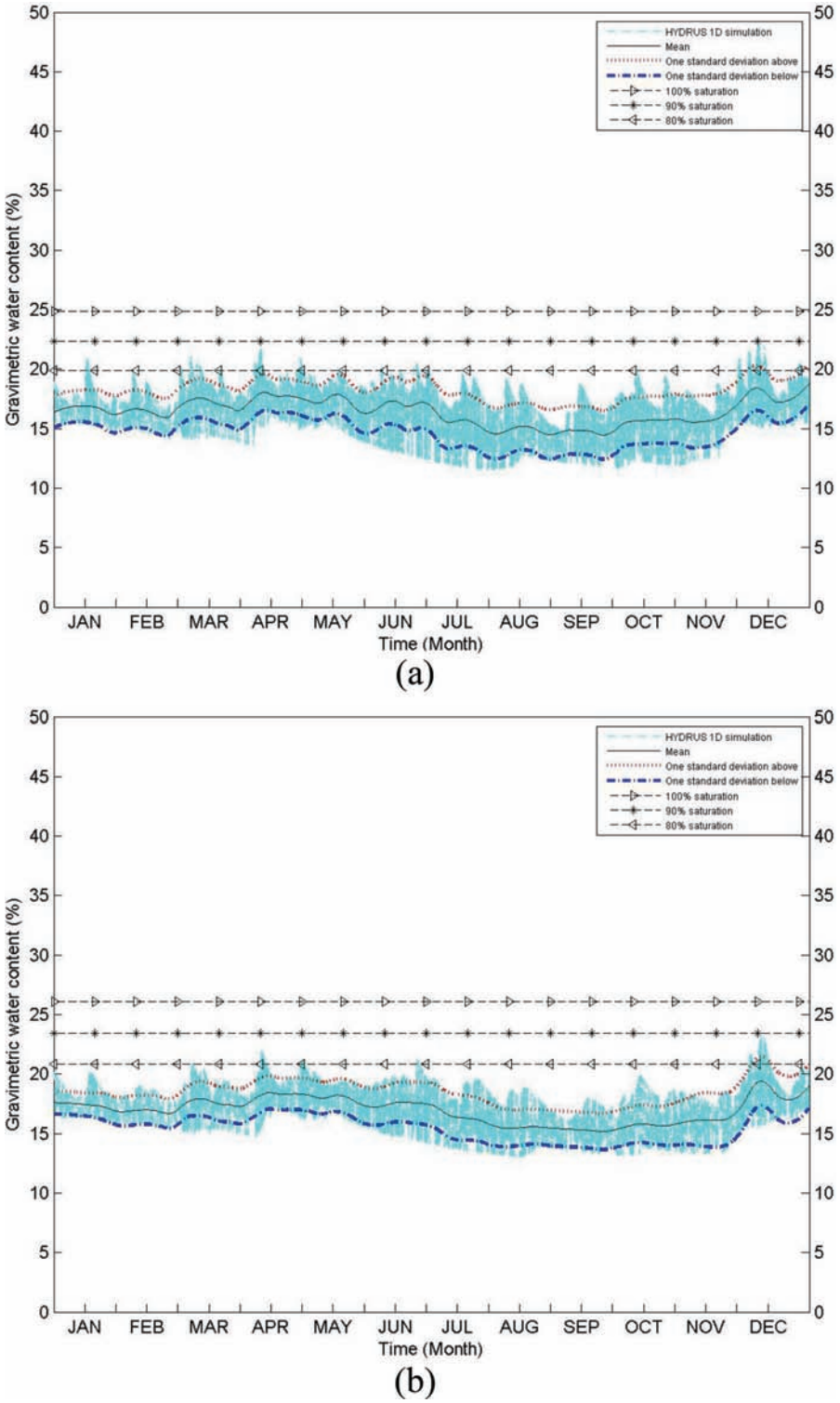

Figure A.18 Annual soil moisture variation for (a) 60 cm depth and (b) 90 cm depth for Franklin County for profile (FRA-1).

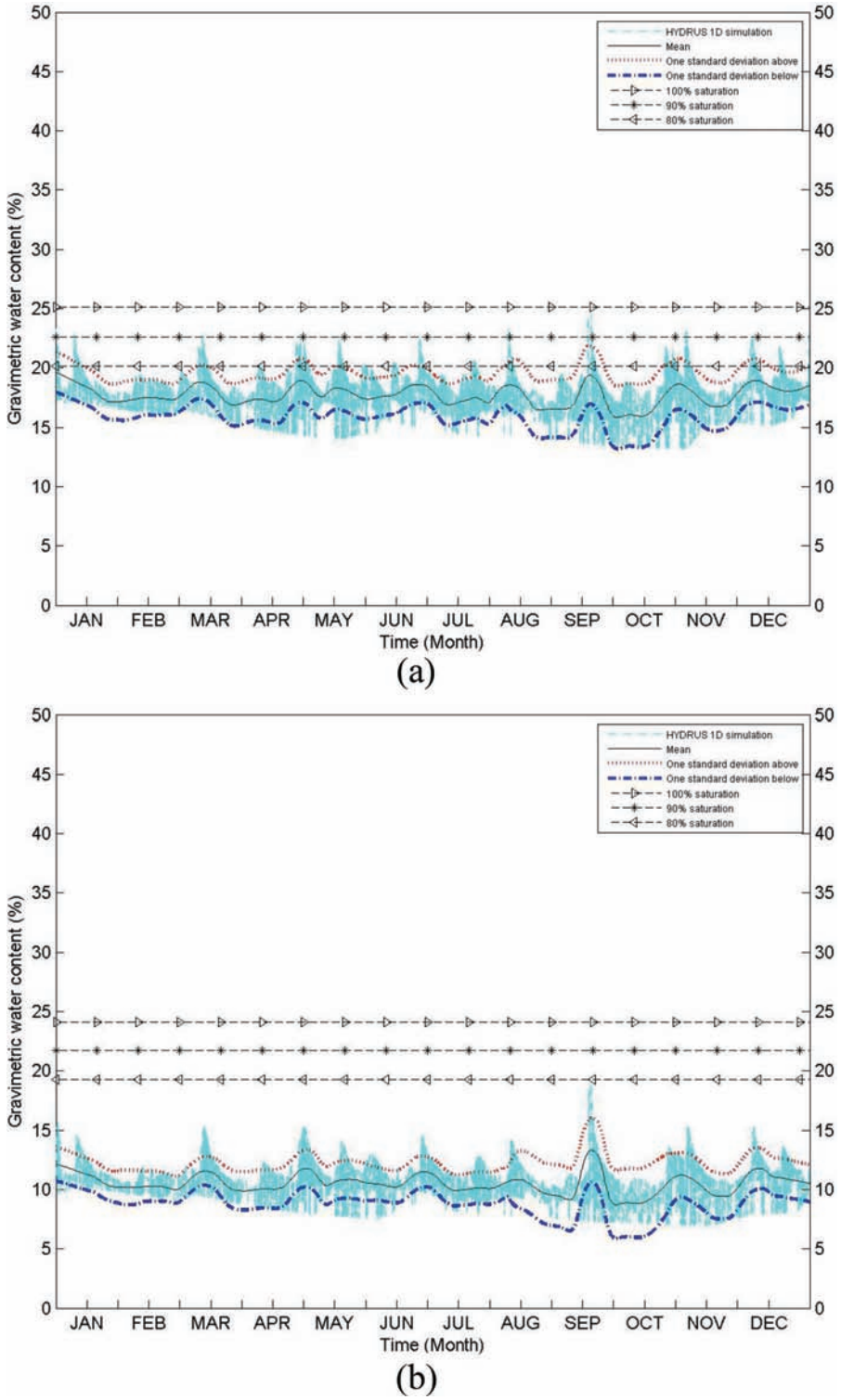

Figure A.19 Annual soil moisture variation for (a) 60 cm depth and (b) 90 cm depth for Fulton County for profile (FUL-1).

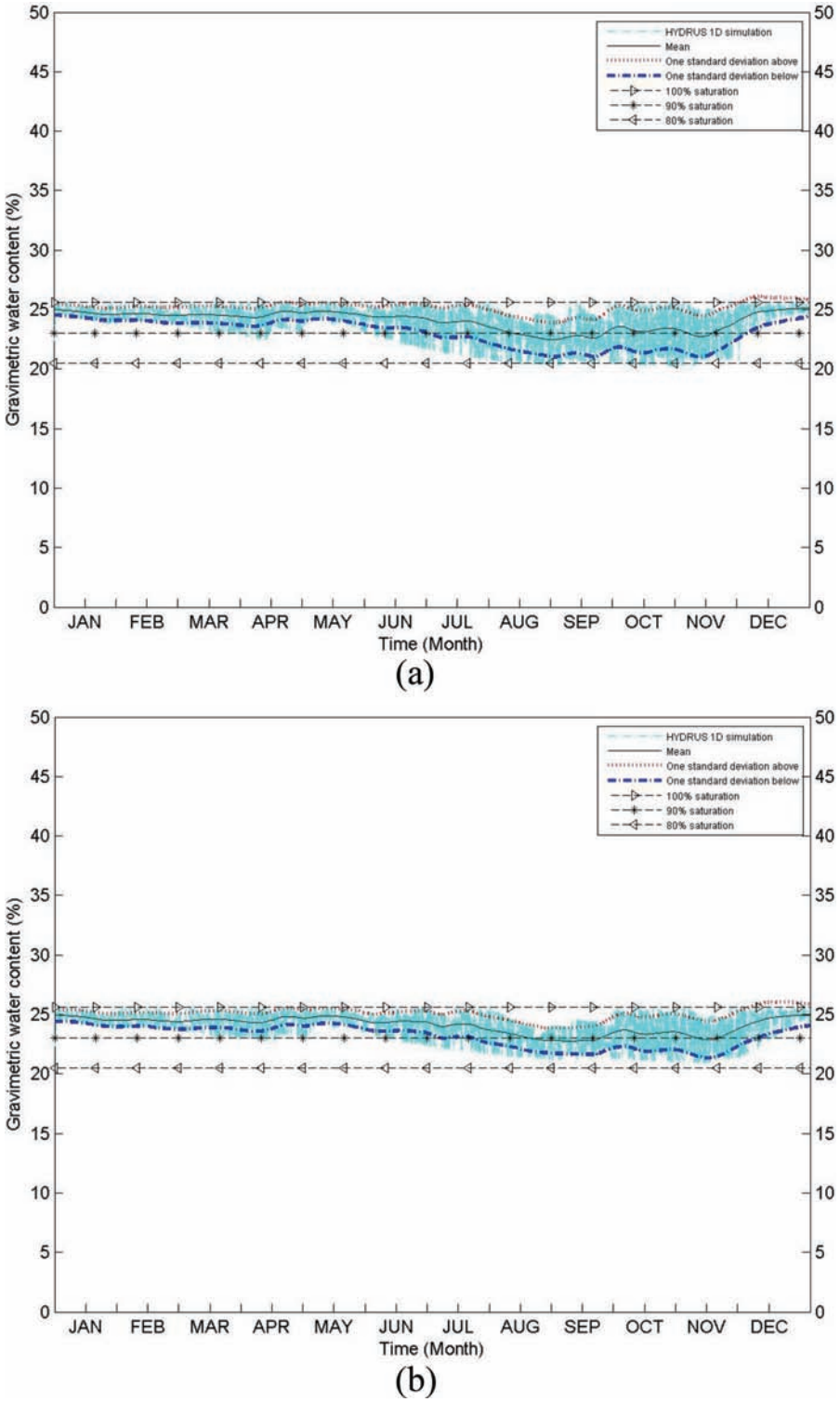

Figure A.20 Annual soil moisture variation for (a) 60 cm depth and (b) 90 cm depth for Gibson County for profile (GIB-1).

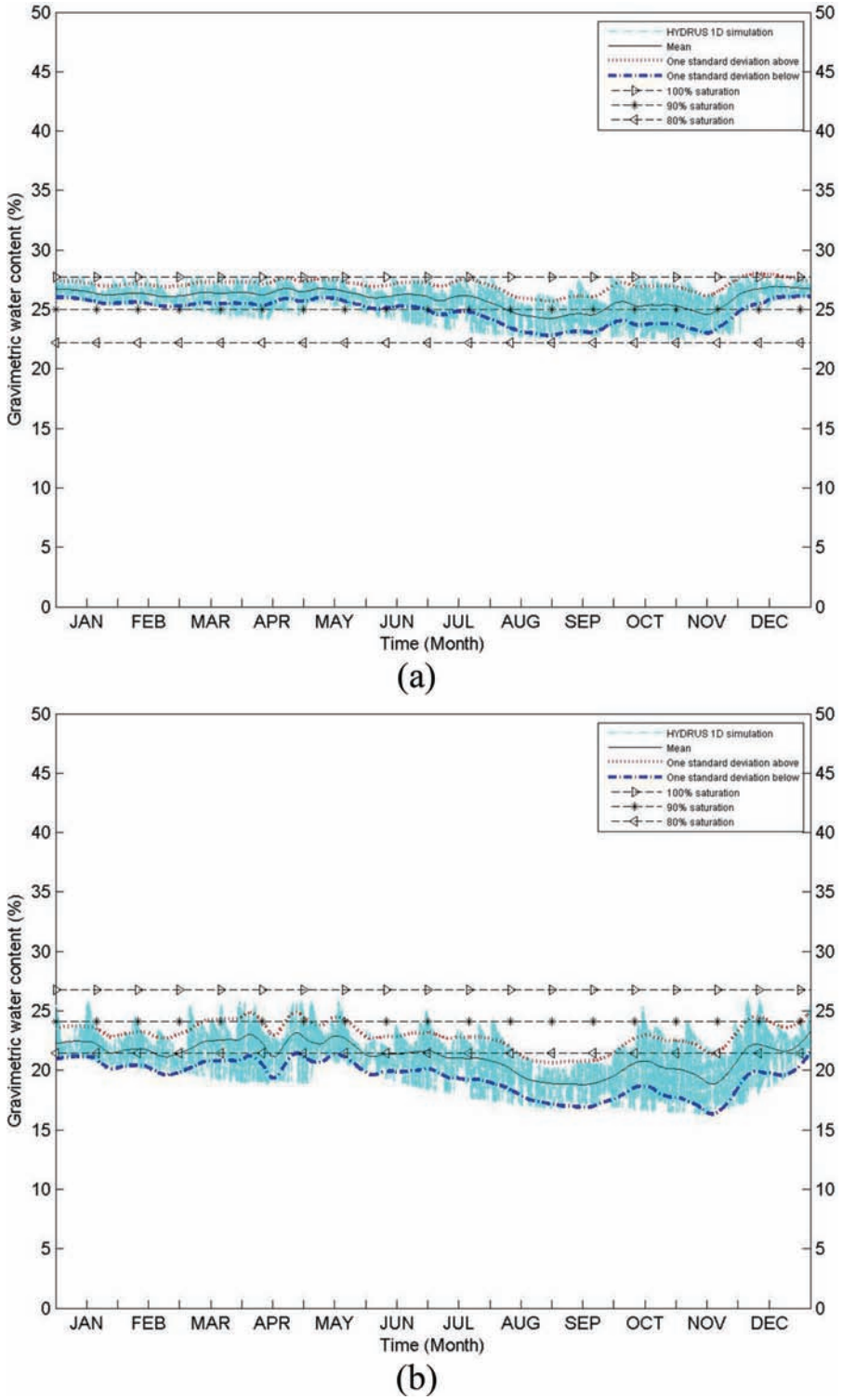

Figure A.21 Annual soil moisture variation for (a) 60 cm depth and (b) 90 cm depth for Green County for profile (GRE-1).

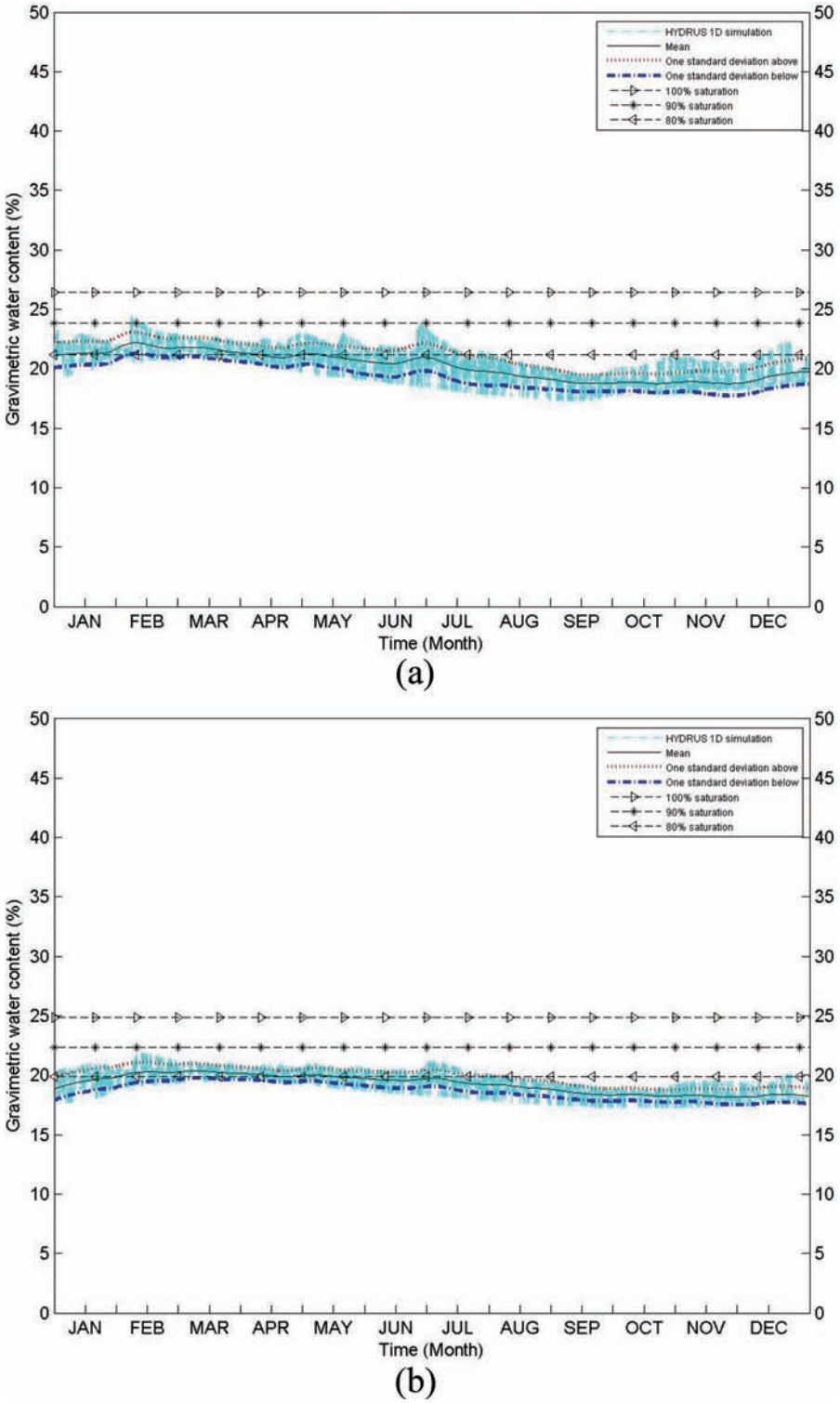

Figure A.22 Annual soil moisture variation for (a) 60 cm depth and (b) 90 cm depth for Hendricks County for profile (HEND-1).

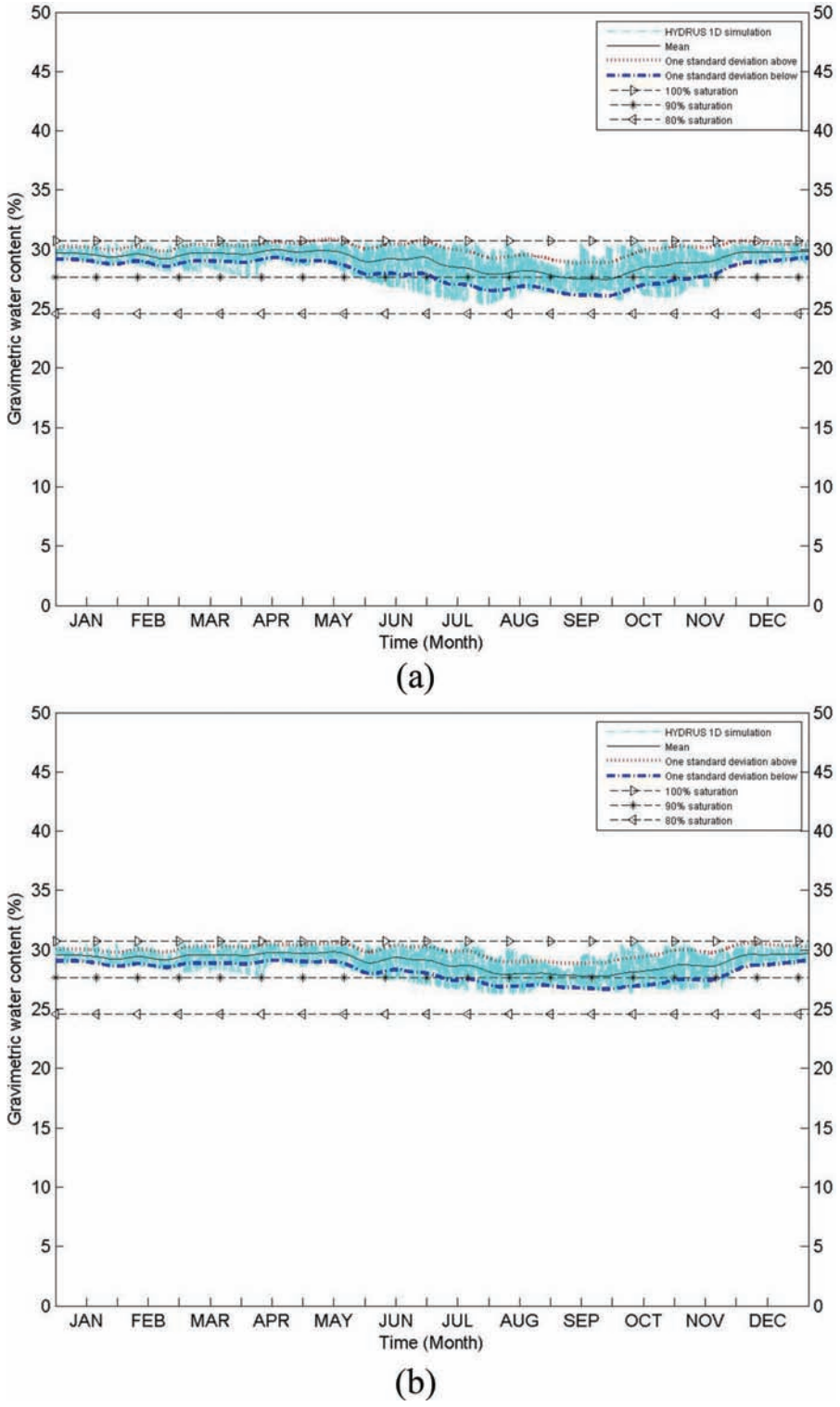

Figure A.23 Annual soil moisture variation for (a) 60 cm depth and (b) 90 cm depth for Henry County for profile (HEN-1).

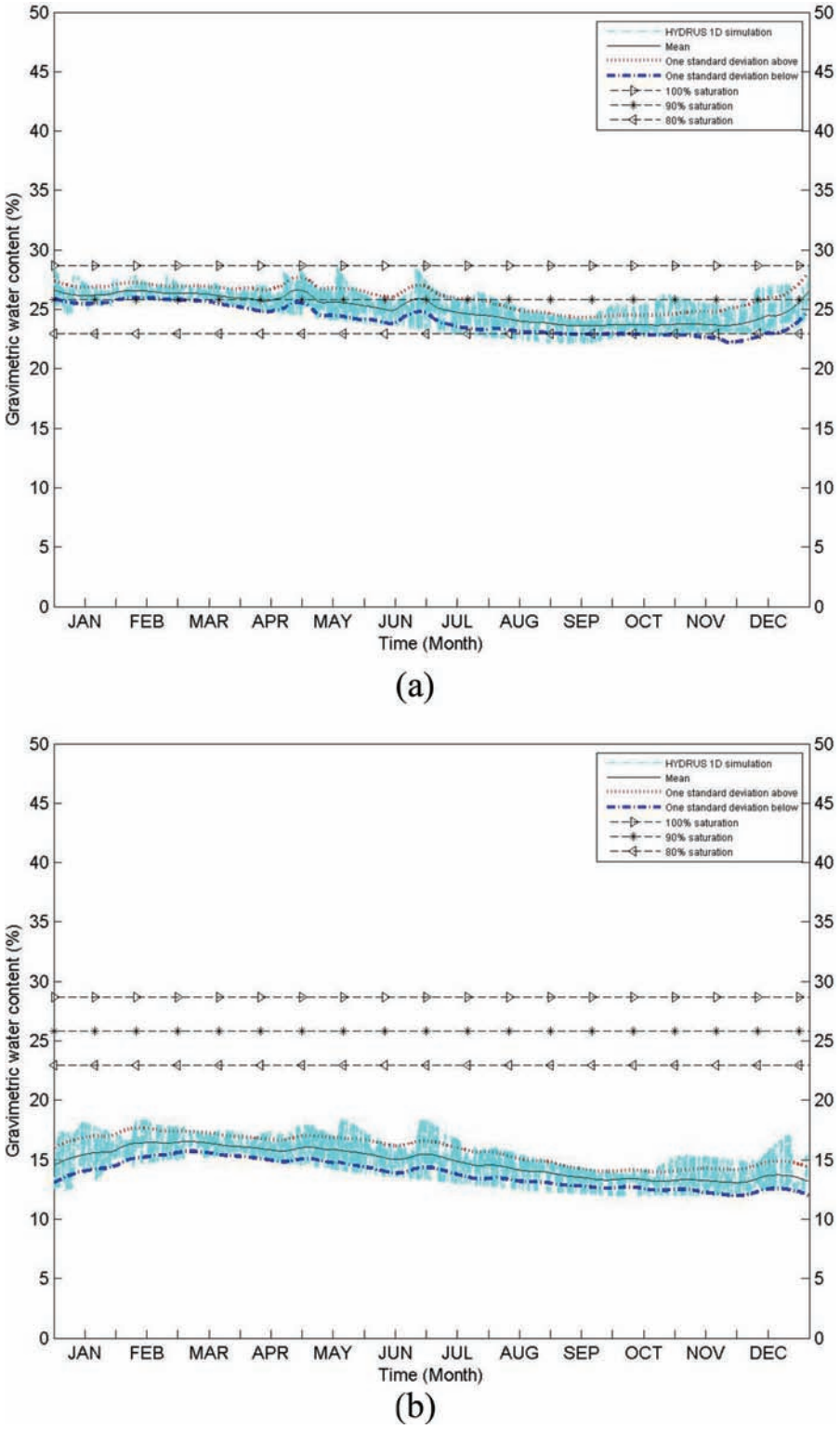

Figure A.24 Annual soil moisture variation for (a) 60 cm depth and (b) 90 cm depth for Howard County for profile (HOW-1).

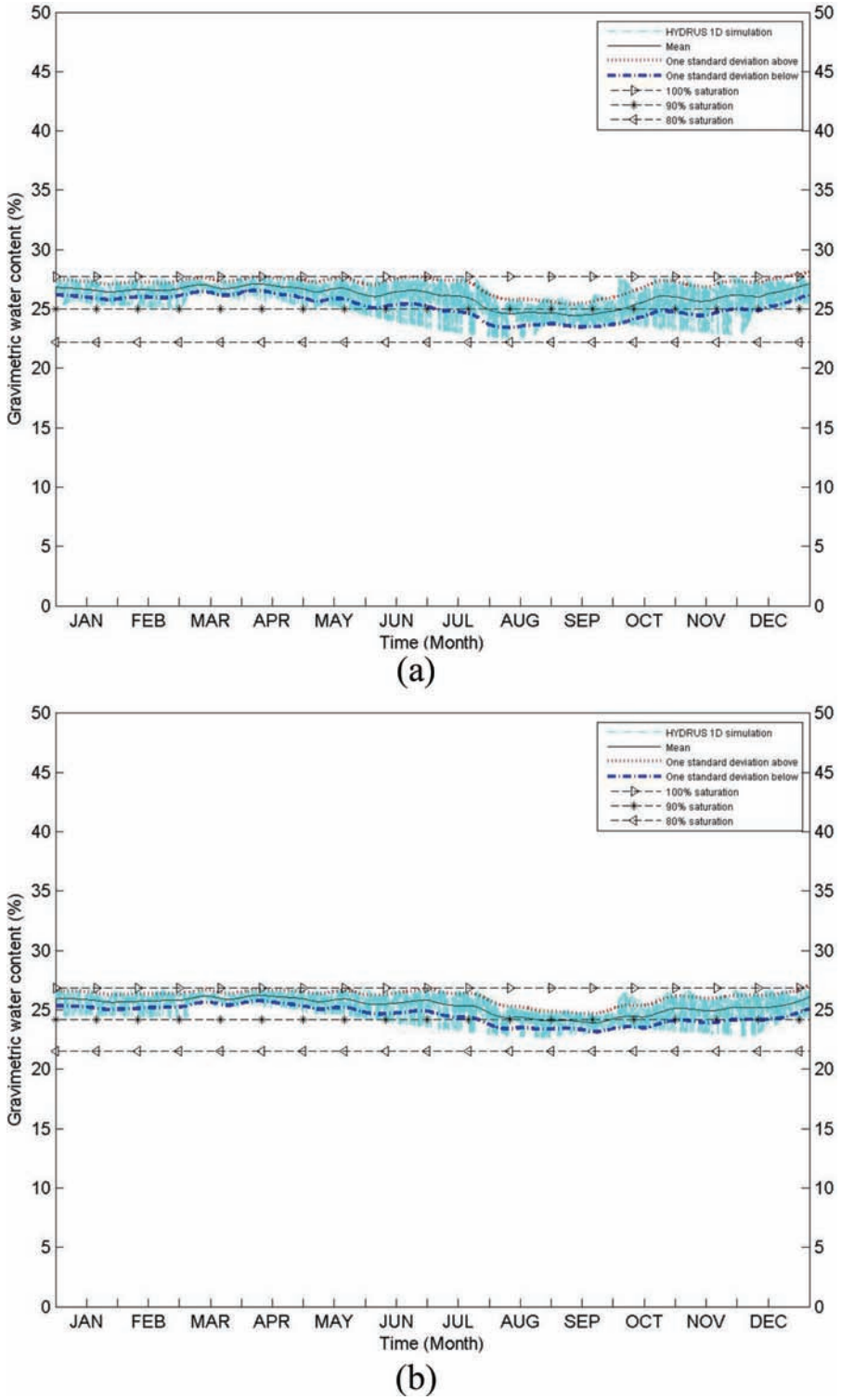

Figure A.25 Annual soil moisture variation for (a) 60 cm depth and (b) 90 cm depth for Huntington County for profile (HUN-1).

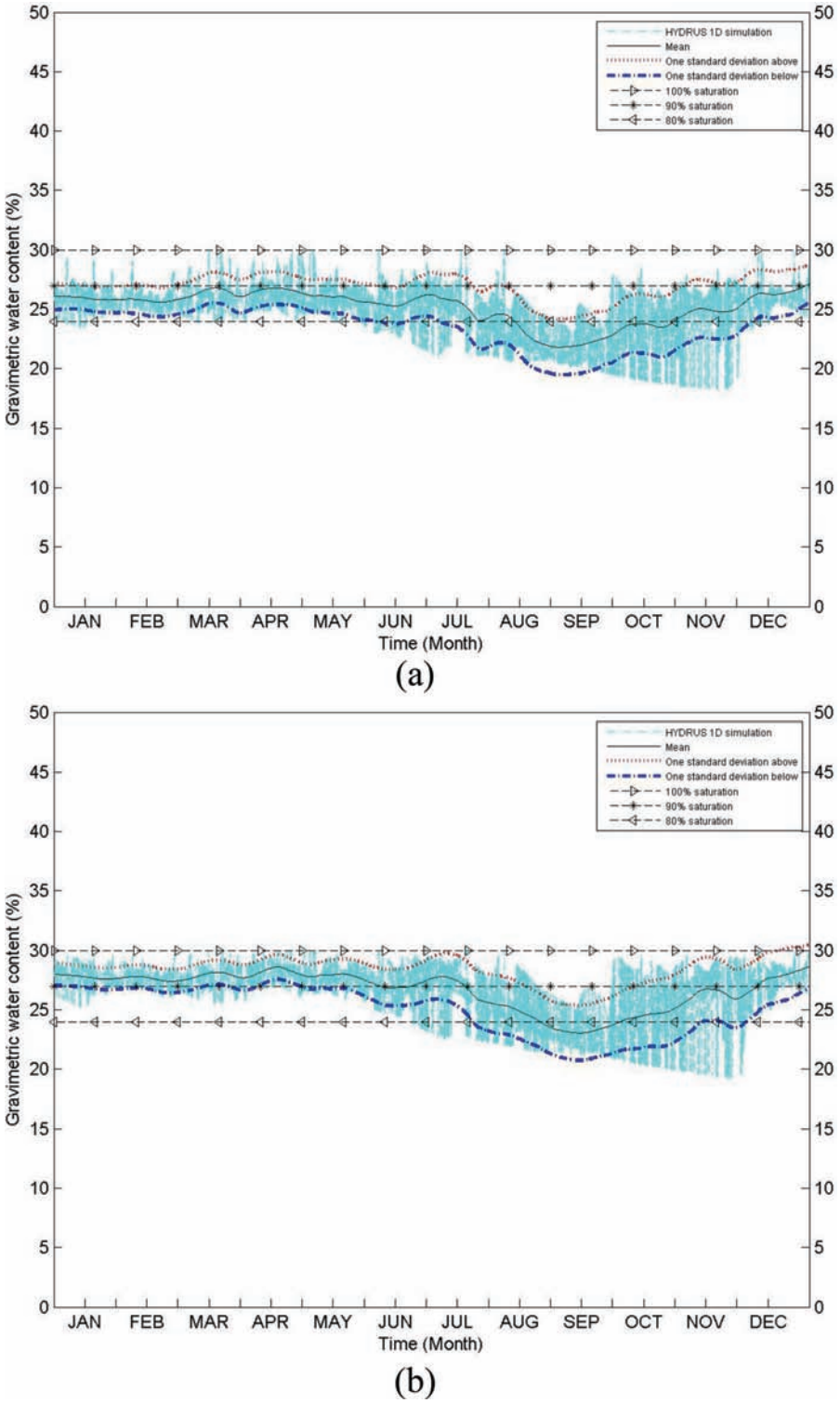

Figure A.26 Annual soil moisture variation for (a) 60 cm depth and (b) 90 cm depth for Jackson County for profile (JAC-1).

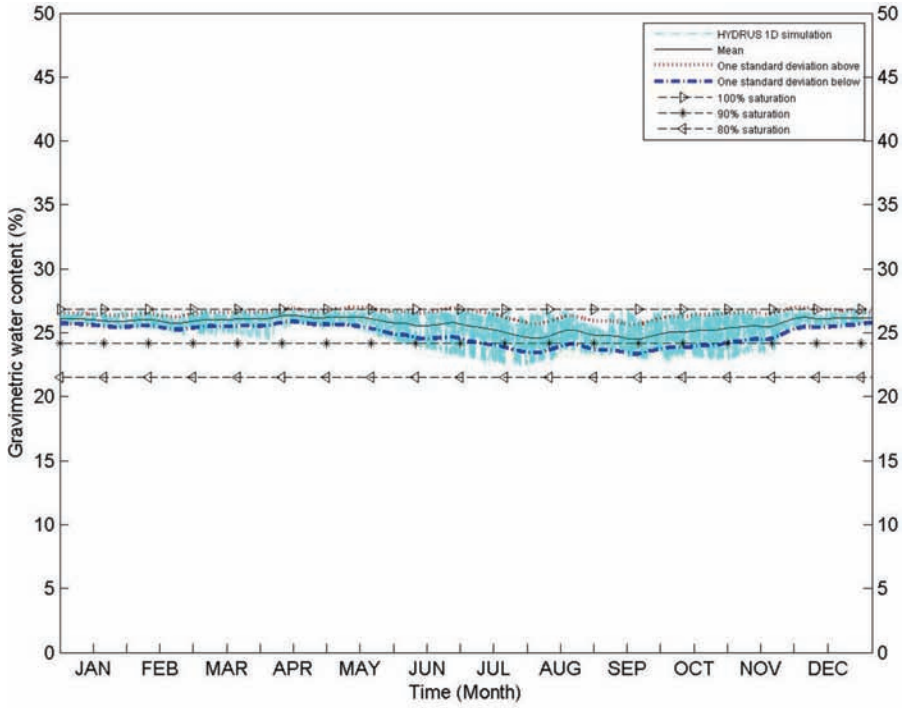

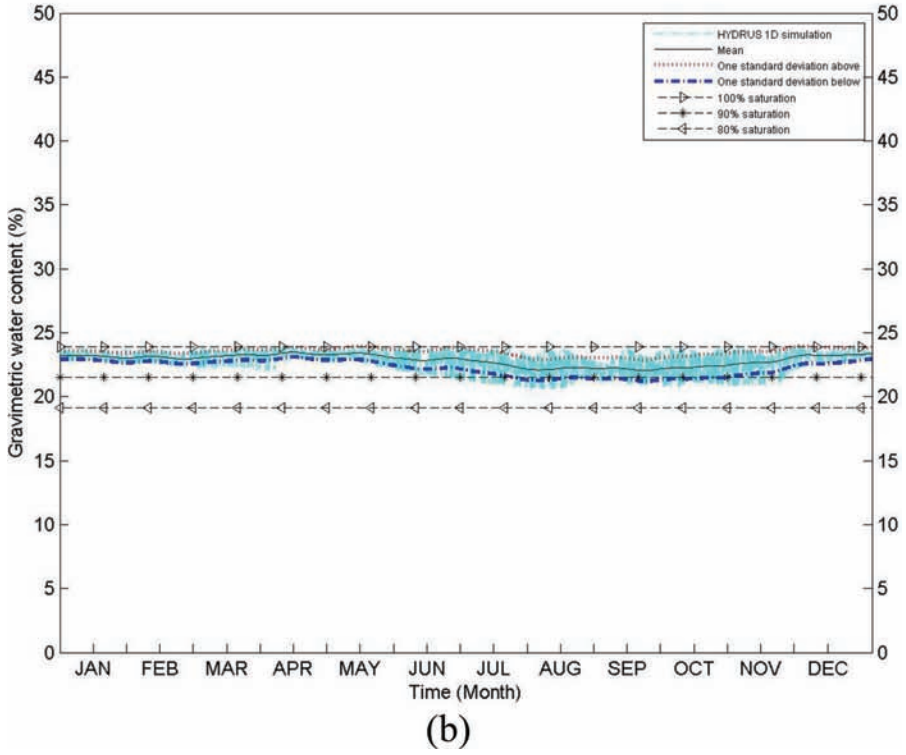

Figure A.27 Annual soil moisture variation for (a) 60 cm depth and (b) 90 cm depth for Jay County for profile (JAY-1).

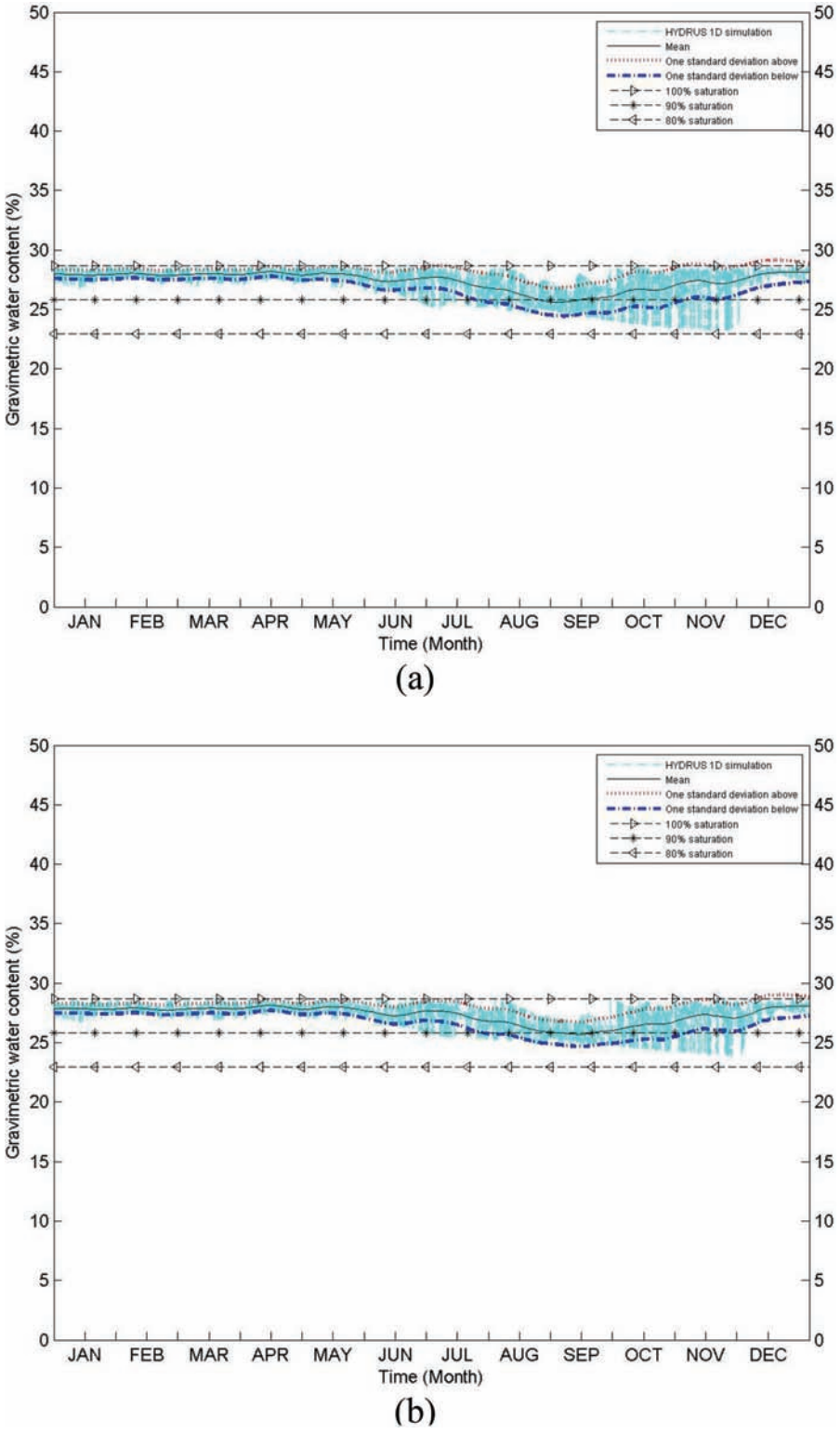

Figure A.28 Annual soil moisture variation for (a) 60 cm depth and (b) 90 cm depth for Jefferson County for profile (JEF-1).

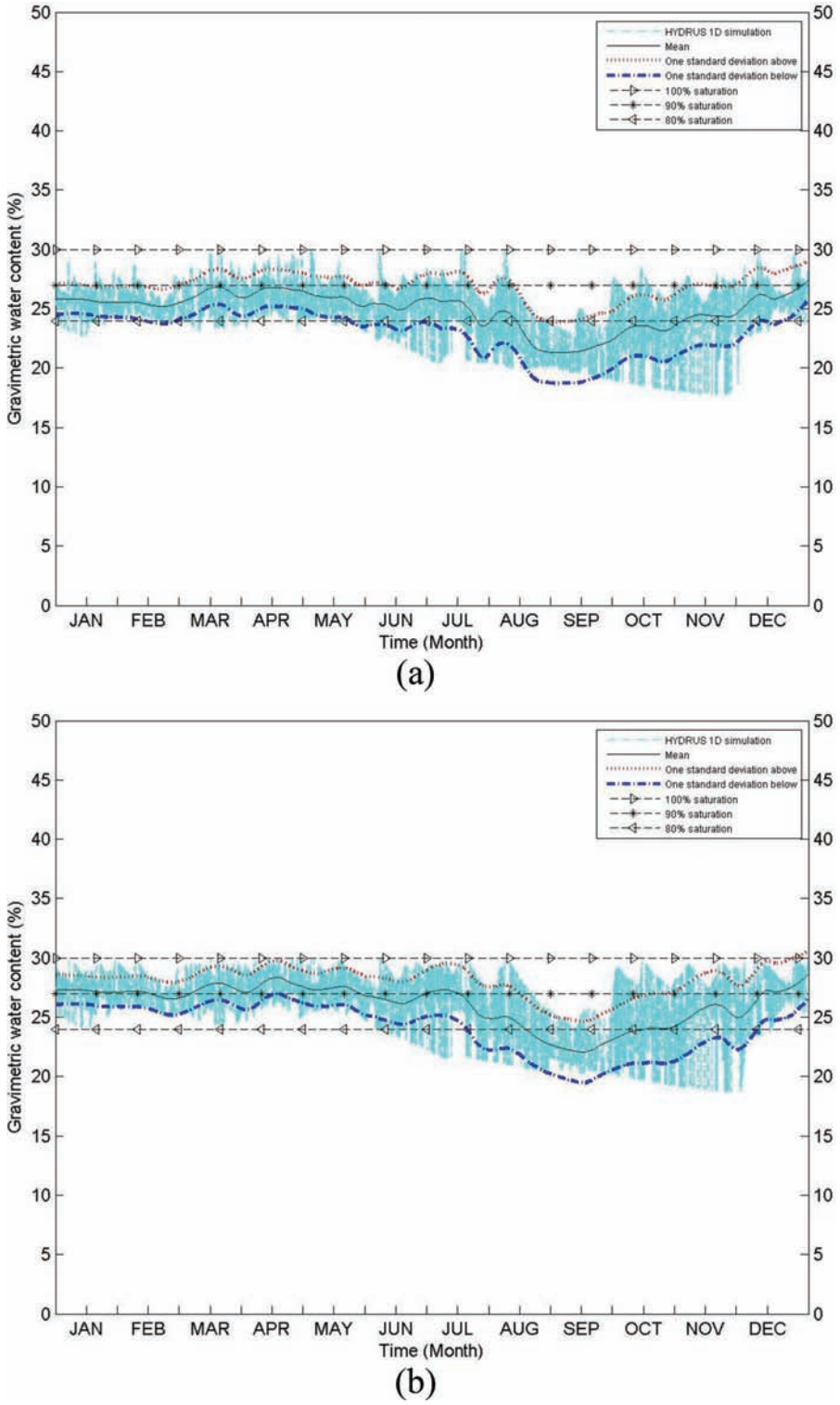

Figure A.29 Annual soil moisture variation for (a) 60 cm depth and (b) 90 cm depth for Jennings County for profile (JEN-1).

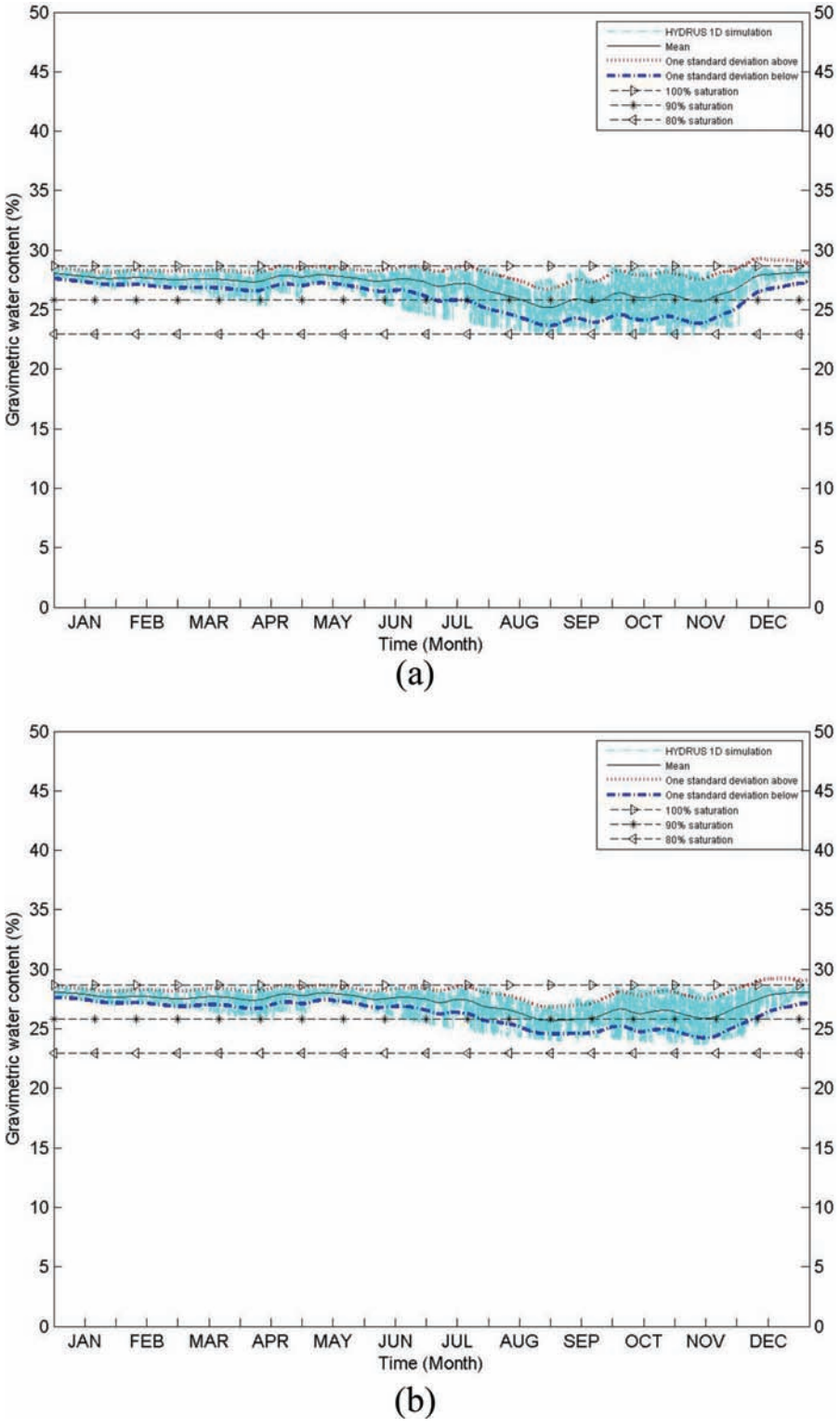

Figure A.30 Annual soil moisture variation for (a) 60 cm depth and (b) 90 cm depth for Knox County for profile (KNO-1).

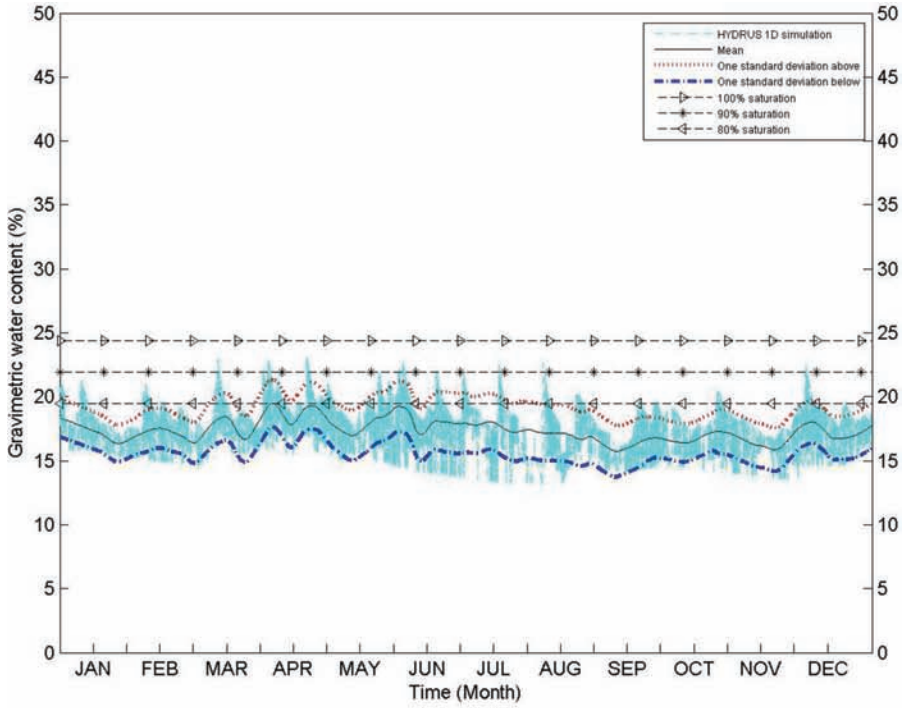

(a)

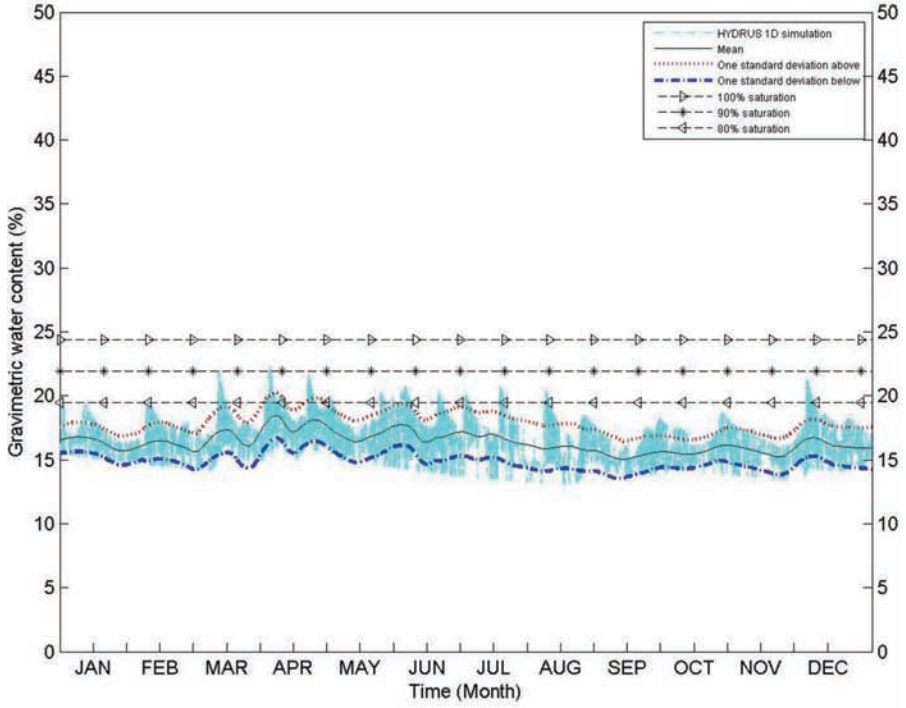

(b)

Figure A.31 Annual soil moisture variation for (a) 60 cm depth and (b) 90 cm depth for Kosciusko County for profile (KOS-1).

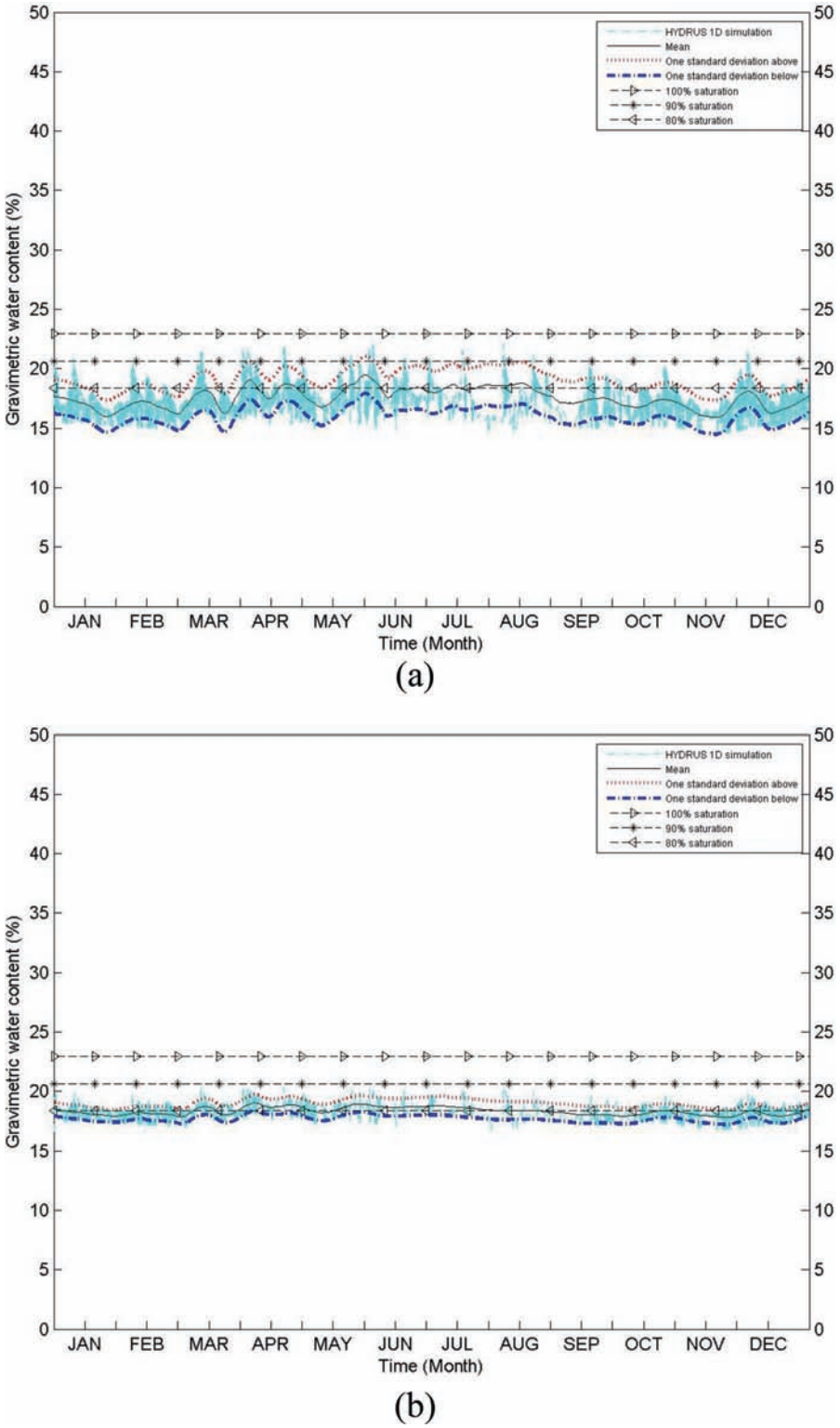

Figure A.32 Annual soil moisture variation for (a) 60 cm depth and (b) 90 cm depth for Lagrange County for profile (LAG-1).

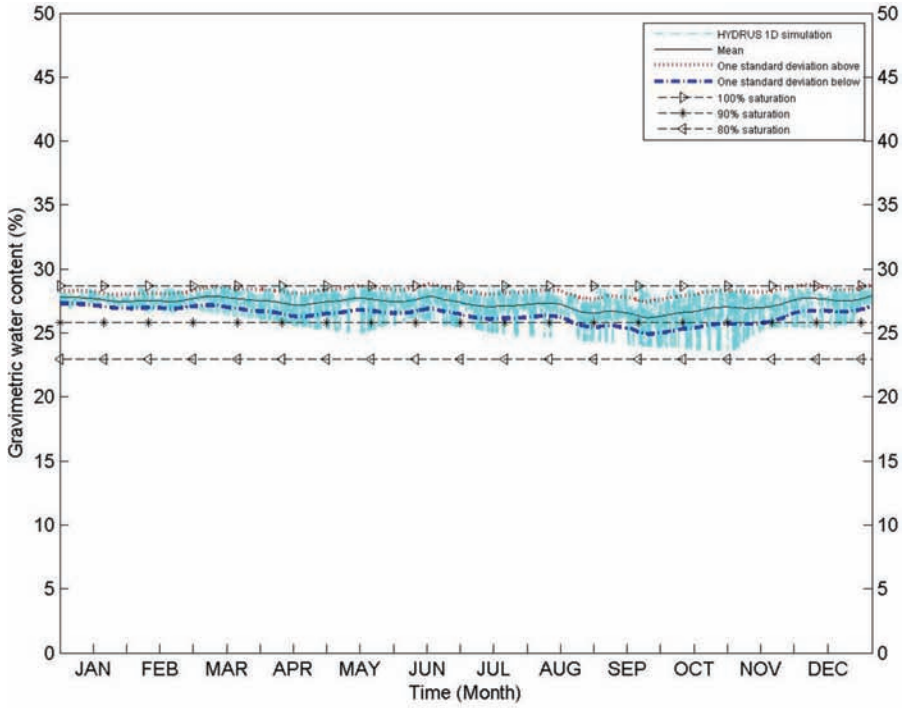

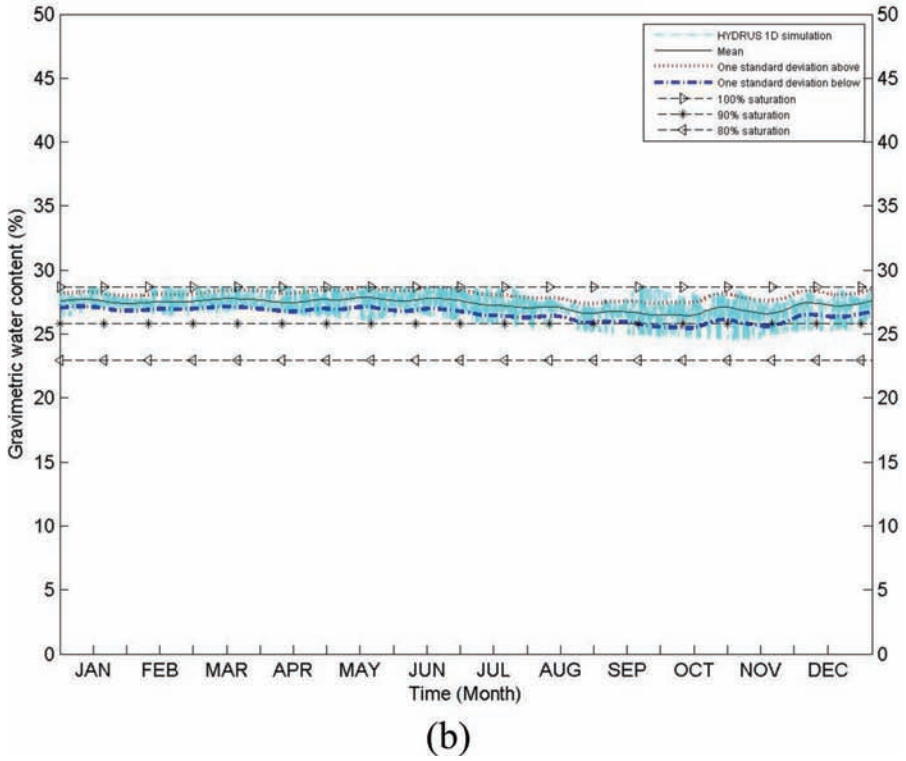

Figure A.33 Annual soil moisture variation for (a) 60 cm depth and (b) 90 cm depth for Lake County for profile (LAK-1).

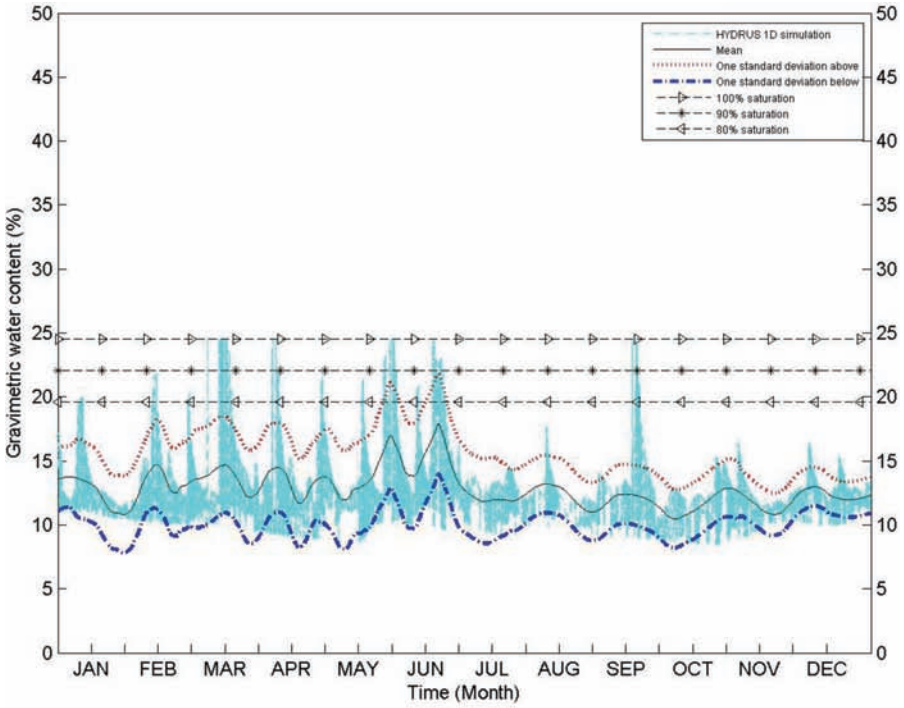

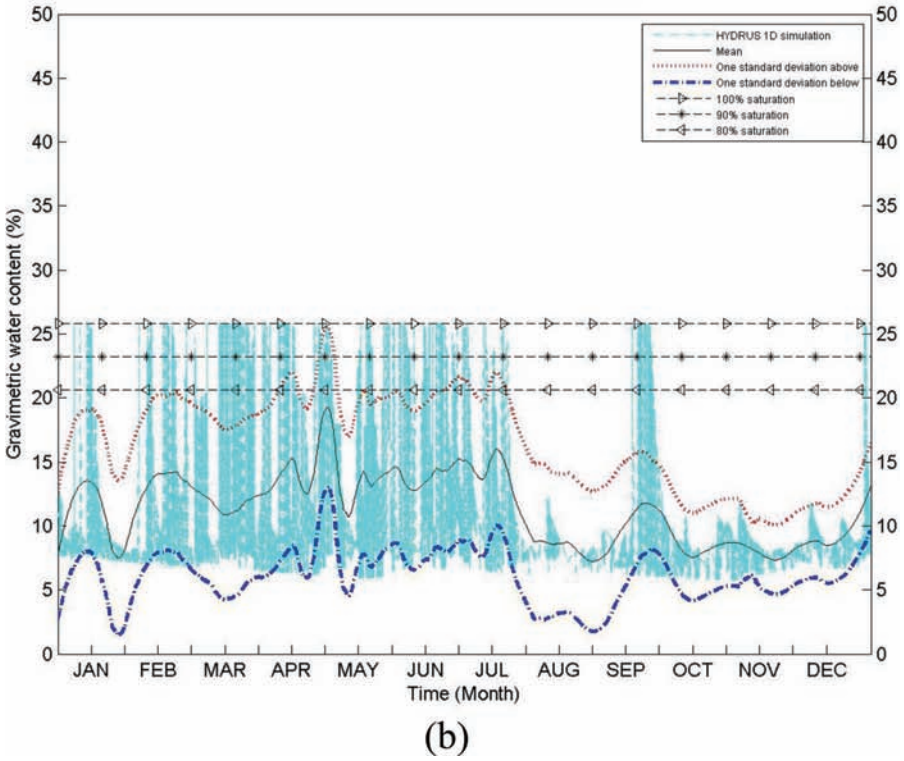

Figure A.34 Annual soil moisture variation for (a) 60 cm depth and (b) 90 cm depth for LaPorte County for profile (LAP-1).

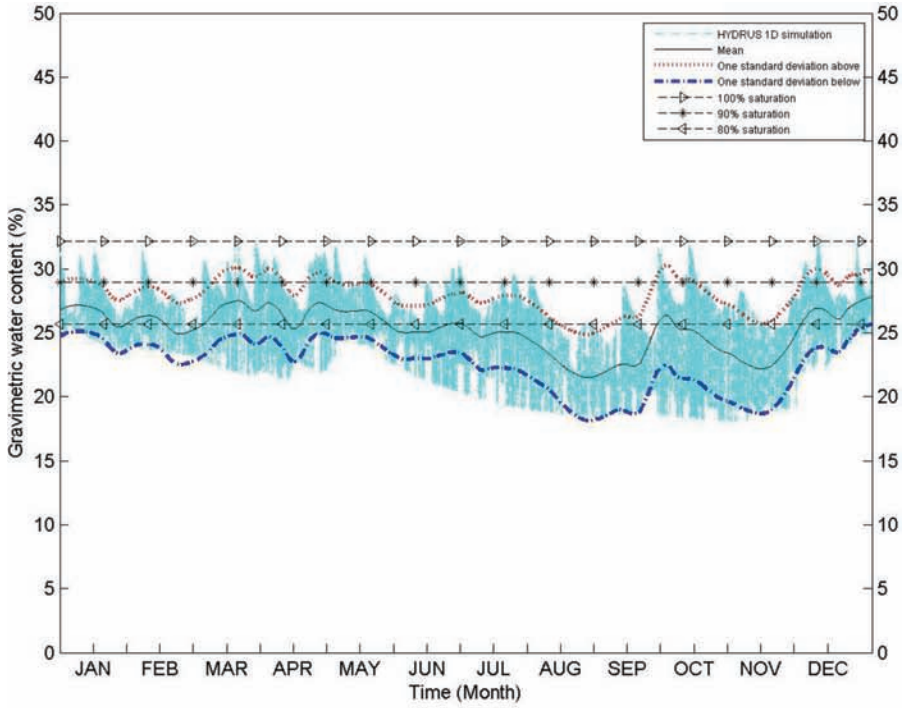

(a)

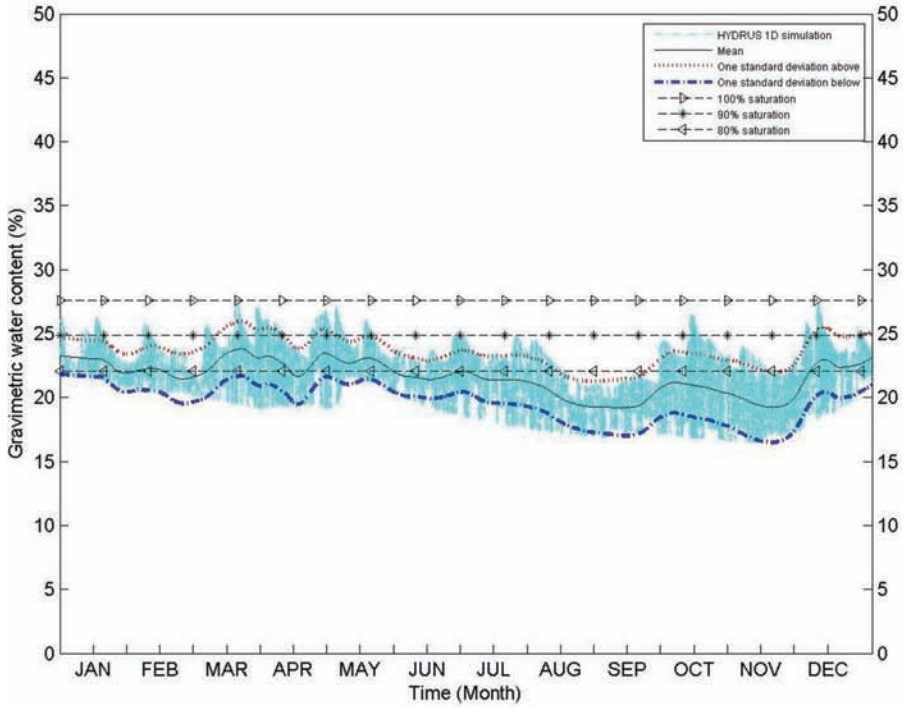

(b)

Figure A.35 Annual soil moisture variation for (a) 60 cm depth and (b) 90 cm depth for Lawrence County for profile (LAW-1).

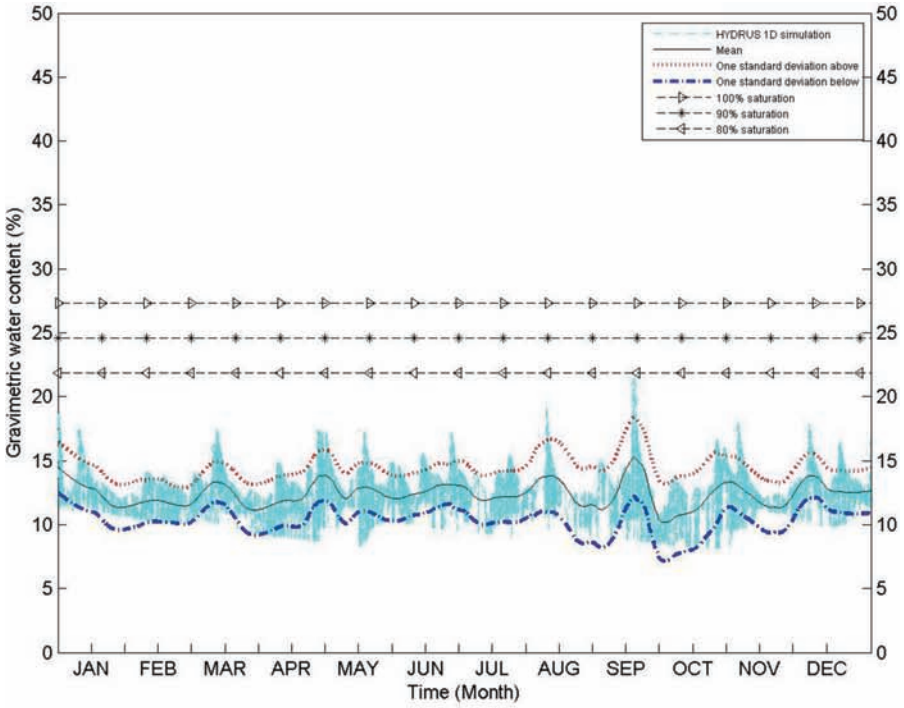

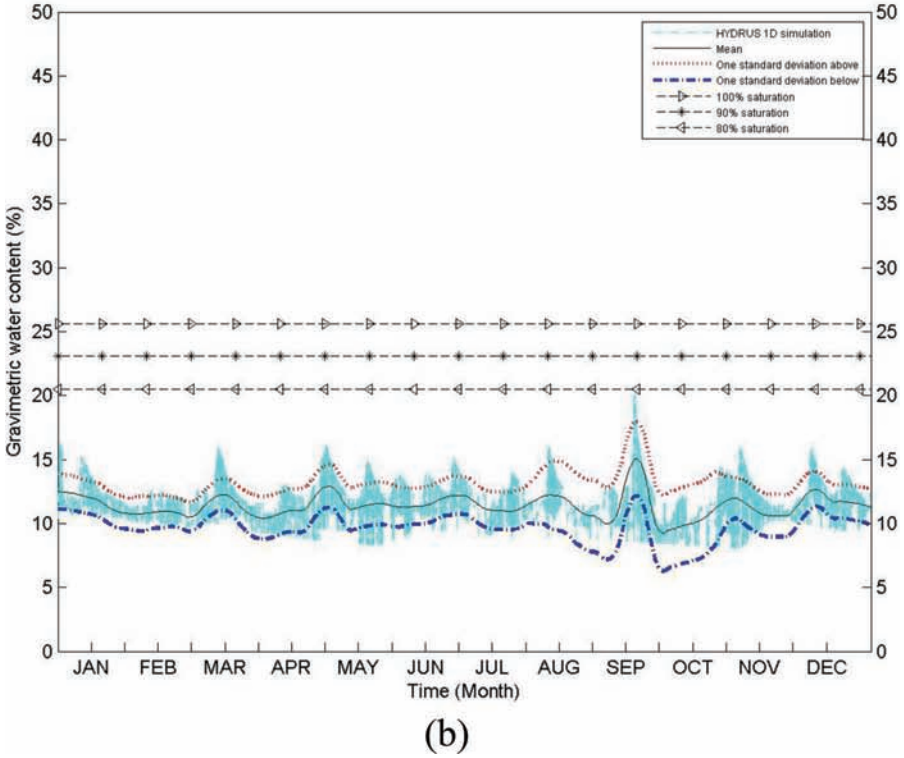

Figure A.36 Annual soil moisture variation for (a) 60 cm depth and (b) 90 cm depth for Marshall County for profile (MARS-1).

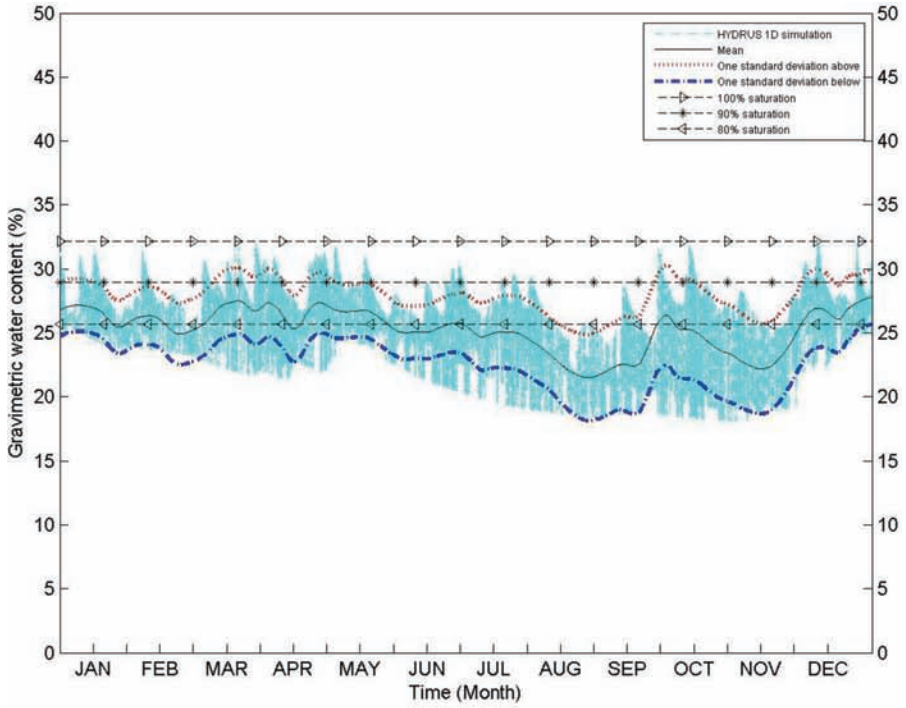

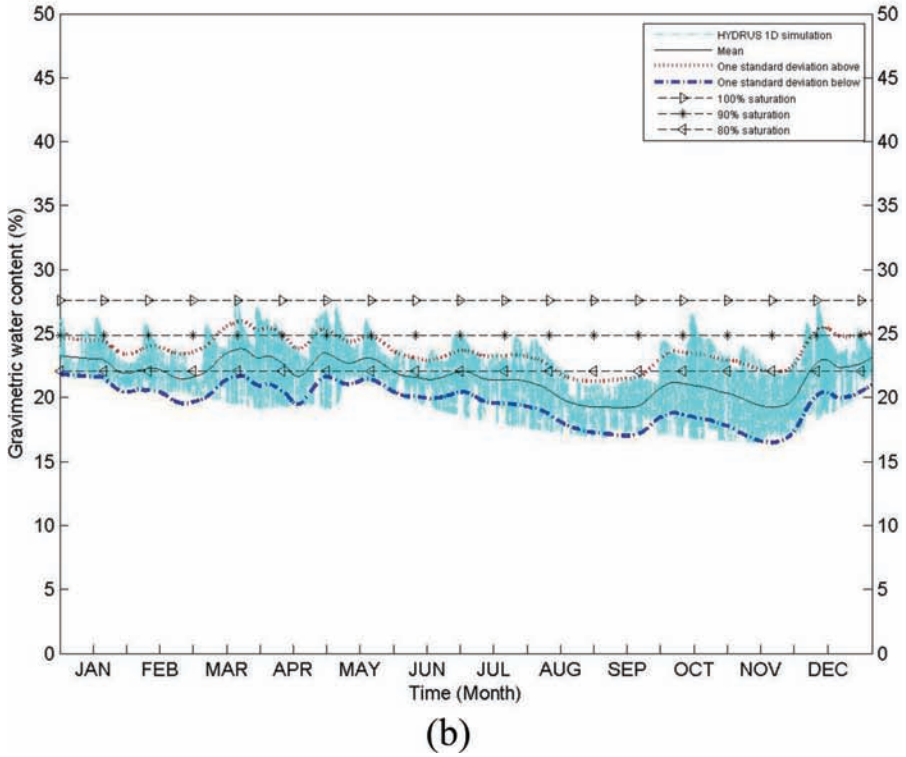

Figure A.37 Annual soil moisture variation for (a) 60 cm depth and (b) 90 cm depth for Martin County for profile (MART-1).

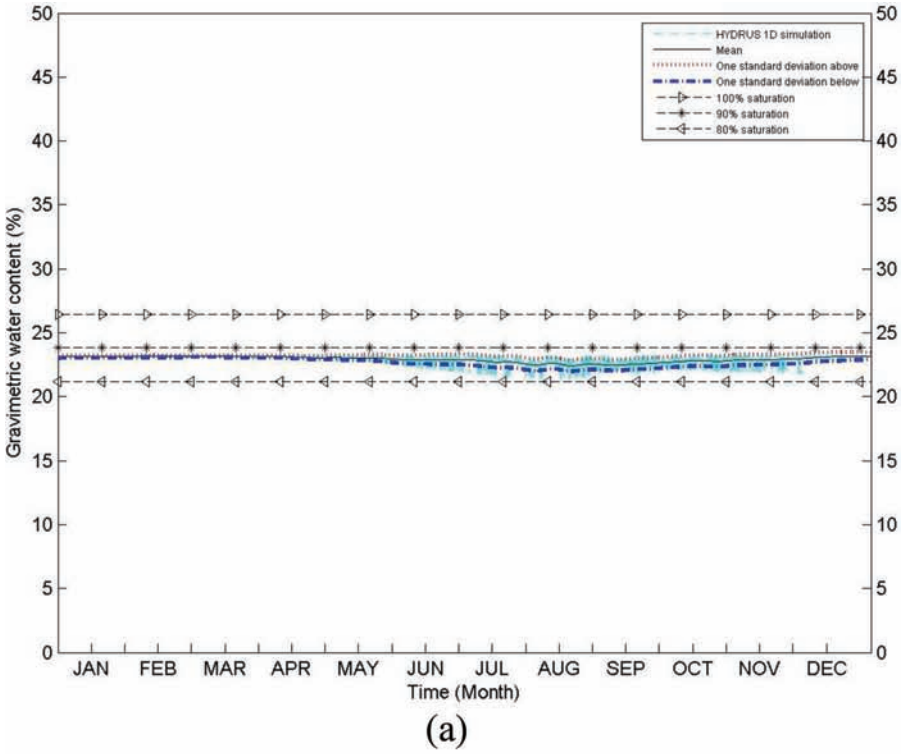

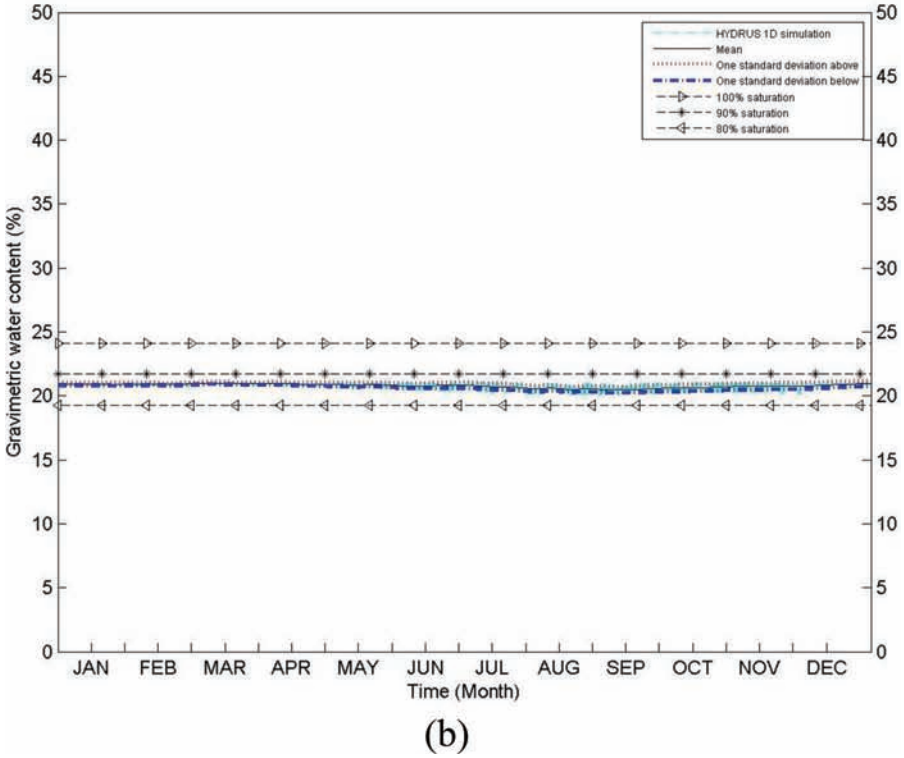

Figure A.38 Annual soil moisture variation for (a) 60 cm depth and (b) 90 cm depth for Miami County for profile (MIA-1).

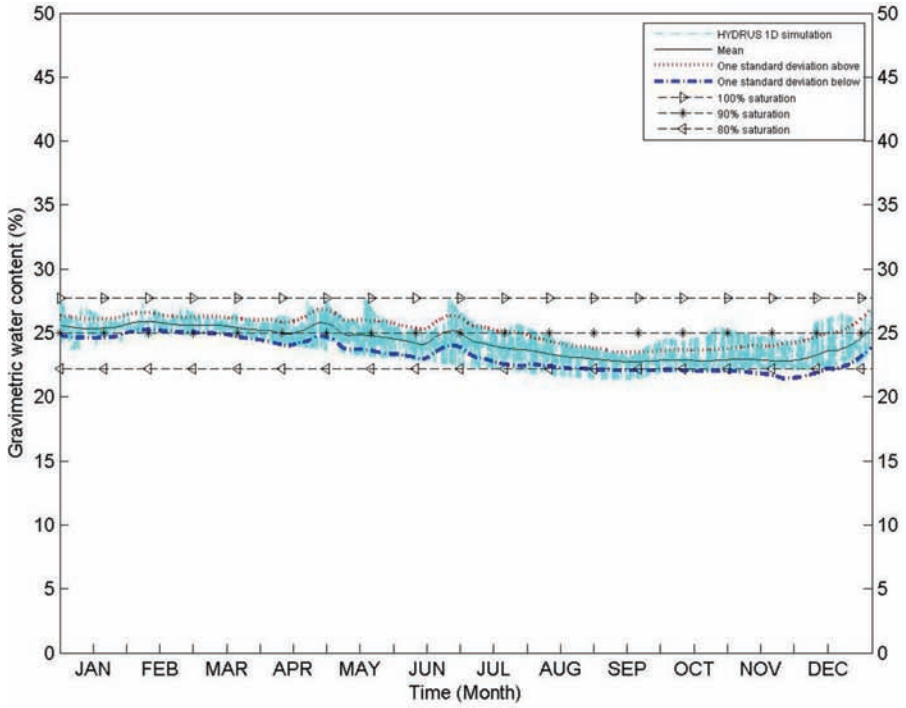

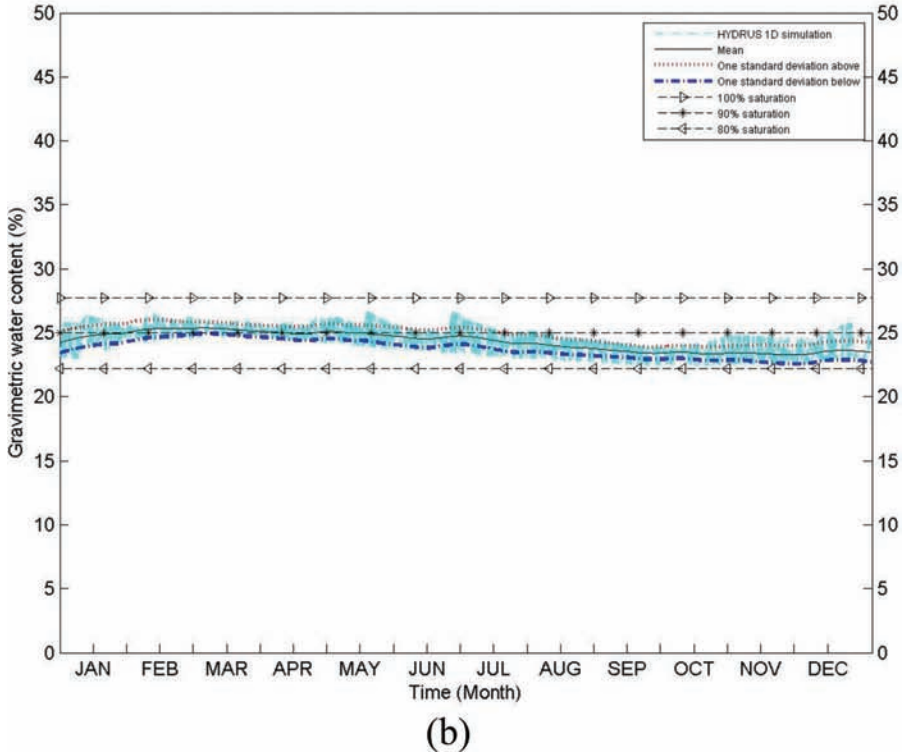

Figure A.39 Annual soil moisture variation for (a) 60 cm depth and (b) 90 cm depth for Montgomery County for profile (MONT-1).

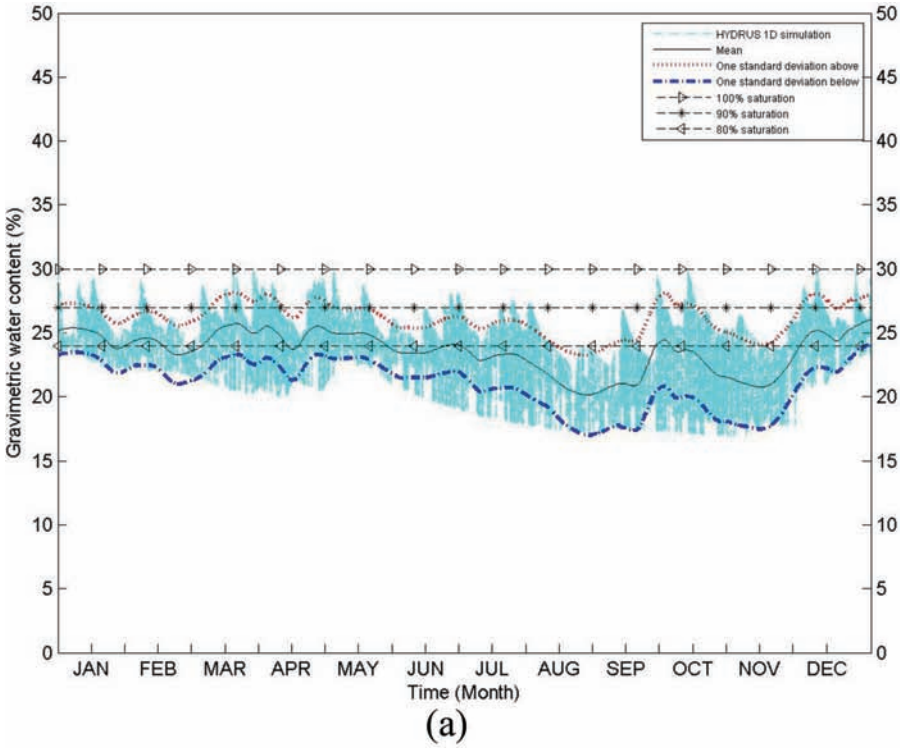

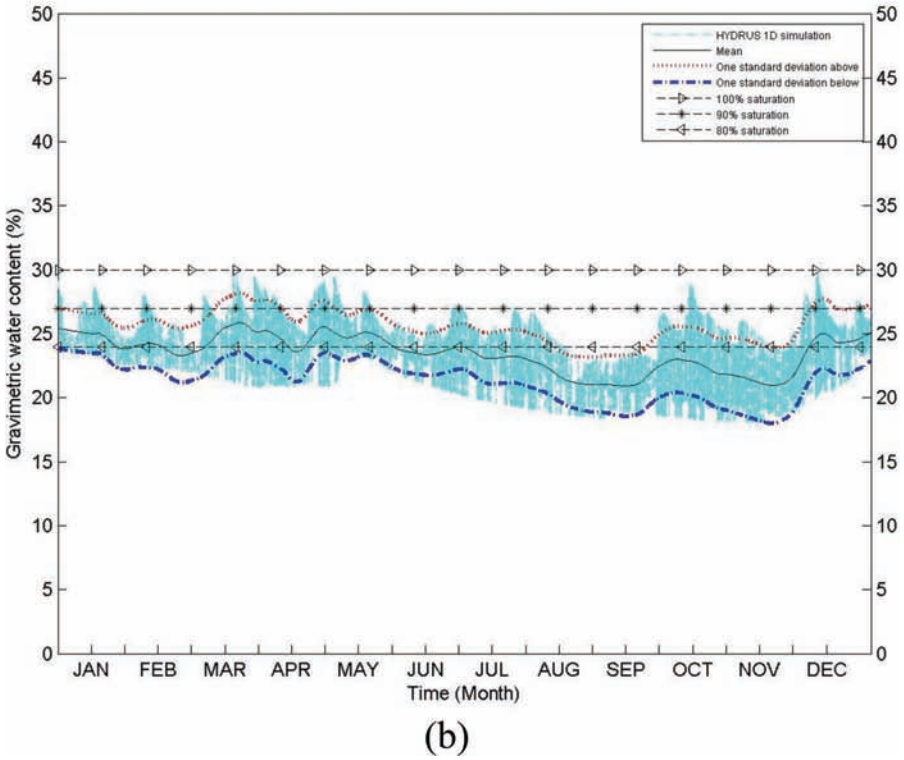

Figure A.40 Annual soil moisture variation for (a) 60 cm depth and (b) 90 cm depth for Morgan County for profile (MOR-1).

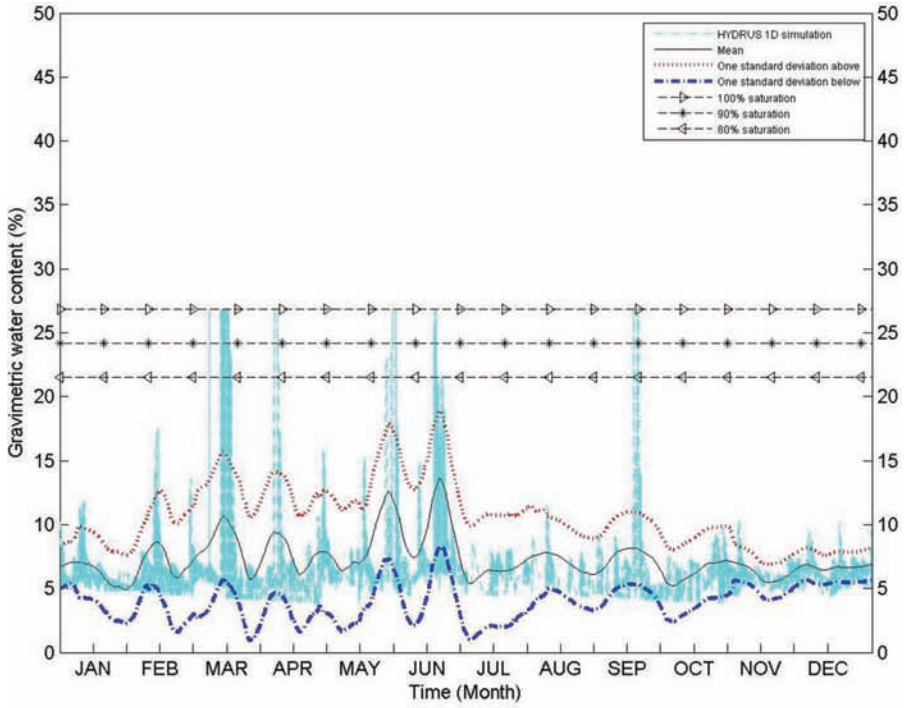

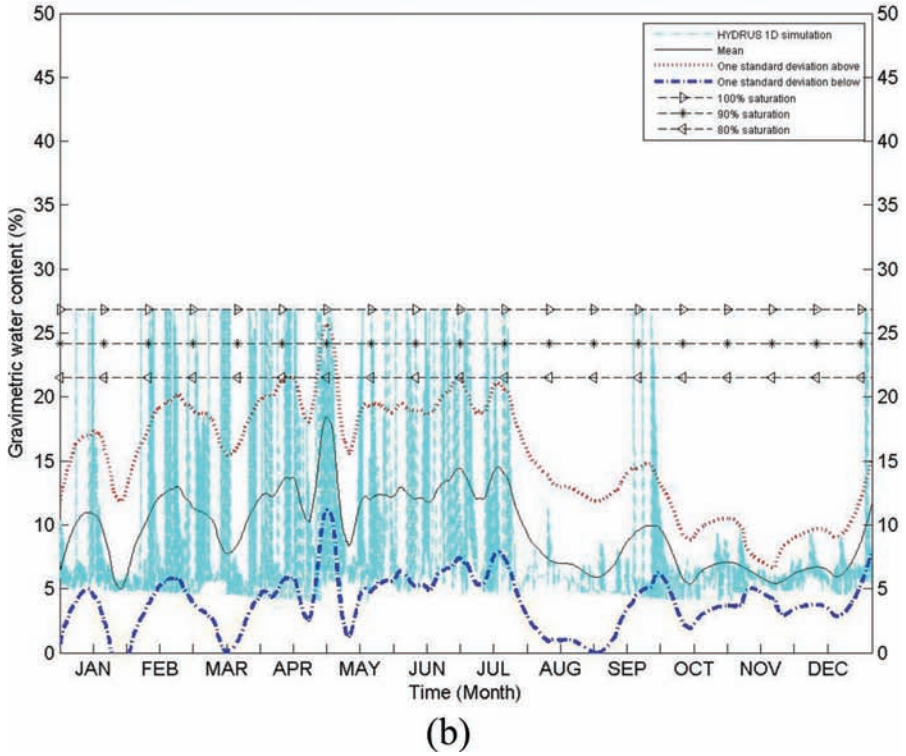

Figure A.41 Annual soil moisture variation for (a) 60 cm depth and (b) 90 cm depth for Newton County for profile (NEW-1).

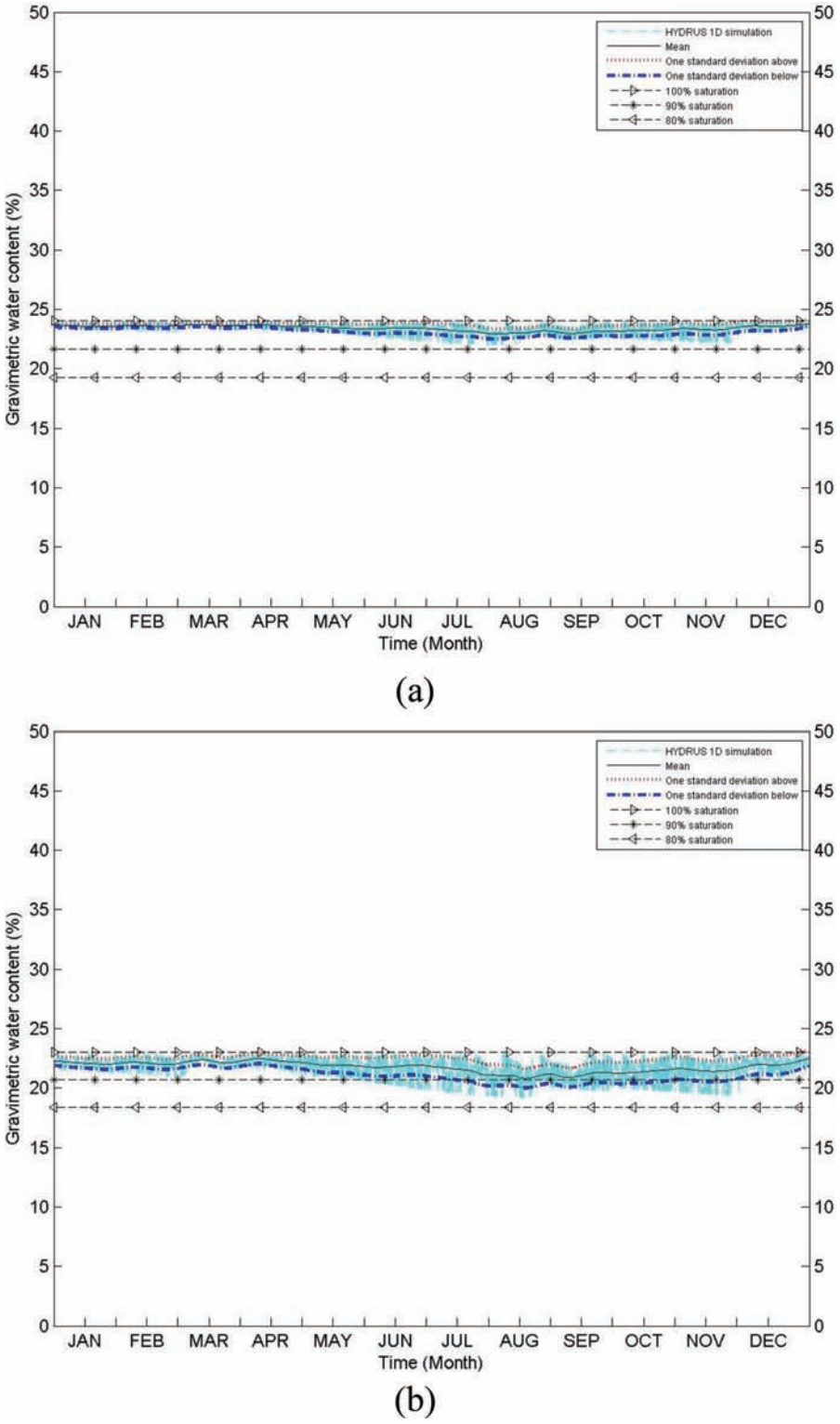

Figure A.42 Annual soil moisture variation for (a) 60 cm depth and (b) 90 cm depth for Noble County for profile (NOB-1).

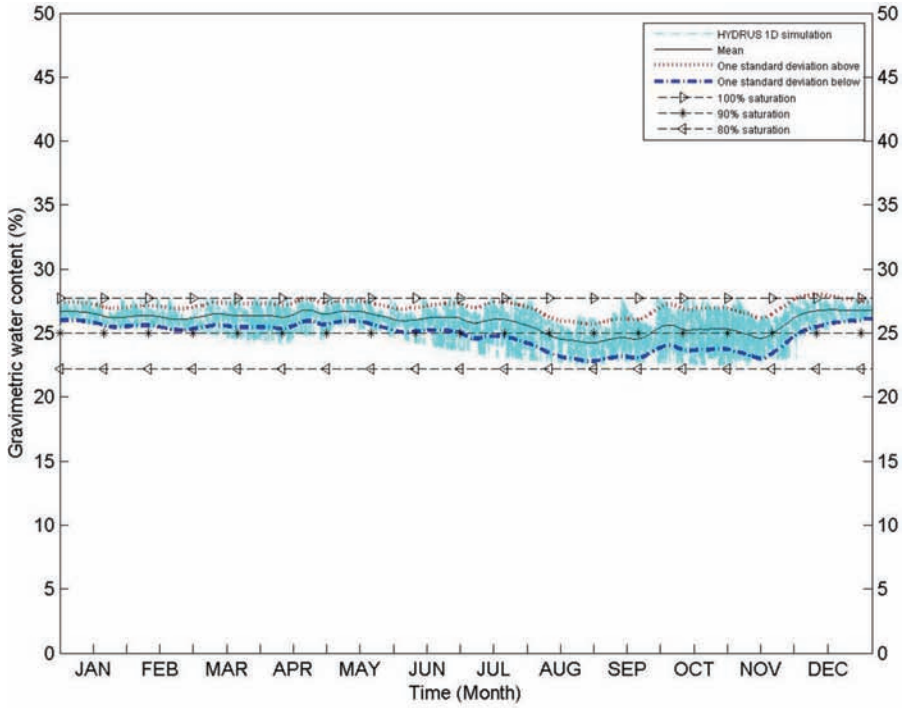

Figure A.43 Annual soil moisture variation for (a) 60 cm depth and (b) 90 cm depth for Owen County for profile (OWE-1).

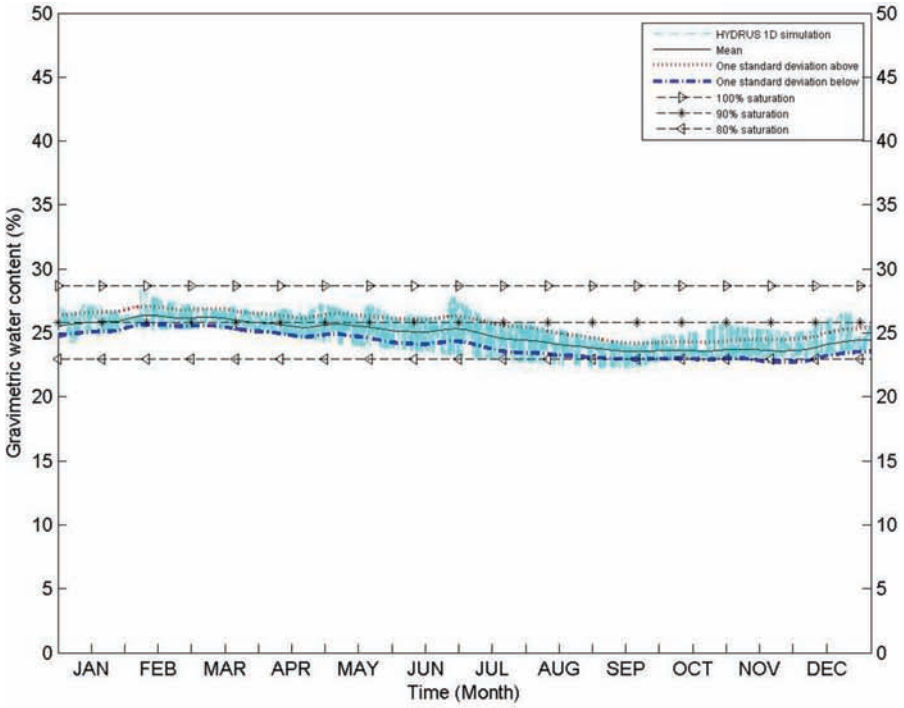

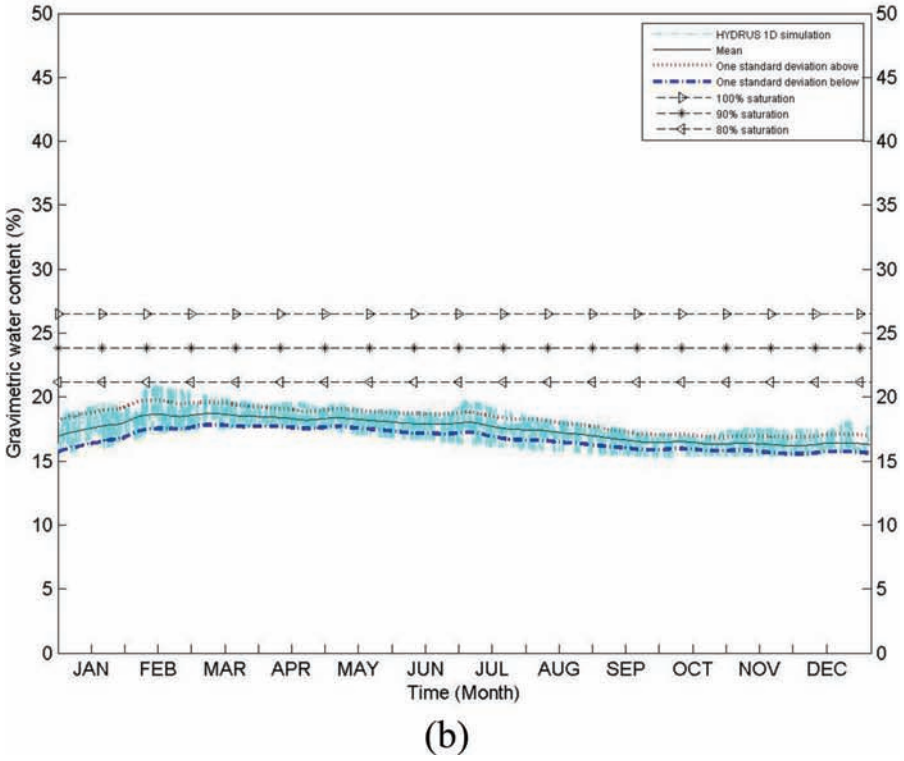

Figure A.44 Annual soil moisture variation for (a) 60 cm depth and (b) 90 cm depth for Parke County for profile (PAR-1).

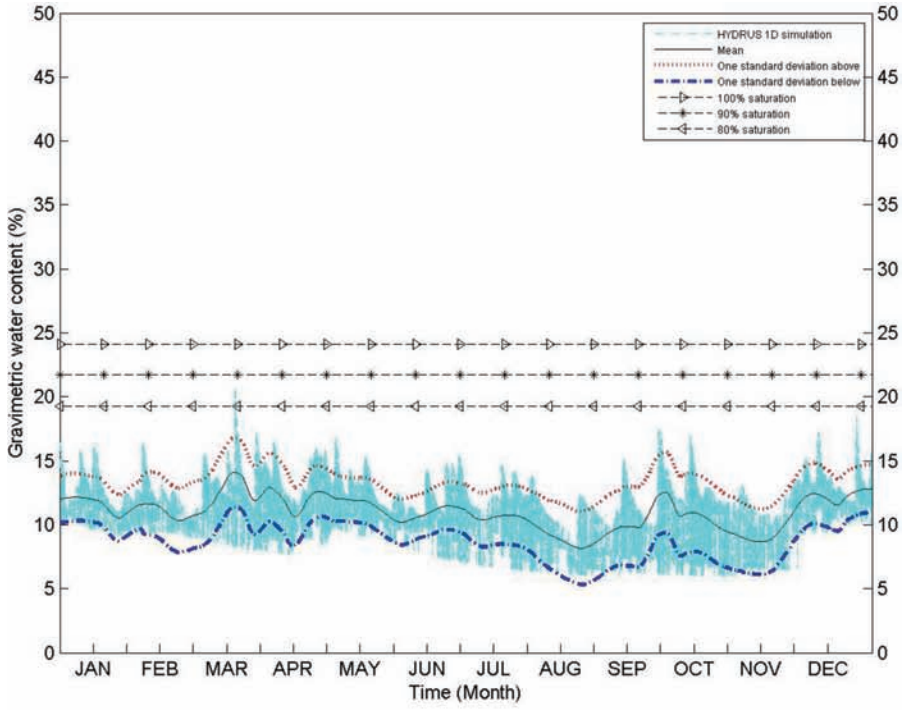

(a)

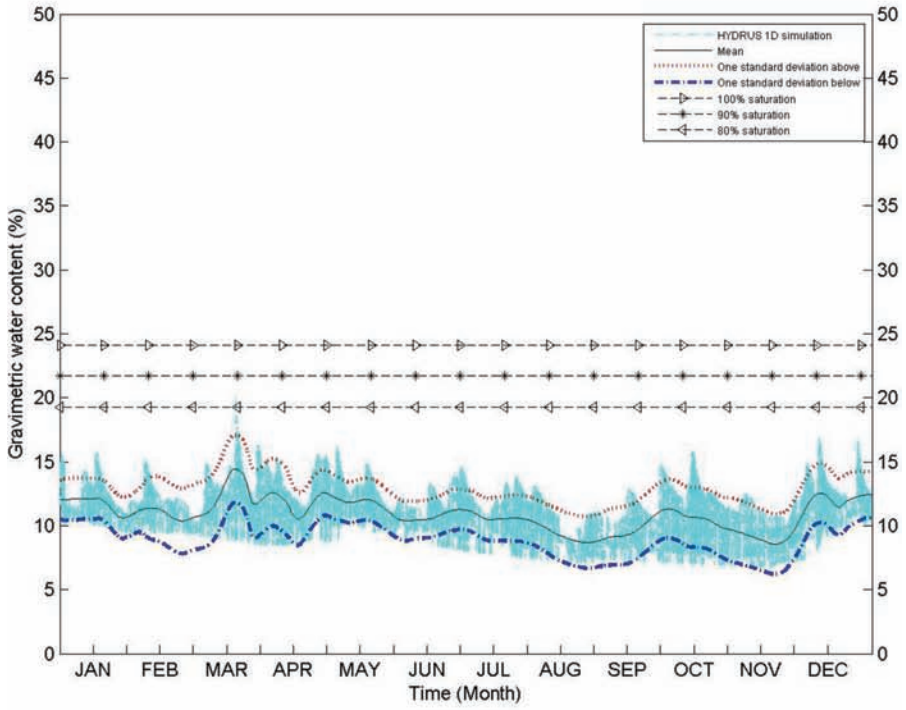

(b)

Figure A.45 Annual soil moisture variation for (a) 60 cm depth and (b) 90 cm depth for Perry County for profile (PER-1).

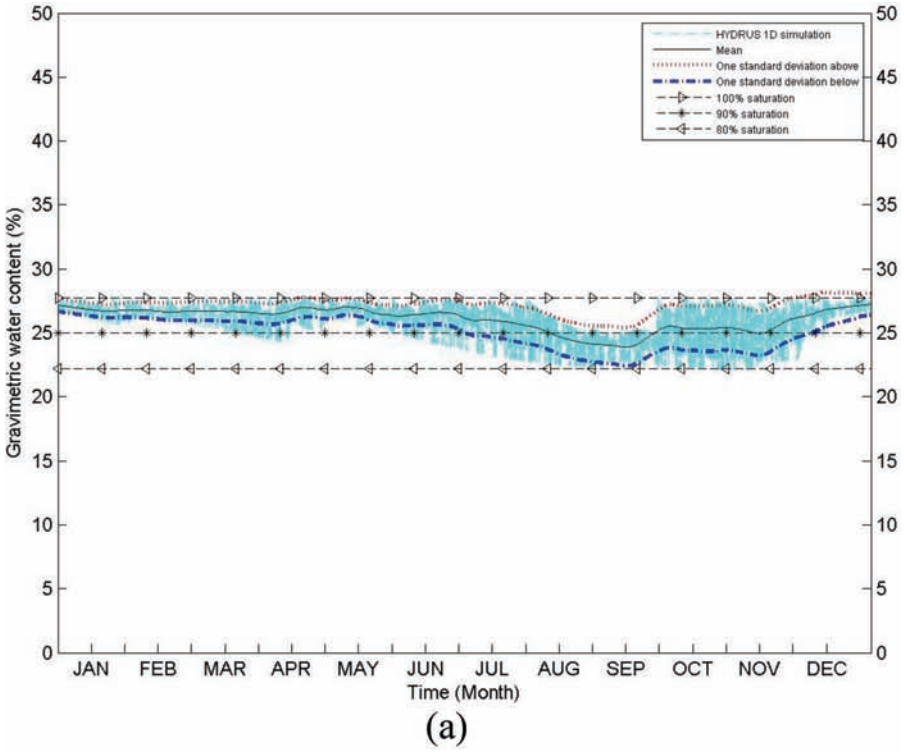

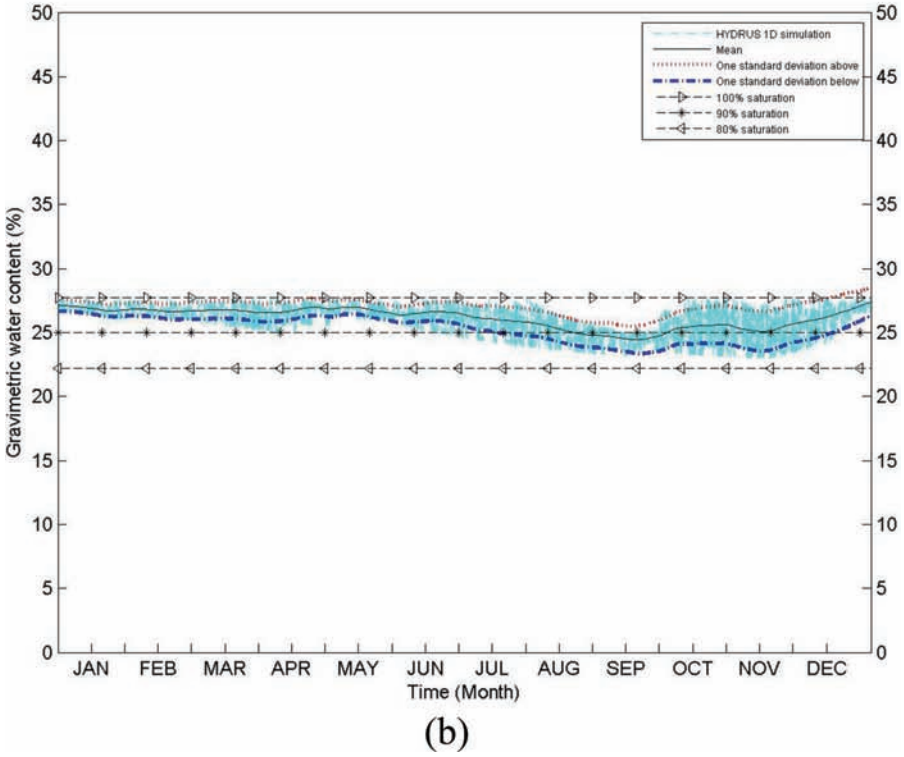

Figure A.46 Annual soil moisture variation for (a) 60 cm depth and (b) 90 cm depth for Pike County for profile (PIK-1).

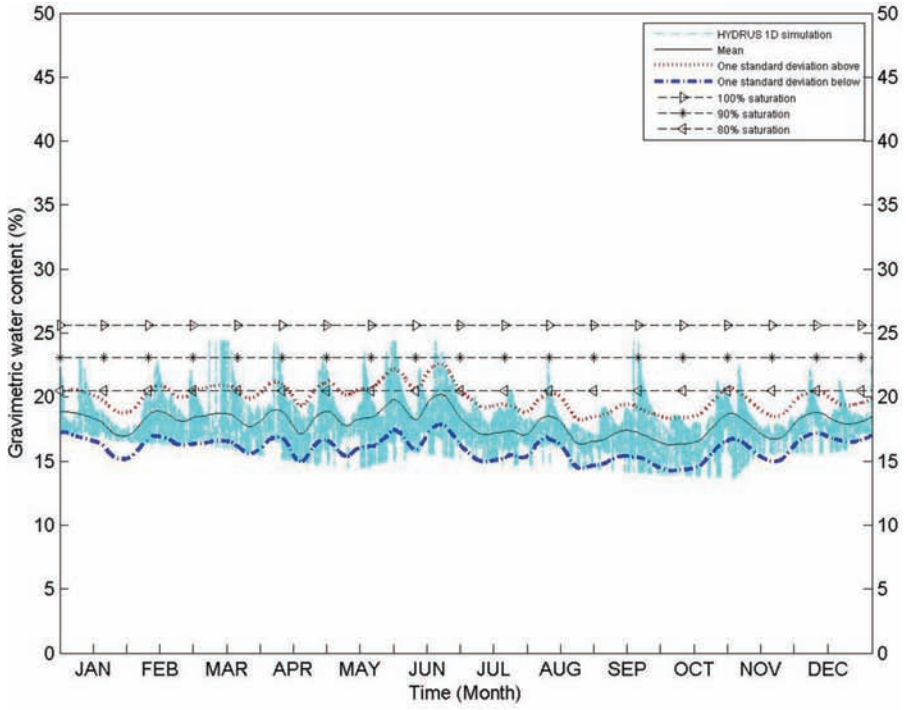

(a)

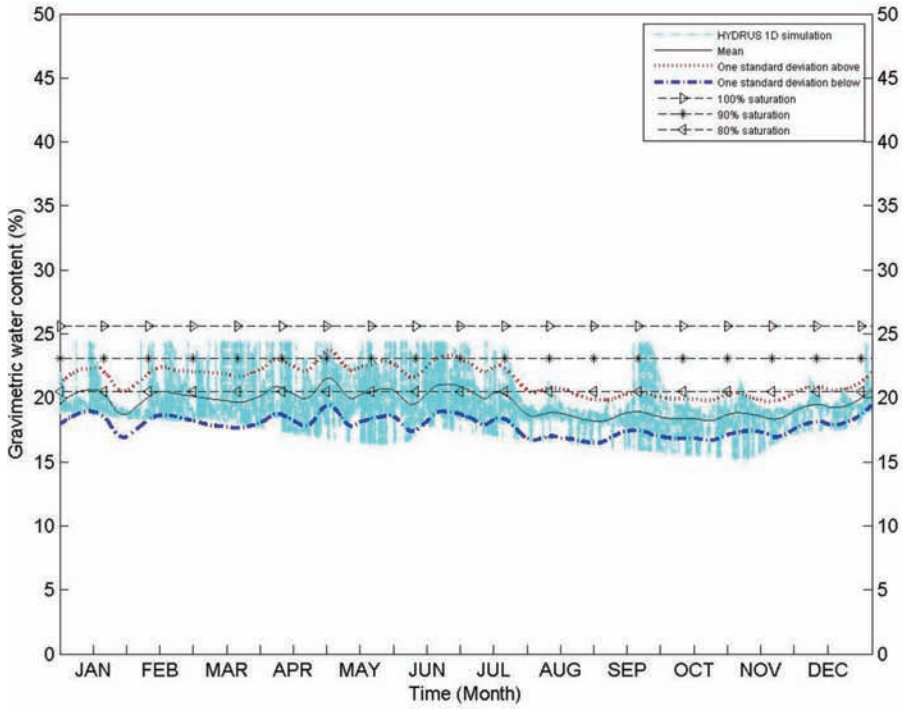

(b)

Figure A.47 Annual soil moisture variation for (a) 60 cm depth and (b) 90 cm depth for Porter County for profile (POR-1).

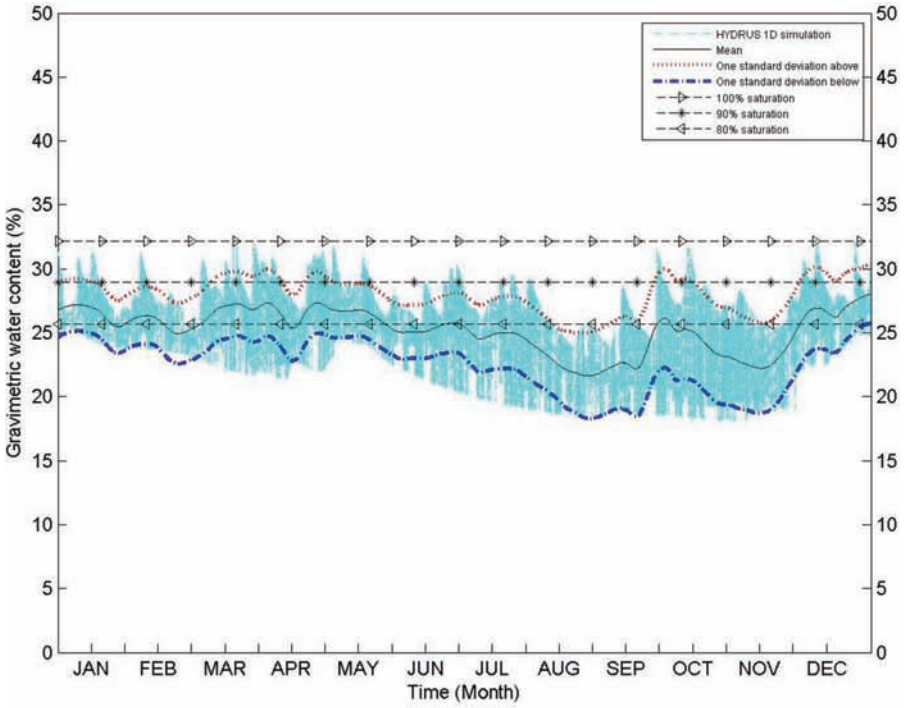

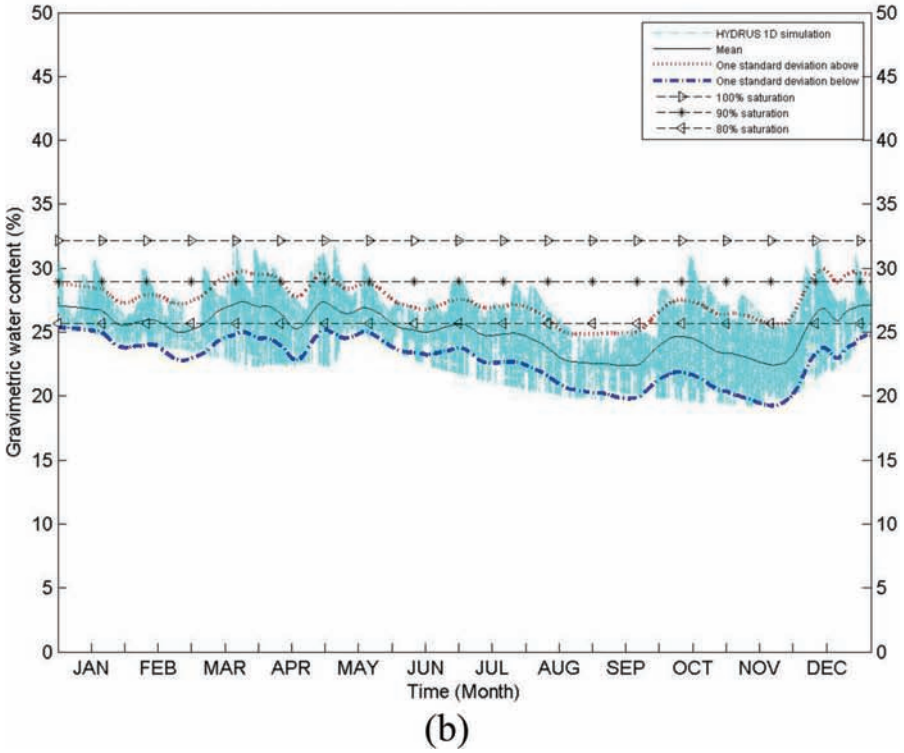

Figure A.48 Annual soil moisture variation for (a) 60 cm depth and (b) 90 cm depth for Posey County for profile (POS-1).

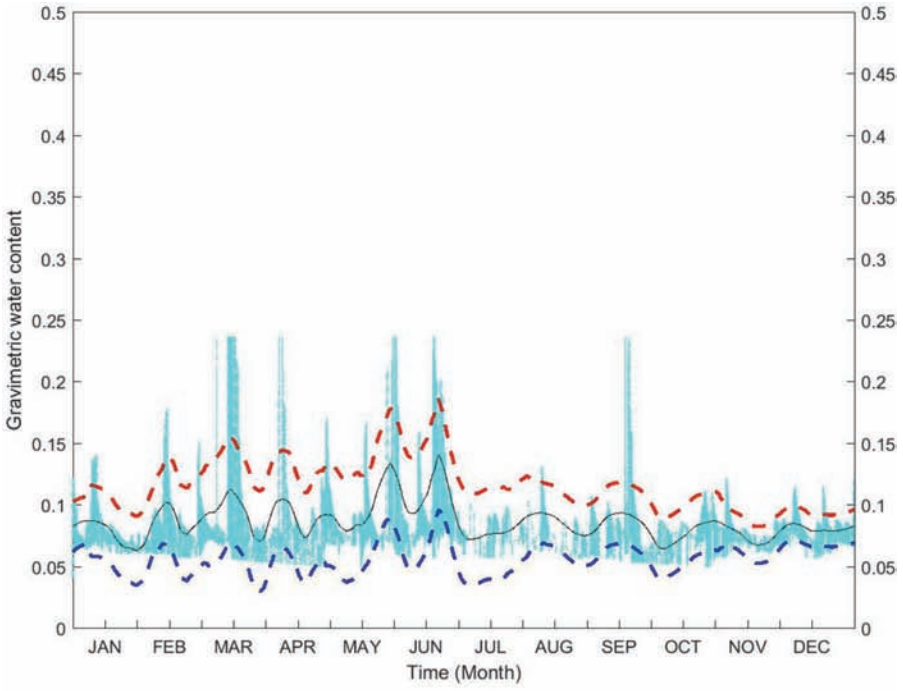

(a)

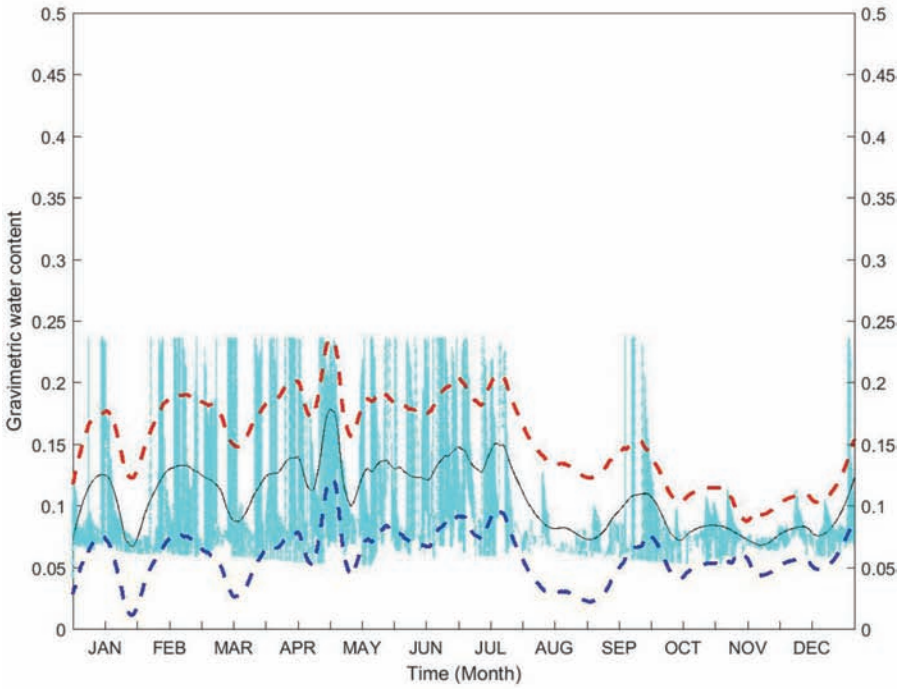

(b)

Figure A.49 Annual soil moisture variation for (a) 60 cm depth and (b) 90 cm depth for Pulaski County for profile (PUL-1).

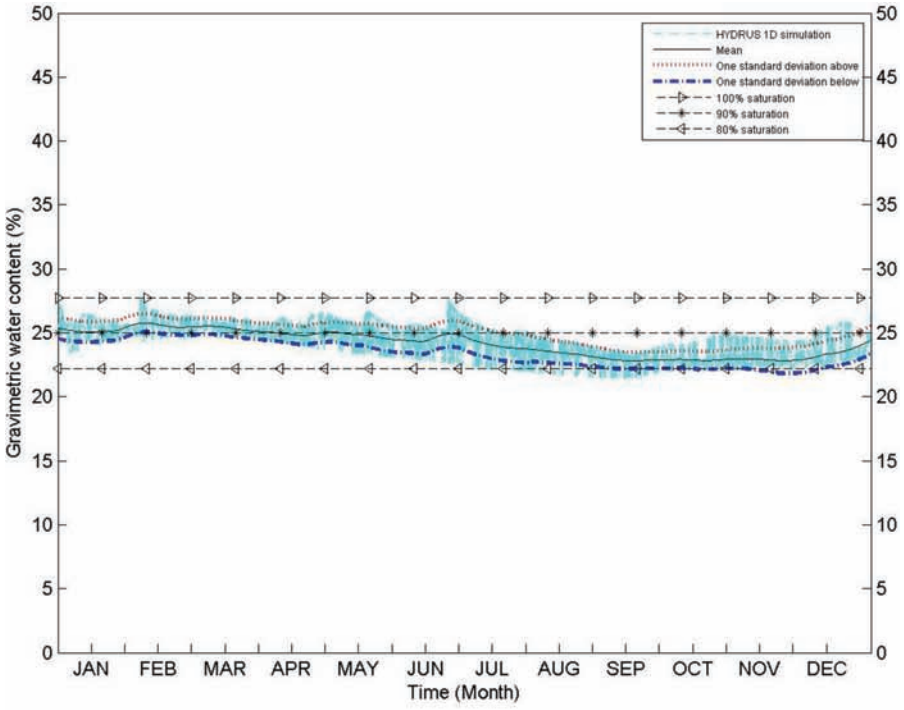

(a)

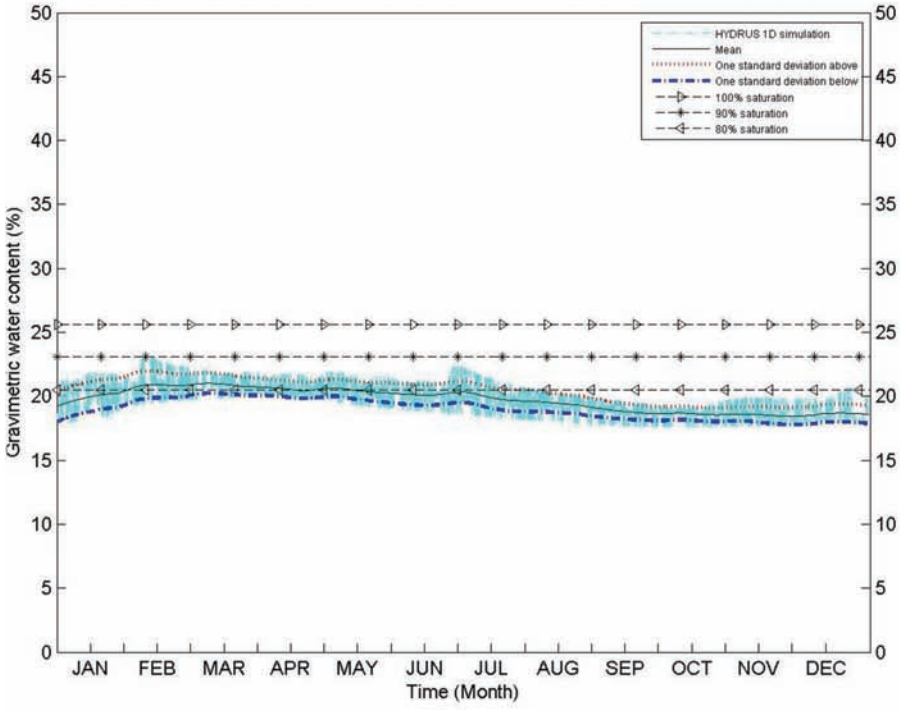

(b)

Figure A.50 Annual soil moisture variation for (a) 60 cm depth and (b) 90 cm depth for Putnam County for profile (PUT-1).

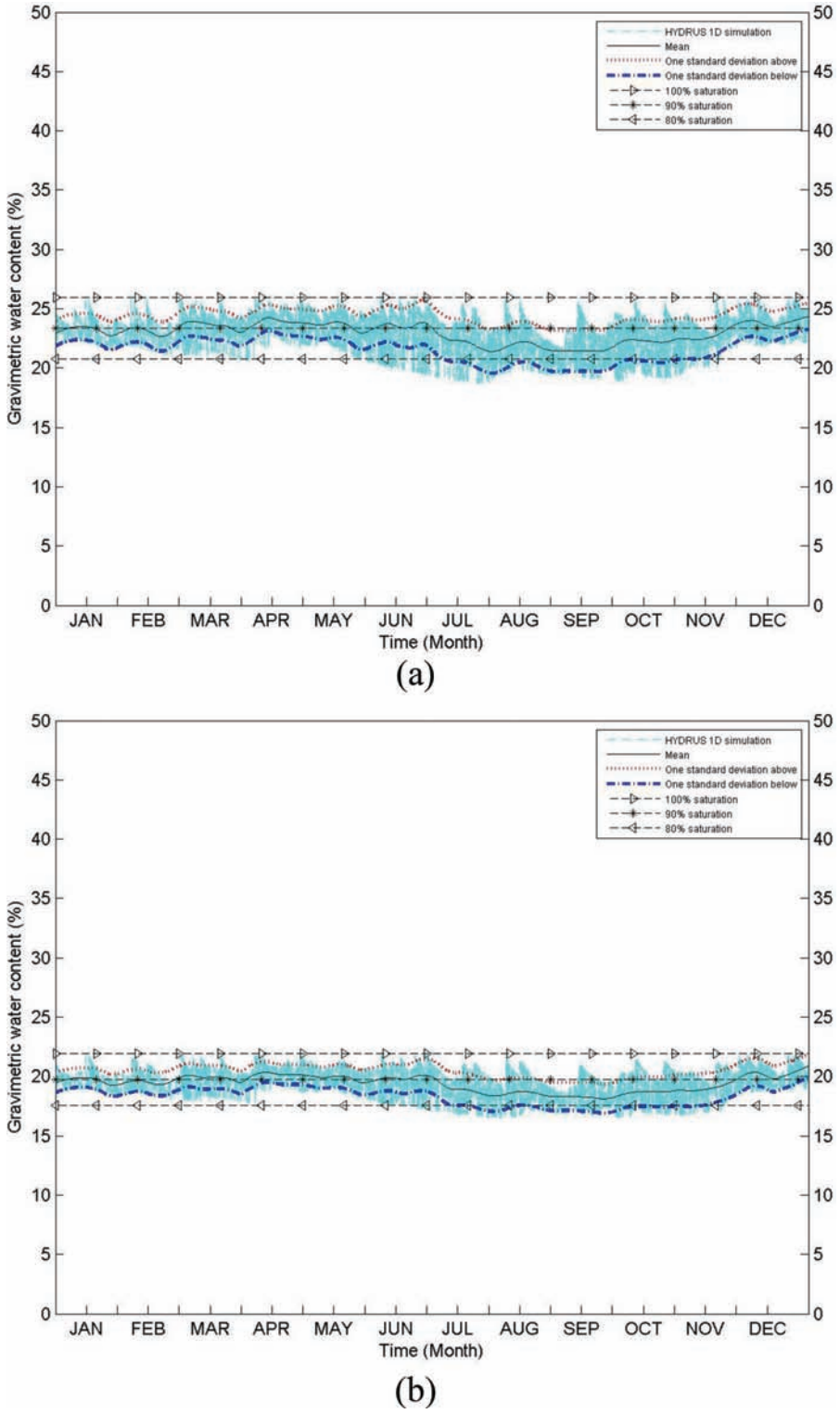

Figure A.51 Annual soil moisture variation for (a) 60 cm depth and (b) 90 cm depth for Randolph County for profile (RAN-1).

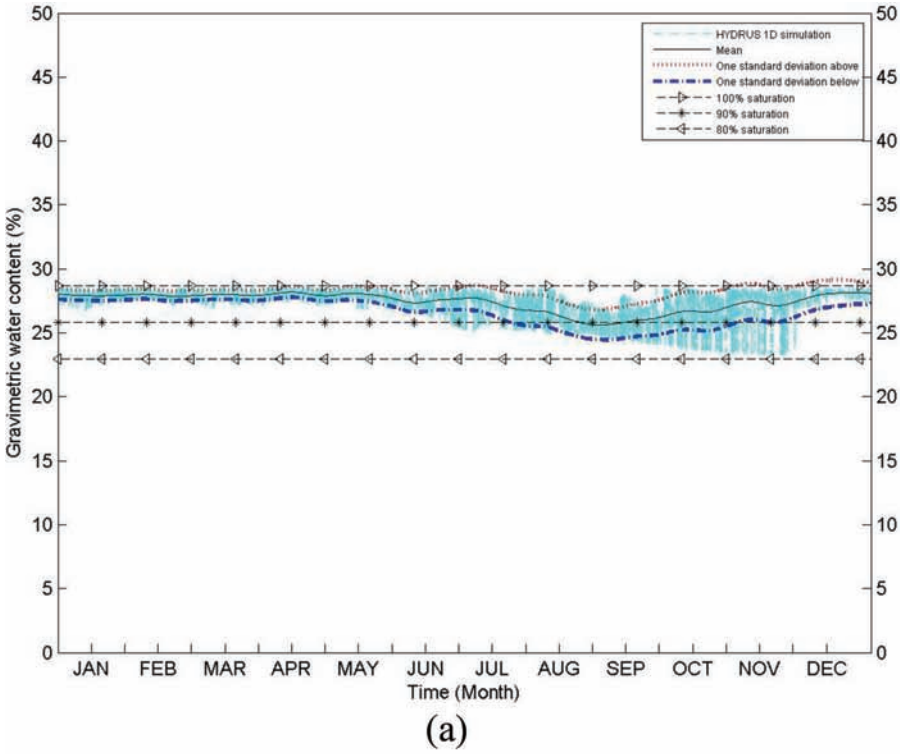

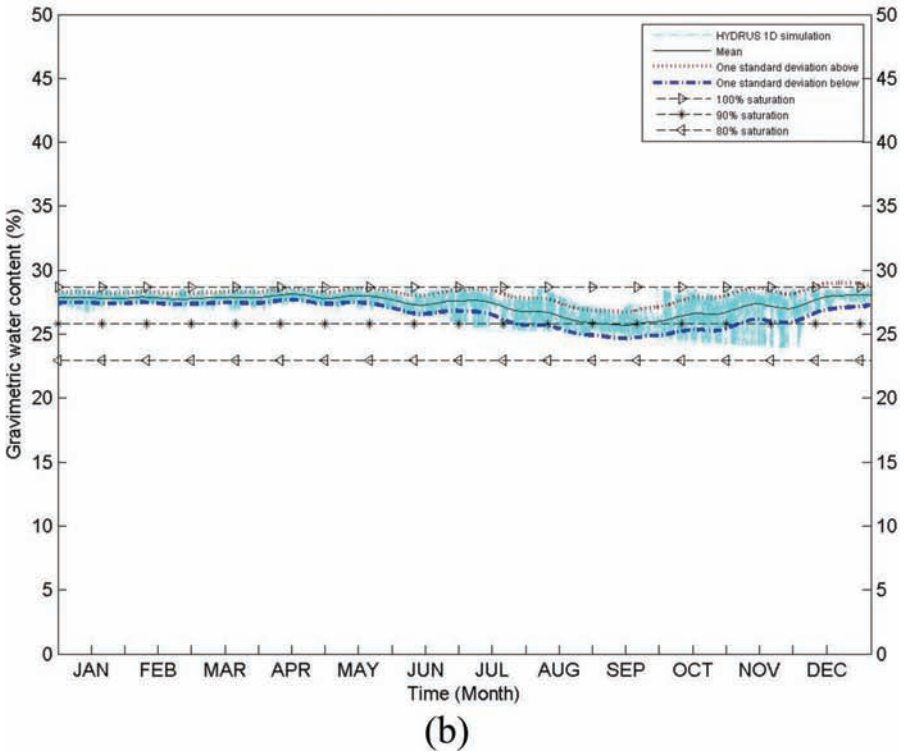

Figure A.52 Annual soil moisture variation for (a) 60 cm depth and (b) 90 cm depth for Ripley County for profile (RIP-1).

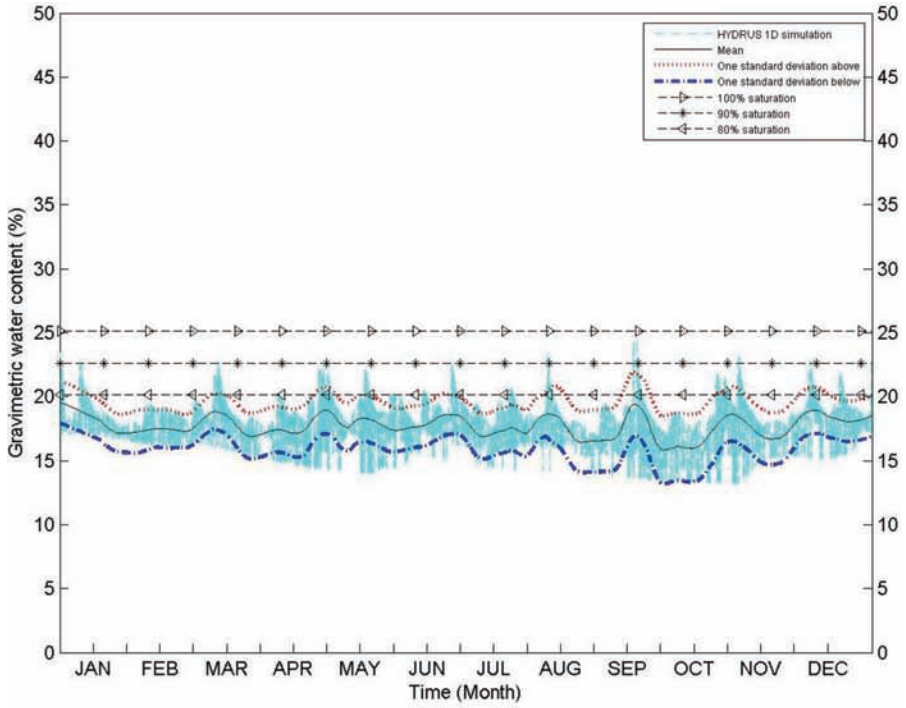

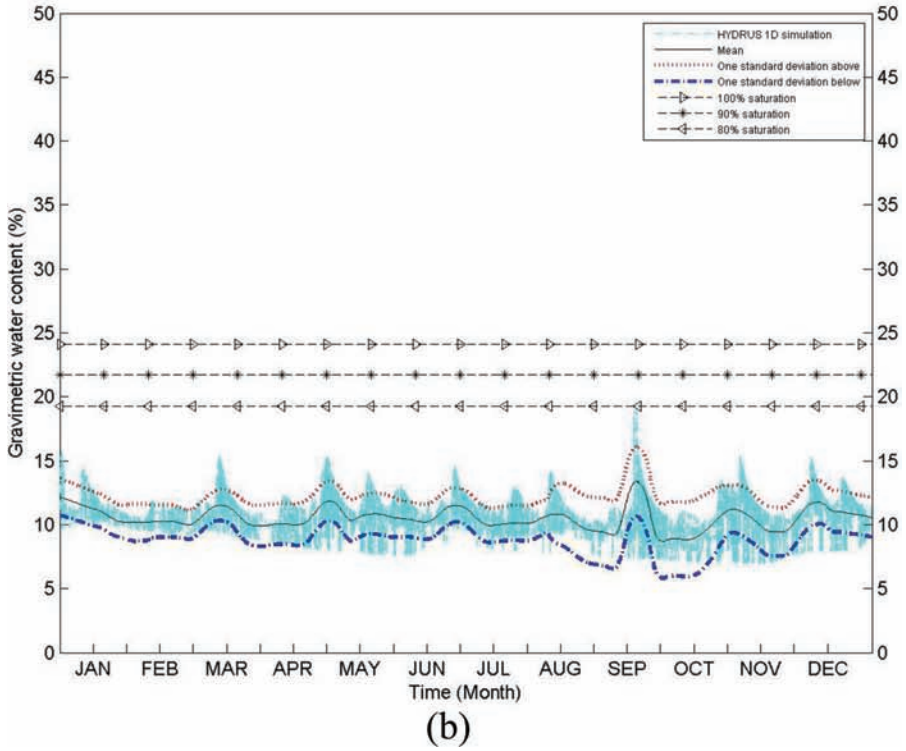

Figure A.53 Annual soil moisture variation for (a) 60 cm depth and (b) 90 cm depth for St. Joseph County for profile (STJ-1).

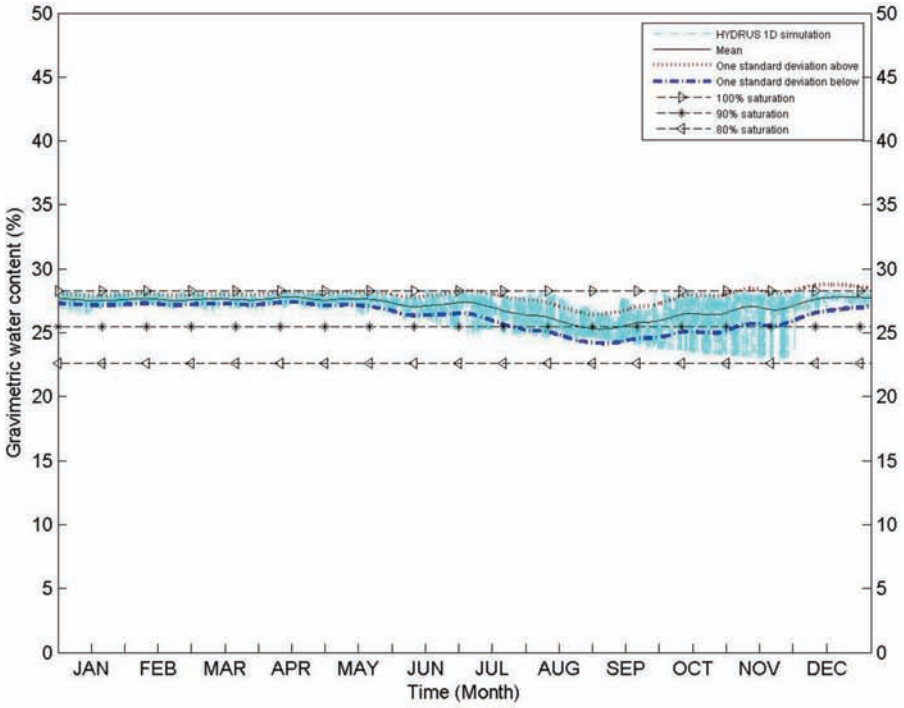

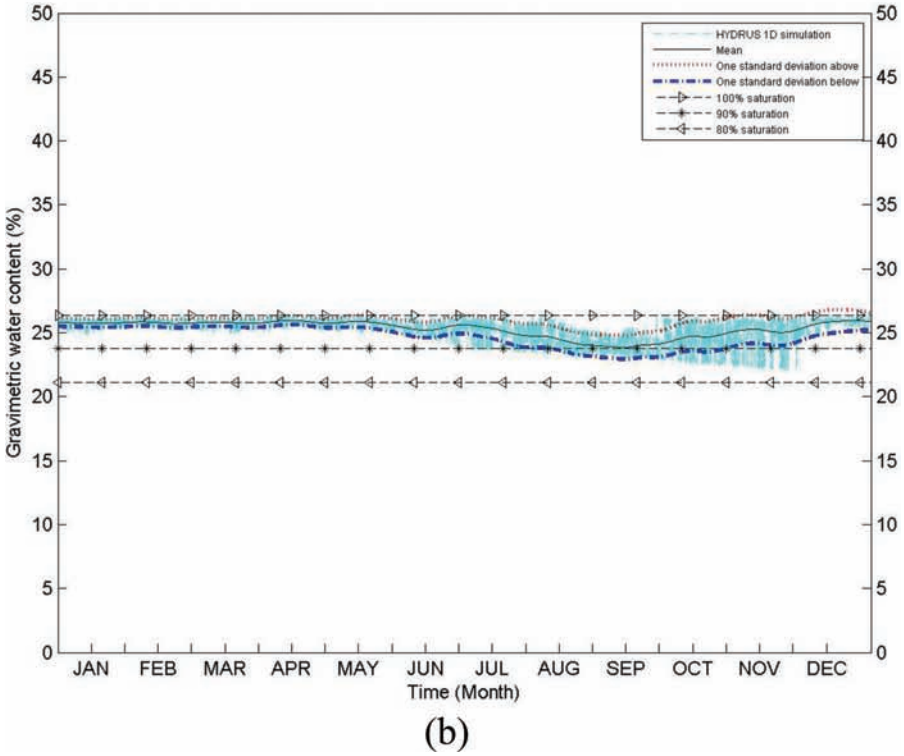

Figure A.54 Annual soil moisture variation for (a) 60 cm depth and (b) 90 cm depth for Scott County for profile (SCO-1).

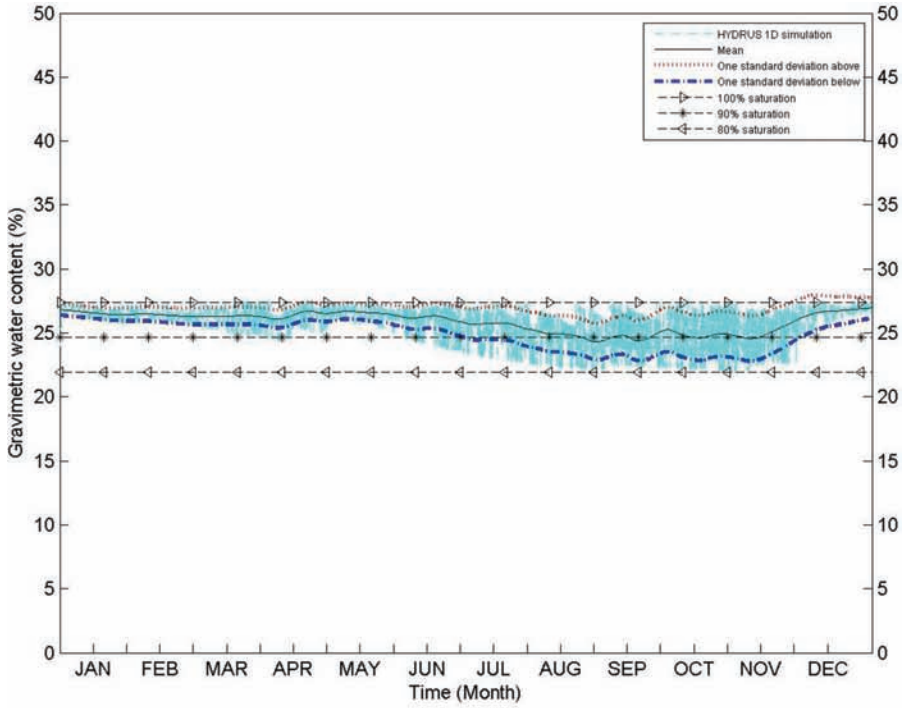

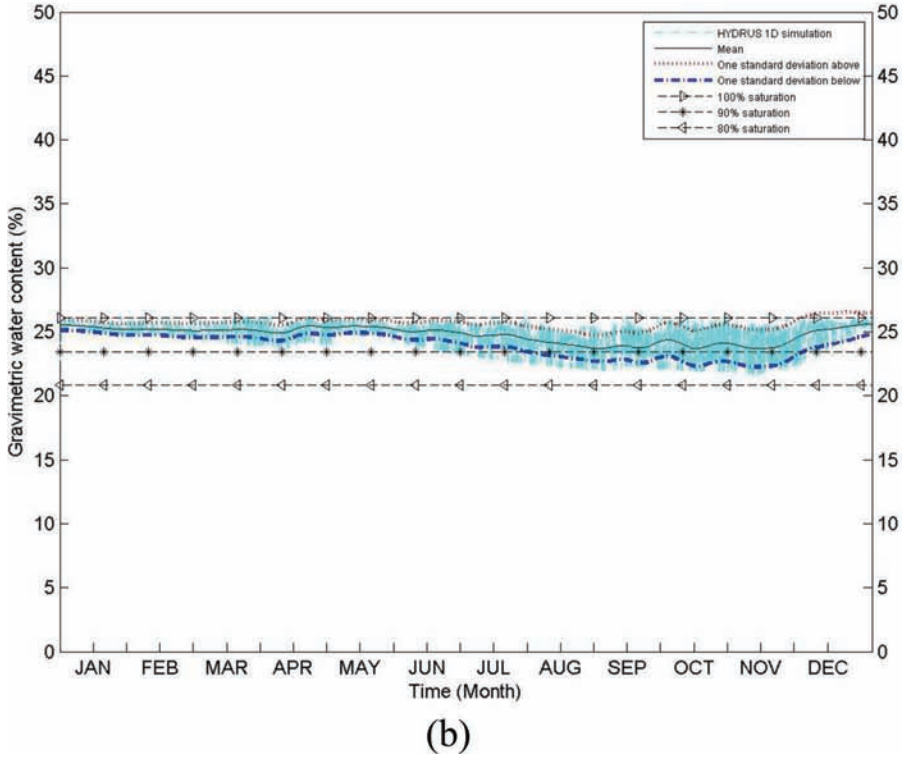

Figure A.55 Annual soil moisture variation for (a) 60 cm depth and (b) 90 cm depth for Spencer County for profile (SPE-1).

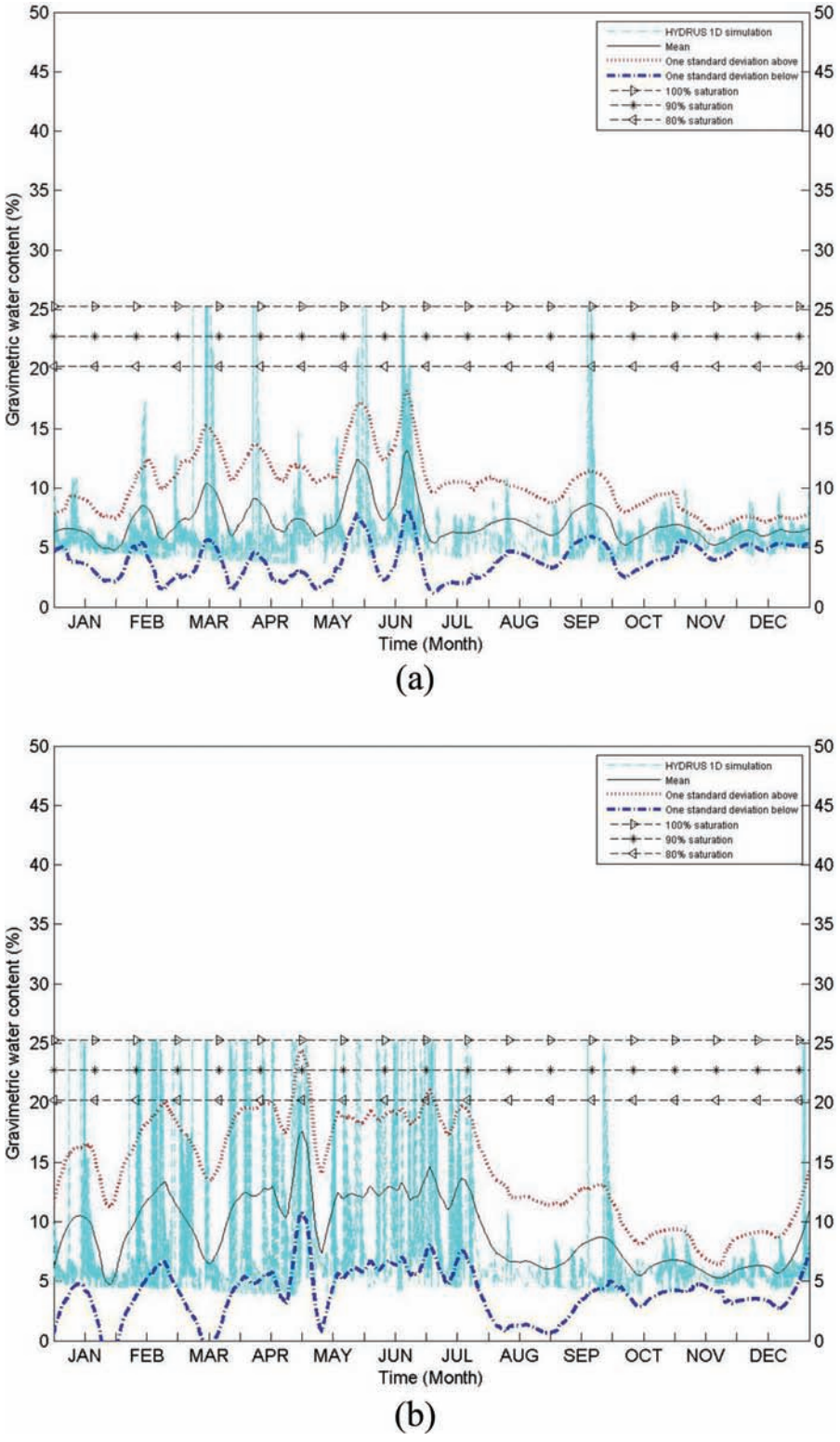

Figure A.56 Annual soil moisture variation for (a) 60 cm depth and (b) 90 cm depth for Starke County for profile (STA-1).

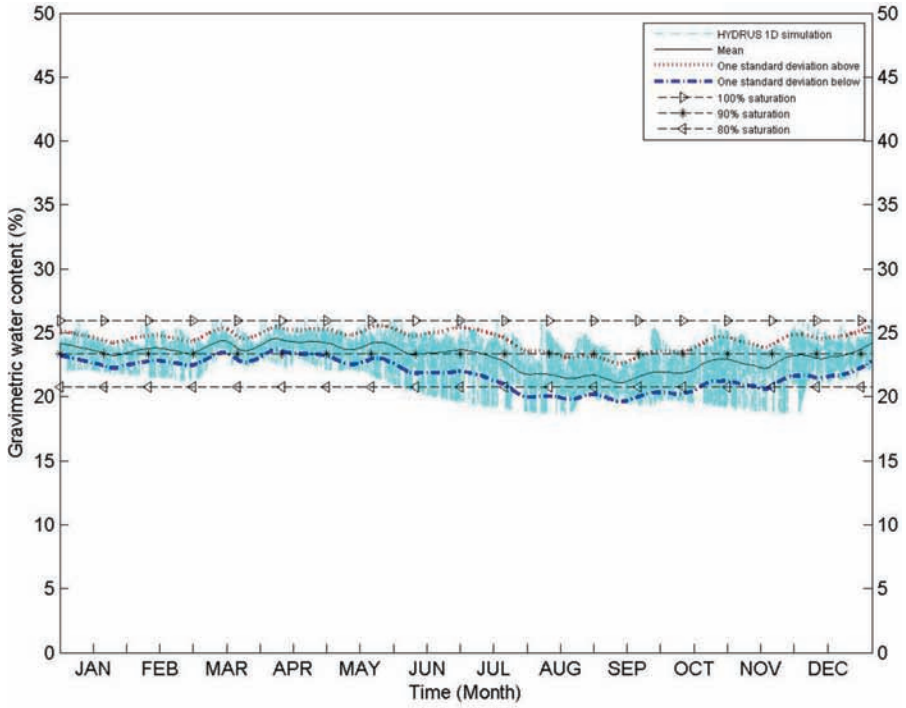

(a)

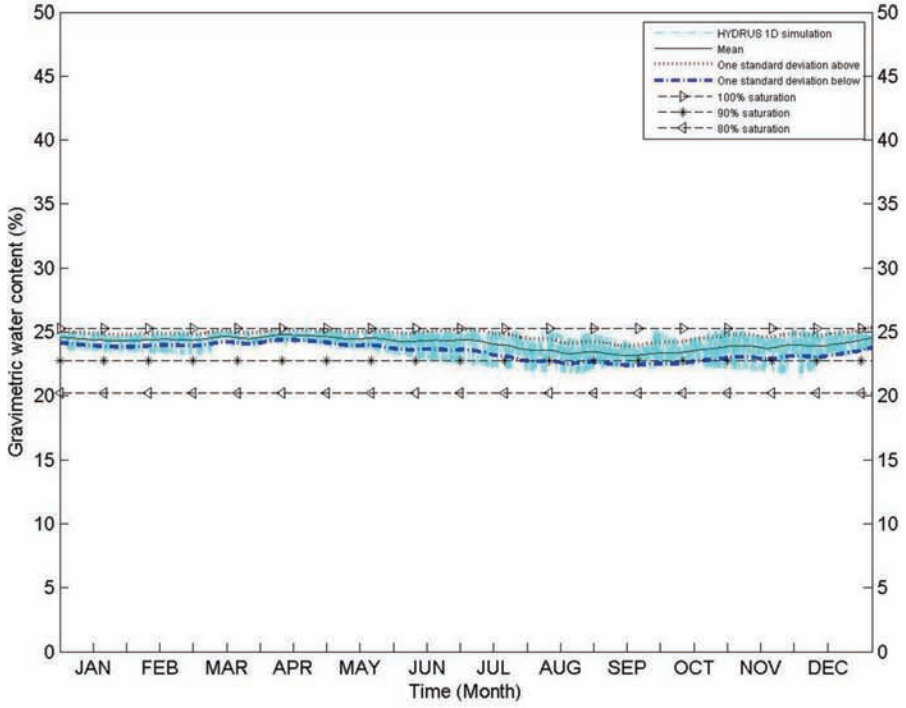

(b)

Figure A.57 Annual soil moisture variation for (a) 60 cm depth and (b) 90 cm depth for Steuben County for profile (STE-1).

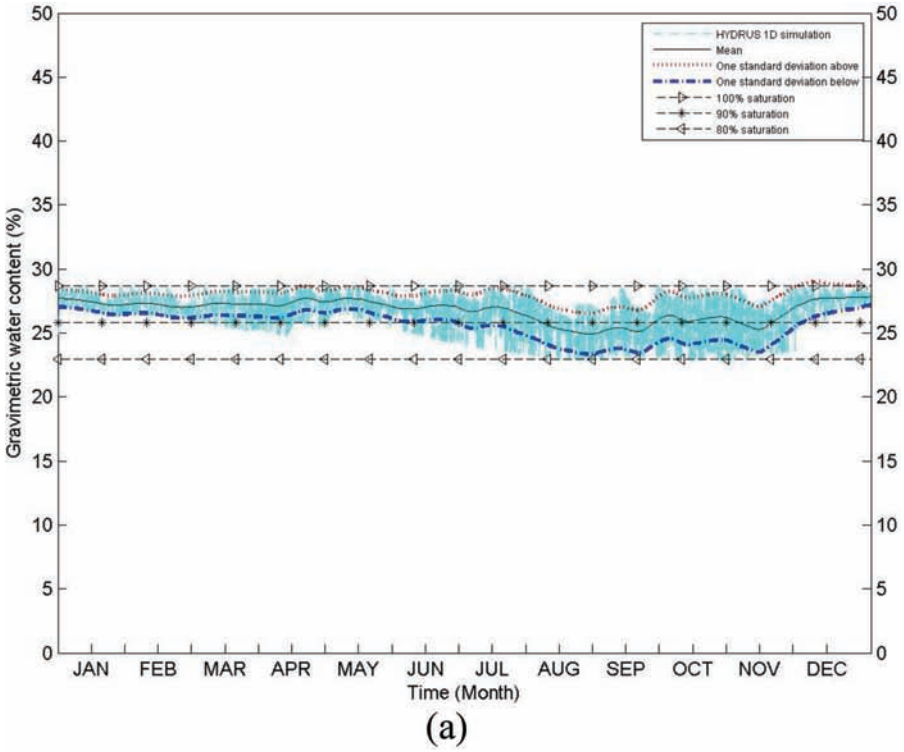

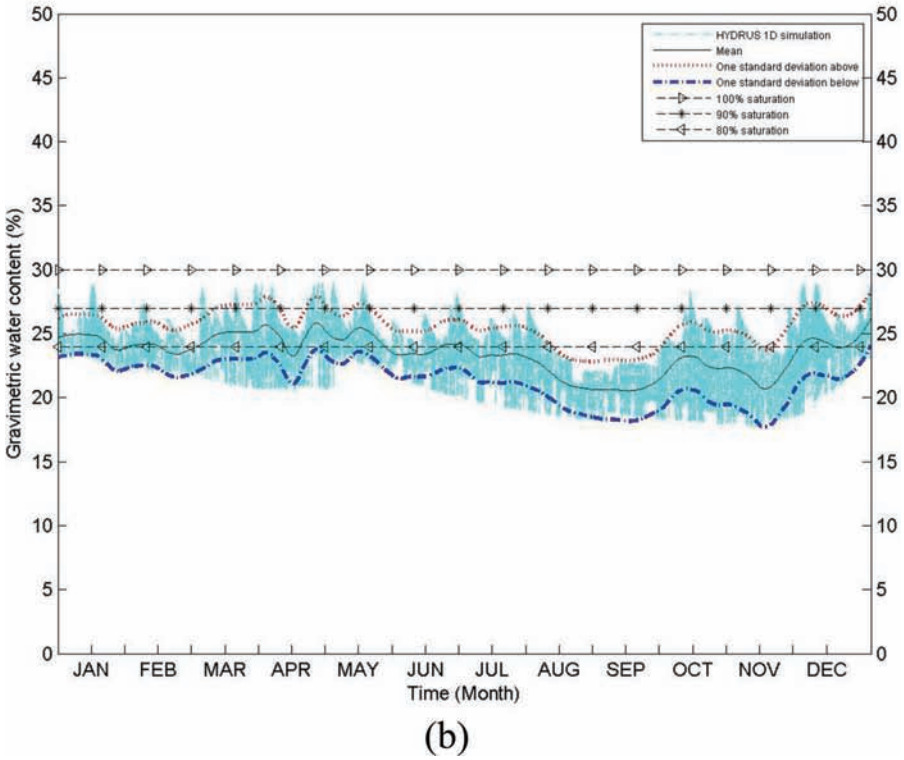

Figure A.58 Annual soil moisture variation for (a) 60 cm depth and (b) 90 cm depth for Sullivan County for profile (SUL-1).

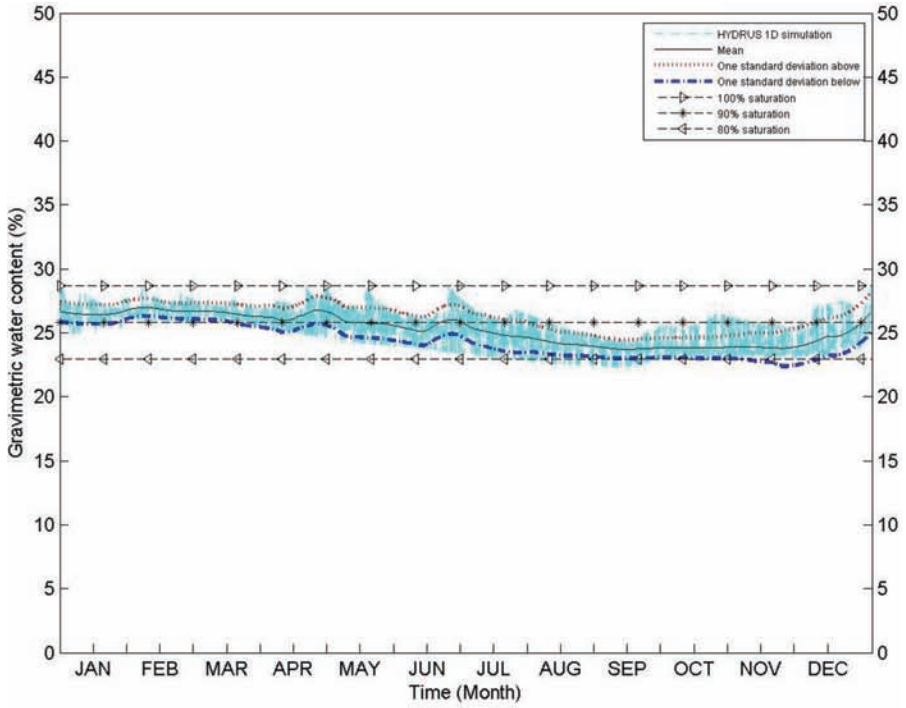

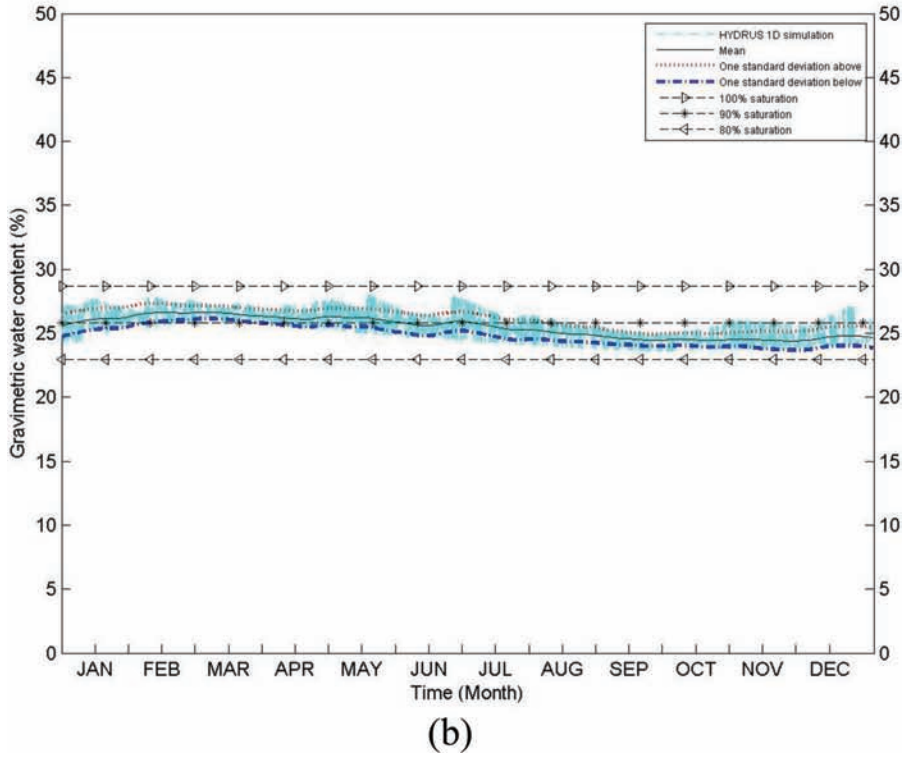

Figure A.59 Annual soil moisture variation for (a) 60 cm depth and (b) 90 cm depth for Tippecanoe County for profile (TIP-1).

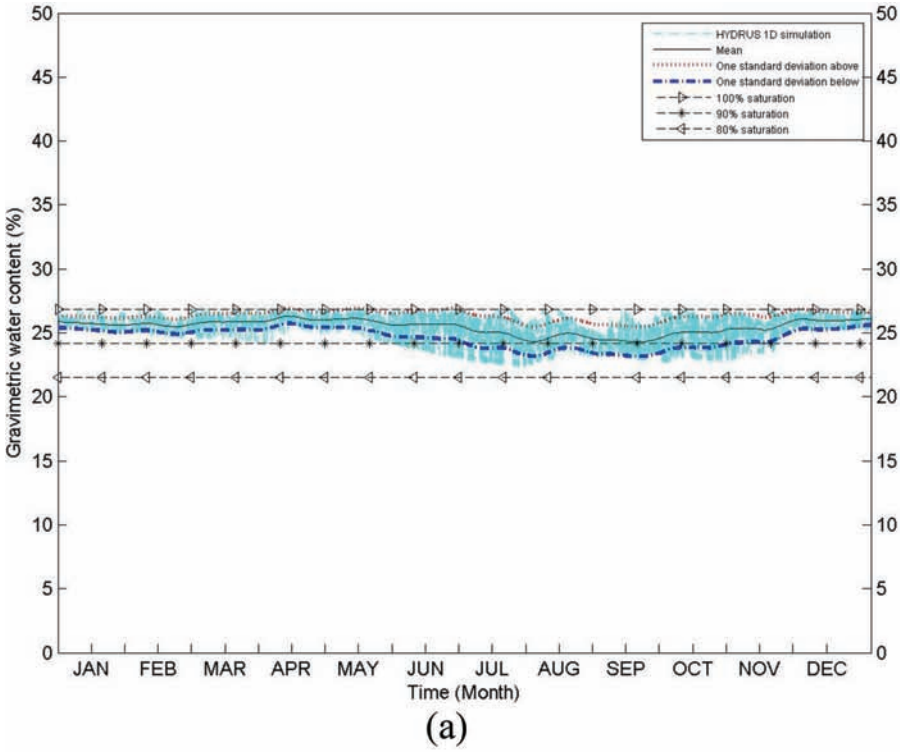

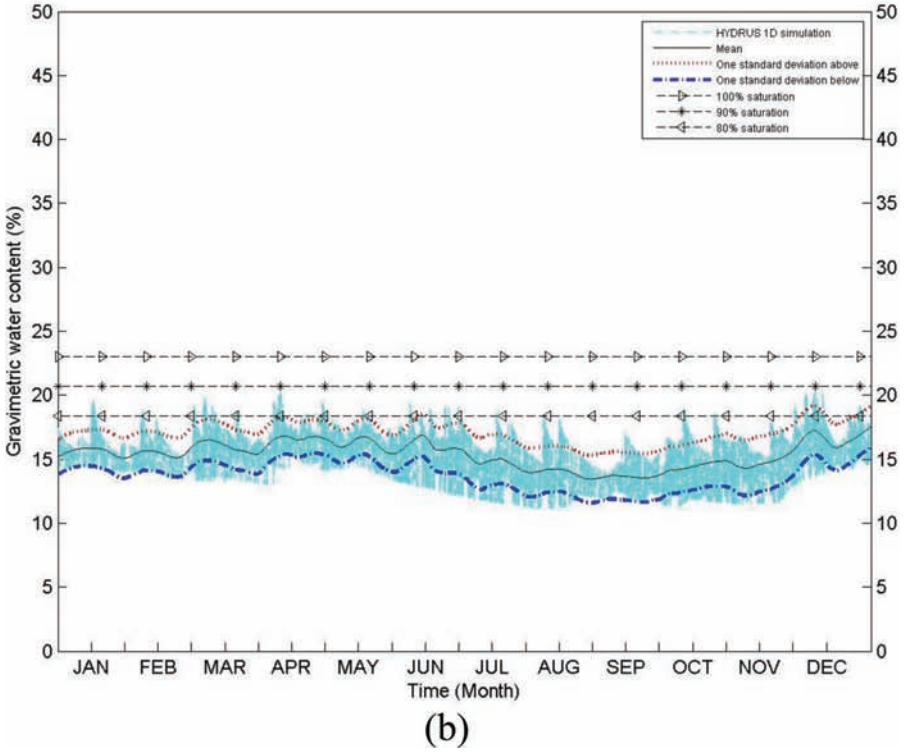

Figure A.60 Annual soil moisture variation for (a) 60 cm depth and (b) 90 cm depth for Union County for profile (UNI-1).

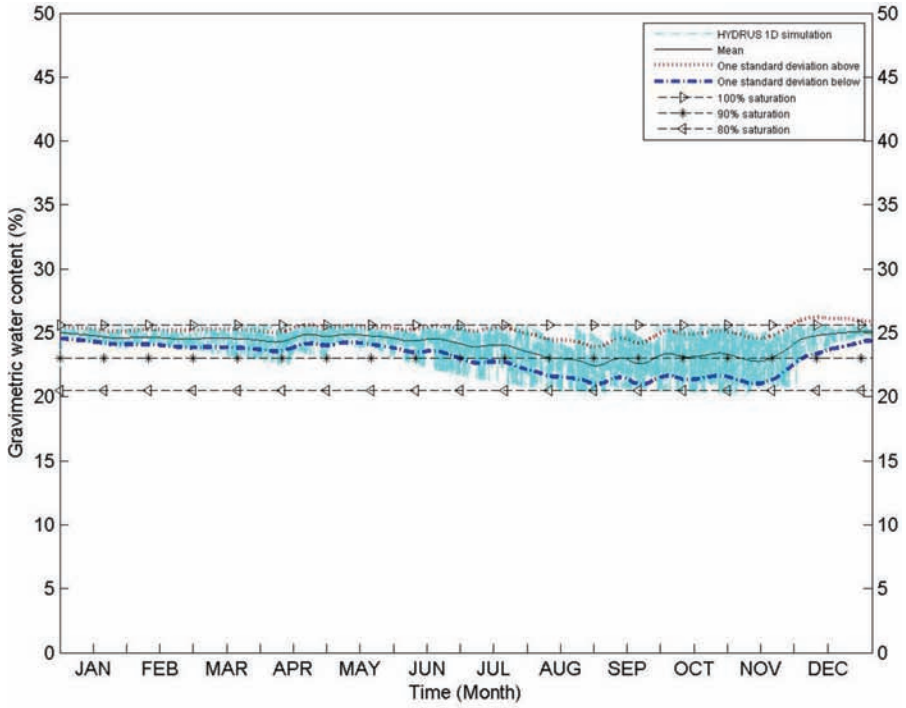

(a)

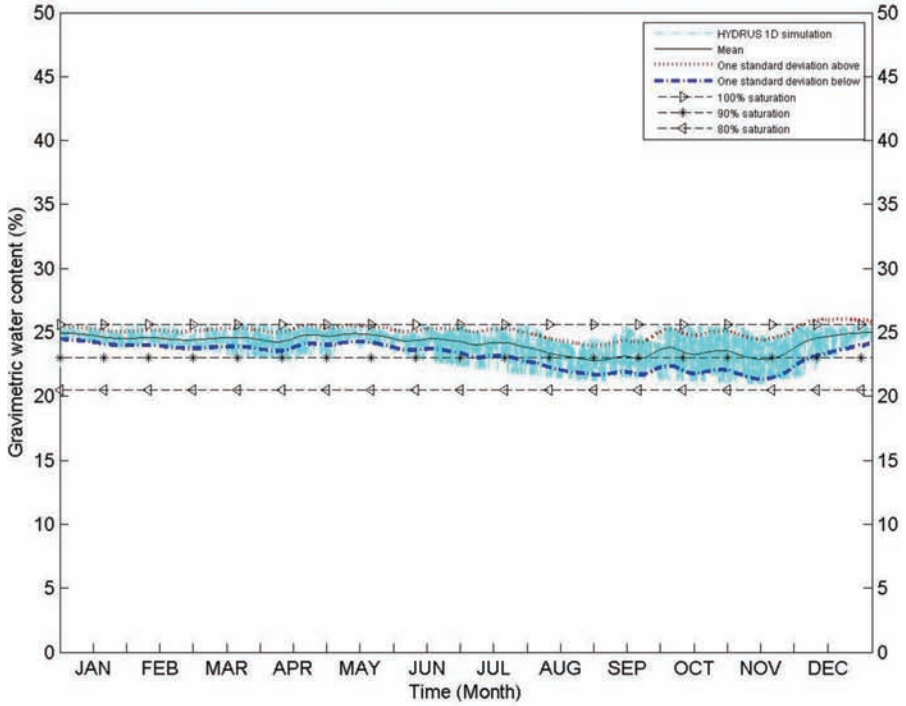

(b)

Figure A.61 Annual soil moisture variation for (a) 60 cm depth and (b) 90 cm depth for Vanderburgh County for profile (VAN-1).

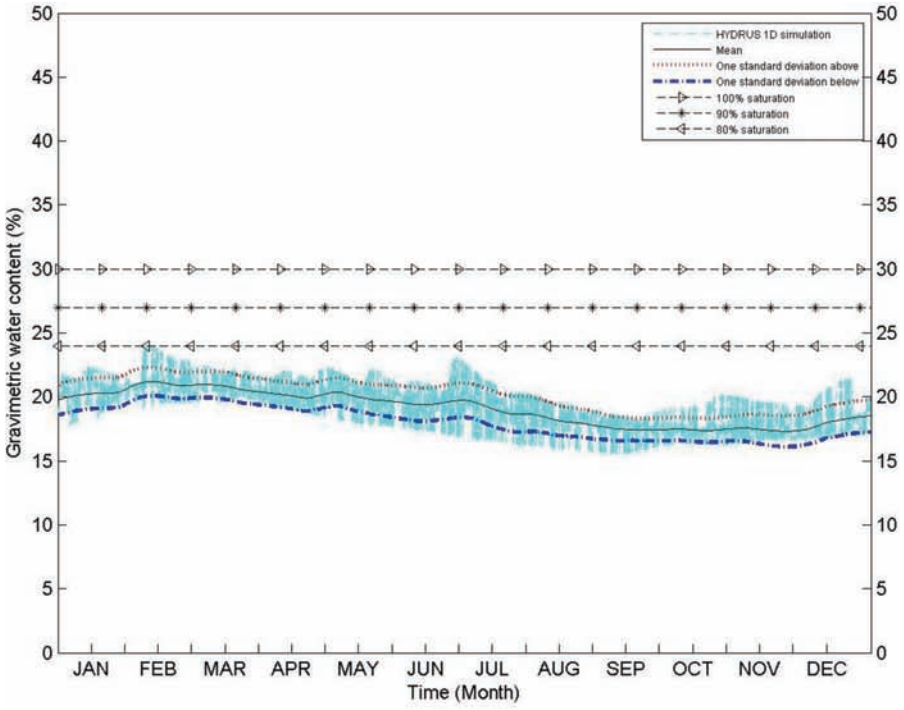

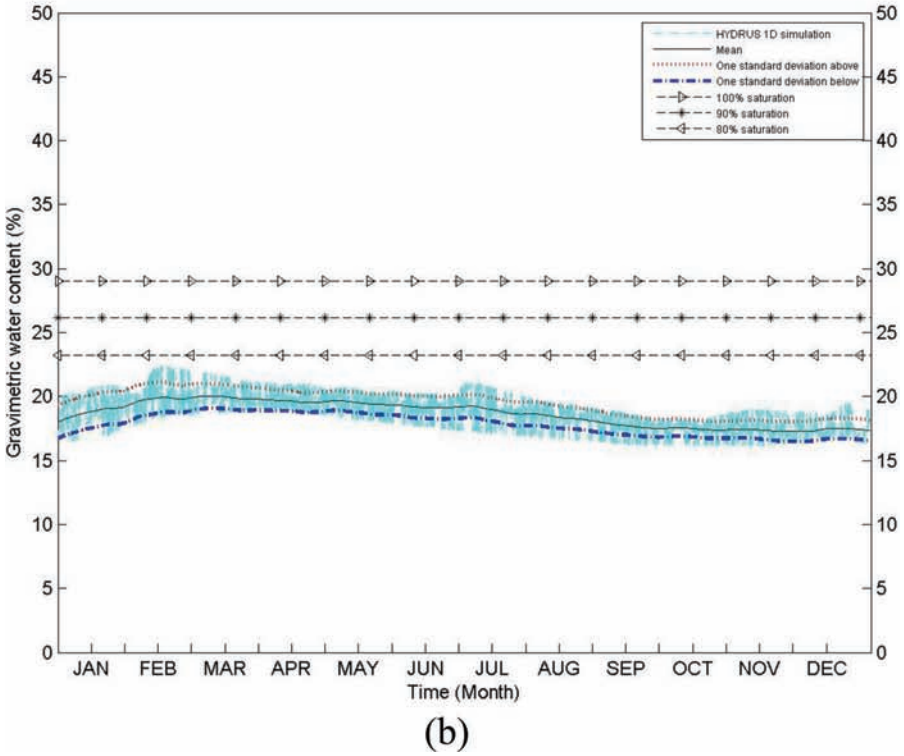

Figure A.62 Annual soil moisture variation for (a) 60 cm depth and (b) 90 cm depth for Vermillion County for profile (VER-1).

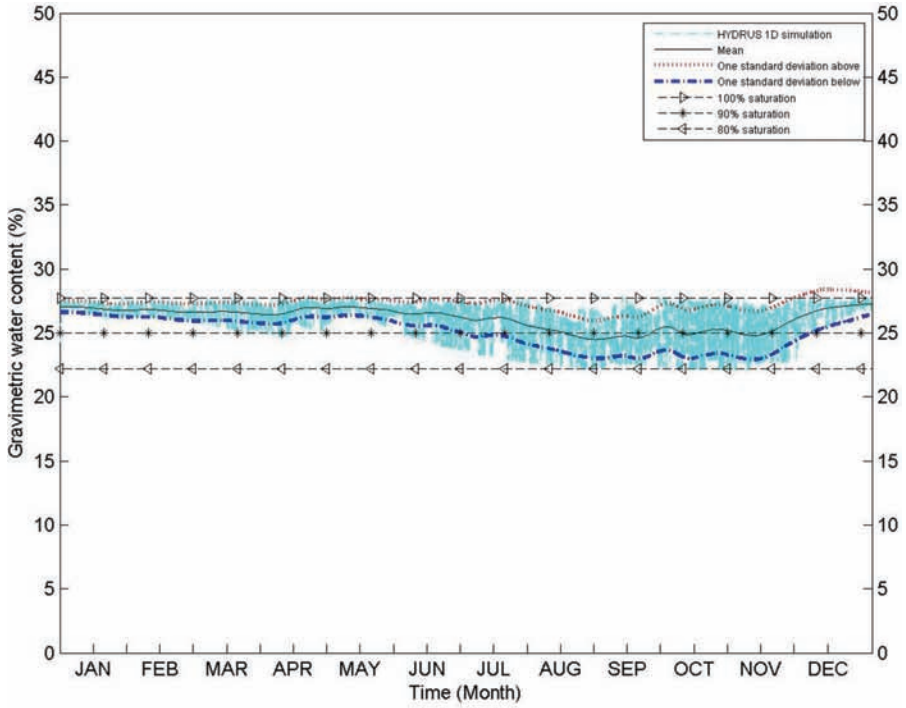

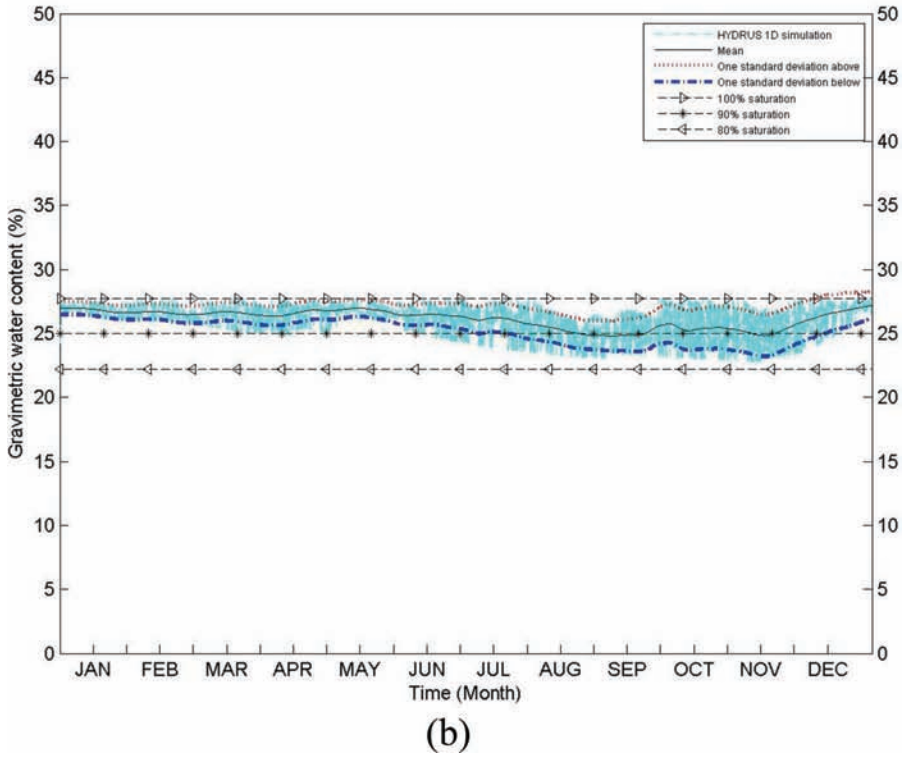

Figure A.63 Annual soil moisture variation for (a) 60 cm depth and (b) 90 cm depth for Vigo County for profile (VIG-1).

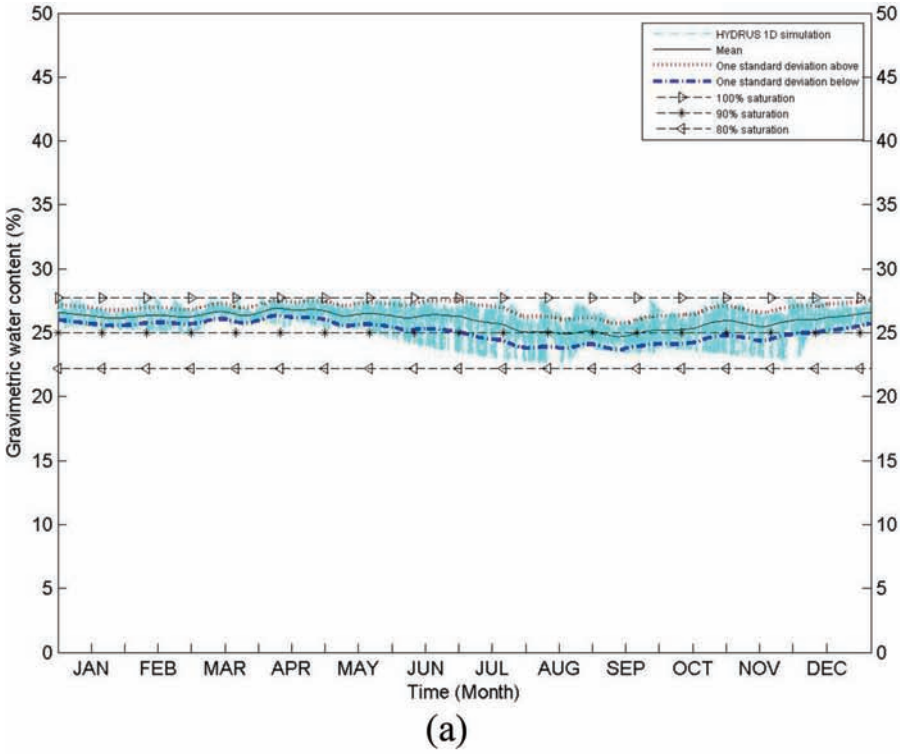

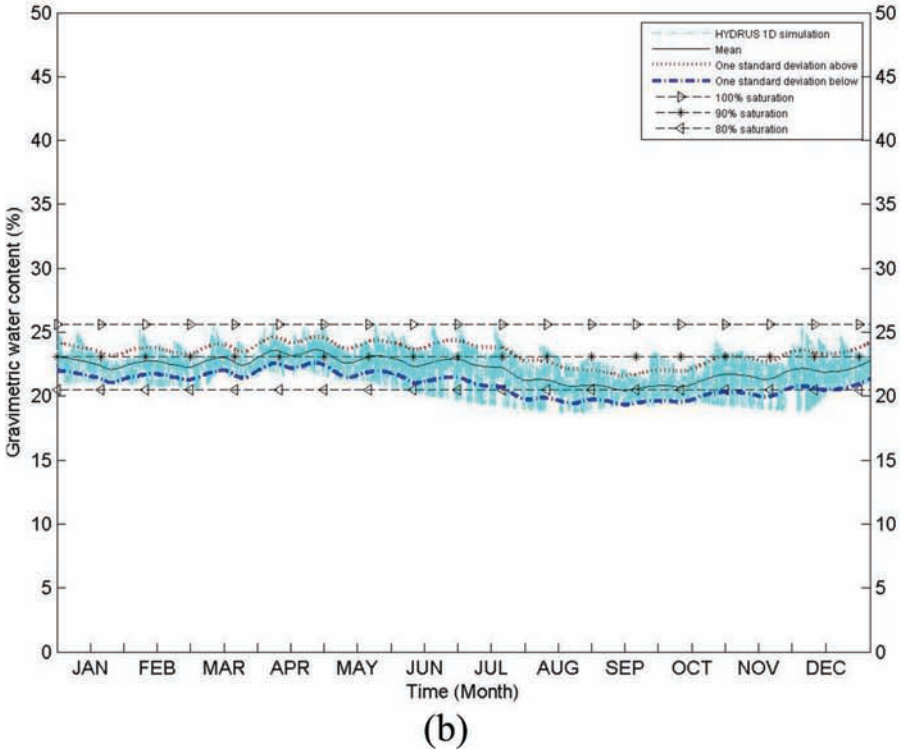

Figure A.64 Annual soil moisture variation for (a) 60 cm depth and (b) 90 cm depth for Wabash County for profile (WAB-1).

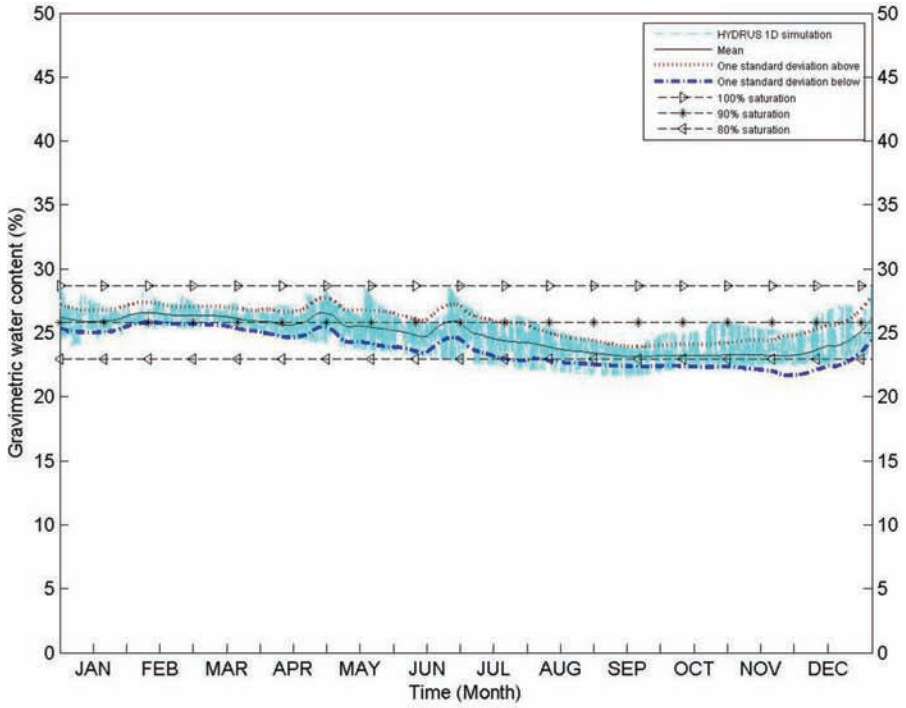

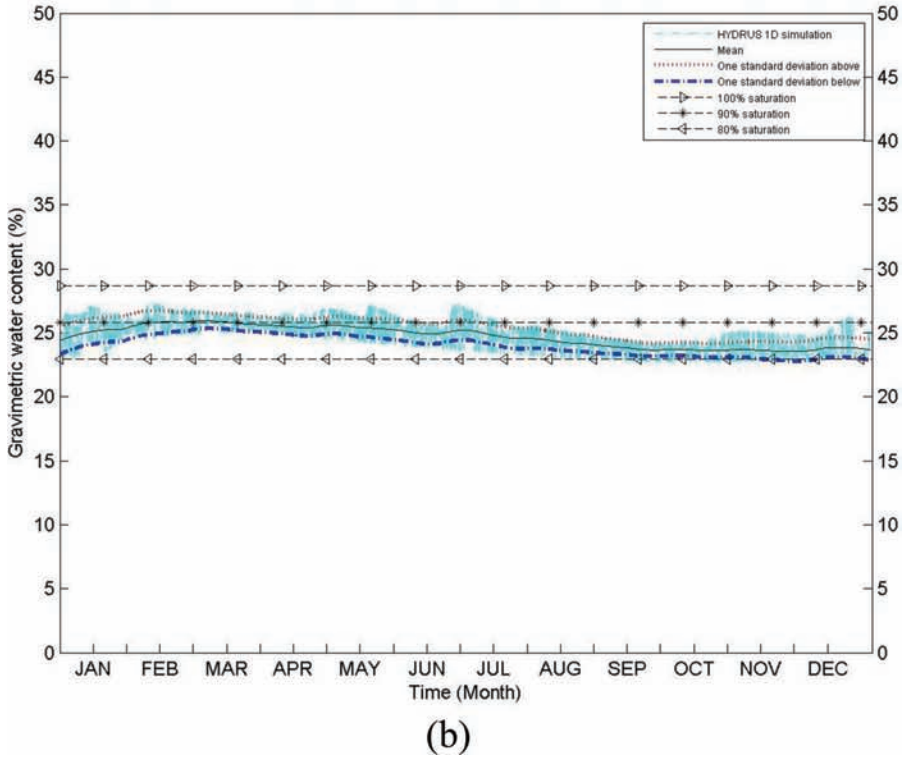

Figure A.65 Annual soil moisture variation for (a) 60 cm depth and (b) 90 cm depth for Warren County for profile (WAR-1).

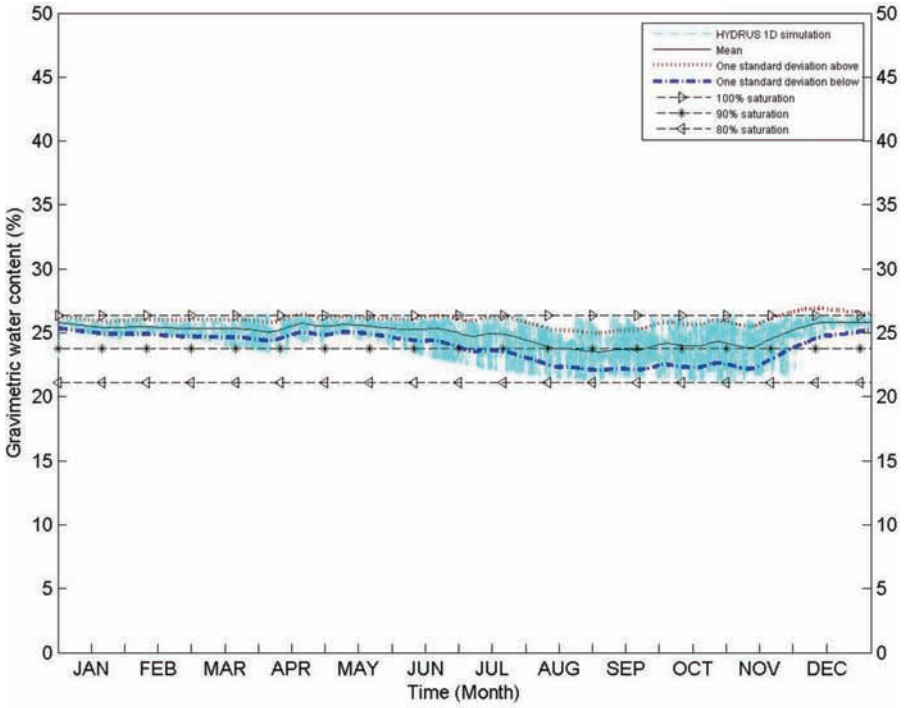

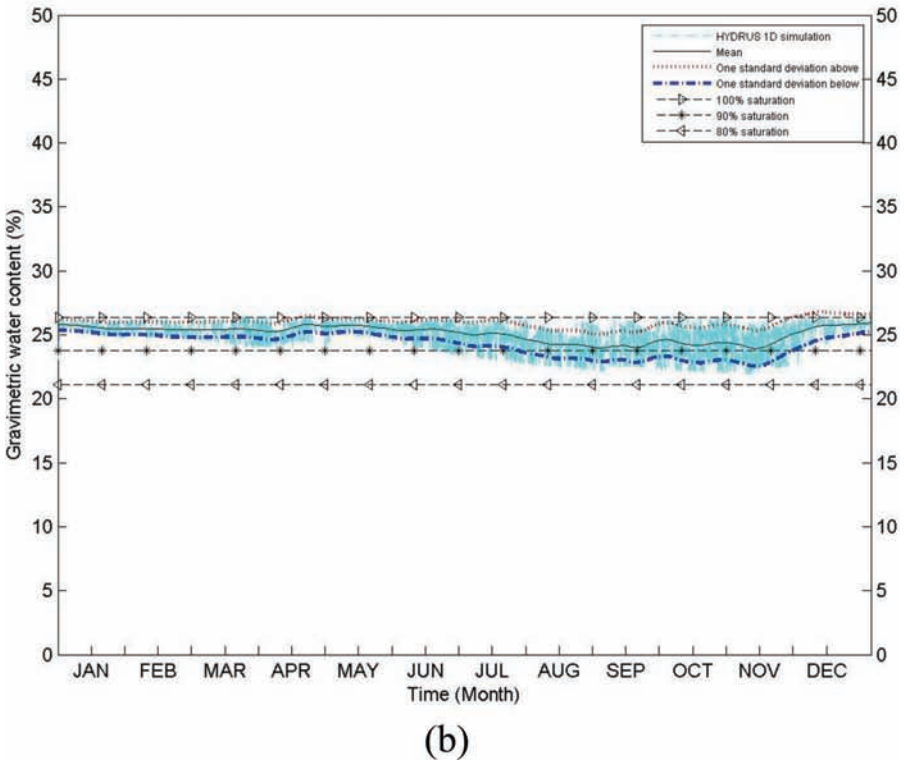

Figure A.66 Annual soil moisture variation for (a) 60 cm depth and (b) 90 cm depth for Warrick County for profile (WARR-1).

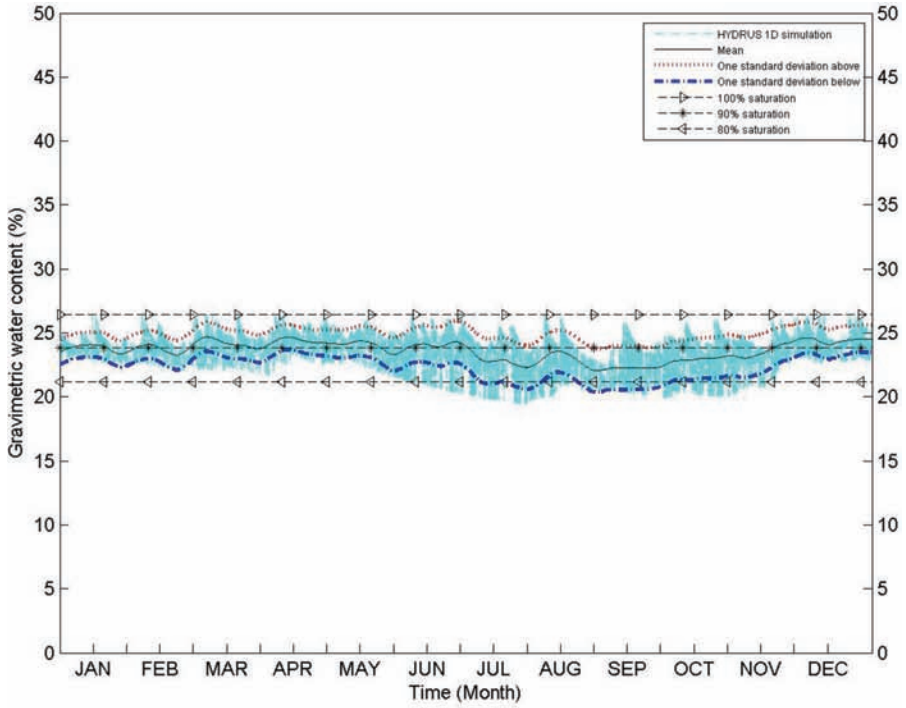

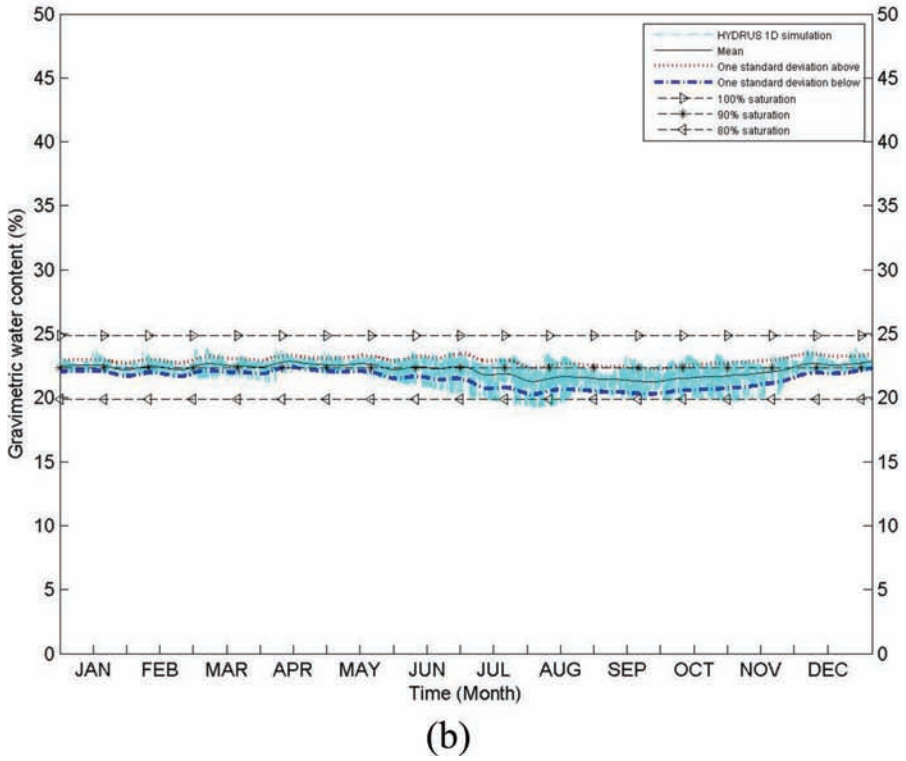

Figure A.67 Annual soil moisture variation for (a) 60 cm depth and (b) 90 cm depth for Wayne County for profile (WAY-1).

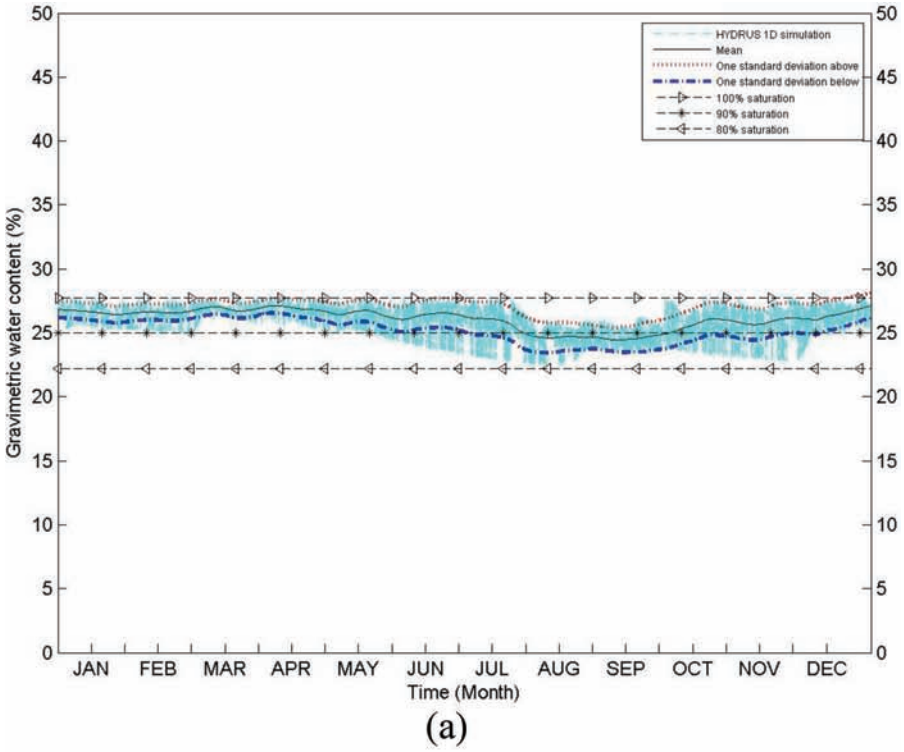

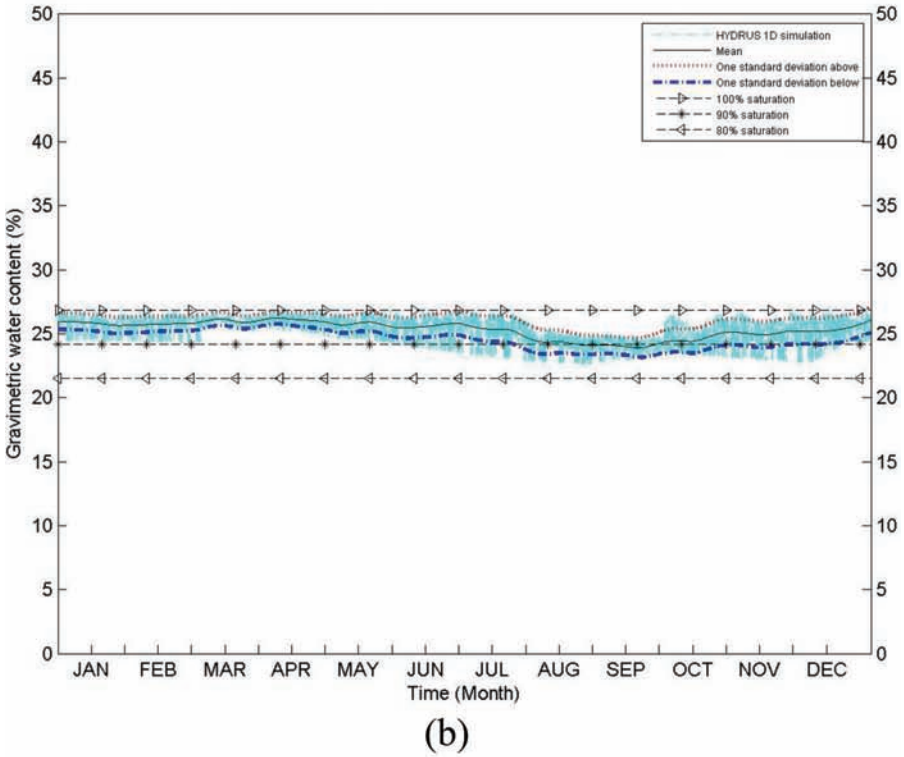

Figure A.68 Annual soil moisture variation for (a) 60 cm depth and (b) 90 cm depth for Wells County for profile (WEL-1).

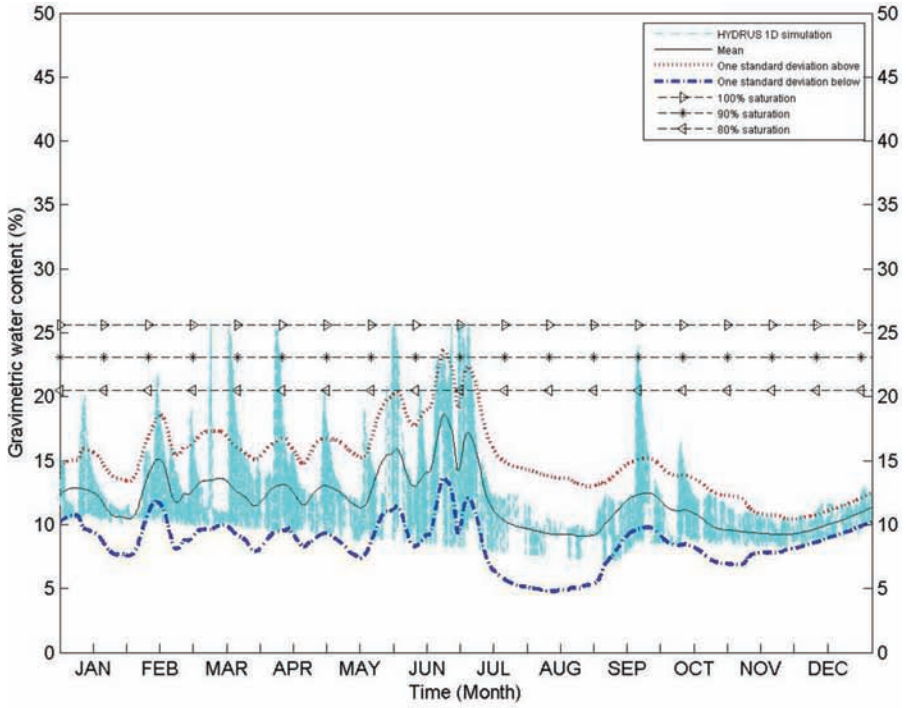

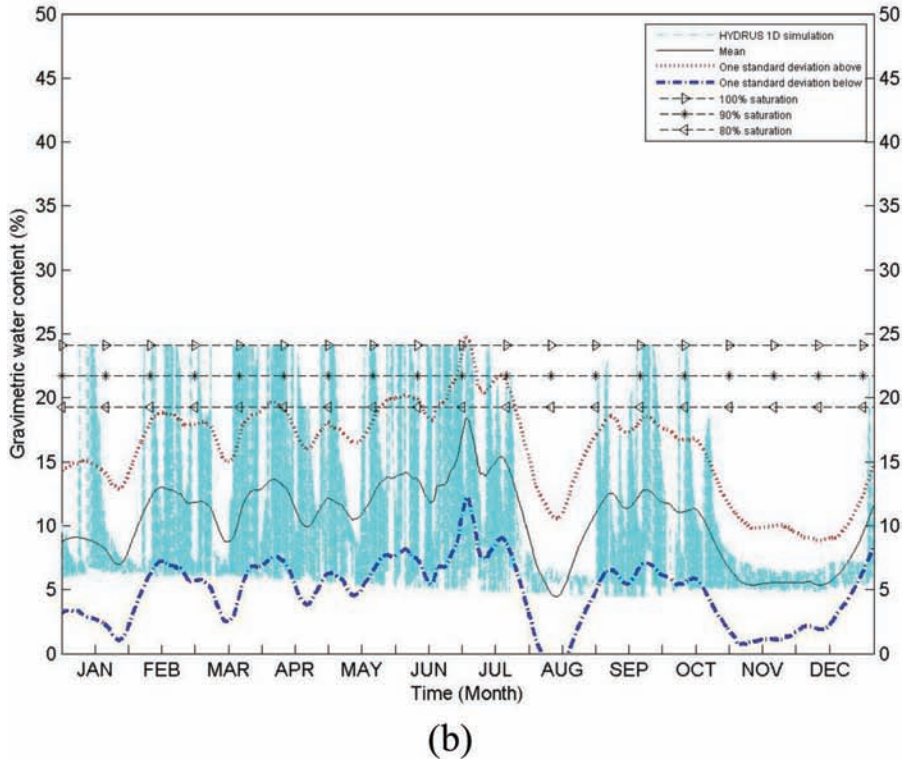

Figure A.69 Annual soil moisture variation for (a) 60 cm depth and (b) 90 cm depth for White County for profile (WHI-1).

APPENDIX B: SOIL INDEX AND HYDRAULIC PROPERTIES

In this appendix, all soil index and hydraulic properties are presented for the soil profiles that were used to generate the soil moisture simulations in Appendix A.

TABLE B.1
Soil index and hydraulic properties for the soil profiles that used to generate the soil moisture simulations.

County	Profile No.	Layer	Layer Thickness (cm)	Classification		LL	PI	γ_{dry} (g/cm^3)
				AASHTO	USDA			
Adams	ADA-1	1	0-28	A-7, A-7-6	silty clay loam	40-60	15-40	1.5
		2	28-86	A-6, A-7-6	silty clay loam	40-55	15-30	1.55
		3	86-119	A-6, A-7-6	silty clay loam	40-55	15-35	1.6
		4	119-145	A-6, A-7-6	silty clay loam	30-45	10-25	1.62
		5	145-201	A-6, A-7-6	silty clay loam	30-45	10-25	1.62
Allen	ALL-1	1	0-28	A-7, A-7	silty clay loam	40-60	10-25	1.57
		2	28-86	A-6, A-7-6	silty clay	40-55	15-30	1.55
		3	86-119	A-6, A-7-6	silty clay	40-55	15-35	1.6
		4	119-145	A-6, A-7	silty clay	30-45	10-25	1.62
		5	145-201	A-6, A-7	clay loam	30-45	10-25	1.62
Bartholomew	BAR-1	1	0-25	A-7-6	silty clay loam	39-43	21-22	1.30
		2	25-36	A-4	silt loam	30-41	7-19	1.30
		3	36-51	A-6, A-7-6	silty clay loam	37-52	17-28	1.385
		4	51-124	A-6	silty clay loam	37-44	17-23	1.395
		5	124-152	A-6, A-7-6	clay loam, loam, silt loam	25-41	6-22	1.445
		6	152-201	A-4, A-6	fine sandy loam, loam, sandy clay loam, sandy loam	20-36	2-17	1.455
Benton	BEN-1	1	0-30	A-6, A-7-6	silty clay loam	35-55	10-30	1.40
		2	30-86	A6, A-7, A-7-6	silty clay loam	35-55	15-35	1.50
		3	86-122	A-4, A-6	silt loam	20-40	5-25	1.60
		4	122-152	A-4, A-6	loam	15-30	NP-15	1.60
Blackford	BLA-1	1	0-23	A-4, A-6	silt loam	30-40	4-20	1.45
		2	23-61	A-6, A-7-6	silty clay loam	40-65	20-40	1.50
		3	61-86	A-6, A-7-6	silty clay loam	30-55	15-30	1.60
		4	86-152	A-6, A-7-6	silty clay loam	25-45	10-25	1.80
Boone	BOO-1	1	0-25	A-4, A-6	silt loam	20-42	3-18	1.45
		2	25-43	A-6, A-7-6	silty clay loam	30-57	12-32	1.45
		3	43-74	A-4, A-7-6	clay loam	27-58	10-35	1.50
		4	74-91	A-6, A-7-6	loam	27-48	9-26	1.65
		5	91-201	A-4, A-6	loam	25-47	9-26	1.875

TABLE B.1
(Continued)

County	Profile No.	Layer	Layer Thickness (cm)	Classification		LL	PI	γ_{dry} (g/cm^3)
				AASHTO	USDA			
Brown	BRO-1	1	0-15	A-2-4, A-4	channery silt loam, silt loam	0-25	NP-7	1.35
		2	15-46	A-2-4, A-4	channery silt loam, very channery silt loam, extremely channery silt loam	0-25	NP-7	1.40
		3	46-91	A-1, A-2-4, A-4	extremely channery silt loam, very flaggy silt loam	0-25	NP-7	1.40
		4	91-152	–	unweathered bedrock	–	–	–
Carrol	CAR-1	1	0-25	A-4, A-6	silt loam	20-35	4-14	1.425
		2	25-33	A-4, A-6	silt loam	20-35	4-14	1.425
		3	33-69	A-6, A-7, A-7-6	silty clay loam	35-55	15-35	1.55
		4	69-127	A-6, A-7	clay loam	30-50	10-30	1.60
		5	127-150	A-4, A-6	clay loam	20-50	3-30	1.875
		6	150-201	A-4, A-6	loam	15-30	3-15	1.875
Cass	CAS-1	1	0-36	A-6	silty clay loam	33-57	10-24	1.34
		2	36-51	A-6, A-7-6	silty clay loam	36-49	17-25	1.395
		3	51-124	A-6, A-7-6	silty clay loam	36-49	17-25	1.41
		4	124-152	A-6, A-7-6	clay loam	26-44	9-21	1.435
		5	152-201	A-4, A-6	loam	21-37	5-17	1.445
Clark	CLAR-1	1	0-28	A-4. A-6	silt loam	23-33	6-12	1.45
		2	28-53	A-4	silt loam	22-32	7-13	1.45
		3	53-102	A-6	silty clay loam, silt loam	33-38	16-19	1.50
		4	102-133	A-6	silty clay loam, silt loam	30-37	15-19	1.65
		5	133-211	A-6	silt loam	29-35	13-18	1.75
		6	211-229	A-6, A-7-6	clay loam	36-50	19-29	1.60
Clay	CLA-1	1	0-28	A-4, A-6	silt loam	23-37	6-13	1.425
		2	28-46	A-4, A-6	silt loam	24-32	7-13	1.475
		3	46-124	A-6	silt clay loam	32-40	15-21	1.55
		4	124-201	A-4, A-6	silt loam	21-31	6-13	1.50
Clinton	CLI-1	1	0-25	A-4, A-6	silt loam	20-35	4-14	1.425
		2	25-33	A-4, A-6	silt loam	20-35	4-14	1.425
		3	33-69	A-6, A-7, A-7-6	silty clay loam	35-55	15-35	1.55
		4	69-127	A-6, A-7	clay loam	30-50	10-30	1.60
		5	127-150	A-4, A-6	clay loam	20-50	3-30	1.875
		6	150-201	A-4, A-6	loam	15-30	3-15	1.875

TABLE B.1
(Continued)

County	Profile No.	Layer	Layer Thickness (cm)	Classification		LL	PI	γ_{dry} (g/cm^3)
				AASHTO	USDA			
Crawford	CRA-1	1	0-23	A-4, A-6	silt loam	23-40	3-15	1.45
		2	23-183	A-4, A-6, A-7-6	silty clay loam	25-50	8-32	1.50
		3	183-203	A-4, A-6	silt loam	15-40	3-20	1.375
Daviess	DAV-1	1	0-20	A-4, A-6	silt loam	22-40	NP-17	1.40
		2	20-58	A-4, A-6, A-7-6	silt loam	23-48	4-27	1.55
		3	58-127	A-4, A-6	silty clay loam	24-40	8-24	1.675
		4	127-203	A-4, A-6	silt loam	23-40	2-17	1.60
Dearborn	DEA-1	1	0-20	A-4, A-6	silt loam	23-40	6-16	1.45
		2	20-78	A-6, A-7-6	silty clay loam	31-41	15-21	1.55
		3	78-183	A-6	loam	29-35	13-18	1.73
		4	183-201	A-7-6	clay loam	34-49	17-28	1.65
Decatur	DEC-1	1	0-25	A-4, A-6	silt loam	20-35	4-14	1.425
		2	25-33	A-4, A-6	silt loam	20-35	4-14	1.425
		3	33-69	A-6, A-7, A-7-6	silty clay loam, silt loam	35-55	15-35	1.55
		4	69-127	A-6, A-7	clay loam, loam	30-50	10-30	1.60
		5	127-150	A-4, A-6	clay loam, loam	20-50	3-30	1.875
		6	150-201	A-4, A-6	fine sandy loam, loam	15-30	3-15	1.875
Dekalb	DEK-1	1	0-20	A-4, A-6	silt loam	25-40	7-15	1.45
		2	20-66	A-6, A-7-6	silty clay	35-55	15-35	1.55
		3	66-76	A-6, A-7	silty clay	30-50	10-30	1.70
		4	76-201	A-6, A-7	silty clay loam	25-45	7-25	1.8
Delaware	DEL-1	1	0-28	A-6, A-7	silty clay loam	35-50	10-25	1.475
		2	28-86	A-6, A-7-6	clay, silty clay, silty clay loam	40-55	15-30	1.55
		3	86-119	A-6, A-7-6	clay, silty clay, silty clay loam	40-55	15-35	1.60
		4	119-145	A-6, A-7	clay, clay loam, silty clay loam	30-45	10-25	1.625
		5	145-201	A-6, A-7	clay loam, silty clay loam	30-45	10-25	1.625
Dubois	DUB-1	1	0-25	A-4, A-6	silt loam	20-39	2-15	1.425
		2	25-79	A-4, A-6	silty clay loam, silt loam	25-50	3-25	1.45
		3	79-152	A-2-4, A-4, A-6	stratified silt loam to loam to sandy loam	15-38	2-15	1.45
Elkhart	ELK-1	1	0-27	A-4, A-6	loam	20-40	NP-17	1.43
		2	27-76	A-6, A-7-6	clay loam	25-50	12-30	1.55
		3	76-203	A-4, A-6	sandy loam	15-40	NP-22	1.7

TABLE B.1
(Continued)

County	Profile No.	Layer	Layer Thickness (cm)	Classification		LL	PI	γ_{dry} (g/cm^3)
				AASHTO	USDA			
Fayette	FAY-1	1	0-28	A-4, A-6	silt loam	20-35	3-14	1.45
		2	28-86	A-6, A-7	silty clay loam, silt loam	35-50	15-32	1.50
		3	86-114	A-6, A-7	clay loam, loam	25-48	8-30	1.60
		4	114-152	A-4, A-6	fine sandy loam, loam	15-30	4-15	1.875
Floyd	FLO-1	1	0-20	A-4, A-6	silt loam	22-40	1-17	1.425
		2	20-89	A-4, A-6, A-7-6	silty clay loam, silt loam	23-50	3-29	1.525
		3	89-109	A-7-6	clay, silty clay	44-75	20-46	1.45
		4	109-183	A-7-6	clay silty clay	44-75	20-46	1.45
		5	183-208	–	bedrock	–	–	–
Fountain	FOU-1	1	0-25	A-4, A-6	silt loam	20-35	4-14	1.425
		2	25-33	A-4, A-6	silt loam	20-35	4-14	1.425
		3	33-69	A-6, A-7, A-7-6	silty clay loam, silt loam	35-55	15-35	1.55
		4	69-127	A-6, A-7	clay loam, loam	30-50	10-30	1.60
		5	127-150	A-4, A-6	clay loam, loam	20-50	3-30	1.875
		6	150-201	A-4, A-6	fine sandy loam, loam	15-30	3-15	1.875
Franklin	FRA-1	1	0-13	A-6	silt loam	29-40	12-18	1.45
		2	13-36	A-6, A-7-6	silty clay loam, silt loam	31-41	15-21	1.55
		3	36-89	A-6	loam, silt loam	29-39	13-21	1.725
		4	89-198	A-7-6	clay loam, loam	34-49	17-28	1.65
		5	198-201	A-6	clay loam, loam	30-44	13-24	1.65
Fulton	FUL-1	1	0-28	a-4, a-6	loam	20-40	np-17	1.43
		2	28-76	a-6, a-7-6	sandy clay loam	25-50	12-30	1.55
		3	76-203	a-4, a-6	sandy loam	15-30	np-15	1.7
Gibson	GIB-1	1	0-25	A-4, A-6	loam, silt loam	20-40	4-18	1.475
		2	25-137	A-4, A-6, A-7-6	clay loam, loam, sandy clay loam	26-47	7-24	1.50
		3	137-152	A-2-4, A-2-6, A-4, A-6, A-7-6	stratified sandy clay loam to clay loam to sandy loam to fine sandy loam	18-45	2-24	1.60
Grant	GRA-1	1	0-28	A-6, A-7	silty clay loam	35-50	10-25	1.475
		2	28-86	A-6, A-7-6	clay, silty clay, silty clay loam	40-55	15-30	1.55
		3	86-119	A-6, A-7-6	clay, silty clay, silty clay loam	40-55	15-35	1.60
		4	119-145	A-6, A-7	clay, clay loam, silty clay loam	30-45	10-25	1.625
		5	145-201	A-6, A-7	clay loam, silty clay loam	30-45	10-25	1.625

TABLE B.1
(Continued)

County	Profile No.	Layer	Layer Thickness (cm)	Classification		LL	PI	γ_{dry} (g/cm^3)
				AASHTO	USDA			
Greene	GRE-1	1	0-20	A-4, A-6	silt loam	25-38	7-15	1.425
		2	20-69	A-6	silty clay loam, silt loam	32-40	15-21	1.55
		3	69-109	A-6	silt loam	30-35	14-18	1.675
		4	109-150	A-4, A-6	loam, silt loam	24-34	9-17	1.75
		5	150-201	A-6	clay loam, loam	28-40	12-21	1.65
Hamilton	HAM-1	1	0-25	A-4, A-6	silt loam	20-42	3-18	1.45
		2	25-43	A-6, A-7-6	clay loam, silty clay loam	30-57	12-32	1.45
		3	43-74	A-4, A-7-6	clay loam	27-58	10-35	1.55
		4	74-91	A-6, A-7-6	clay loam, fine sandy loam, loam	27-48	9-26	1.65
		5	91-201	A-4, A-6	fine sandy loam, loam	25-47	9-26	1.875
Hancock	HAN-1	1	0-20	A-6	silt loam	23-40	6-16	1.45
		2	20-28	A-6	silt loam	23-38	6-16	1.45
		3	28-36	A-6	silt loam	31-37	13-18	1.55
		4	36-71	A-7-6	clay loam, silty clay, silty, clay loam	45-55	25-32	1.55
		5	71-91	A-6	clay loam, fine sandy loam, loam	22-44	6-24	1.65
		6	91-201	A-4	fine sandy loam, loam	20-35	4-16	1.875
Harrison	HAR-1	1	0-10	A-4	gravelly silt loam, silt loam	25-35	4-10	1.30
		2	10-51	A-6, A-7, A-7-6	clay, gravelly clay, gravelly silty clay, silty clay loam	40-87	29-59	1.325
		3	51-117	A-6, A-7, A-7-6	clay, silty clay	40-75	20-48	1.30
		4	117-203	A-7, A-7-6	clay, gravelly clay, gravelly silty clay	50-86	29-59	1.275
Hendricks	HEND-1	1	0-25	A-4, A-6	silt loam	20-42	3-18	1.45
		2	25-43	A-6, A-7-6	clay loam, silty clay loam	30-57	12-32	1.45
		3	43-74	A-4, A-7-6	clay loam	27-58	10-35	1.55
		4	74-91	A-6, A-7-6	clay loam, fine sandy loam, loam	27-48	9-26	1.65
		5	91-201	A-4, A-6	fine sandy loam, loam	25-47	9-26	1.875
Henry	HEN-1	1	0-20	A-6	silt loam	23-40	6-16	1.45
		2	20-28	A-6	silt loam	23-38	6-16	1.45
		3	28-36	A-6	silt loam	31-37	13-18	1.55
		4	36-71	A-7-6	clay loam, silty clay, silty, clay loam	45-55	25-32	1.55
		5	71-91	A-6	clay loam, fine sandy loam, loam	22-44	6-24	1.65
		6	91-201	A-4	fine sandy loam, loam	20-35	4-16	1.875

TABLE B.1
(Continued)

County	Profile No.	Layer	Layer Thickness (cm)	Classification		LL	PI	γ_{dry} (g/cm^3)
				AASHTO	USDA			
Howard	HOW-1	1	0-41	A-7-6	silty clay loam	44-57	19-24	1.45
		2	41-81	A-6, A-7-6	silty clay loam	39-49	19-25	1.50
		3	81-112	A-6, A-7	clay loam, loam	31-49	13-25	1.50
		4	112-154	A-4, A-6	fine sandy loam, loam	23-30	6-11	1.65
Huntington	HUN-1	1	0-28	A-6, A-7	silty clay loam	35-50	10-25	1.475
		2	28-86	A-6, A-7-6	clay, silty clay, silty clay loam	40-55	15-30	1.55
		3	86-119	A-6, A-7-6	clay, silty clay, silty clay loam	40-55	15-35	1.60
		4	119-145	A-6, A-7	clay, clay loam, silty clay loam	30-45	10-25	1.625
		5	145-201	A-6, A-7	clay loam, silty clay loam	30-45	10-25	1.625
Jackson	JAC-1	1	0-25	A-4, A-6	silt loam	22-40	1-17	1.45
		2	25-43	A-4, A-6	silt loam	23-40	2-15	1.475
		3	43-97	A-4, A-6, A-7-6	silty clay loam, silt loam	24-50	4-30	1.50
		4	97-208	A-4, A-6	loam, silty clay loam, silt loam	20-40	7-25	1.725
		5	208-244	A-2, A-4, A-6, A-7-6	clay loam, fine sandy loam, silty clay loam, silt loam	20-50	6-25	1.60
Jasper	JAS-1	1	0-23	A-2-4	loamy sand	0	NP	1.50
		2	23-152	A-2-4, A-3	fine sand, loamy fine sand, loamy sand, sand	0	NP	1.60
		3	152-203	A-2-4, A-3	fine sand, sand	0	NP	1.60
Jay	JAY-1	1	0-23	A-4, A-6	silt loam	30-40	4-20	1.45
		2	23-61	A-6, A-7-6	clay loam, silty clay, silty clay loam	40-65	20-40	1.50
		3	61-86	A-6, A-7-6	clay, clay loam, silty clay loam	30-55	15-30	1.60
		4	86-152	A-6, A-7-6	clay loam, silty clay loam	25-45	10-25	1.80
Jefferson	JEF-1	1	0-30	A-4	silt loam	23-32	6-9	1.45
		2	30-46	A-6	silt loam	21-32	6-13	1.45
		3	46-97	A-6	silty clay loam, silt loam	29-40	13-21	1.50
		4	97-127	A-6	silty clay loam, silt loam	29-37	13-19	1.70
		5	127-216	A-6	silt loam	29-35	13-18	1.70
		6	216-229	A-6, A-7-6	clay loam	36-48	19-27	1.60

TABLE B.1
(Continued)

County	Profile No.	Layer	Layer Thickness (cm)	Classification		LL	PI	γ_{dry} (g/cm^3)
				AASHTO	USDA			
Jennings	JEN-1	1	0-30	A-4	silt loam	23-32	6-9	1.45
		2	30-46	A-6	silt loam	21-32	6-13	1.45
		3	46-97	A-6	silty clay loam, silt loam	29-40	13-21	1.50
		4	97-127	A-6	silty clay loam, silt loam	29-37	13-19	1.70
		5	127-216	A-6	silt loam	29-35	13-18	1.70
		6	216-229	A-6, A-7-6	clay loam	36-48	19-27	1.60
Johnson	JOH-1	1	0-25	A-4, A-6	silt loam	20-42	3-18	1.45
		2	25-43	A-6, A-7-6	clay loam, silty clay loam	30-57	12-32	1.45
		3	43-74	A-4, A-7-6	clay loam	27-58	10-35	1.50
		4	74-91	A-6, A-7-6	clay loam, fine sandy loam, loam	27-48	9-26	1.65
		5	91-201	A-4, A-6	fine sandy loam, loam	25-47	9-26	1.875
Knox	KNO-1	1	0-15	A-4, A-6	silt loam	24-39	7-75	1.45
		2	15-66	A-6, A-7-6	silty clay loam, silt loam	34-46	16-24	1.50
		3	66-185	A-4, A-6, A-7-6	silty clay loam, silt loam	24-42	9-21	1.50
		4	185-201	A-4	silt, silt loam	18-29	4-12	1.375
Kosciusko	KOS-1	1	0-20	A-4	sandy loam	15-30	NP-10	1.45
		2	20-97	A-4, A-6	sandy clay loam	20-50	5-30	1.60
		3	97-152	A-2-4, A-4, A-6	loam	15-30	NP-15	1.60
LaGrange	LAG-1	1	0-46	A-2-4	loamy sandy	0	NP	1.60
		2	46-90	A-2	sandy clay loam	0-50	NP-20	1.70
		3	90-152	A-1	sand	0	NP	1.70
Lake	LAK-1	1	0-19	A-4, A-6	silt loam	25-40	NP-15	1.45
		2	19-90	A-6, A-7-6	silty clay loam	40-60	20-35	1.50
		3	90-152	A-6, A-7-6	clay loam	25-45	10-25	1.80
LaPorte	LAP-1	1	0-74	A-2-4, A-2-5, A-2-6	sandy loam	20-41	3-13	1.50
		2	74-101	A-2-4	loamy sand	15-21	1-5	1.59
		3	101-300	A2-4, A-3	sand	0-19	NP-4	1.63
Lawrence	LAW-1	1	0-18	A-4, A-6	silt loam	22-40	1-17	1.425
		2	18-109	A-4, A-6, A-7-6	silty clay loam, silt loam	23-50	3-29	1.525
		3	109-203	A-7, A-7-6	clay, silty clay	44-75	20-46	1.50
Madison	MAD-1	1	0-41	A-7-6	silty clay loam	44-57	19-24	1.45
		2	41-81	A-6, A-7-6	silty clay loam	39-49	19-25	1.50
		3	81-112	A-7, A-7	clay loam, loam	31-49	13-25	1.50
		4	112-152	A-4, A-6	fine sandy loam, loam	23-30	6-11	1.65

TABLE B.1
(Continued)

County	Profile No.	Layer	Layer Thickness (cm)	Classification		LL	PI	γ_{dry} (g/cm^3)
				AASHTO	USDA			
Marion	MAR-1	1	0-25	A-4, A-6	silt loam	20-42	3-18	1.45
		2	25-43	A-6, A-7-6	clay loam, silty clay loam	30-57	12-32	1.45
		3	43-74	A-4, A-7-6	clay loam	27-58	10-35	1.50
		4	74-91	A-6, A-7-6	clay loam, fine sandy loam, loam	27-48	9-26	1.65
		5	91-201	A-4, A-6	fine sandy loam, loam	25-47	9-26	1.875
Marshall	MARS-1	1	0-20	A-4	sandy loam	15-30	NP-10	1.50
		2	20-33	A-4, A-6	sandy clay loam	10-50	NP-30	1.50
		3	33-254	A-4	sandy loam	15-30	NP-15	1.70
Martin	MART-1	1	0-20	A-4, A-6	silt loam	26-38	9-15	1.425
		2	20-63	A-4, A-6	silty clay loam, silt loam	28-40	12-21	1.525
		3	63-124	A-4, A-6	loam, silty clay loam, silt loam	25-40	10-21	1.675
		4	124-175	A-4, A-6	clay, channery clay loam, very parachannery clay, silty clay	42-76	24-48	1.50
		5	175-229	A-4, A-6	channery sandy loam, loam, sandy clay loam, sandy loam	25-44	9-24	1.55
		6	229-254	–	bedrock	–	–	–
Miami	MIA-1	1	0-25	A-4, A-6	silt loam	25-40	7-15	1.45
		2	25-84	A-6, A-7-6	clay, silty clay, silty clay loam	35-55	15-35	1.55
		3	84-99	A-6, A-7	clay loam, silty clay, silty clay loam	30-50	10-30	1.80
		4	99-201	A-6, A-7	clay loam, silty clay loam	25-45	7-25	1.90
Monroe	MON-1	1	0-18	A-4, A-6	silt loam	27-46	9-18	1.425
		2	18-91	A-6, A-7-6	silty clay loam, silt loam	35-45	16-24	1.525
		3	91-203	A-7-6	clay, silty clay	48-82	28-54	1.50
Montgomery	MONT-1	1	0-38	A-6, A-7, A-7-6	silty clay loam	35-50	10-30	1.425
		2	38-101	A-6, A-7	silty clay loam, silt loam	35-45	15-25	1.55
		3	101-132	A-4, A-6	clay loam, loam, silt loam	22-40	5-20	1.50
		4	132-201	A-4	stratified sand to sandy loam to loam to silt loam	0-40	NP-20	1.60
Morgan	MOR-1	1	0-20	A-6, A-7-6	silt loam	30-45	12-18	1.45
		2	20-102	A-6	loam, silt loam	30-41	12-19	1.50
		3	102-201	A-6	loam, sandy loam, silt loam	22-37	6-17	1.55

TABLE B.1
(Continued)

County	Profile No.	Layer	Layer Thickness (cm)	Classification		LL	PI	γ_{dry} (g/cm^3)
				AASHTO	USDA			
Newton	NEW-1	1	0-35	A-2-4	loamy sand	0	NP	1.45
		2	35-300	A-2-4, A-3	sand	0	NP	1.60
Noble	NOB-1	1	0-23	A-4	sandy loam	15-30	NP-10	1.45
		2	23-36	A-4	sandy loam	15-30	NP-10	1.45
		3	36-51	A-6, A-7-6	clay loam, loam, sandy clay loam	20-50	10-30	1.60
		4	51-86	A-6, A-7-6	clay loam, loam, sandy clay loam	20-50	10-30	1.60
		5	86-119	A-6, A-7-6	clay loam, loam, sandy clay loam	20-50	10-30	1.60
		6	119-132	A-4, A-6	sandy clay loam	20-40	5-25	1.60
		7	132-178	A-4, A-6	loam, sandy loam	15-30	NP-15	1.70
Ohio	OHI-1	1	0-18	A-4, A-6	silt loam	23-40	3-15	1.45
		2	18-61	A-4, A-6, A-7-6	silty clay loam, silt loam	24-45	5-25	1.55
		3	61-99	A-4, A-6	clay loam, loam, silty clay loam, silt loam	24-44	8-25	1.725
		4	99-175	A-7-6	clay, clay loam, silty clay	30-54	20-33	1.60
		5	175-203	A-7	clay, silty clay	40-60	20-40	1.575
Orange	ORA-1	1	0-20	A-4, A-6	silt loam	22-40	3-17	1.375
		2	20-66	A-4, A-6, A-7-6	silty clay loam, silt loam	23-48	4-27	1.525
		3	66-104	A-2, A-4, A-6	clay loam, fine sandy loam, loam, silt loam, sandy loam	20-35	5-15	1.475
		4	104-137	A-1-b, A-2-4, A-4, A-6	clay loam, channery sandy loam, parachannery fine sandy loam, very parachannery sandy loam	16-35	4-15	1.45
		5	137-152	–	weathered bedrock	–	–	–
Owen	OWE-1	1	0-20	A-4, A-6	silt loam	25-38	7-15	1.425
		2	20-69	A-6	silty clay loam, silt loam	32-40	15-21	1.55
		3	69-109	A-6	silt loam	30-35	14-18	1.675
		4	109-150	A-4, A-6	loam, silt loam	24-34	9-17	1.75
		5	150-201	A-6	clay loam, loam	28-40	12-21	1.65
Parke	PAR-1	1	0-30	A-6	silt loam	23-37	6-13	1.45
		2	30-86	A-7-6	silty clay loam, silt loam	37-42	18-21	1.50
		3	86-147	A-6	silt loam	29-40	12-19	1.70
		4	147-201	A-6	loam	27-36	11-17	1.825

TABLE B.1
(Continued)

County	Profile No.	Layer	Layer Thickness (cm)	Classification		LL	PI	γ_{dry} (g/cm^3)
				AASHTO	USDA			
Perry	PER-1	1	0-10	A-4	loam	16-27	2-9	1.425
		2	10-46	A-2-4, A-4	fine sandy loam, loam, sandy loam	14-23	2-7	1.575
		3	46-152	A-1-a, A-2-4	stratified extremely channery coarse sandy loam to extremely channery sandy loam to very channery loam	14-23	2-7	1.70
Pike	PIK-1	1	0-8	A-6, A-7	parachannery silt loam, very parachannery silty clay loam	24-50	10-24	1.50
		2	8-152	A-6, A-7	channery clay loam, very parachannery loam, very parachannery silty clay loam, extremely parachannery silt loam	24-50	10-24	1.60
Porter	POR-1	1	0-31	A-4, A-6	loam	20-40	5-20	1.55
		2	31-93	A-2, A-6, A-7	sandy clay loam	20-60	5-30	1.60
		3	93-300	A-1, A-3	sand	0	NP	1.60
Posey	POS-1	1	0-18	A-4	silt loam	16-28	3-9	1.45
		2	18-74	A-4	silt loam	16-28	3-9	1.40
		3	74-152	A-4	stratified silt loam to loam to sandy loam to fine sandy loam	16-28	3-9	1.40
Pulaski	PUL-1	1	0-149	A-2-4	loamy sand	0	NP	1.7
		2	149-300	A-3	sand	0	NP	1.55
Putnam	PUT-1	1	0-20	A-4	silt loam	23-37	5-13	1.425
		2	20-76	A-7, A-7-6	silty clay loam	38-47	19-25	1.55
		3	76-127	A-6, A-7	clay loam, loam	35-47	16-25	1.60
		4	127-147	A-6	clay loam, loam	30-41	13-21	1.60
		5	147-201	A-4, A-6	fine sandy loam, loam	22-29	7-12	1.875
Randolph	RAN-1	1	0-20	A-4, A-6	clay loam, silt loam	25-40	7-20	1.475
		2	20-66	A-6, A-7-6	clay, clay loam, silty clay loam	35-55	15-30	1.575
		3	66-76	A-6, A-7	clay loam, silty clay, silty clay loam	30-50	10-30	1.70
		4	76-201	A-6, A-7	clay loam, silty clay loam	25-45	7-25	1.875

TABLE B.1
(Continued)

County	Profile No.	Layer	Layer Thickness (cm)	Classification		LL	PI	γ_{dry} (g/cm^3)
				AASHTO	USDA			
Ripley	RIP-1	1	0-30	A-4	silt loam	23-32	6-9	1.45
		2	30-46	A-6	silt loam	21-32	6-13	1.45
		3	46-97	A-6	silty clay loam, silt loam	29-40	13-21	1.50
		4	97-127	A-6	silty clay loam, silt loam	29-37	13-19	1.70
		5	127-216	A-6	silt loam	29-35	13-18	1.70
		6	216-229	A-6, A-7-6	clay loam	36-48	19-27	1.60
Rush	RUS-1	1	0-25	A-6, A-7-6	silty clay loam, silt loam	40-52	16-21	1.40
		2	25-36	A-6, A-7-6	silty clay loam, silt loam	38-54	16-22	1.40
		3	36-91	A-6, A-7-6	silty clay loam, silt loam	36-49	16-25	1.55
		4	91-150	A-6, A-7-6	clay loam, loam, silty clay loam	31-47	13-25	1.55
		5	150-201	A-4	fine sandy loam, loam	20-32	5-13	1.465
St. Joseph	STJ-1	1	0-27	A-4, A-6	loam	2--40	NP-17	1.23
		2	27-76	A-6, A-7-6	sandy clay loam	25-50	12-30	1.55
		3	76-203	A-4, A-6	sandy loam	15-30	NP-15	1.7
Scott	SCO-1	1	0-18	A-4, A-6	silt loam	22-39	6-15	1.415
		2	18-33	A-4, A-6	silt loam	23-33	8-13	1.42
		3	33-84	A-6, A-7-6	silty clay loam, silt loam	31-42	13-21	1.525
		4	84-180	A-6	silty clay loam, silt loam	27-38	12-19	1.625
		5	180-201	A-7-6	clay loam, loam	34-49	16-27	1.49
Shelby	SHE-1	1	0-20	A-6	silt loam	23-40	6-16	1.45
		2	20-28	A-6	silt loam	23-38	6-16	1.45
		3	28-36	A-6	silt loam	31-37	13-18	1.55
		4	36-71	A-7-6	clay loam, silty clay, silty clay loam	45-55	25-32	1.55
		5	71-91	A-6	clay loam, fine sandy loam, loam	22-44	6-24	1.65
		6	91-201	A-4	fine sandy loam, loam	20-35	4-16	1.875
Spencer	SPE-1	1	0-25	A-4, A-6	silt loam	22-40	4-17	1.50
		2	25-81	A-6, A-7-6	silty clay loam, silt loam	32-46	15-24	1.575
		3	81-163	A-6, A-7-6	silty clay loam, silt loam	33-45	11-24	1.65
		4	163-203	A-4, A-6, A-7-6	silty clay loam, silt loam	29-45	10-24	1.60
Starke	STA-1	1	0-300	A-2-4, A-3	sand	0	NP	1.70

TABLE B.1
(Continued)

County	Profile No.	Layer	Layer Thickness (cm)	Classification		LL	PI	γ_{dry} (g/cm^3)
				AASHTO	USDA			
Steuben	STE-1	1	0-23	A-4, A-6	silt loam	25-40	7-20	1.48
		2	23-74	A-6	clay loam	35-55	15-30	1.58
		3	74-200	A-6, A-7	silty clay loam	25-45	7-25	1.70
Sullivan	SUL-1	1	0-20	A-4	silt loam	22-30	3-15	1.45
		2	20-76	A-6, A-7	silt clay loam	35-45	15-25	1.50
		3	76-89	A-4, A-6	silt loam	25-35	6-15	1.50
		4	89-152	A-4, A-6	silt, silt loam	20-35	5-15	1.50
Switzerland	SWI-1	1	0-18	A-4, A-6	silt loam	23-40	3-15	1.45
		2	18-61	A-4, A-6, A-7-6	silty clay loam, silt loam	24-45	5-25	1.55
		3	61-99	A-4, A-6	clay loam, loam, silty clay loam, silt loam	24-44	8-25	1.725
		4	99-175	A-7-6	clay, clay loam, silty clay	30-54	20-33	1.60
		5	175-203	A-7	clay, silty clay	40-60	20-40	1.575
Tippecanoe	TIP-1	1	0-43	A-6, A-7-6	silty clay loam	35-55	10-30	1.40
		2	43-137	A-4, A-6, A-7-6	silty clay loam, silt loam	25-65	4-40	1.50
		3	137-178	A-2, A-4, A-6, A-7	clay loam, loam, sandy clay loam, sandy loam	10-60	NP-30	1.55
		4	178-203	A-2, A-4, A-6, A-7	stratified sandy loam to silty clay loam	10-50	NP-25	1.60
Tipton	TIPT-1	1	0-30	A-7-5	silty clay loam	43-57	19-24	1.305
		2	30-102	A-6, A-7-6	silty clay loam	38-49	19-25	1.365
		3	102-152	A-6	fine sand, fine sandy loam, loam, loamy fine sand, silt loam	19-32	3-13	1.545
Union	UNI-1	1	0-30	A-4, A-6	silt loam	22-36	4-12	1.45
		2	30-84	A-6, A-7	clay, clay loam, silty clay loam	30-50	11-30	1.60
		3	84-152	A-4, A-6	fine sandy loam, loam	15-35	4-15	1.875
Vanderburgh	VAN-1	1	0-20	A-4, A-6	silt loam	22-40	NP-17	1.40
		2	20-58	A-4, A-6, A-7-6	silty clay loam, silt loam	23-48	4-27	1.55
		3	58-127	A-4, A-6	silty clay loam, silt loam	24-40	8-24	1.675
		4	127-203	A-4, A-6	silt loam	23-40	2-17	1.60
Vermillion	VER-1	1	0-25	A-4, A-6	silt loam	20-40	3-15	1.45
		2	25-81	A-4, A-6	loam, silt loam	20-40	3-25	1.50
		3	81-183	A-4, A-6	stratified sandy loam to silt loam to loam	20-50	3-25	1.55

TABLE B.1
(Continued)

County	Profile No.	Layer	Layer Thickness (cm)	Classification		LL	PI	γ_{dry} (g/cm^3)
				AASHTO	USDA			
Vigo	VIG-1	1	0-28	A-4, A-6	silt loam	23-37	6-13	1.425
		2	28-46	A-4, A-6	silt loam	24-32	7-13	1.475
		3	46-124	A-6	silt clay loam, silt loam	32-40	15-21	1.55
		4	124-201	A-4, A-6	silt loam	21-31	6-13	1.50
Wabash	WAB-1	1	0-25	A-4, A-6	silt loam	20-35	4-14	1.425
		2	25-33	A-4, A-6	silt loam	20-35	4-14	1.425
		3	33-69	A-6, A-7, A-7-6	silty clay loam, silt loam	35-55	15-35	1.55
		4	69-127	A-6, A-7	clay loam, loam	30-50	10-30	1.60
		5	127-150	A-4, A-6	clay loam, loam	20-50	3-30	1.875
		6	150-201	A-4, A-6	fine sandy loam, loam	15-30	3-15	1.875
Warren	WAR-1	1	0-30	A-6, A-7, A-7-6	silty clay loam	35-55	10-30	1.35
		2	30-114	A-6, A-7, A-7-6	silty clay loam	35-55	15-35	1.50
		3	114-145	A-4, A-6	fine sandy loam, loam, silt loam	10-40	NP-20	1.50
		4	145-152	A-2-4, A-4	stratified silt loam to sandy loam	10-40	NP-20	1.60
Warrick	WARR-1	1	0-5	A-4, A-6	silt loam	22-40	1-17	1.525
		2	5-13	A-6, A-7-6	loam, silty clay loam, silt loam	22-50	1-27	1.675
		3	13-28	A-6, A-7-6	loam, silty clay loam, silt loam	22-50	1-27	1.725
		4	28-203	A-4, A-6, A-7-6	loam, very parachannery silty clay loam, very parachannery silt loam	30-50	8-25	1.875
Washington	WAS-1	1	0-18	A-4, A-6	silt loam	22-40	1-17	1.425
		2	18-91	A-6, A-7-6	silty clay loam, silt loam	23-50	3-29	1.525
		3	91-203	A-7-6	clay, silty clay	44-75	20-46	1.50
Wayne	WAY-1	1	0-20	A-6	silt loam	23-40	6-16	1.45
		2	20-28	A-6	silt loam	23-38	6-16	1.45
		3	28-36	A-6	silt loam	31-37	13-18	1.55
		4	36-71	A-7-6	clay loam, silty clay, silty clay loam	45-55	25-32	1.55
		5	71-91	A-6	clay loam, fine sandy loam, loam	22-44	6-24	1.65
		6	91-201	A-4	fine sandy loam, loam	20-35	4-16	1.875

TABLE B.1
(Continued)

County	Profile No.	Layer	Layer Thickness (cm)	Classification		LL	PI	γ_{dry} (g/cm^3)
				AASHTO	USDA			
Wells	WEL-1	1	0-28	A-6, A-7	silty clay loam	35-50	10-25	1.475
		2	28-86	A-6, A-7-6	clay, silty clay, silty clay loam	40-55	15-30	1.55
		3	86-119	A-6, A-7-6	clay, silty clay, silty clay loam	40-55	15-35	1.60
		4	119-145	A-6, A-7	clay, clay loam, silty clay loam	30-45	10-25	1.625
		5	145-201	A-6, A-7	clay loam, silty clay loam	30-45	10-25	1.625
White	WHI-1	1	0-36	A-4	fine sandy loam	15-25	NP-10	1.55
		2	36-81	A-2-4	fine sandy loam, sandy loam	10-30	NP-10	1.60
		3	81-97	A-1-b, A-2-4, A-3	loamy fine sand, loamy sand, sand	0	NP	1.70
		4	97-203	A-1-b, A-2-4, A-3	coarse sand, loamy sand, sand	0	NP	1.70
Whitley	WHIT-1	1	0-20	A-4, A-6	silt loam	25-40	7-15	1.45
		2	20-66	A-6, A-7-6	clay, silty clay, silty clay loam	35-55	15-35	1.55
		3	66-76	A-6, A-7	clay loam, silty clay, silty clay loam	30-50	10-30	1.70
		4	76-201	A-6, A-7	clay loam, silty clay loam	25-45	7-25	1.80

About the Joint Transportation Research Program (JTRP)

On March 11, 1937, the Indiana Legislature passed an act which authorized the Indiana State Highway Commission to cooperate with and assist Purdue University in developing the best methods of improving and maintaining the highways of the state and the respective counties thereof. That collaborative effort was called the Joint Highway Research Project (JHRP). In 1997 the collaborative venture was renamed as the Joint Transportation Research Program (JTRP) to reflect the state and national efforts to integrate the management and operation of various transportation modes.

The first studies of JHRP were concerned with Test Road No. 1—evaluation of the weathering characteristics of stabilized materials. After World War II, the JHRP program grew substantially and was regularly producing technical reports. Over 1,500 technical reports are now available, published as part of the JHRP and subsequently JTRP collaborative venture between Purdue University and what is now the Indiana Department of Transportation.

Free online access to all reports is provided through a unique collaboration between JTRP and Purdue Libraries. These are available at: http://docs.lib.purdue.edu/jtrp

Further information about JTRP and its current research program is available at: http://www.purdue.edu/jtrp

About This Report

An open access version of this publication is available online. This can be most easily located using the Digital Object Identifier (doi) listed below. Pre-2011 publications that include color illustrations are available online in color but are printed only in grayscale.

The recommended citation for this publication is:

Ganju, E., Rahman, S., Prezzi, M., Salgado, R., & Siddiki, N. (2016). *Moisture-strength-constructability guidelines for subgrade foundation soils found in Indiana* (Joint Transportation Research Program Publication No. FHWA/IN/JTRP-2016/27). West Lafayette, IN: Purdue University. http://dx.doi.org/10.5703/1288284316354